

FDOT Contract Number: BDV29-977-67

Incorporation of Climatic and Hydrologic Nonstationarity into FDOT Planning and Design Guidelines & Processes

FINAL

Submitted to the Florida Department of Transportation

FDOT Project Manager: **Jennifer Carver, AICP**

Principal Investigator:

Jayantha Obeysekera, Ph.D., P.E.

Sea Level Solutions Center
Institute of Environment
Florida International University

Co-Principal Investigator:

Thomas Wahl, Ph.D.

Department of Civil, Environment, and
Construction Engineering
University of Central Florida

Postdoctoral Researcher:

Anupama John, Ph.D.

Sea Level Solutions Center
Institute of Environment
Florida International University

DISCLAIMER

The opinions, findings, and conclusions expressed in this publication are those of the authors and not necessarily those of the State of Florida Department of Transportation.

TECHNICAL REPORT DOCUMENTATION PAGE

1. Report No.	2. Government Accession No.	3. Recipient's Catalog No.	
4. Title and Subtitle Incorporation of Climatic and Hydrologic Nonstationarity into FDOT Planning and Design Guidelines & Processes		5. Report Date June 2023	
		6. Performing Organization Code:	
7. Author(s) Jayantha Obeysekera, Thomas Wahl, Anupama John		8. Performing Organization Report No.	
9. Performing Organization Name and Address Florida International University 11200 SW 8 th St, Miami, FL 33199		10. Work Unit No.	
		11. Contract or Grant No. BDV29-977-67	
12. Sponsoring Agency Name and Address Office of Research, Development, and Technology Florida Department of Transportation 605 Suwannee Street, MS 30 Tallahassee, FL 32399		13. Type of Report and Period Final Report March 2021 to June 2023	
		14. Sponsoring Agency Code	
15. Supplementary Notes			
16. Abstract Changes in climate and associated extreme weather events are already affecting Florida's inland and coastal communities and infrastructure. Until recently, the field of transportation infrastructure (TI) planning and design has also assumed "stationarity" in climate (past climate represents what is expected in the future) and in environmental drivers such as extreme rainfall, flood discharges, and other variables. When necessary, planning for agile, resilient, and quality TI for the future requires moving from this stationarity assumption to a nonstationarity environment characterized by rising sea levels, changing rainfall patterns and floods, changing land use/land cover, and a rising groundwater table along the coast. This research provides potential modifications to current stationary practices being used for TI planning and design when nonstationarity is detected using statistical tests and confirmed by attribution. The study included a comprehensive review of the current guidance documents and the available datasets for hydrologic drivers such as rainfall, sea levels, and peak discharges in inland rivers to identify statistically significant trends in historical data and systematic trends in future projections, both of which would warrant nonstationary techniques for planning and design of TI. This report provides details of trend detection techniques and relevant tools and the development of up-to-date datasets consisting of historical peak discharges, sea levels, and rainfall extremes in the form of intensity-duration-frequency curves. The study also described new nonstationary techniques that may be used when statistically significant trends in historical data or systematic trends in future projections are present and under what circumstances the current practices based on stationarity may be adequate for future planning. The datasets have been delivered to the University of Florida's GeoPortal with the goal of assisting FDOT in implementing the methods developed in this study.			
17. Key Words: Transportation, Nonstationarity, Trend Detection, Attribution		18. Distribution Statement No restrictions.	
19. Security Classif. (of this report) Unclassified	20. Security Classif. (of this page) Unclassified	21. No. of Pages 178	22. Price

Form DOT F 1700.7 (8-72)

Reproduction of completed page authorized.

EXECUTIVE SUMMARY

This report is the final deliverable of the project entitled *Incorporation of Climatic and Hydrologic Nonstationarity into FDOT Planning and Design Guidelines and Processes*. **For this project, a nonstationary system is defined as a system that changes temporally; hence, patterns or trends of the past cannot be used directly to predict a future state. Nonstationarity in hydrologic drivers pertinent to transportation infrastructure incorporates potential future changes attributable to both climatic and non-climatic factors in planning and design.** The primary objectives of this project are to (a) review the current FDOT and other manuals of practice to determine if nonstationarity approaches need to be considered, (b) develop appropriate nonstationary methods for applications in Florida, and (c) provide data sets and capacity building to support the new methods. In general, resilience against future hazards is an important aspect of Florida's transportation infrastructure planning, and the statewide resiliency goals translate to local efforts through long-range transportation plans (LRTPs). Consideration of nonstationarity is an important aspect of resilience. Through recent legislation, the State of Florida has guided the resilience of transportation infrastructure against future flooding and other impacts.

The research team reviewed 13 FDOT manuals and determined three categories of data currently recommended: rainfall, sea level, and discharge. All the datasets and the methods included in the current manuals are largely based on the stationarity assumption. Circulars and reports by the FHWA and the National Cooperative Highway Research Program (NCHRP), at the national level, provide recommendations for datasets and methods which may be used to incorporate nonstationarity into transportation infrastructure, but their implementation in Florida has not been developed fully.

It is important to note that not all projects need to incorporate nonstationarity in their design process, and factors like design life, cost, risk, and vulnerability should be considered. For example, the FHWA circulars recommend the use of nonstationary data for projects with design lives over 75 years. Only a few FDOT projects are designed beyond 75 years. In addition, the risk and vulnerability of projects that can be quantified using existing assessment tools should be considered in the decision to incorporate nonstationarity. Frameworks that consider these different factors are presented in the NCHRP reports entitled 'Applying Climate Change Information to Hydrologic and Coastal Design of Transportation Infrastructure Final Report' (Kilgore et al., 2019a) and 'Applying Climate Change Information to Hydrologic and Coastal Design of Transportation Infrastructure Design Practices' (Kilgore et al., 2019b). Before embarking on applying nonstationary techniques for planning and design, a logical process needs to be followed to justify their use, and such a process should include the initial screening of data, nonstationary detection, review of literature and data, projected changes in hydrologic drivers, assessment of risk and the application of nonstationary methods only when justified.

Trend detection can quantify if nonstationarity in historical data should be considered in the design process. There are statistical tests, both parametric and nonparametric, and tools (such as the USACE Time Series Analysis tools) that can detect the statistical significance of historical

trends. If nonstationarity is detected, efforts must be initiated to determine the source of the nonstationarity. Abrupt or continuous changes may be attributed to other factors such as changes in land use and water management that are characterized as non-climatic. When considerations of nonstationarity are warranted, this project provides guidance for revisiting the traditional concepts of return period and risk and the methods that may be used by enhancing the current statistical methods. Three relevant hydrologic drivers that were identified, namely, rising sea levels, peak discharges in streams and rivers, and extreme rainfall. While sea levels at almost all tide gages around the state exhibit statistically significant nonstationarity, peak discharge at inland locations did not present similar spatially broad trends in data. The datasets assembled for the project have been delivered for possible inclusion in the University of Florida's GeoPortal.

As the field of climate science is constantly evolving, any effort to incorporate nonstationarity should consider the latest climate datasets, projections, methods, tools, and frameworks available at the time of design. For the State of Florida, Flood Hub is expected to be the centralized resource for the latest science on new sea level and rainfall projections. When nonstationarity is observed and attributed to valid reasons, and or projected, the research in this project provides a new paradigm for treating varying levels of protection expressed as time varying return periods and/or risks. This new paradigm includes methods for revisiting the concept of a fixed return period, and a risk-based infrastructure design in the nonstationary setting.

Finally, "regret" may occur through both underinvestment as well as overinvestment in transportation resiliency. New approaches like Dynamic Adaptive Policy Pathways (DAPP) should be considered to minimize this. Because of uncertainties in projection of climate drivers such as sea level rise, it is almost impossible to predict the evolution of the hazards. In such situations, it is prudent to phase in the implementation of adaptation options through time with proper attention to ensure availability of resources (e.g., land) when needed. This DAPP approach of staging TI infrastructure building will likely save costs ensuring services only when they are needed.

TABLE OF CONTENTS

1. INTRODUCTION	1
1.1. Description of Problem	1
1.2. Objectives	2
1.3. Background	3
1.3.1. Climate Resilience in Florida’s Transportation Planning	3
1.3.2. Recent Legislation	3
1.3.3. Climate Nonstationarity	4
2. ASSESSMENT OF CURRENT METHODS USED IN PRACTICE	7
2.1. Task Objective	7
2.2. Review of Transportation Manuals	7
2.2.1. Rainfall Data	7
2.2.2. Sea Level Data	8
2.2.3. Discharge Data	9
2.3. Other Sources of Climate Data and Projections	9
2.3.1. Rainfall Data from Downscaled Climate Model Outputs	9
2.3.2. Sea Level Projections	11
2.4. Nonstationarity in Transportation Planning	13
2.4.1. Review of FHWA Hydraulic Engineering Circulars (HECs) Incorporating Nonstationarity in Transportation Planning	13
2.4.2. Review of NCHRP Reports Incorporating Nonstationarity	22
2.4.2.1. Design Practices	22
2.4.2.2. Inland Hydrology	24
2.4.2.3. Coastal Applications	29
2.4.2.4. Selecting Sea Level Rise for Design	29
2.4.3. Detecting Nonstationarity	31
2.4.3.1. Trend Detection by Parametric Methods	32
2.4.3.2. Trend Detection by Nonparametric Methods	32
2.5. Conclusions	33
3. NEW PARADIGM AND METHODS FOR TRANSPORTATION SYSTEM PLANNING AND DESIGN USING NONSTATIONARY PRINCIPLES	35

3.1.	Task Objective	35
3.2.	Review of Existing Tools.....	35
3.2.1.	Vulnerability Assessment Scoring Tool	35
3.2.2.	Guide to Assessing Criticality in Transportation Adaptation Planning.....	41
3.3.	Data Assembly	46
3.3.1.	Rainfall.....	46
3.3.2.	Sea Level.....	47
3.3.3.	USGS Peak Discharge Data across Florida.....	49
3.4.	Tools for Nonstationarity Detection	50
3.4.1.	USACE Time Series Toolbox	50
3.4.2.	USGS Trend Assessment for Peak Flow	56
3.5.	Nonstationarity Paradigm for Return Period, Risk, and Uncertainty	58
3.5.1.	Modeling of Stationary and Nonstationary Extremes.....	59
3.5.2.	Statistical Modeling of Extremes	61
3.5.2.1.	AMS Series.....	61
3.5.2.2.	POT Series	61
3.5.2.3.	Modeling Nonstationary.....	62
3.5.2.4.	Change Factors of Rainfall Depth-Duration-Frequency (DDF) Estimates	63
3.5.3.	Review of Stationary Methods for Return Period and Risk.....	64
3.5.4.	Extension to a Nonstationary Paradigm	66
3.6.	Development of Nonstationary Methods for Key Environmental Drivers	69
3.6.1.	Rainfall.....	69
3.6.1.1.	Comparison of DDF.....	69
3.6.1.2.	Spatial Mapping of Change Factor.....	70
3.6.2.	Sea Level.....	73
3.6.3.	Peak Discharge	80
3.6.3.1.	Example risk-based application of FDOT Projects.....	83
3.7.	Conclusions.....	84
4.	DEVELOPMENT OF NEW DATASETS FOR APPLYING THE NONSTATIONARY METHODS.....	86
4.1.	Objective	86
4.2.	Description of Datasets Included	86

4.2.1.	Rainfall.....	86
4.2.2.	Peak Discharge	87
4.2.3.	Sea Level.....	88
4.2.4.	Groundwater	88
5.	KNOWLEDGE TRANSFER.....	89
5.1.	Objective	89
5.2.	Description of Task	89
6.	SUMMARY AND RECOMMENDATIONS	90
6.1.	Summary	90
6.2.	Recommendations.....	92
	REFERENCES.....	95
	APPENDIX A. SUMMARY OF FDOT DOCUMENT REVIEW.....	103
	APPENDIX B. THEORETICAL CONCEPTS	110
	APPENDIX C. EXAMPLES OF INDICATORS AND THEIR POTENTIAL DATA SOURCES.....	116
	APPENDIX D. REPORT ON NONSTATIONARY DETECTION USING USACE’S TIME SERIES TOOLBOX	123
	APPENDIX E. USGS TREND ASSESSMENT TABULAR DATA	159

LIST OF FIGURES

Figure 1-1. Flow chart and crosswalk table developed by USACE for incorporating climate change impacts to inland hydrology in civil works (USACE, 2018)	6
Figure 2-1. The 2019 Unified Sea Level Rise Projections for Southeast Florida. Source: SEFRCC (2019).....	12
Figure 2-2. Sea level rise scenarios for St. Petersburg, Florida from NOAA (2017) recommended for the Tampa Bay Region. Source: CSAP (2019).....	13
Figure 2-3. Projections of GMSLR in this century from Kopp et al. (2014) for (a) RCP8.5, (b) RCP4.5, and (c) RCP2.6. Source: FHWA (2020).....	19
Figure 2-4. GMSLR scenarios (Sweet et al. 2017) and process-based scenarios (Kopp et al., 2014). Source: FHWA (2020).....	20
Figure 2-5. The relationship between survey and tidal datums. Source: FHWA (2020).	21
Figure 2-6. Levels of analysis (Kilgore et al., 2019b).....	23
Figure 2-7. Considerations for choosing a decision-making framework (Kilgore et al., 2019b)...	24
Figure 2-8. Definition of the climate change indicator (CCI) (FHWA, 2016).	27
Figure 2-9. The recommended procedure for projecting 24-hour precipitation quantiles (Kilgore et al. 2019b).....	28
Figure 2-10. A suggested framework for considering GMSLR scenarios for design or planning. Arrows point in the direction of increasing sensitivity, redundancy, or consequence of failure (Kilgore et al. 2019b).....	30
Figure 3-1. Schematic of the process used by the Vulnerability Assessment Tool (VAST) (Source: USDOT, 2015).....	38
Figure 3-2. Vulnerability assessment timeline (Source: USDOT, 2015).	39
Figure 3-3. 10 Criticality scale was applied to each asset based on the asset’s character by the WSDOT (Source: USDOT, 2014).....	45
Figure 3-4. Map of the DDF rainfall stations and zones in Florida.....	47
Figure 3-5. NOAA tide gauge locations were selected for the project.	48

Figure 3-6. Relative sea level rise curves correspond to the intermediate-high scenario obtained from the NOAA 2017 report (Sweet et al., 2017). 48

Figure 3-7. Extreme sea-level curves (design return level versus frequency) correspond to the tide gauges shown in Figure 3-6. The curves are based on the data obtained from the NOAA 2022 report (Sweet et al. 2022). 49

Figure 3-8. Map of the 231 USGS stations that were selected from the HEC-DSSVue database. A second round of filtering resulted in 99 stations (blue dots) while 132 stations were excluded (red dots) for insufficient observations. 50

Figure 3-9. Example of the time series plot of the annual peak flow at Bonnet Creek, Vineland, FL, created using the USACE Time Series Toolbox. 52

Figure 3-10. Nonstationarity detection using the Time Series Toolbox for annual peak flow at Bonnet Creek, Vineland, FL. 54

Figure 3-11. Statistical heat map showing the significant tests for the nonstationary analysis of annual peak flow data at Bonnet Creek, Vineland, FL. 54

Figure 3-12. Segment statistics for the nonstationary analysis of annual peak flow data at Bonnet Creek, Vineland, FL. 55

Figure 3-13. Breakpoints identified by the Time Series Toolbox and the breakpoint segment details for the annual peak flow data at Bonnet Creek, Vineland, FL. 55

Figure 3-14. Map with stations showing the results from the nonparametric trend analysis. 57

Figure 3-15. The plot of the discharge with linear trendlines for stations with significant positive trends. 58

Figure 3-16. (a) Illustration of extracting block maxima (BM) data for modeling extremes and (b) example of a daily rainfall series (open circles) and the (annual) block maxima values (solid circles in red). 59

Figure 3-17. (a) Illustration of extracting peaks-over-threshold (POT) data for modeling extremes (in green) and (b) example of a daily precipitation series and the values above a threshold equal to 2 inches (in red color). 60

Figure 3-18. Illustration of the concept of the change factor. The dashed curve is the adjusted curve using, observed, modeled-current, and modeled-project probability distributions and the change factor defined in the text below. In most cases, the m-c and o-c curves deviate from each other, even in cases when the current and observed periods are identical. 63

Figure 3-19. Examples of stationary and nonstationary annual maximum floods for (a) stationary, and (b) nonstationary. The dashed line in each figure is the fitted location parameter using a stationary and nonstationary GEV distribution respectively for each case. The variables t_0 and t_n denote the beginning and end of the project design life, n , respectively. In addition, z_{q0} is the design quantile, and p_0 and p_n denote exceedance probabilities (area of PDF above the design quantile) (Adapted from Obeysekera and Salas, 2020)..... 66

Figure 3-20. Example return period curve..... 67

Figure 3-21. An example demonstrating changes in the magnitude of risk due to nonstationarity as a function of the project life, n . The dashed lines in this figure correspond to the stationary case, and as shown, risk naturally increases for projects with longer project life. In each case, the corresponding nonstationary curve is shown as a solid curve. Three cases corresponding to the initial return period, $T_0 = 25, 50, \text{ and } 100$ years are shown. 68

Figure 3-22. DDF curves generated for 1-day, 3-day, 7-day, and 10-day storms using the ATLAS 14 data and change factors from downscaled data at the Jacksonville International Airport station..... 70

Figure 3-23. Spatial maps of change factors derived from the LOCA dataset corresponding to the return period of five years. Sample values in selected grid points and the contours using a smoothing algorithm are also shown..... 72

Figure 3-24. Recurrent flood frequency estimates for (a) Virginia Key, Florida, and (b) Pensacola, Florida. Note: to be useful for decision-making, a conversion of the return level to land-based heights (e.g., geodetic datum such as NAVD88) should be made. 75

Figure 3-25. (a) Actual average recurrence interval (due to rising mean sea level) curves (T versus T_0) at each tide gauge. (b) Risk curves as a function of design life: Stationary (black curve), the actual risk resulting from rising relative sea level rise (red curve), and risk curve for a specific risk (blue curve)..... 78

Figure 3-26. Temporal variation of the location parameters with the flood magnitude data. 82

Figure 3-27. The nonstationary return period curve and the risk curves. 82

Figure 3-28. Risk-based nonstationary approach for planning and design..... 83

LIST OF TABLES

Table 2-1. Tools required for each level of analysis.	16
Table 2-2. Data required for each level of analysis.	16
Table 2-3. The service life of projects with levels of analysis.	17
Table 2-4. Numerical coastal models cited in the HEC-25 manual. Source: FHWA (2020).	21
Table 2-5. Level of analysis for inland hydrology.....	23
Table 2-6. Level of analysis for coastal applications.	23
Table 2-7. Climate scenario classification from CMIP3 and CMIP5 archives.	25
Table 2-8. Four recommended high-resolution datasets of temperature and projections (Kilgore et al. 2019b)	25
Table 2-9. Climate sensitivity of Group 1 models (Kilgore et al. 2019b).....	26
Table 2-10. Recommended minimum GMSLR estimates for use in planning and design (Kilgore et al. 2019b, FHWA 2020).	29
Table 3-1. Modeling options for the climate stressors used in the Gulf Coast Study (Source: USDOT, 2015).....	40
Table 3-2. Examples of how the criticality assessment design process is influenced by the purpose of the study and the target audience (Source: USDOT, 2014).....	42
Table 3-3. Applications of the USACE Time Series Toolbox which are presented in the UCF report in Appendix D.....	51
Table 3-4. USGS annual peak flow stations with significant positive trends from the trend assessment.....	57
Table 3-5. Regional frequency analysis (RFA)-based extreme water level (EWL) distribution parameters.....	74
Table 3-6. Summary of design parameters (with numbers rounded) to constrain the recurrent flood frequency, N, to one per year by 2060 (end-year of the design life.....	76
Table 3-7. The parameters of GEV computed using the peaks-over-threshold GPD model (Coles 2001).....	77

Table 3-8. Results of the Risk-Based Design for all tide gauges shown in Figure 3-5. Values in the last column have been rounded to the closest 5-year interval.	80
Table 3-9. Results summarized for the various combinations of the Gumbel - GEV models.	81
Table 6-1. Decision matrix for considering nonstationarity.....	93
Table B-1. ANOVA table for multiple linear regression.....	111
Table C-1. Temperature indicators provided as examples in Vulnerability Assessment Tool (VAST).....	117
Table C-2. Precipitation indicators provided as examples in Vulnerability Assessment Tool (VAST).....	118
Table C-3. Sea Level Rise indicators provided as examples in Vulnerability Assessment Tool (VAST).....	120
Table C-4. Storm surge indicators provided as examples in Vulnerability Assessment Tool (VAST).....	121
Table C-5. Wind exposure indicators provided as examples in Vulnerability Assessment Tool (VAST).....	122
Table E-1. Tabular results from the normality test for the USGS annual peak flow data.....	160
Table E-2. Tabular results from the Kendall Test for the USGS Annual Peak Flow Data.....	163

1. INTRODUCTION

1.1. Description of Problem

Changes in climate and associated extreme weather events are already affecting Florida's inland and coastal communities and infrastructure. Most notably, the frequency of high tide flooding events in some coastal regions of Florida has increased significantly because of sea level rise, higher tides, and storm surge. There are concerns that extreme rainfall is also increasing, which could lead to an increased frequency of flooding in both inland and coastal communities. Flooding is projected to increase further in the next few years to decades, becoming more severe with time (Vogel et al., 2011). Sea level rise has a direct effect on the groundwater table, especially along the coastal belt, and this effect may propagate inland (Befus et al., 2020). Furthermore, increasing storm surge and extreme waves could occur due to future changes in intensity, frequency, and/or tracks of tropical and extra-tropical storms (e.g., Knutson et al., 2021). In recent years, South Florida appears to have experienced unprecedented rainfall from tropical systems causing significant damage to transportation infrastructure (TI), buildings, and other infrastructure along the coast. For instance, the return period associated with rainfall amounts along the track of Hurricane Ian in 2022 was rare, and according to a recent analysis by FIU (unpublished), reaching upwards of 500 years at certain locations.

There has been major research activity in the field of hydrology and water resources to detect and attribute changes in hydrological processes at a range of scales (e.g., Salas et al., 2018; Milly et al., 2008). Before this research, generally, the key statistics for hydrological processes such as the mean and the variance have been assumed to be constant over time, i.e., the concept known as stationarity. Many hydrologists have strongly questioned the assumption of stationarity and suggested that "Stationarity is Dead – Whither Water Management?" (Milly et al., 2008). Others have now developed methods for more realistic design, evaluation, and planning and management of infrastructure to account for potential future changes leading to nonstationarity. The paper by Milly et al. (2008) caught major attention worldwide. However, many others reacted immediately with opposite positions and opinions that are exemplified by the titles of some of the articles published in the literature (see Salas et al. 2018): "Stationarity: Wanted Dead or Alive? (Lins and Cohn, 2011), "Comment on the Announced Death of Stationarity" (Matalas, 2012), "Negligent Killing of Scientific Concepts: The Stationary Case" (Koutsoyiannis and Montanari, 2014), "Modeling and Mitigating Natural Hazards: Stationarity is Immortal!" (Montanari and Koutsoyiannis, 2014), and "Stationarity is Undead: Uncertainty Dominates the Distribution of Extremes" (Serinaldi and Kilsby, 2015). Despite the tremendous increased attention given to this subject, there is no generally agreed-upon set of methods for performing key hydrologic analyses such as the Flood frequency analysis, under nonstationary conditions. Many agencies are updating flood protection design guidelines to account for nonstationarity (e.g., Stedinger and Griffis, 2011; Centre for Ecology and Hydrology 2013; Prosdociimi et al., 2014). It should be noted that hydrologic processes with short and/or long memory (e.g. Koutsoyiannis, 2002) are capable of generating hydrologic sequences that exhibit trends and abrupt shifting

patterns, but they may not be characterized necessarily as nonstationary. The lack of a consensus regarding the use of nonstationary approaches results in part from the uncertainty associated with the ability to detect, attribute, and model past trends. In situations where historical trends are obvious, statistically significant, and attributable to changes in historical land use, climate, and/or water infrastructure, the approaches for planning and design must be updated. However, in many situations, such trends are not statistically significant, and the current practices of planning and design may be adequate, particularly with short spans of design life. Even if the historical trends are not significant, the application of nonstationary methods may be needed if the future projections of the hydrologic driver of interest (e.g. sea level rise) suggest systematic trends.

The impact of longer-term climate and anthropogenic changes in different flooding drivers has not been accounted for in the planning and design of coastal transportation systems except in some regions. The research in this report will provide specific methodologies and data sets for planning TI experiencing changing stresses and shocks from climate and associated impacts but customized for Florida. The incorporation of a new paradigm for TI planning and design and associated datasets based on actionable science in a changing climate will lead to innovation in resiliency planning. This improvement to current standards and guidance will promote the sustainability of transportation infrastructure for many decades.

1.2. Objectives

The research is focused on potential modifications to current manuals of practice being used by the Florida Department of Transportation (FDOT) for transportation project design. When possible, guidance will also be provided on relevant planning practices that may be in use by FDOT. Concerning TI designs, the research will identify which standards may warrant modifications to account for implications of future climate change, especially sea level rise, and changes to extreme rainfall. The final report of this research project will recommend appropriate nonstationary methods and datasets for future use by FDOT engineers and consultants for future planning and design of TI.

Objective 1: Identify potential changes to current FDOT manuals of practice and design standards that require modifications to account for nonstationarity.

This objective will focus on recommended revisions required for addressing evolving conditions associated with climate change and variability such as sea level rise, tides, storm surge, increasing extreme rainfall and river discharge, and rising ground water tables.

Objective 2: Develop new planning and design methods for dealing with nonstationarity.

Based on the current state of actionable science, develop detailed guidelines for treating evolving conditions due to rising sea levels, changing rainfall, rising groundwater tables, and other drivers of consequence to the performance of transportation infrastructure.

Objective 3: Develop datasets for applying new nonstationarity methods.

The research will assess and assemble information available for projections of sea level rise, rainfall, and groundwater levels for applications of the nonstationarity methods. The datasets will include both FDOT and other data that are necessary for applying the nonstationarity methods. Other data sets will include but are not limited to, those that are part of the Sea Level Impact Projection (SLIP) tool. The exact data to be included for FDOT use will be determined in consultation with the FDOT Data Governance Administrator.

Objective 4: Building Capacity among FDOT engineering professionals.

Develop a technology transfer and a training program to inform design professionals including engineers, environmental professionals, and right-of-way professionals on the application of the new methods.

1.3. Background

1.3.1. Climate Resilience in Florida’s Transportation Planning

The FDOT serves the people of the state of Florida with a mission to “provide a safe transportation system that ensures the mobility of people and goods, enhances economic prosperity, and preserves the quality of our environment and communities” (FDOT 2021a). FDOT develops the Florida Transportation Plan (FTP) to guide the statewide efforts to achieve ‘Agile, Resilient, and Quality Transportation Infrastructure.’ Resilience is an important aspect of Florida’s transportation planning and these statewide resiliency goals translate to local efforts through Long Range Transportations Plans (LRTPs), which are developed by Metropolitan Planning Organizations (MPOs). The LRTPs are aligned with the FTPs and are required to consider resilience in their planning and objectives, performance measures, risk and vulnerability assessments, assets and mobility assessments, and projects and actions of the Cost Feasibility Plan. MPOs like the Broward County MPO have identified climate resilience actions that are outlined in the Broward County Climate Change Action Plan. There are also examples of statewide plans, other than the FTP, which address resilience in their infrastructure planning like the Strategic Intermodal System Policy Plan (2022 update), FDOTs Transportation Asset Management Plan (FDOT, 2019a), and the Florida Freight Mobility and Trade Plan (2022). These plans were developed to tackle the challenges posed by the effects of climate change like increased inland flooding, sea level rise, increased frequency of severe storms with higher winds, extreme rainfall, and increased duration of droughts.

1.3.2. Recent Legislation

Some legislations are pertinent to FDOT’s effort to pursue nonstationary approaches for transportation infrastructure planning and design. First, the Senate Bill 1954 (SB 1954 in 2021) creating 380.093 F.S. emphasizes the statewide flooding and sea-level rise resilience. It is worthwhile noting that the State of Florida Legislature recognizes that Florida is particularly vulnerable to adverse impacts of flooding resulting from the increasing frequency and duration of rainfall events, storm surge from more frequent and sever weather systems, and sea-level rise (wording extracted from SB 1954). This observation already acknowledges the changing

conditions and hence requires the exploration of a nonstationary framework. Concerning the mission of the FDOT, SB 1954 includes transportation assets including bridges and major roadways among other types of infrastructure as “critical assets.” Further, Section 380.0933, F.S. established the Florida Flood Hub for Applied Research and Innovation to provide research support in the form of data and modeling for vulnerability assessments, and presumably, this data will need to address future environmental conditions requiring consideration of nonstationarity. Second, House Bill 7053 filed in 2022 also addresses flooding and sea level rise resilience and established the Statewide Office of Resilience and appointment of a Chief Resilience Officer. This Bill requires the development of a “resilience action plan” for the State Highway System based on current conditions and forecasted future events. It also recommends design changes to retrofit existing state highway facilities and to construct new state highway facilities. The traditional stationary approaches need to be revisited to meet such requirements.

1.3.3. Climate Nonstationarity

Until recently, TI planning and design have assumed “stationarity” in climate (past climate represents what is expected to be in the future) in environmental drivers such as rainfall, sea levels, and other design variables. The only exception may be to address sea level rise but even its treatment tends to be limited to projections using historical trends. Planning for agile, resilient, and quality TI for the future, depending on the current design criteria and the use of such approaches as safety factors, may require moving from this stationarity assumption to a nonstationary environment characterized by rising sea levels, changing rainfall patterns and floods, stronger and/or more frequent tropical storms, changing land use/land cover, and a rising groundwater table especially along the coast and extending to some inland locations. While guidance documents such as FHWA (2016) (guidance for riverine systems) provide enhancements to consider, the application of nonstationarity to Florida’s situation requires the development of specific approaches, guidelines, and data sets for the state. Currently, the “Design Return Period” concept is the standard practice, but recent research on nonstationarity indicates that this concept needs to be revisited since the return period and future risks are dynamic (Salas et al. 2019) as they vary with time. A new paradigm, which incorporates changing exceedance probabilities (failure probabilities), risks, and innovative planning criteria based on future projections, is needed. Florida is a state where rising sea levels, changing rainfall, and other impacts are being experienced already, and hence changes to the current planning and design guidelines are needed.

Before embarking on applying nonstationary techniques for TI planning and design, a logical process needs to be followed to justify their use. Because there are many factors (land use change and climate) may contribute to any apparent nonstationarity in data, careful adherence to this process may be needed. Such a process should essentially include the following general steps:

- I. Initial screening to assess vulnerability using tools like Vulnerability Assessment Scoring Tool (VAST)

- II. Detection of nonstationarity in relevant climatic and non-climatic drivers using data in the vicinity of the project site
- III. Literature review to determine the possible presence of climate change in the project area
- IV. Projected change in relevant climate drivers
- V. Assess risk to project features
- VI. Develop planning and design options to address potential nonstationarity

An example of such a process, developed by the US Army of Corps of Engineers is shown in Figure 1-1.

It should be noted that the prediction of future climatic conditions, including sea level rise, is inherently associated with significant uncertainties, particularly for rare extremes. Such uncertainties are the result of inadequacies in science and the modeling of future predictions. While there are many methods to deal with “deep uncertainties,” one approach that is becoming increasingly popular is scenario testing. When uncertainty estimates of projections are available, they should be used along with the best available trajectories for future conditions for the development of adaptation strategies with due consideration to risks of failure. When TI planning and design methods include significant factors of safety, these may already cover the future conditions reflecting nonstationarity. All the above factors need to be considered in the application of nonstationarity approaches developed in this report.

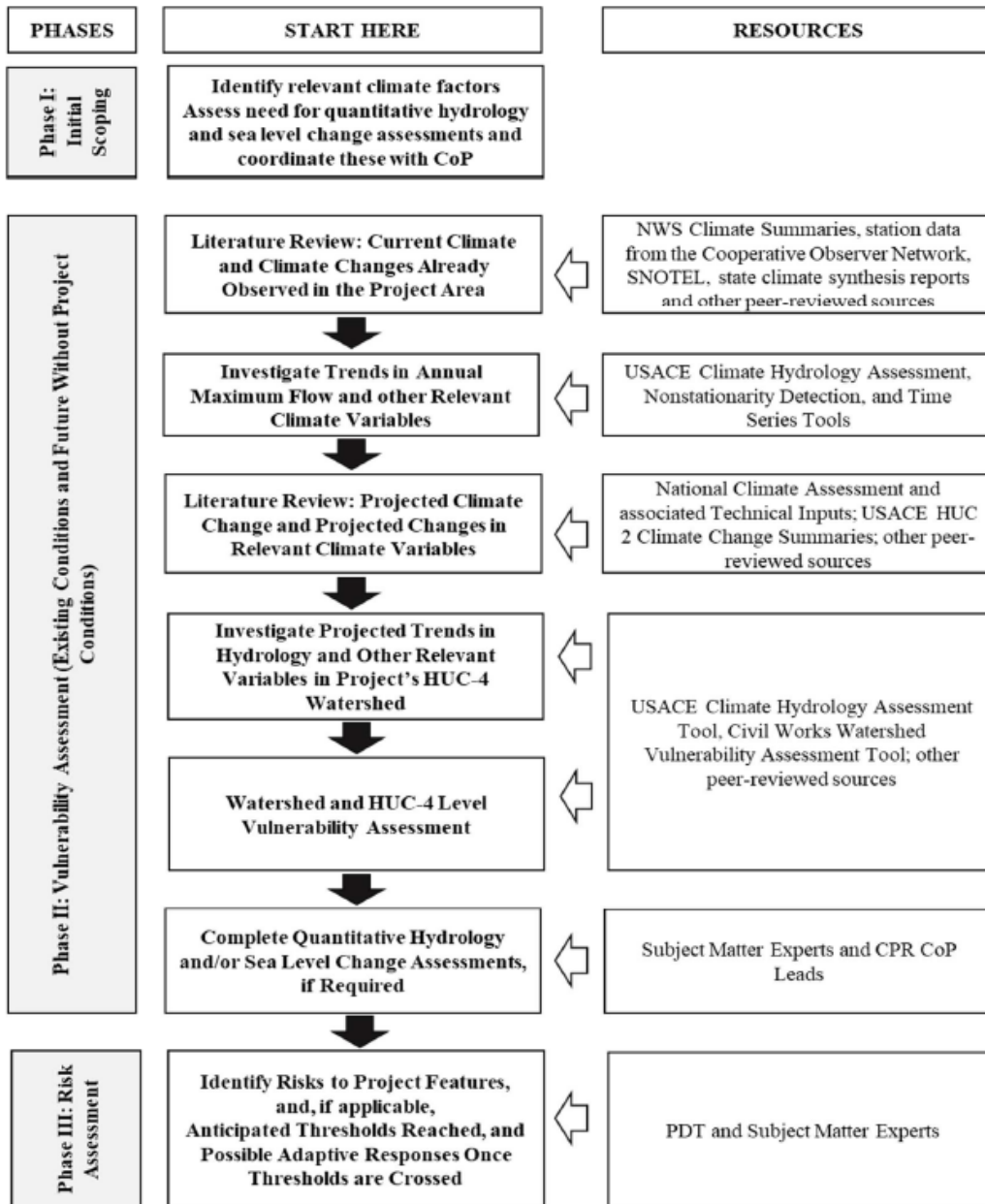


Figure 1-1. Flow chart and crosswalk table developed by USACE for incorporating climate change impacts to inland hydrology in civil works (USACE, 2018).

2. ASSESSMENT OF CURRENT METHODS USED IN PRACTICE

2.1. Task Objective

Review relevant literature, manuals, and standards to determine the changes that may be necessary to incorporate peer-reviewed research on nonstationarity into the manuals of practice.

2.2. Review of Transportation Manuals

To identify necessary changes to incorporate nonstationarity, this effort first reviewed the following manuals of practice and other relevant documents:

- FDOT Drainage Manual (FDOT, 2021a)
- FDOT Drainage Design Guide (FDOT, 2020a)
- FDOT Drainage Handbook – Drainage Connection Permits (FDOT, 2020b)
- FDOT Structures Manual (FDOT, 2022a)
- FDOT Soils and Foundations Handbook (FDOT, 2021b)
- FDOT Flexible Pavement Design Manual (FDOT, 2022b)
- FDOT Rigid Pavement Design Manual (FDOT, 2022c)
- FDOT Pavement Type Selection Manual (FDOT, 2019b)
- FDOT Manual of Uniform Minimum Standards for Design, Construction, and Maintenance for Streets and Highways (FDOT, 2018)
- FDOT Project Development & Environment Manual (FDOT, 2020c)
- FDOT Local Agency Program Manual (FDOT, 2012)
- FDOT Utility Accommodation Manual (FDOT, 2017)
- FDOT Utility Procedures Manual (FDOT, 2021c)

Appendix A presents a tabular, summarized review of the FDOT manuals with pertinent climate data. Based on the review, three categories of data were identified: 1) rainfall, 2) sea level, and 3) peak discharge. The following sections provide the datasets and their applications identified in the manuals for each category.

2.2.1. Rainfall Data

Engineers and planners rely on design storms for rainfall estimates used in the planning and design of drainage projects. Design storms can be defined using Depth-Duration-Frequency (DDF) or Intensity-Duration-Frequency (IDF) curves, which are objective probabilistic assessments of rainfall occurrence (Panthou et al., 2014). DDF/IDF curves present the depth/intensity and duration of rainfall for storms with different frequencies (defined either in terms of exceedance probability or return period) and are developed by (1) fitting a probability distribution function (PDF) to rainfall data for different durations, (2) relating the maximum rainfall depth to the corresponding return period from the cumulative distribution function, and (3) determining the maximum rainfall depth from the known cumulative frequency and duration using a theoretical distribution function (Srivastav et al., 2015; FHWA, 2016). Typically, historical observations have been used to derive DDF/IDF curves; however, with the recent developments in climate

nonstationarity research, there is concern about their reliability for future climate scenarios (Irizarry-Ortiz and Stamm, 2021).

The FDOT Drainage Manual (FDOT, 2021a), FDOT Drainage Design Guide (FDOT, 2020a), and the FDOT Drainage Handbook – Drainage Connection Permits (2020b) all require design storm frequencies for storm drain system design, cross drain hydraulics, temporary facility design, and calculating peak flow using the Rational method. The previous versions of the FDOT design manuals (FDOT Drainage Manual, 2021 and the FDOT Drainage Handbook, 2020b) recommended the use of the FDOT IDF curves, which were available for 11 zones in Florida. However, FDOT now recommends the use of NOAA Atlas 14 rainfall data. The dataset consists of statistical rainfall depth developed using Regional Frequency Analysis (RFA). Depth-Duration-Frequency (DDF) curves are available at 242 locations in Florida. The dataset provides precipitation frequency estimates for storm durations of 5 minutes through 60 days at average recurrence intervals of 1 year through 1000 years. These estimates assume climate stationarity (Perica et al., 2013).

2.2.2. Sea Level Data

Increasing rates of sea level rise (SLR) pose risks to coastal and tidally influenced communities and their infrastructure. Globally, the sea level has risen about 8 inches in the last century; however, the rate of increase in the last two decades is twice that of the last century. From 1971 to 2018, thermal expansion and ice melt from ocean warming contributed to about 50% and 42% of sea level rise, while 8% is attributed to changes in land storage (IPCC, 2021). Dealing with SLR has been especially challenging for a state like Florida with its 1100-mile-long coastline, low elevation, and porous geology. In addition, many of the state's larger communities/economies, and their infrastructure, are in coastal areas vulnerable to the consequences of SLR like coastal inundation, impairment of infrastructure like roadways, drainage systems, sewers, and septic systems, saltwater intrusion of drinking water supply, displacement, and decrease in property values. Some communities in Florida have already begun planning for and/or implementing SLR adaptation strategies.

It is important to measure the local sea levels with tide gauges as Global Mean Sea Level Rise (GMSLR) is not homogenous across the oceans. These measurements are referenced to a stable vertical point on land and include local factors of sea level change such as changes in ocean circulation, gravitational and other changes due to redistribution of ice melt, and vertical land movement (VLM) from subsidence, glacial rebound or tectonic motion. Coastal applications of sea level use the relative sea level rise (RSLR) trend, which is the change in local sea level over time. Typically, approaches used in planning for sea level change involve combining RSLR for an area with projections of global sea level change.

The historical tidal records gathered by the National Water Level Observation Network (NWLON) and managed by NOAA's Center for Operational Oceanographic Products and Services (CO-OPS) can be used to estimate the relative sea level trend data (<https://tidesandcurrents.noaa.gov/nwlon.html>). The NWLON data collection platforms measure water levels in lakes, estuaries, and oceans, as well as some oceanographic and meteorological

parameters. The long-term historical (some stations with data as far back as 1850) and current water levels are useful in computing local sea level trends and studying patterns of high tide events. Tidal datums are vertical elevations that describe tidal fluctuations. Some common tidal datums include 1) Mean high water (MHW) – base elevation for structure heights, bridge clearances, etc., and mean low water (MLW) – officially designated navigational chart datum for the United States. Tidal benchmarks are used to reference tidal datums.

Sea level data are required in FDOT Drainage Manual (FDOT, 2021a) and FDOT Drainage Design Guide (FDOT, 2020a) for tailwater elevations in storm drains, cross drains, and coastal ponds. Typically, regression of historical tide gauge data is used for these applications; however, the FDOT now proposes the use of NOAA (2017) projections for estimating future sea levels (FDOT, 2021a).

2.2.3. Discharge Data

Stream/canal discharge data is used for the design and analysis of open channels, cross drains, and bridges. Typically, observations from gauge data are used to perform frequency analysis for open channels and cross drains. Gauge data may be available through the United States Geological Survey (USGS), as well as regional water management districts like the South Florida Water Management District.

For projects where gauge data may not be available, the FDOT Drainage Manual (FDOT, 2021a) recommends the use of local or regional regression equations that are available through USGS. If the project area is less than 600 acres, the Drainage Manual (FDOT, 2021a) recommends the use of the Rational Equation to calculate flow. It is worth noting that this method requires a rainfall intensity, and depending on the source of this data, it may be prone to stationarity. In the case of bridge hydraulic analysis, the Drainage Manual (FDOT, 2021a) recommends that gauge data be used to determine the peak flow rates and provide the starting water surface elevations. Gauge data is also recommended to provide boundary conditions for bridge models.

2.3. Other Sources of Climate Data and Projections

2.3.1. Rainfall Data from Downscaled Climate Model Outputs

A possible way of incorporating nonstationarity into rainfall estimates is using rainfall data from downscaled climate model estimates. Global Climate Models (GCMs) are one of the best available tools to predict atmospheric variables under future climate scenarios (GHG emissions, land-use, energy production, global and regional economy, and population growth) (Srivastav et al., 2015). The World Climate Research Programme's (WCRP's) Coupled Model Intercomparison Project (CMIP) has produced high-quality GCMs like the CMIP3 and CMIP5, which have been widely applied in climate studies. More recently, they have developed the CMIP6.

The Intergovernmental Panel on Climate Change defined four scenarios called Representative Concentration Pathways (RCPs): RCP2.6, RCP4.5, RCP6.0, and RCP8.5. The number in the RCP is the end of the century radiative forcing (in watts per square meter, representing the GHG effect in the atmosphere). RCP2.6 is the pathway necessary to keep the global temperature increase

below 2°C, whereas RCP8.5, which represents the highest concentration scenario, assumes a strong dependence on fossil fuels. RCP4.5 and RCP6.0 are in-between moderate-low and moderate-high scenarios.

GCM outputs need to be downscaled before application to represent local-scale processes. There are two types of commonly applied downscaling methods: 1) dynamical – a physically-based method using computational cells much smaller than the GCM, or 2) statistical – a statistically-based method of developing relationships between observed data and hindcast GCM output. Statistically downscaled methods are more flexible, require less computational resources, and have been found to match observations better than dynamical downscaling methods; hence, they are more popular. However, they are highly dependent on observational records. More recently, there have been data products developed from hybrid techniques to overcome the limitations of each.

There have been many applications of using statistically downscaled GCM data to predict extreme rainfall due to climate change. SLSC-FIU (2021), leveraging an ongoing USGS study by Irizarry-Ortiz and Stamm (2021), applied statistically downscaled rainfall products to update statewide extreme rainfall projections for the state of Florida. Rainfall durations of 1, 3, 7, and 10 days were considered along with return periods of 5, 10, 25, 50, 100, and 200 years. Change factors to update the DDF curves were generated for two future periods of analysis, 2030-2069 and 2060-2099 using a baseline period of 1966-2005. The following list presents statistically downscaled products commonly applied in extreme rainfall studies:

1. Coordinated Regional Climate Downscaling Experiment (CORDEX)

The Coordinated Regional Climate Downscaling Experiment (CORDEX) uses boundary conditions from the GCM simulations from the CMIP5 as boundary conditions to derive outputs from Regional Climate Models (RCMs). Results for most of North America are available at North American CORDEX (NA-CORDEX) at spatial resolutions of 0.22° (25 km) or 0.44° (50 km) from 1950-2100 under different Representative Concentration Pathways (RCPs) which are future greenhouse gas scenarios.

2. Localized Constructed Analogues (LOCA)

The Localized Constructed Analogues (LOCA) method constructs the downscaled field using a single analog day (from a pool of 30 days) that best matches weather in the local region around the point being considered. The best matching observed day is scaled to match the amplitude of the modeled day being downscaled (additively for precipitation) and produce the final downscaled value (Pierce et al., 2014). The LOCA dataset covers North America from central Mexico through southern Canada at a 1/16th degree spatial resolution.

3. Multivariate Adaptive Constructed Analogs (MACA)

The Multivariate Adaptive Constructed Analogs (MACA) method identifies the 30 best matching analog days in the historical occurrence and combines these analog days, using

a weighted average method, to reproduce the target pattern (Abatzoglu and Brown, 2012; Pierce et al., 2014). The datasets cover the contiguous United States.

The USDOT developed the CMIP Climate Data Processing Tool for downloading and processing downscaled climate projections from the Downscaled CMIP3 and CMIP5 Climate and Hydrology Projections (DCHP) website (USDOT, 2015). This tool was produced to assist transportation agencies in assessing vulnerabilities and evaluating adaptation strategies. The tool is capable of processing raw GCM output to produce relevant projections for transportation planners. Climate projections from three downscaling techniques are made available on the DCHP website: 1) monthly bias-corrected spatial disaggregation (BCSD), 2) daily bias-corrected constructed analog (BCCA), and 3) daily LOCA.

2.3.2. Sea Level Projections

FDOT has proposed the use of NOAA (2017) sea level rise projections (same as Sweet et al., 2017) for planning. For the Fifth National Climate Assessment under development, NOAA, NASA, and other federal agencies are also updating the sea level projections, which have been released recently. Based on NOAA (2017) report (same as Sweet et al., 2017), several regional institutions and agencies in Florida have developed regional sea level projections for local/regional applications. Some of them are summarized below.

The Unified Sea Level Rise Projection for Southeast Florida was prepared by the Southeast Florida Regional Climate Change Compact's Sea Level Rise Ad Hoc work group, which is a team of experts from the academic community and federal agencies. The objective of the Work Group was to develop a unified regional sea level rise projection, using existing projections at local, regional, and global scales, and scientific literature. After its first report was released in 2011, the work group reconvened in 2014 and again in 2019 to provide updated projections. In the 2019 report, which includes the NOAA (2017) report (same as Sweet et al., 2017) and the IPCC (2014) report, the work group recommends using the NOAA high curve, the NOAA intermediate high curve, and the median of the IPCC AR5 RCP8.5 scenario for the regional sea level rise projections for 2040, 2070, and 2120, planning horizons (Figure 2-1). If the projects involve critical infrastructure with design lives exceeding 50 years, the NOAA high curve with 54 inches of mean SLR in 2070 and 136 inches of mean SLR in 2120 is recommended. For most other infrastructure projects before 2070, the IPCC lower, blue-shaded region is recommended.

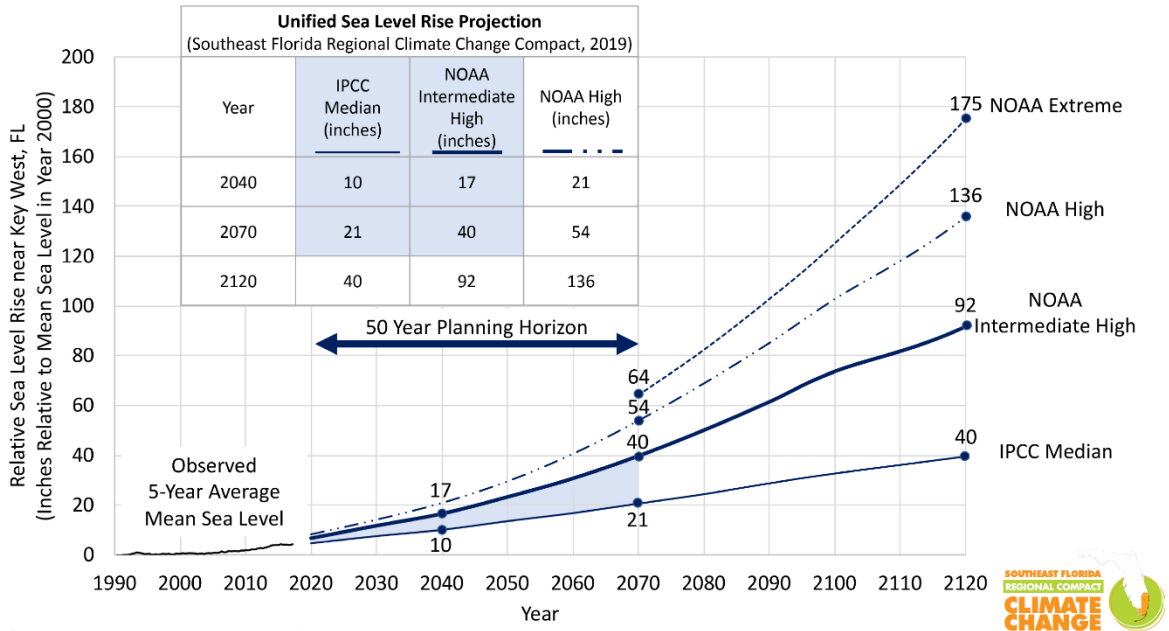


Figure 2-1. The 2019 Unified Sea Level Rise Projections for Southeast Florida. Source: SEFRCC (2019).

The Tampa Bay Climate Science Advisory Panel (CSAP), a network of scientists and resource managers working in the Tampa region, collaboratively produced science-based recommendations to aid local governments and agencies in adapting to climate change and sea level rise. For data collection, the CSAP recommends using the St. Petersburg tide gauge to adjust the first two parameters required to predict SLR, as it has the longest reliable record for the region. The final parameter may be derived from SLR projections from the IPCC or the U.S. National Climate Assessment. Despite the differences in models, both methods have similar estimates of SLR. The CSAP recommends using the NOAA Intermediate-Low as the lowest plausible bound and the NOAA High as the upper bound for sea level change until the science on new instability mechanisms in the ice sheet processes is settled (Figure 2-2). The CSAP strongly recommends against the use of the NOAA Low scenario for planning. All local governments and agencies are also advised to use RCP8.5 to assess the likelihood of SLR scenarios until meaningful efforts to reduce GHGs are implemented.

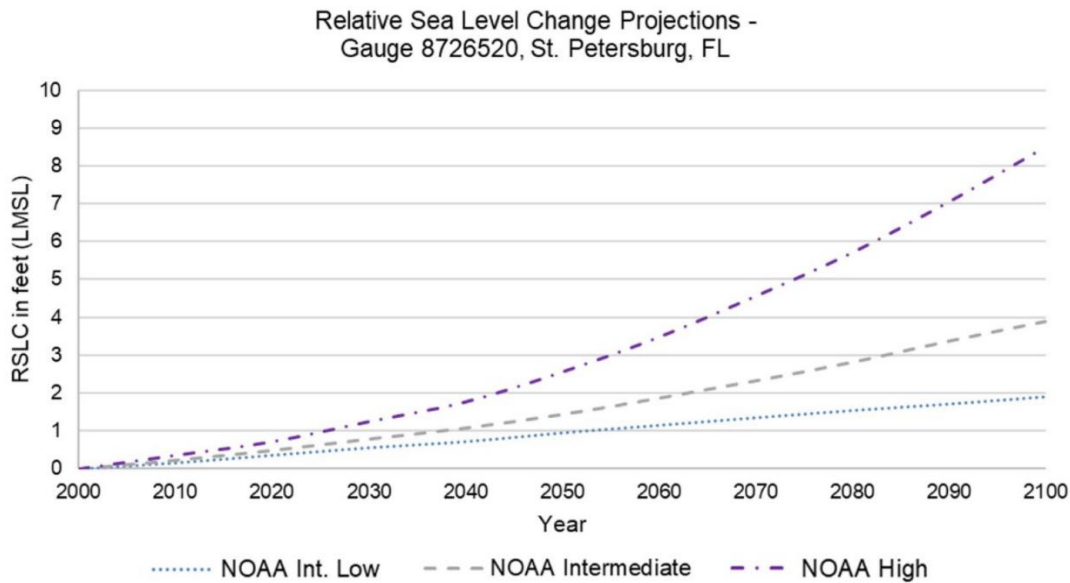


Figure 2-2. Sea level rise scenarios for St. Petersburg, Florida from NOAA (2017) recommended for the Tampa Bay Region. Source: CSAP (2019)

2.4. Nonstationarity in Transportation Planning

A nonstationary system is a system that changes temporally; hence, patterns or trends of the past cannot be used directly to predict a future state. Hydrology, specifically, is reliant on historical measurements of flow, rainfall, and watershed characteristics to define future systems and develop design criteria; however, nonstationarity adds additional sources of uncertainty (beyond measurement uncertainty) and its incorporation would limit the use of historical records. The main sources of nonstationarity in hydrology are changes in climate and land use.

2.4.1. Review of FHWA Hydraulic Engineering Circulars (HECs) Incorporating Nonstationarity in Transportation Planning

For this review, two other relevant documents were included, reviewed, and referenced when necessary:

1. Hydraulic Engineering Circular No. 17 Highways in the River Environment – Floodplains, Extreme Events, Risk, and Resilience. Publication No. FHWA-HIF-16-018. (FHWA, 2016)
2. Hydraulic Engineering Circular No. 25 Highways in the Coastal Environment. Publication No. FHWA-HIF-19-059 (FHWA, 2020)

FHWA (2016) is a technical guidance manual for assessing riverine highways for floods, floodplain policies, extreme events, climate change, risks, and resilience. The manual was reviewed to identify relevant methods and data for quantifying exposure to extreme floods considering sources of nonstationarity, primarily focusing on climate change and land use/land cover change.

FHWA (2016) defines nonstationarity as:

- A significant and lasting shift in the statistical distribution of weather patterns around the average conditions;
- A significant shift in the measures of climate lasting an extended period of time, and
- A non-random shift in climate that is measured over several decades or longer. The change may result from natural or human-induced causes.

FHWA (2016) presents a review of literature that analyzed trends in precipitation and flood frequency along with the data and methods used for each. A more detailed explanation of some methods of detecting nonstationarity in flood data for gradual trends (like the Mann-Kendall test) and abrupt changes (like the Pettitt test) is also presented. The manual also provides several approaches for adjusting nonstationary data, if nonstationarity is detected. The adjustments include adjustment to urbanization, ensuring homogeneity by using subsets of data, and statistical adjustment to the mean (McCuen et al., 2002; Sauer et al., (1983); Salas and Obeysekera, 2014). Some strategies for projecting flood frequency using rainfall/runoff modeling and statistical methods are briefly introduced.

Chapter 5 of the FHWA (2016) presents an excellent overview of climate modeling including descriptions of global climate models (GCMs), regional climate models (RCMs), emission scenarios, and downscaling techniques. Some sources of data include:

- Downscaled CMIP3 and CMIP5 Climate and Hydrology Predictions (DCHP) (https://gdo-dcp.ucllnl.org/downscaled_cmip_projections/dcpInterface.html#Welcome)
- USGS Geo Data Portal (<https://cida.usgs.gov/gdp/>)
- Coordinated Regional Climate Downscaling Experiment (CORDEX) – (<https://na-cordex.org/>) Presented in Section 2.3.1
- North American Regional Climate Change Assessment Program (NARCCAP)

Due to the evolutionary nature of climate science, the FHWA recommends getting expertise from various organizations. A list of tools for climate change adaptation is also presented. Some of these tools like the Guide to Criticality in Transportation Adaptation Planning and the Vulnerability Assessment Scoring Tool will be discussed in the following sections of this report (Section 3.2.1)

FHWA (2016) also presents a risk and vulnerability assessment framework for transportation infrastructure in the riverine environment in Chapter 7. This framework was created with the best available science and methods at the time, and it is meant to be an evolving with new data and tools. The purpose of this framework is to support state DOTs in their consideration of “extreme events and climate change in the planning, design, implementation, and management of their transportation assets.”

The framework consists of multiple levels of analysis with the intention that ultimately designers will select the appropriate level based on risks evaluations (asset criticality, vulnerability, and cost) and the service life of the project. The five levels of analysis, as presented in the FHWA (2019), are as follows:

- Level 1 – Historical discharges. At level 1, the design team applies standard hydrologic design techniques based on historical data to estimate the design discharge. In addition, the design team qualitatively considers changes in the estimated design discharge based on possible future changes in land use and climate.
- Level 2 – Historical discharges/confidence limits. At level 2, the design team estimates the design discharge based on historical data and qualitatively considers future changes in land use and climate as in level 1. In addition, the design team quantitatively estimates a range of discharges (confidence limits) based on historical data to evaluate plan/project performance.
- Level 3 – Historical discharges/confidence limits with precipitation projections. At level 3, the design team performs all level 2 analyses and quantitatively estimates projected changes in precipitation for the project location. The design team evaluates the projected changes in precipitation to determine if a higher level of analysis is appropriate.
- Level 4 – Projected discharges/confidence limits. At level 4, the design team completes all level 3 analyses and develops projected land use and climate data, where feasible. The design team performs hydrologic modeling using the projected land use and climate data to estimate projected design discharges and confidence limits.
- Level 5 – Projected discharges/confidence limits with expanded evaluation. At level 5, the design team performs the equivalent of the level 4 analyses based on custom projections of land use and climate. The design team also expands to include appropriate expertise in climate science and/or land use planning to secure site-specific custom projections.

Based on the levels of analysis, the types of tools (Table 2-1), data (Table 2-2), and service lives (Table 2-3) of the projects may differ. This framework is intended only as a guidance, it is ultimately the responsibility of the design team to select the required level of analysis, techniques, and data. The proposed framework is intended to be versatile and not limited to specific structures. The guidance presented here will be further explored in the subsequent tasks of this project.

Table 2-1. Tools required for each level of analysis.

Class	Tool	Level 1	Level 2	Level 3	Level 4	Level 5
Rainfall/Runoff	Rational	X	X			
	NRCS Graphical Peak	X	X	X	X	
	Unit Hydrograph	X	X	X	X	X
	Continuous Simulation	X	X	X	X	X
	Advanced Models					X
Statistical	Gaged Discharge Data	X	X			
	Gaged Discharge Data (with trend)		X			
	Regional Regression*	X	X	X	X	X
Other	Programmatic Tools	X	X	X	X	X
	Trend Analysis		X	X	X	X
	Confidence Limits		X	X	X	X
	Comparison of Historical and Projected Precipitation			X	X	X
	Resilience Assessment (Qualitative)	X				
	Resilience Assessment (Quantitative)		X	X	X	X

*Regional regression equations may not be available for levels 4 and 5.

Table 2-2. Data required for each level of analysis.

Period	Data	Level 1	Level 2	Level 3	Level 4	Level 5
Historical	Precipitation (D = 24-h)	X	X	X	X	X
	Precipitation (1-h < D < 24-h)	X	X			
	Precipitation (D < 1-h)	X	X			
	Temperature (mean winter)				X	X
	Discharge (annual peak)	X	X	X	X	X
	Land Use/Land Cover	X	X	X	X	X
Projected	Programmatic Information	X	X	X	X	X
	Precipitation (D = 24-h)			X	X	X
	Precipitation (1-h < D < 24-h)				X	X
	Temperature (mean winter)				X	X
	Land Use/Land Cover				X	X

Table 2-3. The service life of projects with levels of analysis.

Service Life	Level 1	Level 2	Level 3	Level 4	Level 5
Less than 30 years	X	X	X	X	
30 to 75 years	X	X	X	X	X
More than 75 years			X	X	X

The 3rd edition of the Hydraulic Engineering Circular No. 25 (FHWA, 2020), entitled “Highways in the Coastal Environment,” is a technical guidance manual for highways in the coastal environment, to integrate coastal engineering principles and practices in the planning and design of highways to make them more resilient. The manual provides modeling and engineering tools for the planning, design, and operation of coastal highways. It also presents engineering approaches for integrating climate change and sea level rise into highway design. FHWA (2020) was reviewed to identify methods and data that are recommended for incorporating the implications of climate change. The focus of this review was on how water levels, storm surge, and waves need to incorporate implications of climate change, particularly sea levels, in engineering designs. Another topic of interest is the potential interaction of coastal storm surge and rainfall-induced runoff from watersheds near the coast. This is one of the potential cases of compound flooding which is expected to be addressed in a future project.

The manual presents the foundational concepts in sea level rise including an overview of the terminology (RSLR – relative sea level rise, GMSLR- global mean sea level rise), causes for sea level rise, and sources of historical data (NOAA tide gauges, satellite data, geologic record). Two broad types of sea level rise projections are presented:

- Process-based, scientific estimates of the physical processes controlling sea level rise
- Scenarios for planning that are based on the range of scientifically possible sea levels

The first is developed for each of the IPCC’s Representative Concentration Pathways (RCPs) which are based on future population growth, technological advancement, and societal responses. Figure 2-3 presents an example of process-based sea level projections developed for three RCP scenarios: 1) RCP8.5 (high emissions scenario), 2) RCP4.5 (intermediate emissions scenario), and 3) RCP2.6 (low emissions scenario). The shaded areas show 90% confidence while the dark blue line shows the median projection. The sixth assessment report of IPCC (AR6) uses a different definition of emission scenarios known as Shared Socioeconomic Pathways (SSPs).

The second type of sea level rise projection is based on the scenario approach. This approach overcomes the challenge of uncertainty ranges of the process-based approaches and is commonly used in planning. Using the same process-based approach, RSLR projections are developed for six GMSLR scenarios (0.3, 0.5, 1.0, 1.5, 2.0, and 2.5 meters of GMSLR named Low, Intermediate Low, Intermediate, Intermediate-High, High, and Extreme) with arbitrary half-meter increments. Figure 2-4 presents a comparison of GMSLR scenarios by Sweet et al. (2017) with process-based projections by Kopp et al., (2014). The HEC-25 manual (FHWA, 2020)

recommends using the site-specific RSLR estimates from the Sea Level Rise Interagency Task Force to evaluate scenario-based data for transportation projects. The three considerations for SLR values aligned with the National Cooperative Highway Research Program (NCHRP) 15-61 report (Kilgore et al., 2019a) are also presented and discussed in this HEC-25 manual (FHWA, 2020), they are:

1. Include future RSLR projections in planning and design.
2. Use minimum projections of RSLR throughout the remainder of this century, corresponding to design.
3. Encourage engineers to be aware of the uncertainty in future RSLR projections and account for it appropriately in design. To illustrate, consider higher projections of RSLR when overall project performance is very sensitive (i.e. fragile) to design sea levels and/or when designing long-lived or expensive infrastructure.

The HEC-25 manual (FHWA, 2020) also presents the concepts of the astronomical tides also called “semidiurnal” tides. A good overview of the characteristics of astronomical tides, tidal and survey datums, along with the common terminology (mean high water – MHW, mean higher high water – MHHW, mean low water – MLW, and mean lower low water – MLLW) are presented (Figure 2-5).

Chapter 4 of the HEC-25 manual (FHWA, 2020) also presents information on storm surges, their characteristics (magnitude, duration, hydrograph), and storm surge modeling (concepts, techniques, and models). In addition, Webb (2017) is recommended as a good introductory resource in coastal hydrodynamic modeling for transportation engineers. The Advanced CIRCulation (ADCIRC) model developed by the USACE is discussed in detail. In addition, the manual provides additional numerical coastal models (Table 2-4).

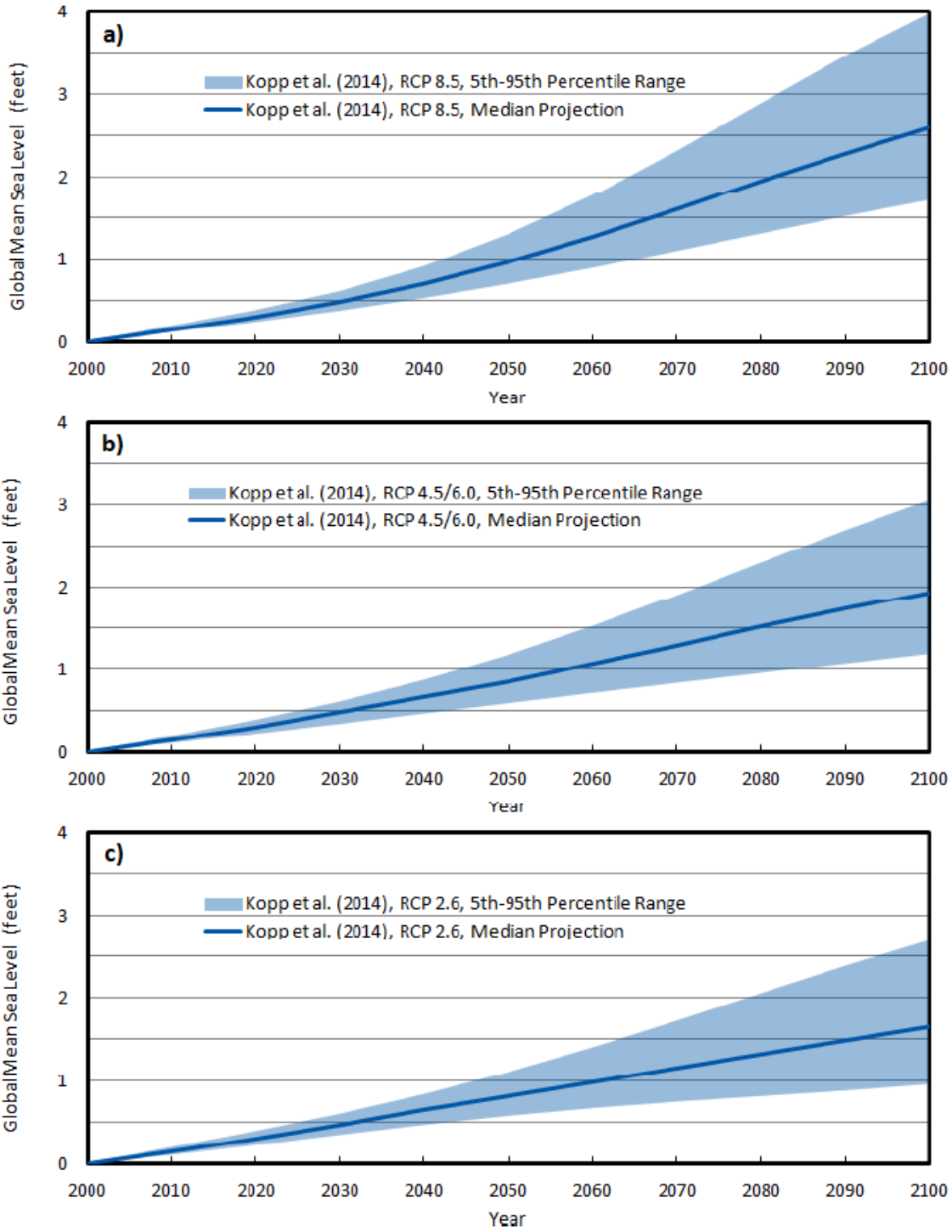


Figure 2-3. Projections of GMSLR in this century from Kopp et al. (2014) for (a) RCP8.5, (b) RCP4.5, and (c) RCP2.6. Source: FHWA (2020).

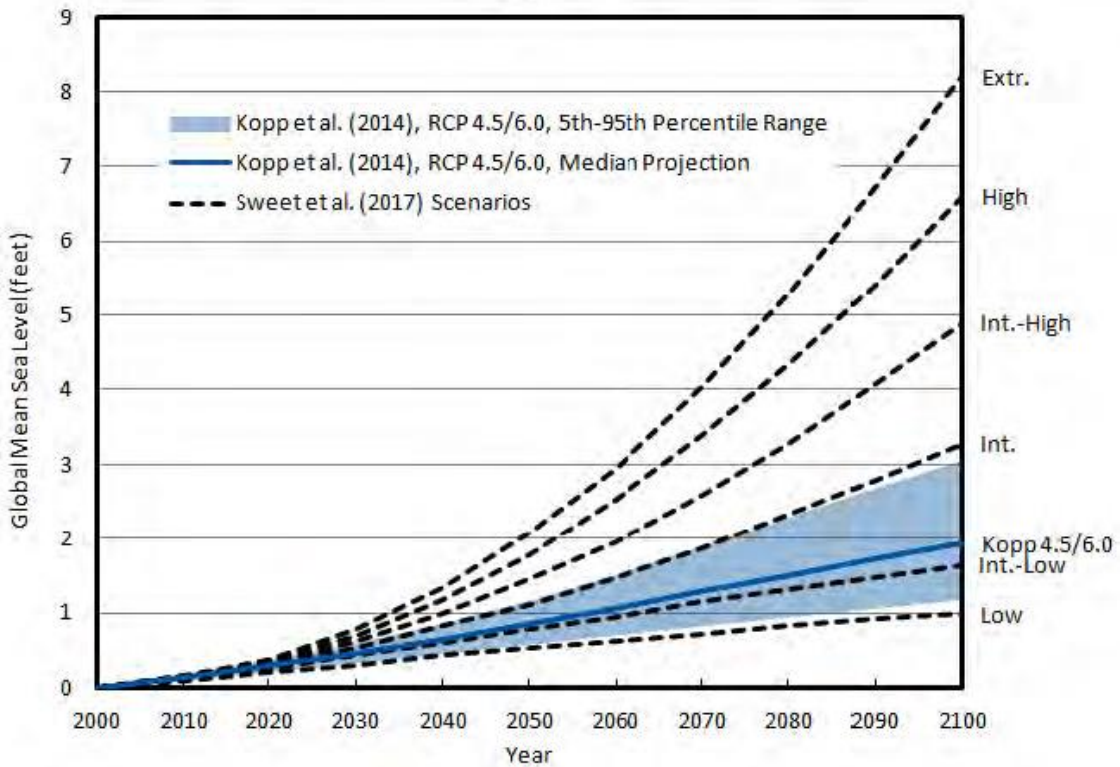
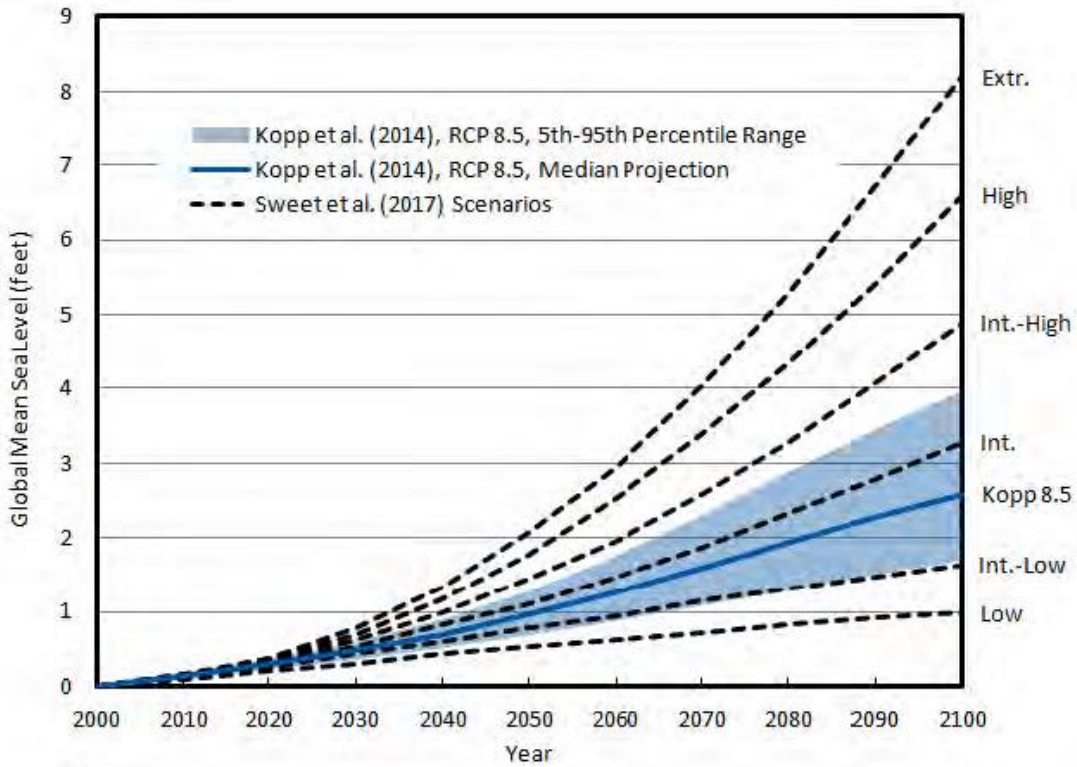


Figure 2-4. GMSLR scenarios (Sweet et al. 2017) and process-based scenarios (Kopp et al., 2014). Source: FHWA (2020).

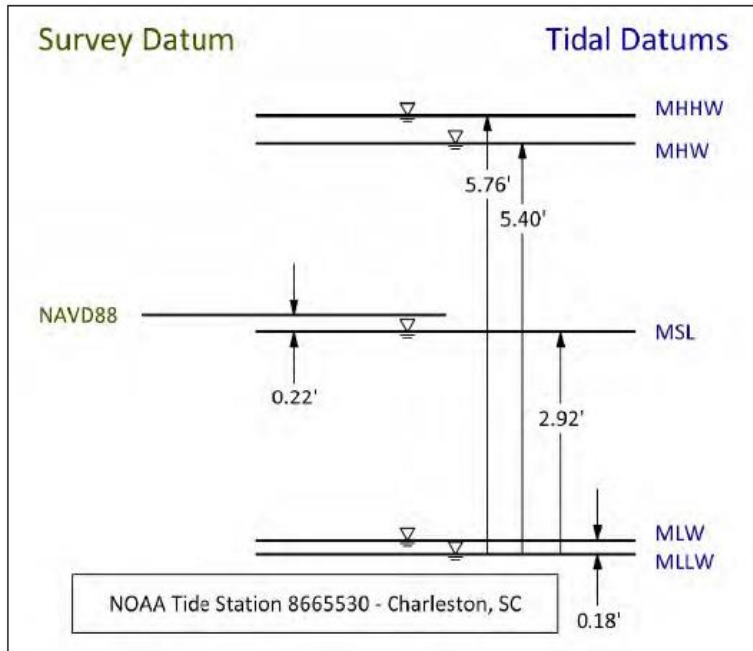


Figure 2-5. The relationship between survey and tidal datums. Source: FHWA (2020).

Table 2-4. Numerical coastal models cited in the HEC-25 manual. Source: FHWA (2020).

Model/Program	Comments
ADCIRC	Hydrodynamic model (often used to model storm surge)
SLOSH	Storm surge model
ET-SURGE	Storm surge forecasting model
DELFT-3D	Hydrodynamics, waves, and morphology model
MIKE-21	Hydrodynamics, waves, and morphology model
FVCOM	Hydrodynamic model
WAM	Wave model
STWAVE	Wave model
CMS	Hydrodynamics, waves, and morphology model
SWAN	Wave model
CH3D	Hydrodynamic model
EDUNE	Dune erosion model
SBEACH	Cross-shore morphology model
XBEACH	Hydrodynamics, waves, and morphology model
CSHORE	Cross-shore wave and morphology model
CHAMPS	Cross-shore wave and morphology model

2.4.2. Review of NCHRP Reports Incorporating Nonstationarity

This review included two other important draft publications that include important information and guidance for incorporating climate change into the planning and design of transportation Infrastructure (TI). They are:

1. *Applying Climate Change Information to Hydrologic and Coastal Design of Transportation Infrastructure* (Final Report, NCHRP Project 15-61, 384 pages, Kilgore et al., 2019a), and
2. *Design Practices* accompanying the above final report (145 pages, Kilgore et al., 2019b)

Both reports were prepared for the National Cooperative Highway Research Program of the Transportation Research Board (TRB) by a group of consultants. They cite methods and procedures of other guidance documents, FHWA (2016) and FHWA (2020), relevant to this literature review. The following sections provide a very brief summary of extensive guidance provided in the Design Practices (henceforth known as the “Guide”).

2.4.2.1. Design Practices

Both of the above reports recognize the current practice based on “stationarity”, in which the planners and engineers assume historical data to represent future conditions. Such an approach may not be prudent because of new and evolving risks such as sea level rise, temperature increase, and changes in precipitation patterns. The basis for suggested guidance to account for climate change is the potential “failure” of TI due to changing risks and compromises in operational characteristics associated with such evolving risks. The new paradigm proposed in the Guide may be characterized as “nonstationary.” The Guide provides a comprehensive framework for incorporating climate change into (a) inland hydrology, and (b) coastal analyses, when appropriate.

The Guide recognizes that, depending on costs, risks, and vulnerability, not all projects may require the same attention and introduces the concept of “levels of analysis” and provides two frameworks for planning and design of TI which are based on (a) traditional (top-down) and (b) threshold approaches. The traditional approach is deemed to be the dominant practice in the design of TI today whereas the threshold approach is becoming increasingly popular when uncertainties due to climate change are important. The Guide also recognizes another important concept, “regret.” One regret is underinvestment in TI to prepare for climate change whereas another regret is associated with the overinvestment of resources that may otherwise be used elsewhere. Because of large uncertainties in climate change outcomes, minimizing regrets may not be feasible, but it can be managed using the threshold approach which is also similar to the Dynamic Adaptive Policy Pathways (DAPP).

The concept of the levels of analysis for both inland hydrology and coastal projects is illustrated in Figure 2-6 and Table 2-5 and Table 2-6. The appropriate level of analysis depends on a variety of factors: (a) the criticality of the project; (b) expected service life; (c) the vulnerability to climate

change, (d) the functional classification (roadway, bridge, or tunnel), (e) regulatory requirements; and (e) resources available for the project.

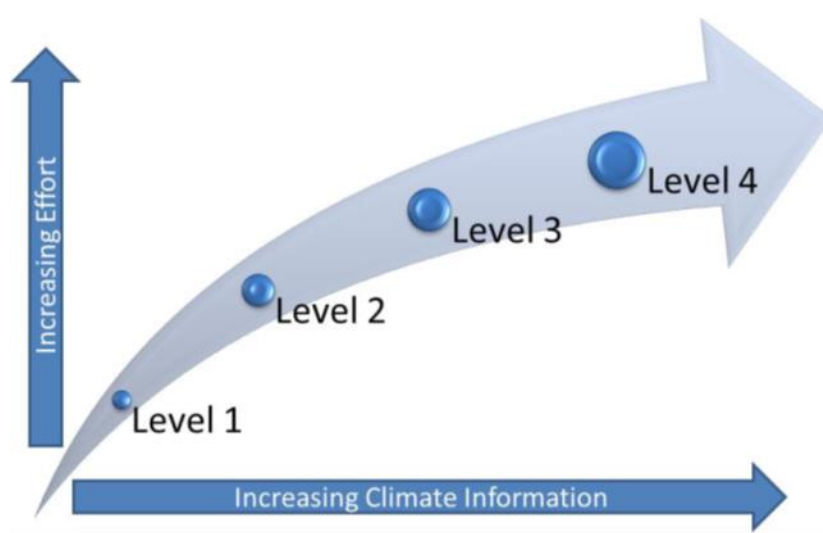


Figure 2-6. Levels of analysis (Kilgore et al., 2019b).

Table 2-5. Level of analysis for inland hydrology.

Level	General Approach
Level 1	Design based on historical data
Level 2	Design based on historical data/confidence limits
Level 3	Design based on projected information/confidence limits
Level 4	Design based on projected information/confidence limits/custom evaluation

Table 2-6. Level of analysis for coastal applications.

Level	General Approach
Level 1	Use of existing data and resources
Level 2	Original modeling of storm surge and waves
Level 3	Modeling in a probabilistic risk framework

Because of uncertainties associated with climate change in inland hydrology and coastal analyses, planners and designers are often challenged by the Traditional Approach. Increasingly, they favor the use of the Threshold Approach (bottom-up) as the decision-making framework. In such an approach, the objective is to assess vulnerabilities and seek robust solutions in an attempt to

minimize the aforementioned regrets. In this paradigm, fundamental questions are “how does my system work?” and/or “under what circumstances it may fail?”

The selection of a particular decision framework (Traditional vs Threshold) depends on the project context and adaptability. Factors that contribute to this selection, generally are on a continuum as shown in Figure 2-7. If a TI project is new with fixed design criteria, then the Traditional Approach is preferred. However, if the goal is to explore options for enhancing an existing or a new system by considering vulnerabilities due to climate change, then the Threshold Approach is valuable.

2.4.2.2. Inland Hydrology

In an environment of a changing climate, historical observations will become less representative of the future conditions that will be experienced during the lifetime of TI. The nonstationary approach proposed in the Guide suggests the combination of historical data with the projected climate for the future. The General Circulation Models (GCMs) typically used for projecting future climate scenarios are too coarse for most TI applications and their outputs are commonly downscaled to higher spatial and temporal resolutions using one of two approaches: (a) Regional Climate Models (RCM) which are similar to GCMs but designed particularly for regional/local climatological processes, and (b) Empirical-Statistical downscaling Models (ESDMs). Both provide projections that quantify the future change of climate variability and extremes under multiple future scenarios for mimicking a range of possibilities over a future period. The GCM outputs are provided by the Coupled Model Intercomparison Project (CMIP) archives. Currently, the commonly used generations of CMIPs are CMIP3 and CMIP5 (see Table 2-7). The CMIP6 class of datasets is just becoming available. As CMIP6 is new, the Guide does not provide any options for using them. Some downscaled products like LOCA are now available for CMIP6. The CMIP6 climate scenarios are presented in Table 2-7.

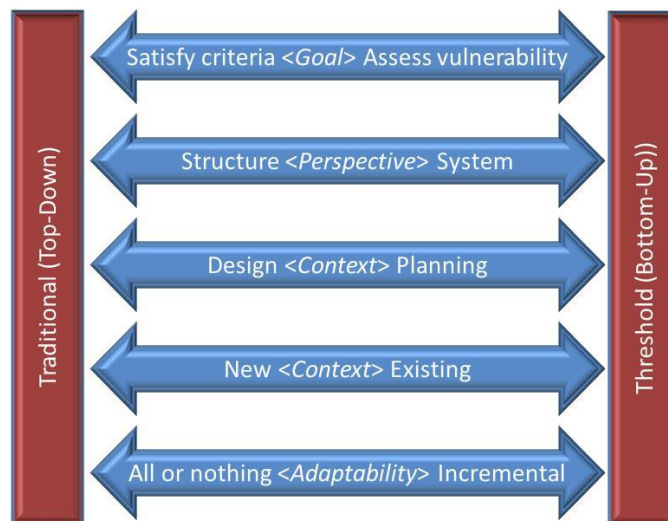


Figure 2-7. Considerations for choosing a decision-making framework (Kilgore et al., 2019b).

Table 2-7. Climate scenario classification from CMIP3, CMIP5 and CMIP6.

CMIP	Higher	Mid-High	Lower	Even Lower
CMIP3	SRES A1F1	SRES A2	SRES B1	N/A
CMIP5	RCP8.5	RCP6.0	RCP4.5	RCP2.6
CMIP6	SSP585	SSP370	SSP245	N/A

The Guide recommends that, if the project service life is 30 years or less, then the selection of future climate scenarios is not critical because the spread of climate realizations during the next several decades is not large. However, if it is greater than 30 years, the scenario selection may be critical but at a minimum, one lower and one higher scenario should be considered. For projects requiring site-specific precipitation and/or temperature, ESDM datasets are appropriate; however, if they require multiple climate variables, or if they are in a region with sparse historical data, then an RCM is preferred. After considering eight different high-resolution gridded climate model outputs, the Guide recommends the four datasets shown in Table 2-8.

Table 2-8. Four recommended high-resolution datasets of temperature and projections (Kilgore et al. 2019b)

Characteristic	ESDM Datasets		RCM Datasets	
	ARRM	LOCA	NARCCAP	NA-CORDEX
CMIP Generation	CMIP3	CMIP5	CMIP3	CMIP5
Future Scenarios	A1FI, A2, A1B, B1	RCP4.5, RCP8.5	A2	RCP4.5, RCP8.5
Time Period of Output	1960-2099	1950-2100	1968-2000, 2038-2070	1950-2100
Time Frequency	Daily	Daily	3-hourly	Daily
Spatial Resolution	1/8 th degree (~12 km)	1/16 th degree (~6 km)	50 km	25-50 km
Obs. Training Dataset	Maurer ¹	Livneh ²	not applicable	not applicable
Number of GCMs	16	30	4	6
Number of Group 1 GCMs	13	14	3	0
Number of RCMs	not applicable	not applicable	8	6

¹ USBR. (2013).

² Livneh et al. (2013).

For the TI design to be robust, the Guide recommends the use of multiple GCMs for analysis. Further recommendations include prioritization of what is known as “Group 1 GCMs” shown in Table 2-9. For LOCA data, the use of both lower (RCP4.5) and higher (RCP8.5) is recommended. For inland projects, future conditions design flows using hydrologic models should be based on the range of plausible values estimated using multiple scenarios separately.

2.4.2.2.1. Precipitation Extremes: Climate Change Indicator

The HEC-17 guidance document (FHWA 2016) provides a simpler approach for incorporating the projected change in 24-hour precipitation that may be useful for all levels of analyses mentioned above. A measure known as the Climate Change Indicator (CCI) is defined for modifying the 24-hour, daily precipitation extreme for a given Annual Exceedance Probability (AEP), or equivalently the Return Period when the projected future change is large compared to the historical variability (Figure 2-8).

Table 2-9. Climate sensitivity of Group 1 models (Kilgore et al. 2019b).

CMIP	Low		Medium		High	
CMIP3	CCSM3	2.7°C	CGCM3.1 (T47)	3.4°C	IPSL-CM4	4.4°C
	GISS-EH	2.7°C	CGCM3.1 (T63)	3.4°C	MIROC3.2(hires)	4.3°C
	GISS-ER	2.7°C	CSIRO-Mk3.0	3.1°C	MIROC3.2(medres)	4.0°C
	INM-CM3.0	2.1°C	ECHAM5-MPI-OM	3.4°C	UKMO-HadGEM1	4.4°C
			GFDL-CM2.1	3.4°C		
			MRI-CGCM2.3.2	3.2°C		
			UKMO-HadCM3	3.3°C		
CMIP5	GISS-E2-H*	2.3°C	BCC-CSM1.1	2.8°C	CSIRO-Mk3.6.0*	4.1°C
	GISS-E2-H-CC	2.3°C	BCC-CSM1.1-m*	2.9°C	GFDL-CM3*	4.0°C
	GISS-E2-R*	2.1°C	CCSM4*	2.9°C	HadGEM2-A	4.6°C
	GISS-E2-R-CC	2.1°C	CNRM-CM5*	3.3°C	HadGEM2-CC*	4.6°C
	INM-CM4	2.1°C	CNRM-CM5-2	3.3°C	HadGEM2-AO*	4.6°C
	IPSL-CM5B-LR	2.6°C	GFDL-CM2.1	3.4°C	IPSL-CM5A-LR*	4.1°C
	MRI-CGCM3*	2.6°C	HadCM3	3.3°C		
			MIROC5*	2.7°C		

*Model simulation available from the Localized Constructed Analogs (LOCA) statistically downscaled dataset.

The CCI is defined as

$$CCI = \frac{P_{24,T,P} - P_{24,T,O}}{P_{24,T,O,U} - P_{24,T,O}}$$

Where, $P_{24,T,P}$ is the projected T-year, 24-hour precipitation, $P_{24,T,O}$ is the Observed T-year, 24-hour precipitation, and $P_{24,T,O,U}$ is the upper 90% confidence limit of T-year, 24-hour precipitation estimated from the observed data.

As a broad guideline, CCI values less than 0.4 suggest that the evaluation of a project based on the historical confidence limits in Level 2 will provide a reasonable basis (i.e. change associated with climate change is within the bounds of sampling variability). On the other hand, a CCI value greater than 0.8 suggests that further analysis of conditions due to climate change may be

warranted. In between these two limits, the required assessment may depend on other factors associated with the project.

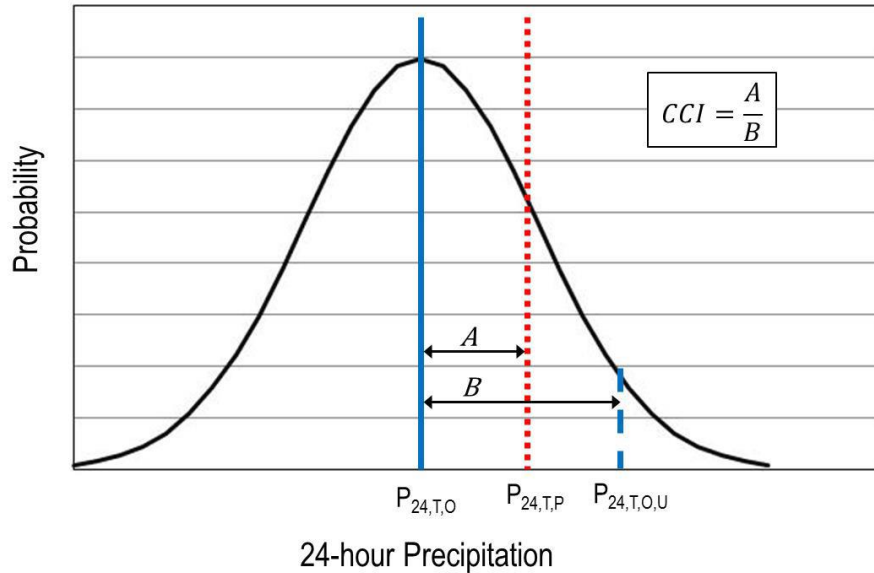


Figure 2-8. Definition of the climate change indicator (CCI) (FHWA, 2016).

2.4.2.2.2. Projections Based on Trends in Historical Discharges

When gauged records in a watershed are available, design flows are typically determined by fitting an appropriate probability distribution to the annual maxima or peaks over threshold discharges. However, in such applications, a fundamental assumption is that the data are homogeneous in time (i.e. stationary). One approach to incorporate nonstationarity when trends are present is to assume that the parameters of the probability distribution vary with time or as a function of another variable (e.g. land use). A simple form of nonstationarity is when only the mean of annual maximum discharges are varying with time. Such an approach requires several steps which may include: (a) estimate the time-varying mean and determine if the trend is statistically significant, (b) develop a hypothesis for the cause of the trend and if the extrapolation of such a trend is warranted, (c) fit a time-varying probabilistic model for the data; and (d) compute design flow quantiles. Depending on the trend, there may be a diminishing benefit to considering the variation of parameters other than the mean.

2.4.2.2.3. Projections Based on Future Precipitation and Rainfall/Runoff Models

Projecting future discharges, particularly in sparsely gauged watersheds, often requires the use of projected precipitation estimates and rainfall/runoff models, particularly when Levels 3 and 4 analyses are necessary. When only the 24-hour precipitation is adequate for estimating the discharge, the Guide provides a 10-step procedure for estimating future, 24-hour precipitation quantiles (Figure 2-9). This procedure includes two loops based on the number of future

scenarios and the number of downscaled GCM outputs that are appropriate for a particular project. As shown in Figure 2-9, steps 5 through 9 are repeated for each future scenario, and steps 5 and 6 are repeated for each GCM selected for the project. The computation of future precipitation is accomplished by using the following equations (in steps 8 and 9):

$$RFB_{q,n,m} = \frac{PF_{q,n,m}}{PB_{q,n,m}}$$

where $RFB_{q,n,m}$ is the Ratio of the future to baseline 24-hour precipitation quantile (q) for the grid (n) and model (m); $PF_{q,n,m}$ is the Future 24-hour precipitation quantile (q) for grid (n) and model (m); and $PB_{q,n,m}$ and Baseline 24-hour precipitation quantile (q).

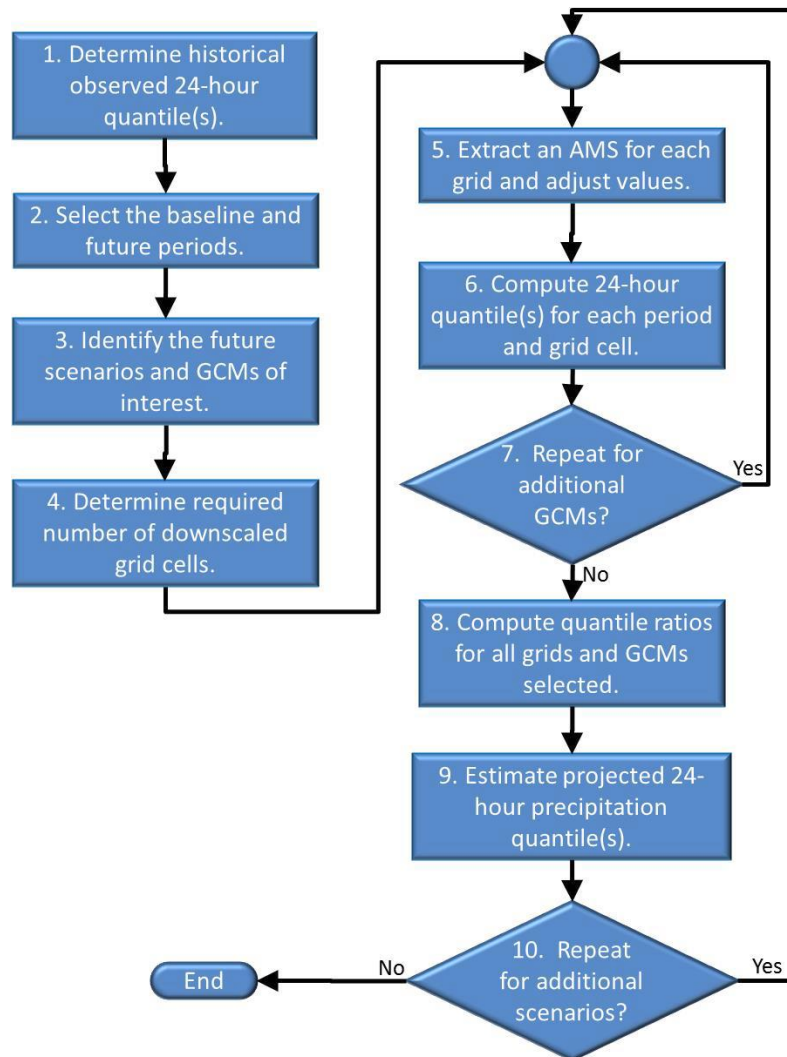


Figure 2-9. The recommended procedure for projecting 24-hour precipitation quantiles (Kilgore et al. 2019b).

The RFB values are then averaged to compute a mean ratio (RFB_q) for each quantile which in turn is used to compute the projected 24-hour precipitation quantile (q), $P_{q,p}$ as

$$P_{q,p} = P_{q,h}(RFB_q)$$

where $P_{q,h}$ is the Historical 24-hour precipitation quantile (q).

The Guide also provides several methods to convert the 24-hour quantiles to Sub-Daily, Precipitation, and the Intensity-Duration-Frequency (IDF) curves. They are (a) Linear scaling using historical IDF curves (Killgore et al., 2016), and (b) the Simonovic approach (Simonovic et al., 2016). When working with large watersheds, the point estimates of precipitation need to be adjusted by using appropriate Areal Reduction Factors (ARF).

2.4.2.3. Coastal Applications

In coastal environments, TI projects require consideration of two primary elements and they are (a) selection of appropriate sea level rise (SLR) estimates, and (b) estimation of potential hazards associated with SLR, combined with projected wave environment (Killgore et al. 2019b, FHWA 2020). The general steps for project assessment are:

1. Determine critical infrastructure elevations, performance/safety thresholds, or structure capacity;
2. Estimate Relative Sea Level Rise (RSLR) at the project site;
3. Estimate hazards associated with the water level and wave environment for the projected SLR; and
4. Compare the engineering demand (loads, scour, etc.) in Step 3 to the structure capacity defined in Step 1.

2.4.2.4. Selecting Sea Level Rise for Design

Selection of an appropriate SLR projection requires consideration of the following decision criteria:

1. Risk tolerance, system sensitivity, and redundancy
2. Policy choices (e.g. projection versus retreat)
3. Time Frame (e.g. short-term preparedness versus long-term planning).

The Guide and HEC-25 (FHWA 2020) specify minimum Global Mean Sea Level Rise projections for use in planning and design unless regionalized projections are available for the project. They are shown in Table 2-10.

Table 2-10. Recommended minimum GMSLR estimates for use in planning and design (Killgore et al. 2019b, FHWA 2020).

	Unit	2020	2030	2040	2050	2060	2070	2080	2090	2100
GMSLR (relative to MSL of 2000: mid- point of 1991- 2009)	m	0.08	0.12	0.18	0.23	0.29	0.36	0.43	0.51	0.59
	ft	0.26	0.41	0.58	0.76	0.96	1.18	1.42	1.67	1.94

The recommended minimum GMSLR projection is generally equal to or greater than the Intermediate-Low scenario of Sweet et al. (2017). The values in Table 13 were based on the assumption that projections that reach about 4 feet of GMSL this century are recommended as higher values to be considered for the planning and design of high-value assets which are sensitive to RSLR. They have been computed to match the 2000 to 2100 projected 95th percentile GMSLR value of 3.97 feet of Kopp et al., (2014) for RCP 8.5 (FHWA, 2020). There is a 95% chance that GMSLR will be less than the values in Table 6 even under the extreme scenario of RCP 8.5.

The Guide also provides a framework for considering GMSLR scenarios (Figure 2-10). It is based on the simple premise that, as the risk tolerance decreases, a more conservative SLR estimate should be considered. The types of TI may fall into three categories denoted as A through C.

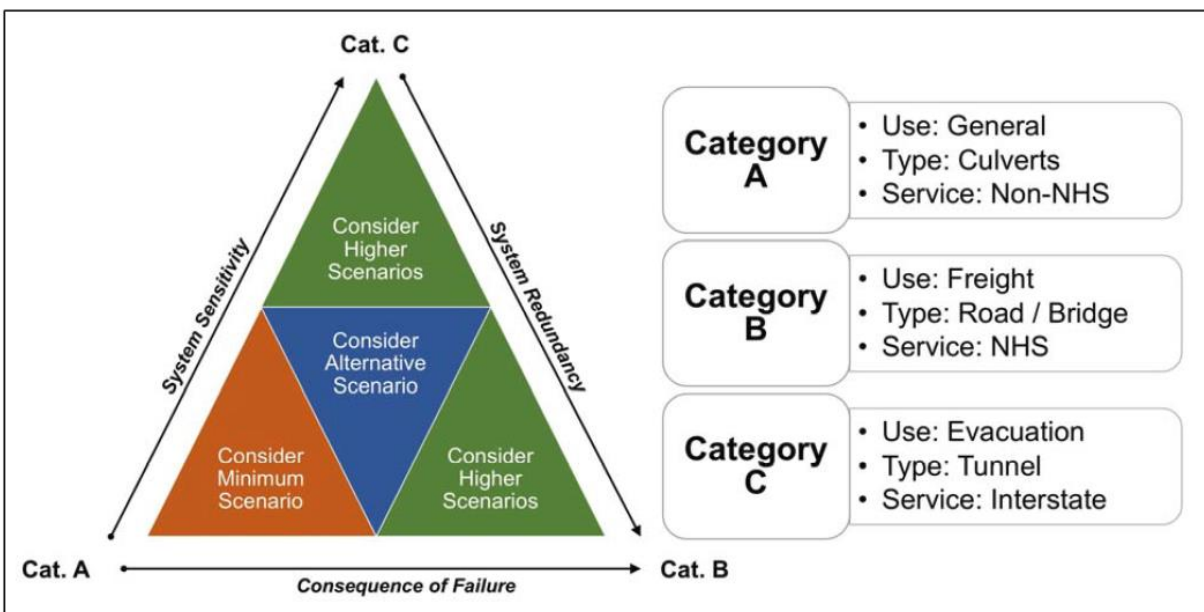


Figure 2-10. A suggested framework for considering GMSLR scenarios for design or planning. Arrows point in the direction of increasing sensitivity, redundancy, or consequence of failure (Kilgore et al. 2019b).

2.4.2.4.1. Combining Coastal Hazard and Climate Change

The transportation infrastructure is impacted by elevated water levels such as those due to storm surge, wave, and velocities. All of these are sensitive to the water depth at a location that increases with rising sea levels. Particularly for Level 2 and Level 3 analyses, coastal numerical models should be used for numerical simulation of the effects of RSLR (relative sea level rise) and increased water depth. Projects that are small, non-critical, and unaffected significantly by rising sea levels may not require such elaborate analyses.

The Guide provides a set of simplified equations for assessing the effect of sea level rise on coastal TI. It is noted that the procedures summarized below do not account for potential non-linear hydrodynamic effects attributable to RSLR.

In this simplified procedure, an estimate of the future flood elevation or flood depth due to a specified RSLR increase may be computed as

$$\eta_2 = \eta_1 + (AR) (SLR)$$

where η_2 is the flood elevation in the future, and η_1 is today's flood elevation, AR is the Application Ratio ($0.7 \leq AR \leq 1.5$), and SLR is the relative SLR increment of the selected scenario. The AR coefficient represents the effect of SLR on the increasing flood depth. Its range indicated above has been determined from hydrodynamic modeling results. For locations in coastal floodplains with a higher degree of non-linearity, a large value of AR is warranted, whereas for those in open locations where such effects are lower, the value of AR may be closer to 1.

Modification to wave heights to account for SLR is estimated by

$$H_2 = H_1 \left(\frac{d + \eta_2}{d + \eta_1} \right)$$

where H_2 is the future "zero moment" wave height, and H_1 is the same for the present, and d is the present water depth. The change in wave period due to SLR may be estimated as

$$T_2 = T_1 \sqrt{\frac{H_2}{H_1}}$$

where T_2 and T_1 are the future and present peak wave periods respectively. Water velocity decreases with SLR, unlike water level, wave height, and wave period. Modification to water velocity due to SLR may be estimated as

$$V_2 = V_1 \left(\frac{d + \eta_1}{d + \eta_2} \right)$$

where V_2 and V_1 are water velocities under future and present conditions respectively. The Guide provides a discussion of the assumptions and limitations of the above-simplified approach. It should be noted that the most comprehensive approach to simulate the potential effect of climate-change-related hazards is to use hydrodynamic models, particularly in Level 2 and Level 3 analyses as they capture the potential non-linear effects more accurately.

2.4.3. Detecting Nonstationarity

Before applying nonstationary methods, it is necessary to ensure that any apparent trend in data is not due to natural variability in a stationary environment. Changes resulting in nonstationarity may be abrupt like the construction or removal of dams on rivers, periodic variability like multi-year cycles of wet or dry periods, or a trend like increased impervious area through watershed development. Detecting nonstationarity requires the examination of all available data including paleoflood, historical information, and the most current records. Examining the full record can help identify useful representative records while preventing erroneous conclusions. Statistical analysis is commonly applied to historical data to identify gradual or abrupt changes.

Stationarity is assumed when statistical properties do not change over time. A more formal definition of a stationary stochastic process is one where the joint probability distribution of $X_{t_1}, X_{t_2}, \dots, X_{t_n}$ is the same as the joint distribution of $X_{t_1+m}, X_{t_2+m}, \dots, X_{t_n+m}$ for all values of m and n

(Nason 2006). A starting point of any time series modeling is to verify if the underlying time series is stationary (Douglas et al., 2000; Yue et al., 2012; Madsen et al., 2014). A simple plot of the time series may reveal quite a lot about possible nonstationarity in the data, and often, the focus is on the temporal variation in the mean and variance. Another useful technique is to compute the autocorrelation function or spectrum on two different parts of the given time series to investigate some evidence of nonstationarity. However, this generally requires that the sample data are of enough length. Often, a realization from a known stationary process may appear as nonstationary particularly if the process has temporal dependence, and for this reason, more formal statistical tests are desirable to determine the choice between stationarity and nonstationarity (Cohn and Lins, 2005).

In this section, commonly used tests for detecting statistically significant changes are described. For the situation of continuous changes, both parametric and nonparametric methods are described.

2.4.3.1. Trend Detection by Parametric Methods

Linear Model for Single Trends

Smooth changes with time are referred to as trends. The simplest type of change is a linear trend, which may be a continuous increase or decrease over time. In some cases, the continuous trend may depend on other variables besides time. If the temporal variation of the variable of interest is deemed to be linear, the starting point for modeling such a process is linear regression, and many textbooks and tutorials describe its application. An excellent textbook that covers the topic of linear models is by Draper and Smith (2014). Chapter 10 of this book also includes an extensive description of linear models. A summary of the theoretical concepts of linear models is presented in Appendix B.

2.4.3.2. Trend Detection by Nonparametric Methods

The parametric methods require certain distributional assumptions. More specifically, the data should be normally distributed, although other exceptions such as the presence of autocorrelation may be dealt with by special methods. However, many hydrologic time series are skewed, and they do not follow a normal distribution. Often, transforming the variables through such an approach as taking the log transformation may help to satisfy this requirement of normality. Thus, alternative methods are needed to detect nonstationarity, such as distribution-free nonparametric methods.

Shapiro-Wilk normality Test

The Shapiro-Wilk test is used to determine if a sample, X_i , $i = 1, 2, \dots, n$ is drawn from a normal distribution with the population mean, μ , and variance, σ^2 , respectively. Hypothesis testing is used to determine if the sample was drawn from a normal population (null hypothesis) versus a non-normal population. More information on the Shapiro-Wilk statistic is presented in Appendix B.

Trend Detection Using the Mann-Kendall and the Sen-Theil Regression Tests

One of the most common, nonparametric tests for detecting trends is the Mann-Kendall test (Mann, 1945; Kendall, 1938, 1976). This method for detecting trends is an improvement to the Ordinary Least Squares (OLS) regression method because of its ability to handle outliers and influential data. It is also a robust test that can detect non-linear monotonic trends in non-normally distributed data which may contain missing or censored data.

The Sen-Theil trend line (Theil, 1950; Sen, 1968) is the nonparametric alternative to linear regression that can be used in conjunction with the Mann-Kendall trend test. It assumes that residuals are statistically independent and that the relationship between the variables is linear. It can also handle missing and censored values.

2.5. Conclusions

The objective of Task 1 was to review FDOT manuals of practice to determine the changes that may be necessary to incorporate peer-reviewed research on nonstationarity into the manuals of practice. The following manuals were reviewed:

- FDOT Drainage Manual (FDOT 2021a)
- FDOT Drainage Design Guide (FDOT 2020a)
- FDOT Drainage Handbook – Drainage Connection Permits (FDOT 2020b)
- FDOT Structures Manual (FDOT 2022a)
- FDOT Soils and Foundations Handbook (FDOT 2021b)
- FDOT Flexible Pavement Design Manual (FDOT 2022b)
- FDOT Rigid Pavement Design Manual (FDOT 2022c)
- FDOT Pavement Type Selection Manual (FDOT 2019b)
- FDOT Manual of Uniform Minimum Standards for Design, Construction, and Maintenance for Streets and Highways (FDOT 2018)
- FDOT Project Development & Environment Manual (FDOT 2020c)
- FDOT Local Agency Program Manual (FDOT 2012)
- FDOT Utility Accommodation Manual (FDOT 2017)
- FDOT Utility Procedures Manual (FDOT 2021c)

The FDOT manuals were reviewed for the applications of climate data, their criteria, and the types of datasets typically used or recommended. Through the review, the research team identified three types of data: 1) rainfall, 2) sea level, and 3) peak discharge.

- **Rainfall data** is used in FDOT manuals for drainage design and calculations. Design storm frequencies are required in design calculations of open channels, storm drain systems, cross-drains, etc. Typically, these are obtained from DDF or IDF curves. FDOT recommends the use of NOAA Atlas 14 data for estimating design.
- **Sea Level data** is typically applied in FDOT designs for calculating tailwater elevation of tidally influenced storm drains, cross drains, coastal ponds, etc. FDOT manuals

recommend obtaining historical sea level data from NOAA's NWLON and tidal benchmarks from NOAA CO-OPS and FDEP LABINS. For assessing the vulnerability of flooding during the design life of infrastructure, FDOT Drainage Manual (FDOT, 2021a) and the FDOT Design Guide (2020) recommend using straight-line extrapolation of historical sea level data based on the design life of the project. An obvious drawback of this method is that it will not account for accelerating rates of sea level rise that have been recorded in recent decades.

- **Stream/canal discharge data** is used for the design and analysis of open channels, cross drains, and bridges. Typically, observations from gauge data are used to perform frequency analysis for open channels and cross drains. If gauge data is not available, either the USGS regional or local regressions equations may be used, or for drainage areas up to 600 acres, the rational equation may be used. In the case of bridge hydraulic analysis, gauge data can be used to determine the peak flow rates and provide starting water surface elevations or boundary conditions for bridge models.

Additionally, the team also investigated some popular datasets for incorporating nonstationarity. They were:

- Downscaled climate model data
- Sea level projections

The research team also conducted a review of FHWA and NCHRP manuals for methods of incorporating nonstationarity into the transportation planning process. Based on the review, the following were noted:

- For most projects, the NOAA Atlas 14 data is recommended (FHWA, 2016). Since most FDOT projects have a design life of 75 years or less, this would influence the level of analysis that is required for considering nonstationarity.
- FHWA (2016) recommends the use of downscaled climate data for projects with a level of analysis of 4 or higher, according to FHWA (2016).
- For sea level, FHWA (2020) recommends a procedure for calculating RSLR from GMSLR estimates and tide gauge data.
- The FHWA (2016) recommends deriving flood frequency curves directly from the gauge data.
- The NCHRP Design Practices guide (Kilgore et al., 2019a) describes two methods for incorporating nonstationarity: (a) trend estimation using historical discharges, including the use of PeakFQ and the USACE tool for trend detection; and (b) using time-varying parameters for statistical distribution.

The following task will look into how some of the data, methods, projections, and scenarios will be considered in the next task of this project.

3. NEW PARADIGM AND METHODS FOR TRANSPORTATION SYSTEM PLANNING AND DESIGN USING NONSTATIONARY PRINCIPLES

3.1. Task Objective

This task includes three subtasks:

- a. Development of datasets and methods for detecting nonstationarity (Sections 3.3 & 3.4);
- b. Defining a new paradigm for defining concepts of the return period, risk, and uncertainty under nonstationarity (Section 3.5); and
- c. Development of new methods for specific environmental drivers (Section 3.6).

3.2. Review of Existing Tools

As recommended by the project team, two US DOT tools were reviewed. A brief description of these tools is provided in the ensuing sections.

3.2.1. Vulnerability Assessment Scoring Tool

The U.S. DOT Vulnerability Assessment Scoring Tool (VAST) is an Excel-based application developed to help State DOTs, MPOs, and other organizations perform an indicator-based desk review type vulnerability assessment using a range of indicators. The purpose of the assessment as described in the tool is “to determine which assets are *likely* to be vulnerable and which assets are probably not particularly vulnerable to climate change.” The main limitation of the tool is that it does not incorporate risk, it is limited to vulnerability assessments only.

The tool operates using two key premises:

1. Vulnerability is a function of exposure, sensitivity, and adaptive capacity.
2. Certain characteristics of assets can serve as indicators of their exposure, sensitivity, or adaptive capacity.

The tool calculates a vulnerability score for each asset on a scale of 1 to 4 using a weighted average of its vulnerability to three vulnerability components:

- Exposure – whether an asset will experience a given stressor
- Sensitivity – whether an asset will be damaged or disrupted from exposure to a stressor
- Adaptive Capacity – how well the transportation system can cope with damage or disruption to a specific asset

The vulnerability score of each component is calculated as weighted averages from the asset scores for several indicators. One of the key shortcomings of VAST is that there is a lack of guidance on the setting of weights for exposure, sensitivity, or adaptive capacity.

The tool defines indicators as “a characteristic of an asset that suggests if the asset is likely to be vulnerable to a given stressor, either through being exposed, being sensitive, or having low adaptive capacity”. The tool provides the following guidelines for choosing indicators:

- Whether you think it will serve as a reasonable descriptor of vulnerability for a particular asset in your experience and your region
- Whether you believe data exists that will inform your rating of that indicator for a given asset or set of assets.

Examples of indicators from the Gulf Coast Study are provided with the tool. VAST is an indicator library for threat-asset pairs for exposure, sensitivity, and adaptive capacity. In addition, the sensitivity of the asset is available in the Sensitivity Matrix.

There are six steps to the process used by the VAST approach as shown in Figure 3-1 and their timeline is presented in Figure 3-2. Each step is described below:

Step 1 – Select Climate Stressor and Asset Types

VAST defines a climate stressor as “an external change in climate that may cause damage to the transportation system.” The tool provides a list of stressors used in the Gulf Coast Study, they are temperature changes, precipitation changes, sea level rise, or severe storms; however, there is an option to specify other stressors. After all the stressors are specified, the user is required to specify the number (up to six) and types of assets. Asset types may be roads, bridges, rail lines, ports, airports, transit assets, buildings, etc.

Step 2 – Enter Specific Assets

For each asset type, the asset ID, asset name, latitude, and longitude must be specified.

Step 3 – Browse and Select Indicators

The tool defines exposure as “the nature and degree to which an asset is exposed to significant climatic variations.” Exposure can be estimated using indicators that provide information about which assets are more likely to be vulnerable. For projects that lack time or resources, indicators may be a better option than traditional modeling of stressors (Example of Gulf Coast Study modeling options for stressors presented in Table 3-1). The tool provides an example of how the ADCRIC model results can provide information about storm surge inundation depths which can then be used to estimate storm surge exposure. Exposure can also be estimated from indicators like distance from the coastline and elevation. The VAST Excel breaks up step 3 into 4 tabs as presented below:

3a_Exp Indicator Library – presents examples of exposure indicators that can be used in the vulnerability assessment (see Appendix C for a complete list of indicators presented in the tool). There is an option to select the indicators for the next step.

3b_Exp Indicators – up to three indicators for each of the climate stressors (selected in Step 1) can be entered here. Indicators selected in the Indicator Library will appear here.

3c_S&AC Indicator Library - presents examples of sensitivity and adaptive capacity indicators. Indicators may be selected for the next step. Examples of sensitivity and adaptive capacity indicators are presented here.

3d_S&AC Indicator Library – this tab is used to enter the indicators to derive sensitivity and adaptive capacity scores. Up to 10 indicators per climate stressor and asset type may be entered here.

Step 4 – Exposure Data

This step is for collecting two types of data: Exposure data and asset data. The tool provides options to enter exposure data for multiple climate scenarios if required. The values for the exposure indicators selected are entered here. Based on these values, exposure scores will be assigned in the next step. VAST has a second tab in step 4 to provide the asset data.

Step 5 – Adjust Scoring

In this step, the raw exposure data as well as the scoring data for each asset are entered. A higher score means the asset is more exposed. The weights of the indicator can also be adjusted in this step. This process is performed for exposure, sensitivity, and adaptive capacity separately.

Step 6 – Full Vulnerability Results

The results from the vulnerability analysis are presented in this tab. The tool allows for the adjustment of weights of the vulnerability components in this step.

The following tips are recommended in the VAST Intro tab:

1. Start small with just one asset and one climate stressor
2. For easier navigation, keep separate copies of the tool – one for each asset type
3. Solicit input on vulnerability assessment assumptions, assets to include, asset data, and scoring approaches from people in departments like planning, engineering, and operations and maintenance.

The exposure, sensitivity, and adaptive capacity indicators and their data sources will be considered in the development of new data sets for applying nonstationary methods.

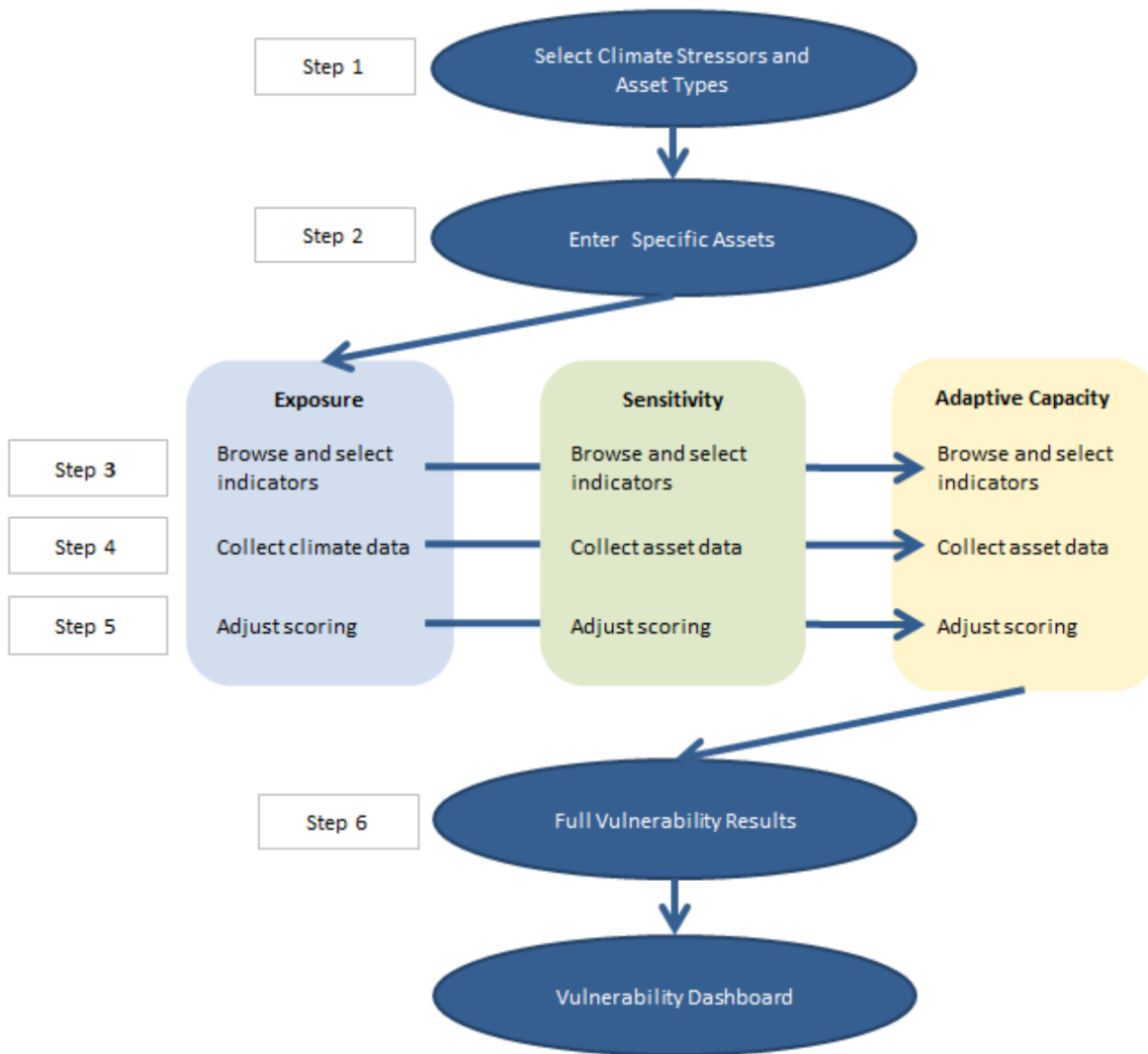


Figure 3-1. Schematic of the process used by the Vulnerability Assessment Tool (VAST) (Source: USDOT, 2015).

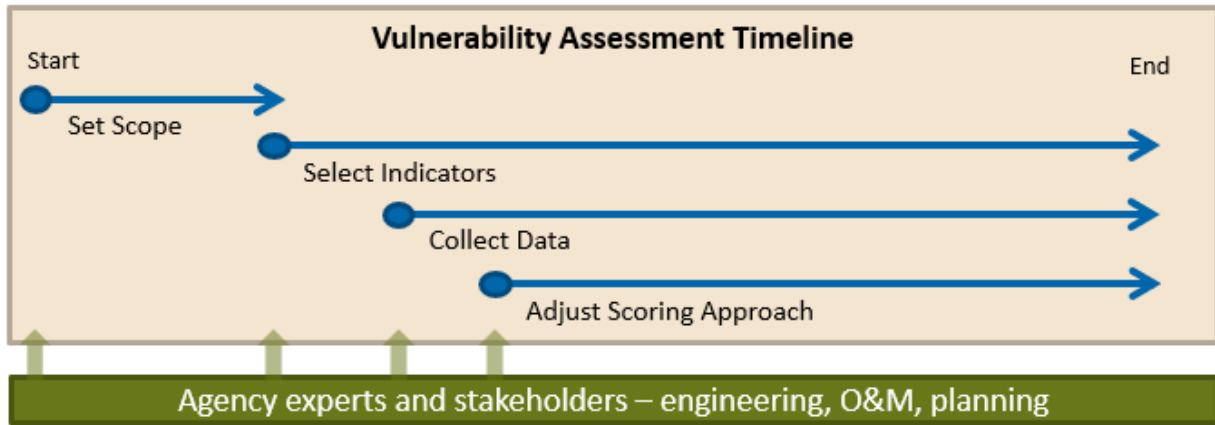


Figure 3-2. Vulnerability assessment timeline (Source: USDOT, 2015).

Table 3-1. Modeling options for the climate stressors used in the Gulf Coast Study (Source: USDOT, 2015).

Stressor	Modeling Options and Resources
Temperature changes	<ul style="list-style-type: none"> • DOT CMIP Climate Data Processing tool – uses CMIP3 and CMIP5 results to provide projected changes in several temperature variables for a single location • USGS NEX DCP30 data viewer – provides projected changes in temperature variables at the county and state levels. Variables include monthly and annual means and changes in the 90th percentile temperatures based on downscaled CMIP5 climate models. • SimCLIM for ArcGIS – provides projected temperature information in an ArcGIS format • Template for Assessing Climate Change Impacts and Management Options (TACCIMO) • The Nature Conservancy's Climate Wizard
Precipitation changes	<ul style="list-style-type: none"> • DOT CMIP Climate Data Processing tool – uses CMIP3 and CMIP5 results to provide projected changes in several precipitation variables for a single location • USGS NEX DCP30 data viewer – provides projected changes in precipitation variables at the county and state levels. Variables include monthly and annual means and changes in the 90th percentile 24-hour rainfall based on downscaled CMIP5 climate models. • SimCLIM for ArcGIS – provides projected precipitation information in an ArcGIS format • Template for Assessing Climate Change Impacts and Management Options (TACCIMO) • The Nature Conservancy's Climate Wizard
Sea Level Rise	<ul style="list-style-type: none"> • Sea level rise bathtub model • NOAA Digital Coast Sea Level Rise and Coastal Flooding Impacts Viewer
Storm Surge	<ul style="list-style-type: none"> • ADvanced CIRCulation (ADCIRC) model • STWAVE - Steady State spectral WAVE model • USGS Coastal Change Hazards: Hurricanes and Extreme Storms web viewer • NOAA Sea, Lake, and Overland Surges from Hurricanes (SLOSH) model
Wind	<ul style="list-style-type: none"> • ADvanced CIRCulation (ADCIRC) model • USGS Coastal Change Hazards: Hurricanes and Extreme Storms web viewer

3.2.2. Guide to Assessing Criticality in Transportation Adaptation Planning

This section presents the review of the United States of America Department of Transportation's (USDOT's) Assessing Criticality in Transportation Adaptation Planning memorandum. The information from this review is useful in defining criticality and selecting values that define critical assets, understanding the process of a criticality study, and selecting the types of nonstationary data that might be useful to these assessments.

The memorandum defines criticality, presents the challenges faced by criticality assessments, identifies methods to define the scope and apply criteria to perform these assessments, and presents examples of such assessments.

Before defining criticality, the memorandum presents some of the common challenges associated with assessing criticality, which are:

- Vague definitions of criticality
- Identifying what constitutes an asset
- Defining the boundaries and relationships in the system
- Gathering relevant data for the studies
- Integrating the data with different formats, spatial referencing, etc.

The document then discusses how some of these challenges can be overcome by first identifying the goals and audience for the vulnerability information. Critical assets are assets of the greatest importance. Based on the purpose and audience of the study, the values that define importance may vary. These values may be economic, cultural, health and safety, emergency evacuation, social connectivity, or other values. Defining the purpose and audience can help select the values to include and the extent to which they should be included. Table 3-2 presents some examples of how the design process is influenced by the purpose of the study and the target audience.

Table 3-2. Examples of how the criticality assessment design process is influenced by the purpose of the study and the target audience (Source: USDOT, 2014).

Purpose of Study	Target Audience(s)	Intended Outcomes	Study Scope	Stakeholder Roles	Potential Criticality Criteria
Raise public awareness of climate risk to transportation assets	General public	Public support for adaptation projects	Limit study to a few high-profile assets across a diverse range of modes	Identify many stakeholders (including non-experts) and involve them throughout the process	Assets with highest use, assets providing access to key employment centers, health and safety
Begin implementing adaptation projects (particularly asset design)	High-level decision makers within transportation agency	Design planned bridge infrastructure for updated design storm characteristics	Limit study to assets that the agency owns and operates; include planned assets if possible	Include engineers, O&M, and other “boots on the ground” stakeholders in meetings to determine criticality	High-cost assets, assets with a long design life
Encourage increased coordination and communication among relevant agencies	Point people from each agency, agency partnerships	Work to share information, increase coordination around emergency events	Focus on assets at the intersection of involvement from multiple agencies	Include mid- and senior-level staff from different agencies in meetings to determine criticality	Assets that are multi-modal or at the intersection of multiple system types (communications, electricity, water); evacuation routes
Research potential risk management strategies	Academia, regional NGOs	Arrive at a consensus on best practices for risk assessment	Include a wide range of modes and assets in the assessment; determine criticality of many assets rather than focusing on a select few	Develop an approach that can be applied in other regions	Criteria that can be used in different regions across the United States; criteria that are cross-cutting and encompass a wide range of decision makers

Some key factors to consider when developing a criticality assessment include:

- Depth of the study – A few key issues were studied deeply versus a broader study
- Range of transportation modes included – one versus many
- Drivers used to define criticality – economic, health and safety, replacement costs, or others
- Stakeholders and when to involve them
- The adaptability of the assessment for other purposes and the adaptability of existing assessments

The general definition of a critical asset is “an asset that is so important to the study area that its removal would result in significant losses.” This definition does not specify what an asset is, where the study area would be, and or who defines significant losses. To address these specifics and narrow the definition, first, the target audience must be identified. For example, the Gulf Cost Study engaged local and regional stakeholders and determined the following major categories of “critical” assets:

- Socioeconomic importance – contributing to not just the economic viability (major transportation facilities providing interstate travel) but also the social viability of communities (like access to households, schools, libraries, places of worship, government centers, etc.).
- Operational importance – assessed by considering each link and how it contributes to the transportation network (by measuring average daily traffic, ridership to transit, annual gross tonnage for rail lines, and cargo volumes for ports).
- Health and safety – contributing to evacuation plans, disaster relief, and recovery plans, moving hazardous materials, inclusion in the national defense system, and access to health care.

When defining the scope of the criticality assessment, the following considerations should be made:

- Geographic Scope – State and local agencies and their jurisdictional borders
- Temporal Scope – Short term versus long term. Long-term plans should also include the design lives as well as the future assets planned
- Modal Scope – Depending on the audience may include highways, public transport, aviation, maritime, pipelines, bicycle and pedestrian facilities, and railroads
- Ownership – Limiting the assets to those owned and operated by the agency

Once the scope, purpose, and intended audience are defined, the memorandum describes three approaches to developing the criticality assessment criteria:

Approach 1 Desk Review

This method involves modal experts using available data and prioritization schemes to place and rank assets with little to no locally specific elements.

The memorandum provides two examples of the desk review approach:

VDOT/Hampton Roads Pilot Approach – To evaluate transportation priorities, the Virginia Department of Transportation (VDOT) partnered with the University of Virginia to identify 30 high-risk assets from 1000 existing assets by using a multicriteria method consisting of traffic volume, elevation relative to mean sea level, location on a maintenance priority route, and location on a hurricane evacuation route.

New Jersey Pilot Approach – To understand how to make strategic capital investments in light of climate change, the North Jersey Planning Authority led an interagency effort in two geographic areas of focus. Criticality criteria were developed using the extent to which each asset connects critical destinations. Factors were determined from 1) the importance of destinations, 2) the magnitude of connects, and 3) the emergency function of routes. The assets were grouped into: “low and medium,” “high,” and “extreme” criticality.

Approach 2 Stakeholder Elicitation

Feedback from regional stakeholders with expertise, selected by the project leaders, is used to identify critical assets.

The memorandum provides two examples of the stakeholder elicitation approach:

The Oahu MPO Pilot Approach – Iterative discussions, facilitated through a workshop, between climate scientists, local planners, engineers, and management professionals identified and prioritized transportation asset groups based on the social and economic consequences of asset failure due to climate change.

The WSDOT Approach – To identify assets vulnerable to climate change and prioritize those assets for a proactive response, the Washington State Department of Transportation (WSDOT) engaged O&M and engineering stakeholders in facilitated workshops. A rating from a 1 to 10 criticality scale was used applied to each asset based on the asset’s character, its general function, and use (Figure 3-3).




Very low to low				Moderate		Critical to Very Critical			
1	2	3	4	5	6	7	8	9	10
Criticality of asset									
<p>Notice that along with the qualitative terms there is an associated scale of 1 to 10, this is to serve as a facilitation tool for some people who may find it useful to think in terms of a numerical scale – although the scoring by each individual is of course subjective. The scale is a generic scale of criticality where “1” is very low (least critical) and “10” is very critical.</p>									
									
<p>Typically involves: non-NHS low AADT alternate routes available</p>				<p>Typically involves: some NHS non-NHS low to medium AADT serves as an alternative for other state routes</p>		<p>Typically involves: Interstate Lifeline some NHS sole access no alternate routes</p>			

Figure 3-3. 10 Criticality scale was applied to each asset based on the asset’s character by the WSDOT (Source: USDOT, 2014).

Approach 3 Hybrid Approach

This method combines aspects from both the desk review and the stakeholder elicitation approaches.

Examples of the hybrid approach are listed below:

San Francisco/MTC Pilot Approach – Climate vulnerability and risk for four types of transportation facilities (road network; transit network; storage, operations, maintenance, and control facilities; and bicycle and pedestrian networks) for Alameda County. The pilot first filtered the assets by those that are located within the end-of-century sea level rise inundation area. A second filter, which analyzed the environmental, economic, and equity characteristics was applied to limit the list of representative assets to three or fewer per category except in the case of the road network. Since the road network has hundreds of discrete arterial, collector, and local streets, a workshop where participants could affix stickers of importance to inundation maps was organized.

Gulf Coast Phase 2 Approach – To determine the criticality of transportation assets in Mobile, the study considered assets of socioeconomic, operational, and health and safety importance. The audience of the project was transportation agencies across the country as well as regional decision-makers. As the goals were overarching and the audience broad, a hybrid approach, which consisted of a desk review in conjunction with periodic

input from a working group was adopted for the Gulf Coast Phase 2 Criticality Assessment. The working group provided feedback on the initial approach, the categories of criteria, and the mode-specific criteria before the transportation experts evaluate data and scored assets from 1 to 5 (low to high) and then categorized them into high, medium, and low criticality. The results were presented to stakeholders and their feedback was incorporated.

3.3. Data Assembly

This project focuses on **Florida-specific data** for the following hydrologic variables: (a) Rainfall; (b) Peak Discharge; and (c) Sea Levels. This section presents the data that has been collected and analyzed.

3.3.1. Rainfall

The Change Factors (CF) derived from three statistically downscaled climate datasets (described in Section 2.3.1) available from a project conducted by SLSC-FIU (2021) for the Florida Building Commission were used. The datasets were:

- I. Localized Constructed Analogues (LOCA), statistically downscaled
- II. Multivariate Adaptive Constructed Analogs (MACA), statistically downscaled
- III. Coordinated Regional Downscaling Experiment (CORDEX), dynamically downscaled. Because of an error in the code used by the original providers of this dataset, updated data have been acquired and are now being incorporated.

The CF values were developed for five climate divisions (see Figure 3-4) for rainfall durations of 1, 3, 7, and 10 days at return periods of 5, 10, 25, 50, 100, and 200 years. SLSC-FIU (2021) developed changed factors for two future periods: NEAR (2030-2069) and FAR (2060-2099) from a baseline period of 1966-2005. For demonstration, the change factors from the NEAR period were applied in this work.

At each of the ATLAS 14 stations shown in Figure 3-4, DDF plots showing the rainfall intensity versus return period for ATLAS 14 stations were produced. The plot also shows the 95th percentile upper and lower bounds for the ATLAS 14 stations. In addition, ATLAS 14 values were multiplied by the Change Factors from the NEAR scenario of the FIU-SLSC (2021) study and plotted, the 17th and 83rd percentile values of the Change Factors were also applied and plotted. Example output plots are presented in Section 3.6.1.1. All plots will be included in the data transfer as specified in Section 5.2

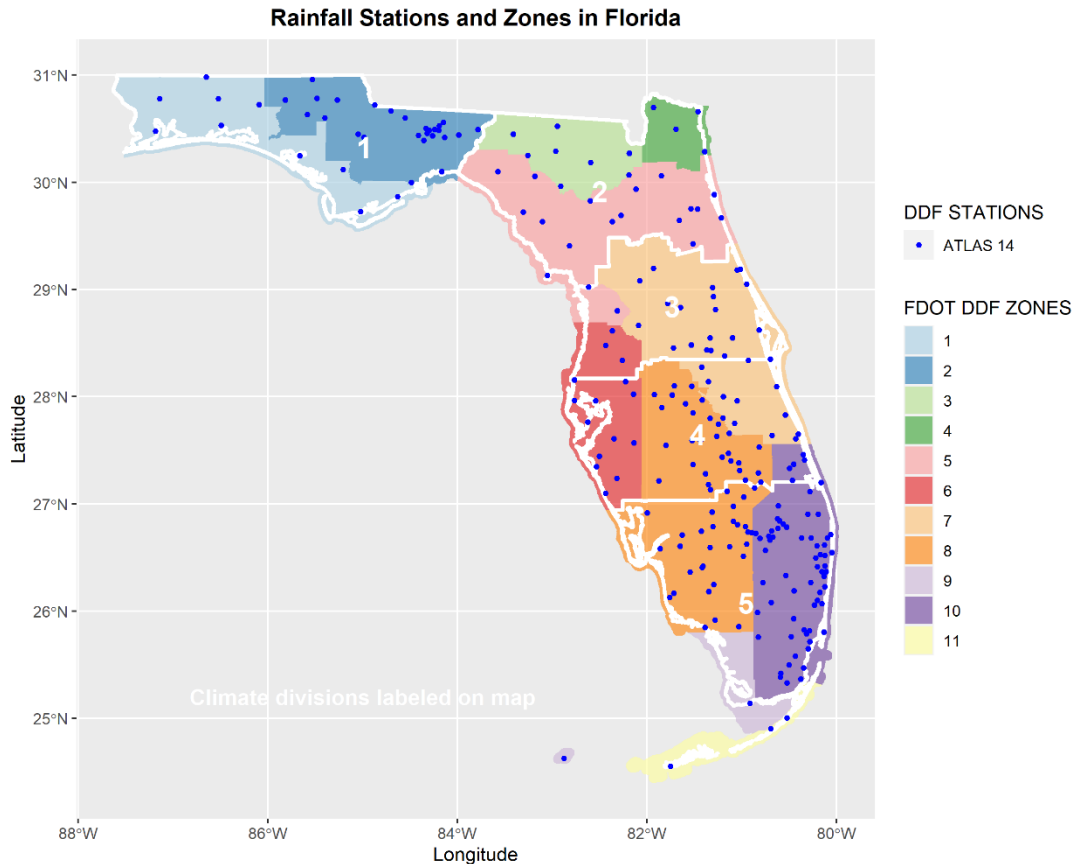


Figure 3-4. Map of the DDF rainfall stations and zones in Florida.

3.3.2. Sea Level

Sea Level scenarios available for locations covered in the NOAA 2017 report (Sweet et al., 2017) were downloaded from the spreadsheet accompanying this report. For this project, the focus was on the scenarios listed in the NOAA 2017 report (Sweet et al., 2017) although several new scenarios are available from a new federal, interagency report published by NOAA (2022). In this regard, it is noted that the scenarios in NOAA 2017 report (Sweet et al., 2017) were the only ones cited in State’s legislation on vulnerability assessment. However, the methods described in the current project can be extended easily to scenarios available from the NOAA 2022 report (Sweet et al., 2022). One exception to using the NOAA 2022 report (Sweet et al., 2022) was on sea level extremes as mentioned below.

The scenarios corresponding to 14 NOAA tide gauges (Figure 3-5) were extracted. For illustration, the corresponding Relative Sea Level scenarios are shown in Figure 3-6. The corresponding extreme sea level curves obtained from the NOAA 2022 report (Sweet et al., 2022) are shown in Figure 3-7. As seen from Figure 3-6 regional mean sea level curves around the state are tightly packed together with little deviation among them. In other words, there is a trivial difference in regional sea level rise scenarios along the coastline of Florida. However, Figure 3-7 shows that the extreme sea level curves have significant differences among the tide gauge locations.

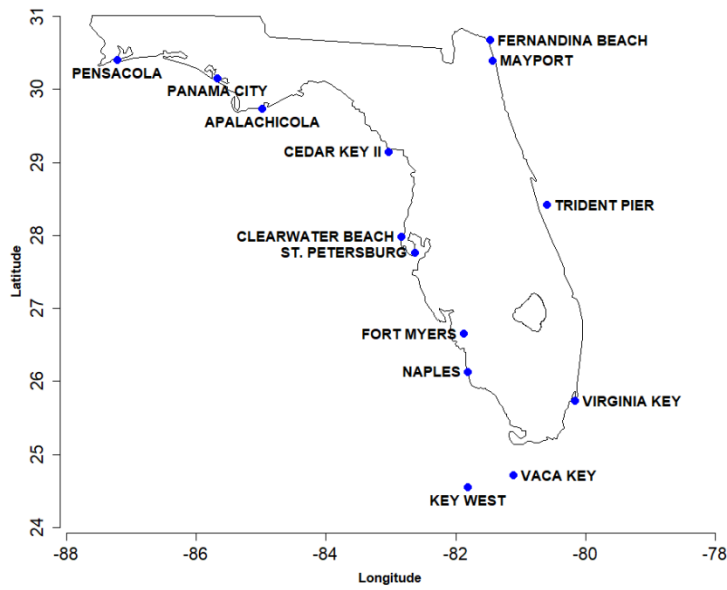


Figure 3-5. NOAA tide gauge locations were selected for the project.

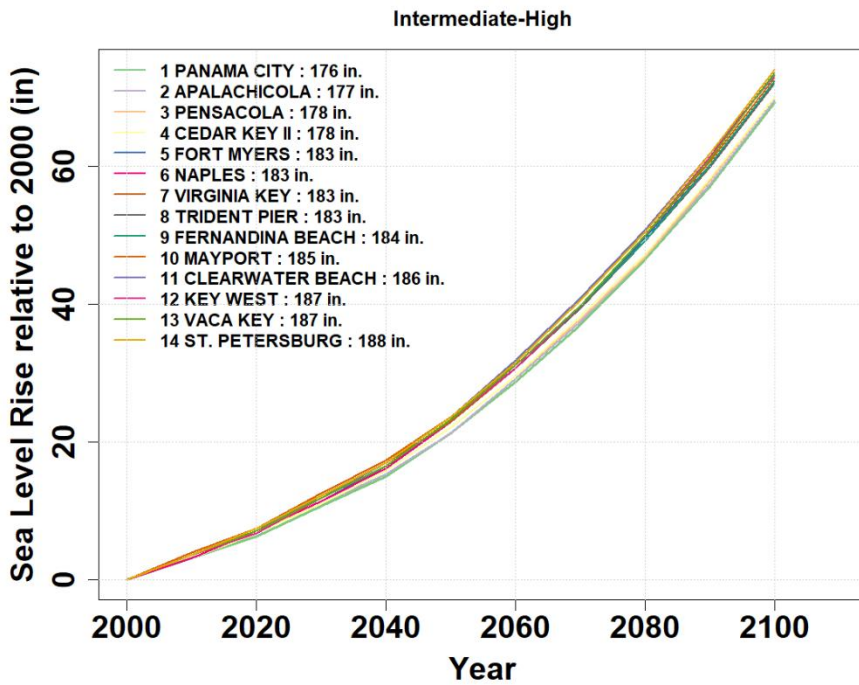


Figure 3-6. Relative sea level rise curves correspond to the intermediate-high scenario obtained from the NOAA 2017 report (Sweet et al., 2017).

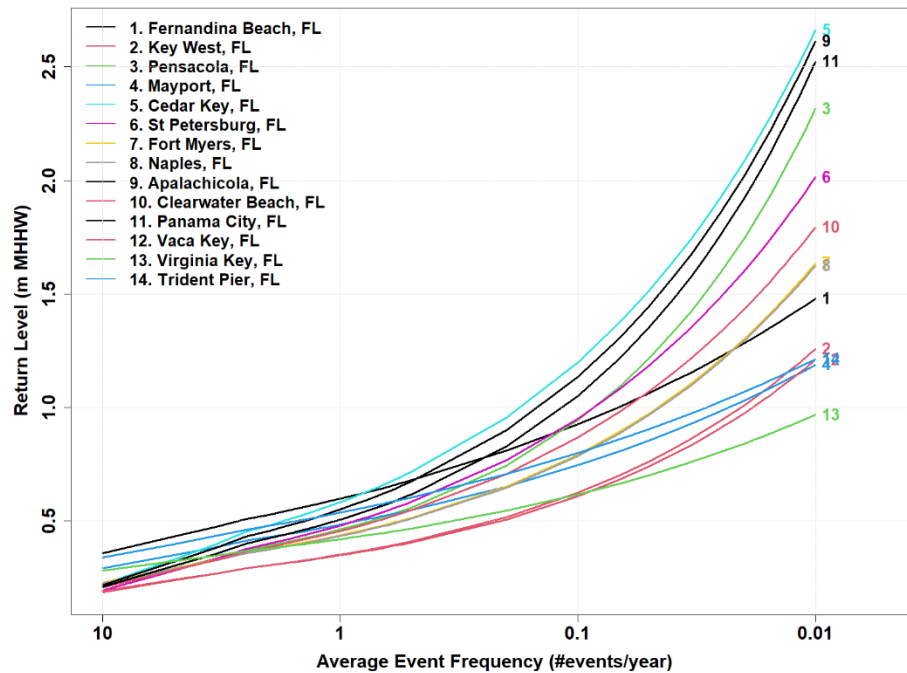


Figure 3-7. Extreme sea-level curves (design return level versus frequency) correspond to the tide gauges shown in Figure 3-6. The curves are based on the data obtained from the NOAA 2022 report (Sweet et al. 2022).

3.3.3. USGS Peak Discharge Data across Florida

HEC-DSSVue and an R code were used to extract, transform, and process the USGS data. The HEC-DSSVue, developed by the U.S. Army Corps of Engineers' Hydrologic Engineering Center, is a Java-based program that can plot, tabulate, edit, manipulate, and visualize hydrologic data in an HEC-DSS database file. HEC-DSSVue can directly import USGS flow data by state. In this work, the HEC-DSSVue was used to import the USGS annual peak discharge data. HEC-DSSVue catalogs the data by region name, station name, data type, date range, frequency, and agency. Using the catalog, data were filtered to include only annual peak flow records. The records were then manually filtered to include stations with a minimum 30-year date range. The resulting 231 stations are exported as CSV files.

Upon closer inspection of the CSV files, some stations with the minimum 30-year date range were found to have large gaps or missing data, resulting in a small number of observations. A second round of filtering was performed using an R-script which removed stations that had less than 40 observations or a data gap exceeding five years. Through this process of elimination, 99 stations were selected from the 231 stations for performing statistical analysis (Figure 3-8). In addition, the R-script also created CSV files of each 231 stations in a format that can be read by the USACE Nonstationary Analysis tool (presented in Section 3.4.1). Statistical methods applied to further analyze this data are presented in Section 3.4.2.

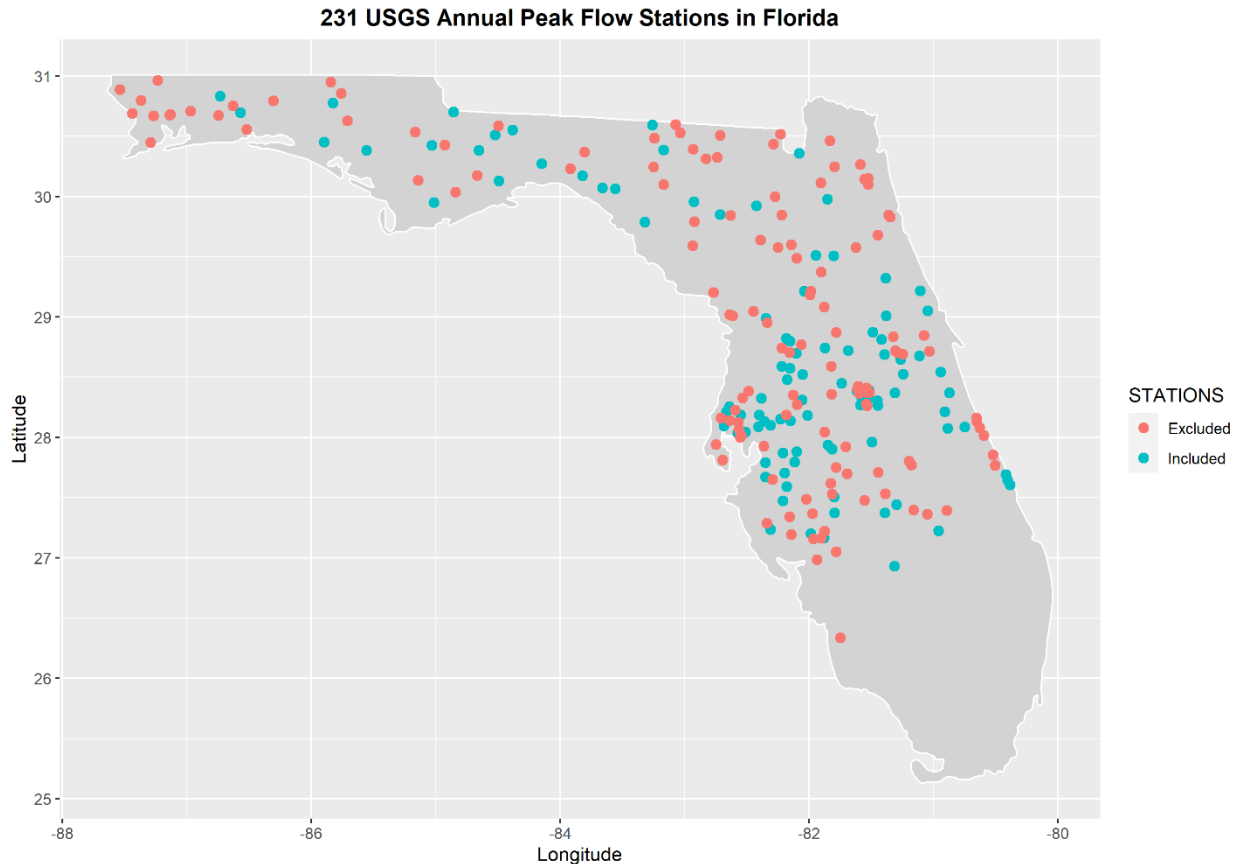


Figure 3-8. Map of the 231 USGS stations that were selected from the HEC-DSSVue database. A second round of filtering resulted in 99 stations (blue dots) while 132 stations were excluded (red dots) for insufficient observations.

3.4. Tools for Nonstationarity Detection

One of the key steps in the proposed methodology is the detection of the possible existence of nonstationarity. Often, natural variability exhibits episodic nonstationary-like characteristics which may not represent persistent, systematic trends that are statistically significant. This research explored existing tools, particularly those from federal agencies such as the US Army Corps of Engineers (USACE), and the United States Geological Survey (USGS), and customize their applications to locations in Florida.

3.4.1. USACE Time Series Toolbox

The USACE Time Series Toolbox is an online tool where users without programming expertise can upload time series data, and perform trend analysis, nonstationarity detection, and time series modeling. This work reviews the data exploration, model-based analysis (trend analysis), and nonstationary detection methods presented in the Toolbox. In addition, a report by the UCF affiliates on the use of the Toolbox for nonstationary detection of sea-level, precipitation, and discharge (as shown in Table 3-3) is available in Appendix D.

Table 3-3. Applications of the USACE Time Series Toolbox which are presented in the UCF report in Appendix D.

Data Type	Monthly mean	Annual Mean	Annual Max
Sea-level	X	X	x (from hourly data)
Precipitation		X	x (from daily data)
Discharge		X	x (from daily data)
Surge			x (from hourly data)

Explore Data

Only csv files may be uploaded to the time series toolbox. The csv files should be formatted to contain two columns the first is date in the mm/dd/yyyy, mm-dd-yyyy, or yyyy format, and the second is the value. Once the data is uploaded the user can specify the title, x-axis label, and y-axis label. The Toolbox offers a few methods to deal with missing values in the time series. The options are:

1. Leave them blank
2. The last observation carried forward
3. Linear interpolation.

Once the data is uploaded, a time series plot of the data with title and axis labels specified by the user is generated (Figure 3-9).

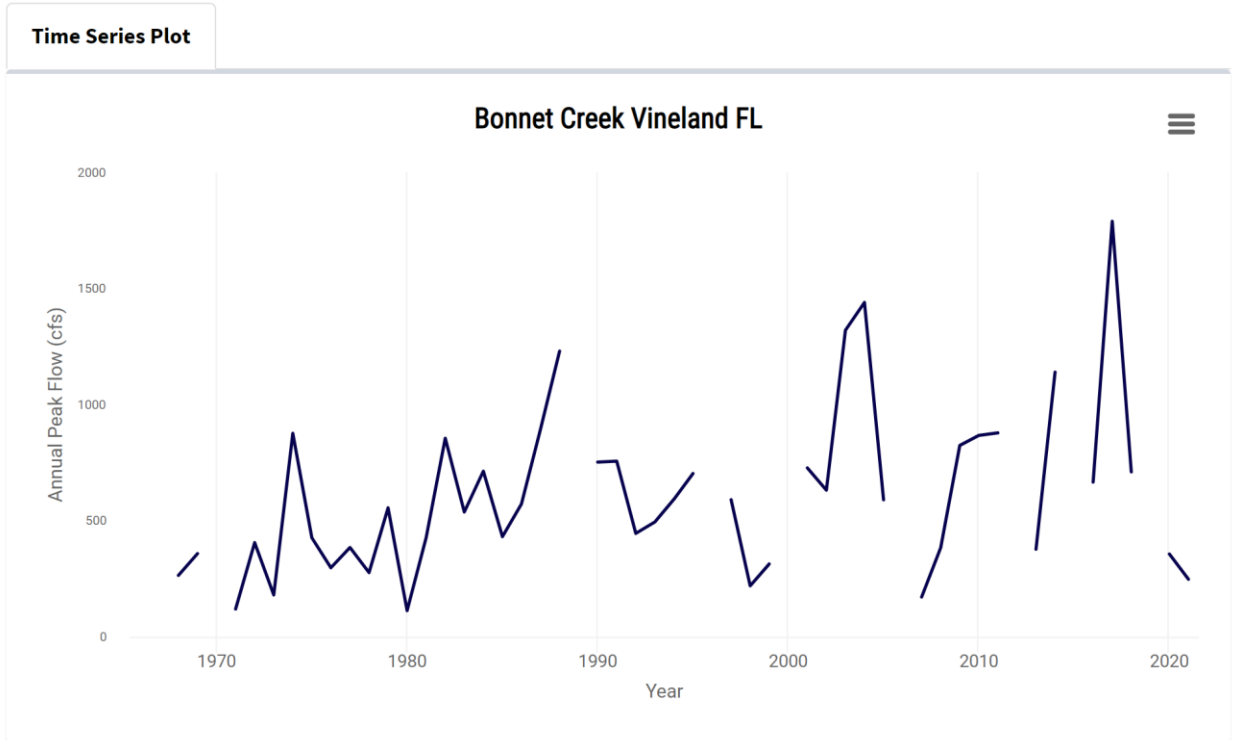


Figure 3-9. Example of the time series plot of the annual peak flow at Bonnet Creek, Vineland, FL, created using the USACE Time Series Toolbox.

The second tab of the Explore data section presents the data summary including tabulated raw data, start and end data of the data, the number of entries per year, the number of missing values, and the total entries.

The third tab presents the Magnificent Seven Analysis, which are summary statistics in data characterization and classification as presented in Archfield et al. (2013). These are:

- L-Mean – Average value of the data provides a measure of the location. Refer to Hosking (1996, p.14) for calculations.
- Coefficient of L-Variance (LCV) – the ratio of standard deviation to the mean of the data. Refer to Hosking (1990) and Hosking (1996) for more information.
- L-Skewness – a measure of the asymmetry of the probability distribution. Values greater than 0.3 indicate large skewness. Refer to Hosking (1990) and Hosking (1996) for more information.
- L-Kurtosis – a measure of the tail density of the probability distribution. For example, a normal distribution would have a value of 1/6. Refer to Hosking (1990) and Hosking (1996) for more information.
- AR1 – autoregressive lag coefficient, represents how predictive the previous value in the time series is of the next. Values can be positive or negative.
- Amplitude – Measures the best-fitting annual sinusoidal curve height.

- Phase – the measure in radians of the angle of the best fitting, annual sinusoidal curve at time zero.

Model-Based Analysis

The model-based trend analysis section of the Toolbox measures the slope, directionality (positive or negative), and intercept for both the traditional linear slope method, as well as Sen's slope method. Trend hypotheses are tested at a 0.05 significance level for the following tests:

- T-test
- Mann-Kendall
- Spearman Rank-Order.

Nonstationary Detection

The algorithm uses statistical testing to examine the data for nonstationarity, that is, changes in the data mean, variance, or distribution. The following tests are applied to detect nonstationarity:

- Lombard Wilcoxon
- Pettitt
- Kolmogorov-Sminov (CPM)
- Bayesian
- Mood (CPM)
- LePage (CPM)
- Energy Divisive Method
- Segment Statistics – Mean, Variance, Standard Deviation.

An example of nonstationarity detection using the Toolbox for annual peak flow data is presented in Figure 3-10. The Toolbox also presents a graphical view of the tests with significant results and the data type tested (Figure 3-11). The Toolbox can show segmented trend lines with slope, intercept, and directionality, and the significance of the trend is tested using t-Test (Figure 3-12).

The algorithm can also perform a breakpoint analysis (Figure 3-13). Breakpoints represent sharp changes in behavior necessitating segment statistics to accurately reflect the data series. The following metrics are used to determine the breakpoints:

- Residual Sum of Squares (RSS)
- Bayesian Information Criteria (BIC)
- Root Mean Square Error (RMS)

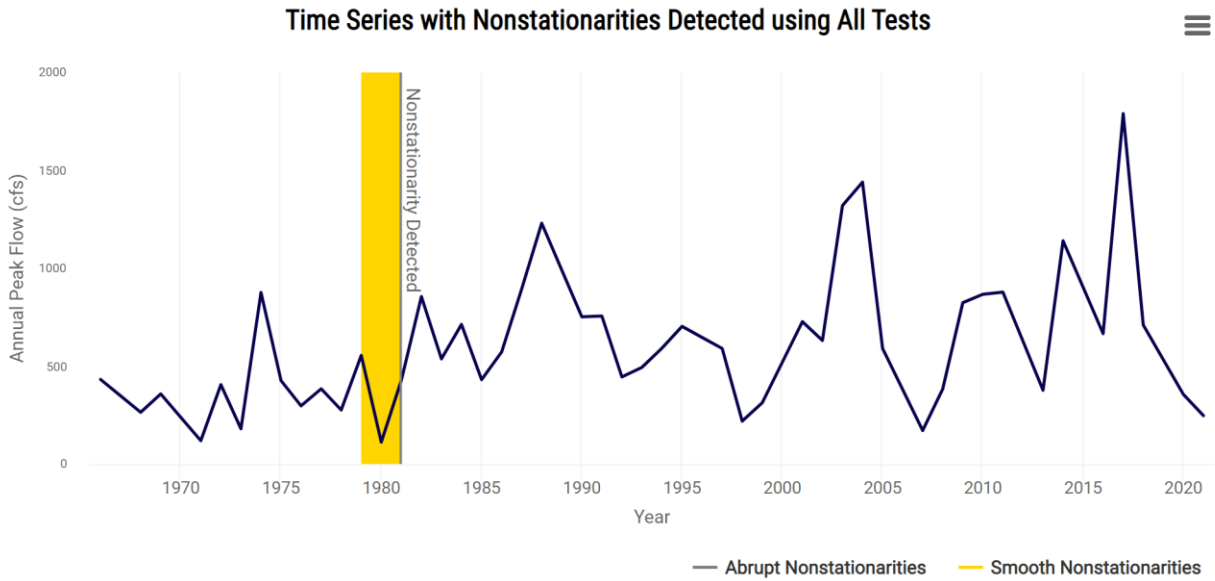


Figure 3-10. Nonstationarity detection using the Time Series Toolbox for annual peak flow at Bonnet Creek, Vineland, FL.

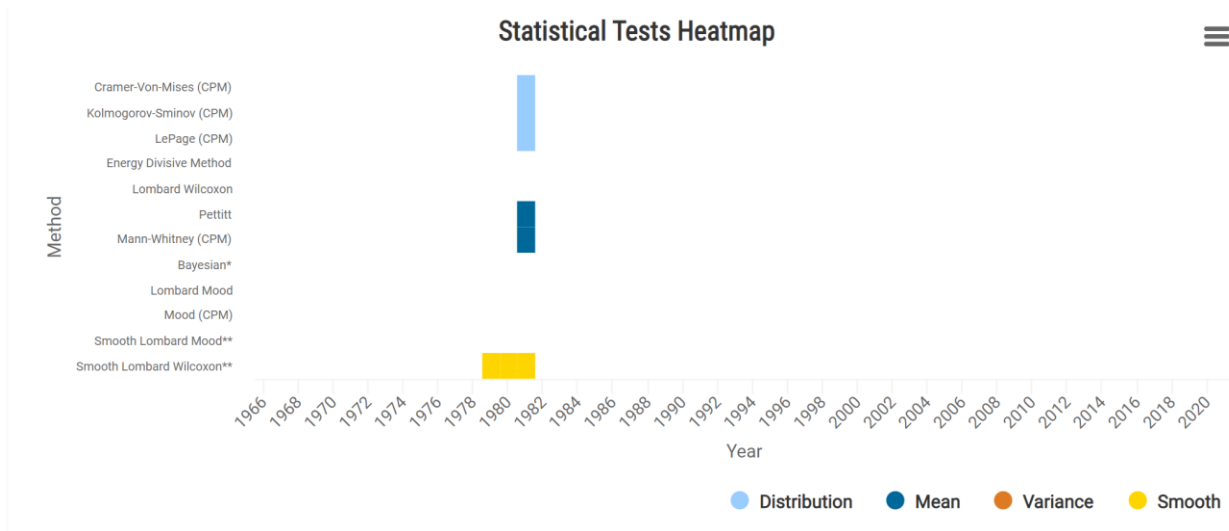


Figure 3-11. Statistical heat map showing the significant tests for the nonstationary analysis of annual peak flow data at Bonnet Creek, Vineland, FL.

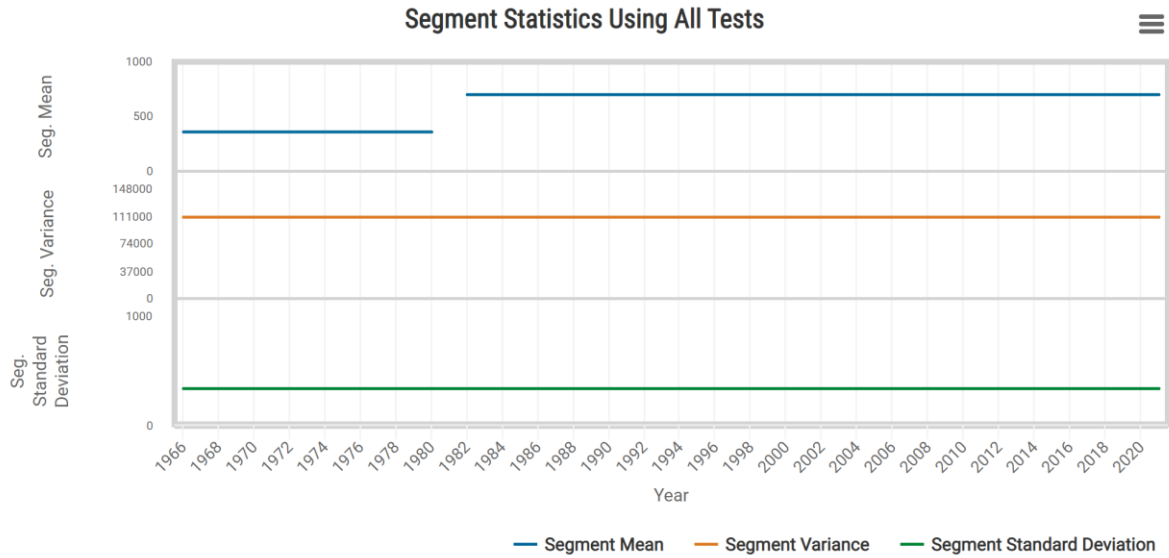


Figure 3-12. Segment statistics for the nonstationary analysis of annual peak flow data at Bonnet Creek, Vineland, FL.

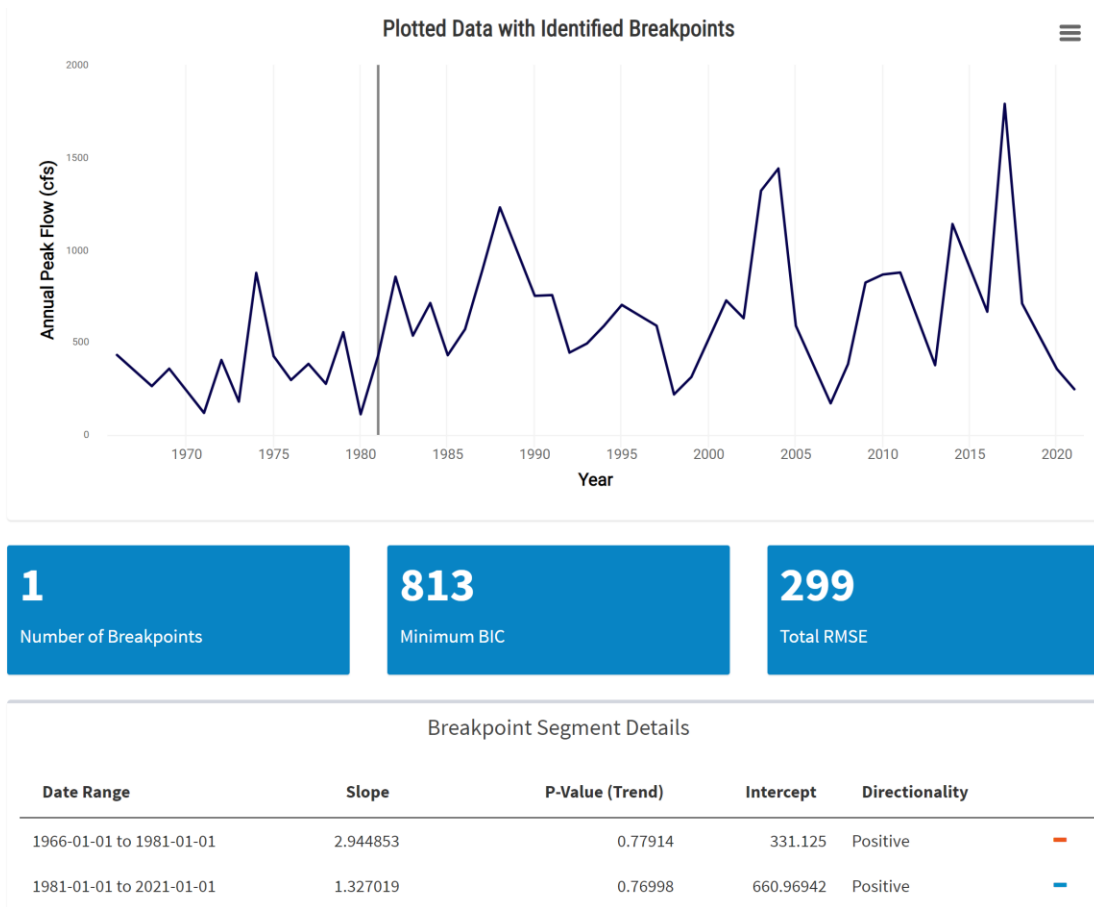


Figure 3-13. Breakpoints identified by the Time Series Toolbox and the breakpoint segment details for the annual peak flow data at Bonnet Creek, Vineland, FL.

When applying the findings of the nonstationary analysis, the following criteria, generally used by researchers are recommended:

1. Consensus: Nonstationarity is considered strong if it is detected by two or more tests
2. Robustness: A statistically significant nonstationarity is robust if at least two statistical properties (mean, variance, standard deviation, or distribution)
3. Magnitude: Nonstationarities produced by greater changes in the statistical properties of the datasets should be taken into consideration.

3.4.2. USGS Trend Assessment for Peak Flow

Trend assessment was performed using R scripts on 99 USGS peak flow stations in Florida that met the conditions as described in Section 3.3.3. The R-script first performed a normality test at a significance of 0.05. Linear regression analysis was also performed. Because the normality tests showed that the Gaussian assumption inherent in the regression modeling was not valid at almost all gauge locations, the Mann-Kendall nonparametric trend assessment was performed. For this task, missing data were filled in using log-linear interpolation. The results from the nonparametric trend assessment tests are presented in Figure 3-14. At a large number of station locations, there was no statistically significant trend (see “white” dots in Figure 3-14). The analysis also showed that the trend was negative (blue dots in Figure 3-14) at many stations. However, statistically significant trends were detected at 9 stations as shown by the “red” dots in Figure 3-14. The exact reason for the nonstationarity at these locations was not explored.

Table 3-4 presents the stations with significant positive trends. The time series plots with superimposed linear trendlines for the 9 stations are presented in Figure 3-15.

Nonparametric Trend Assessment

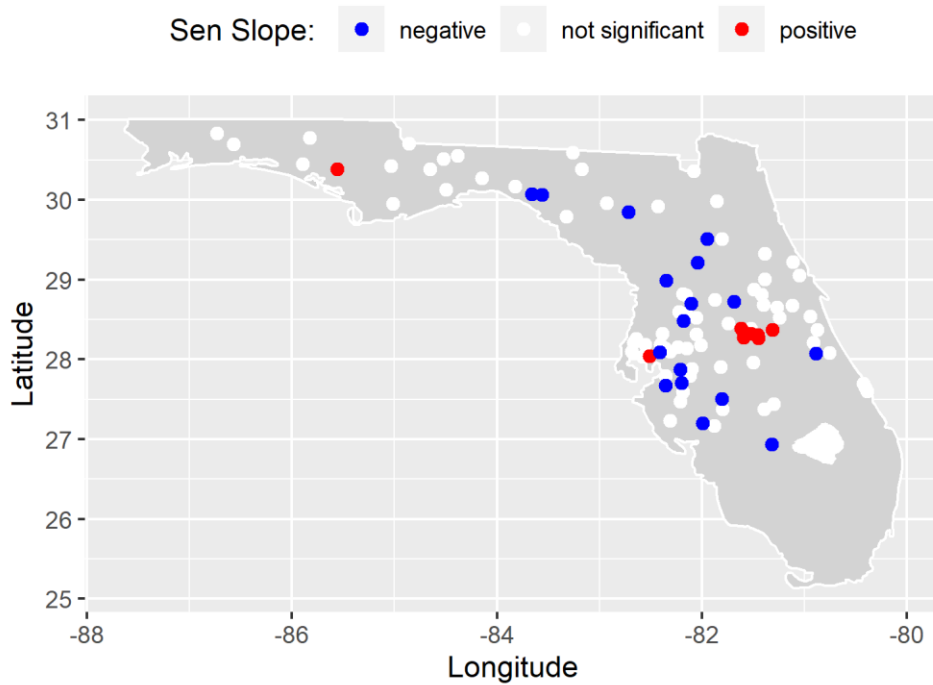


Figure 3-14. Map with stations showing the results from the nonparametric trend analysis.

Table 3-4. USGS annual peak flow stations with significant positive trends from the trend assessment.

STATION NAME	STATION ID	LATITUDE	LONGITUDE
BONNET CREEK VINELAND, FL	2264100	-81.52	28.33
WHITTENHORSE CREEK VINELAND, FL	2266200	-81.62	28.39
REEDY CREEK VINELAND, FL	2266300	-81.58	28.33
DAVENPORT CREEK LOUGHMAN, FL	2266480	-81.59	28.27
SWEETWATER CREEK SULPHUR SPRINGS FL	2306500	-82.51	28.04
ECONFINA CREEK BENNETT, FLA	2359500	-85.56	30.38
SHINGLE CREEK CAMPBELL, FL	2264495	-81.45	28.27
SHINGLE CREEK AIRPORT NEAR KISSIMMEE, FL	2263800	-81.45	28.30
BOGGY CREEK TAFT, FL	2262900	-81.31	28.37

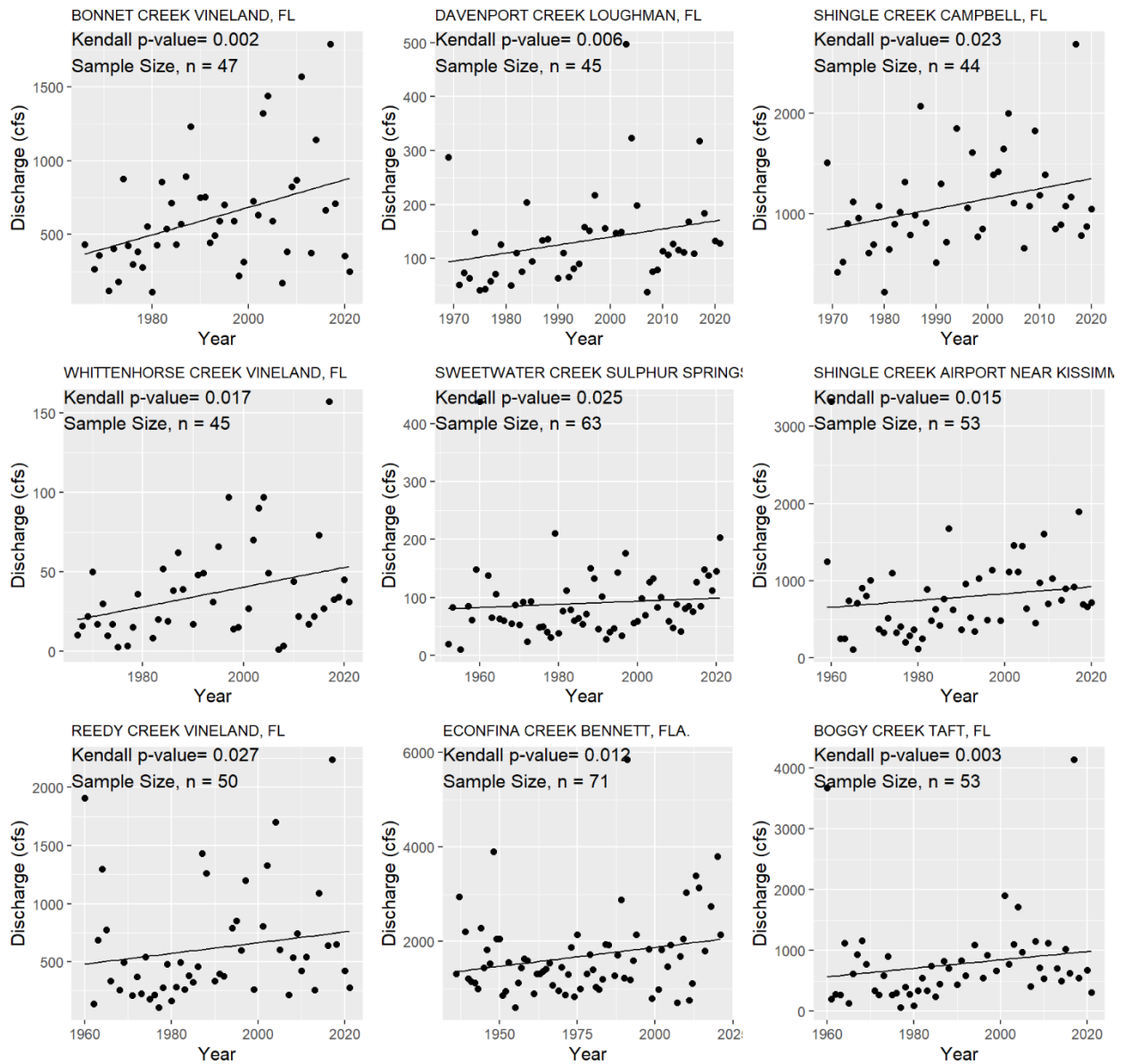


Figure 3-15. The plot of the discharge with linear trendlines for stations with significant positive trends.

3.5. Nonstationarity Paradigm for Return Period, Risk, and Uncertainty

Transportation and other infrastructure built for serving communities from the impact of extreme hydrologic events have largely been designed based on concepts such as return period and risk assuming the concept of “stationarity”, which implies that the past climate represents what is to be expected in the future. Traditionally, the features of Transportation Infrastructure (TI) are designed using a fixed return period which is the basis of stationarity. The current drainage design manual, for example, provides specifications for a fixed return period magnitude that should be used for various features such as canals, stormwater drainage, bridges, roadways, and major highways. However, in an environment of change, whether is it due to anthropogenic

or natural but systematic changes, (e.g., rising sea level, increasing rainfall intensity), the notion of a fixed return period is no longer appropriate. A roadway designed for say, a 50-year return period, will decrease its level of flood protection with time yielding, say, a 25-year level of protection at the end of the design life. In this section, a foundation for a new paradigm based on the assumption that the hydrologic variable of interest is nonstationary is presented. It is important to determine that the hydrologic data indeed do demonstrate trends validated by statistically significant trends with further confirmation by assessing physical reasons for such behavior. The nonstationary design methods discussed in this report are based on the concepts of (a) Expected Waiting Time (EWT), another interpretation of Return Period; (b) Risk; and (c) Expected Number of Events (ENE). First, a summary of the current concepts associated with the stationary approach is presented. Next, a summary of extensions to the concepts of Expected Waiting Time (EWT), which is equivalent to Return Period, Risk (R), and Expected Number of Events (ENE) will be discussed with suggestions as to how they could be used for hydrologic design when the primary variable of interest is nonstationary.

3.5.1. Modeling of Stationary and Nonstationary Extremes

There are two common ways of modeling extremes of hydrologic variables such as floods, precipitation, temperature, and wind. They are based on (a) Block maxima (BM) data or in the case when the “block” is one year, the annual maxima series (AMS), and (b) peaks-over-threshold (POT) data, as shown graphically in Figure 3-16 and Figure 3-17 respectively.

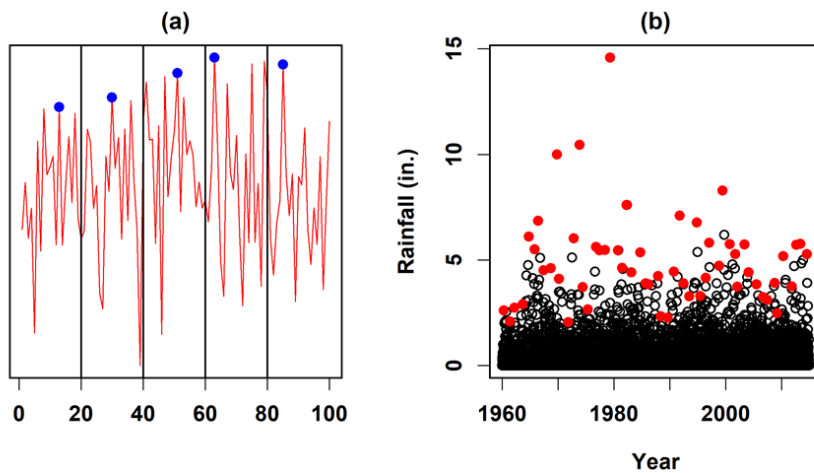


Figure 3-16. (a) Illustration of extracting block maxima (BM) data for modeling extremes and (b) example of a daily rainfall series (open circles) and the (annual) block maxima values (solid circles in red).

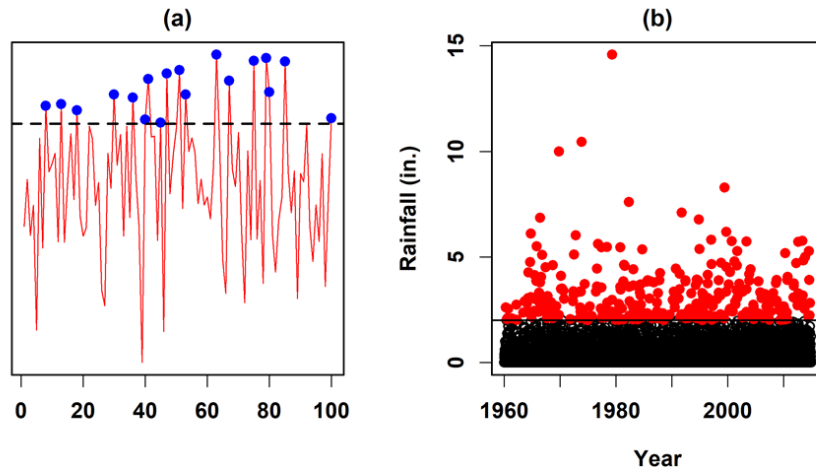


Figure 3-17. (a) Illustration of extracting peaks-over-threshold (POT) data for modeling extremes (in green) and (b) example of a daily precipitation series and the values above a threshold equal to 2 inches (in red color).

Block maxima (BM) is defined as the maximum value of a given block of observations. The length of the block is typically one year, but it could also be an individual season (e.g., a wet or a dry period). A common example of block maxima data is the annual floods which are the highest discharges in a calendar or a water year. This approach has been generally used in actual practice. A limitation of such an approach is that the sample size available for modeling the time series is small due to the use of only one extreme event per year. Often, there are other extreme events (second or third highest) that can be useful for the statistical analysis of the largest events in the records. There are cases where the second largest flood each year may outrank the annual maxima in other years, and yet in the block maxima approach, such events will not be used for extreme value modeling.

The peaks-over-threshold (POT) method uses extreme events (e.g., floods) above a selected threshold (also known as a base flood in case of floods) within a given year or season. The selection of the threshold and the POT values are important from both physical and statistical points of view, and they will be discussed subsequently in this section. It is expected that using POT values will improve the estimation of design events because of the large sample of extremes that can be extracted from the historical dataset. The POT methods require a higher frequency of data in a time series (e.g., hourly or daily) as opposed to block maxima (e.g., annual floods). In some situations, some annual extremes may not even be selected as POT events. The POT modeling approach provides additional flexibility in representing extreme events as compared to the block maxima approach but at a cost of added complexity (Lang et al. 1999). Unlike the BM approach in which the data set is well defined, however, the POT approach can be subjective. Although some criteria have been developed (Coles 2001), standard guidelines for its application are lacking. It is noted that, in hydrology, the POT method is also known as the partial duration series (PDS) method. Both stationary and nonstationary approaches are available for modeling BM and POT data.

3.5.2. Statistical Modeling of Extremes

3.5.2.1. AMS Series

The probability distribution of annual extremes that is becoming increasingly popular is the Generalized Extreme Value distribution (GEV). A good reference for GEV is the classic book by Coles (2001). The Probability Density Function (PDF) for GEV is given by

$$f(z; \mu, \sigma, \xi) = \frac{1}{\sigma} \left[1 + \xi \left(\frac{z - \mu}{\sigma} \right) \right]^{-\frac{1}{\xi} - 1} \exp \left\{ - \left[1 + \xi \left(\frac{z - \mu}{\sigma} \right) \right]^{-\frac{1}{\xi}} \right\} \quad (1)$$

where μ , σ , and ξ are the location, scale, and shape parameters, respectively. When $\xi = 0$ GEV reduces to the well-known Gumbel Distribution that may be expressed as

by inverting the above equation and it is given by

$$z_T = \mu - \frac{\sigma}{\xi} \left[1 - y_p^{-\xi} \right], \quad (2)$$

where

$$y_p = -\log(1 - p), \quad (3)$$

And z_T is the return level for the return period $T = 1/p$.

3.5.2.2. POT Series

The POT approach was first developed by hydrologists in the 1970s. This method fits a stochastic model to exceedances over a threshold (u) and an independent exponential random variable to the model the amount of exceedance (Davison and Smith, 1990). The main advantage of employing the POT method is the increased sample size which results in more robust estimations of the shape parameter. The POT approach used in this project is based on the family of distributions called GPDs. The GPD, which implies the classical Pareto Distribution (Picklands, 1975; Davison and Smith, 1990; Madsen et al., 1997), models the amount of exceedance and the probability density (PDF) function is given by (Coles, 2001):

$$f(z; u, \sigma, \xi) = \frac{1}{\tilde{\sigma}} \left[1 + \xi \left(\frac{z - u}{\tilde{\sigma}} \right) \right]^{-\frac{1}{\xi} - 1} \quad (4)$$

Where u is the threshold used for determining the peaks. Besides u , there are two other parameters of this model (scale, $\tilde{\sigma}$, and shape ξ).

The N -year return level (or quantile) is given by (Coles, 2001):

$$z_N = u + \frac{\tilde{\sigma}}{\xi} \left[(Nn_y \zeta_u)^{-\xi} - 1 \right], \quad (5)$$

where n_y is the number of periods in a year (for daily this is 365.25), and ζ_u is the probability of individual observations exceeding the threshold. This probability is typically estimated as the ratio of the number of exceedances and the length of the entire time series.

The details of parameter estimation, model selection, and uncertainty estimation are beyond the scope of this report as it is covered well in classic textbooks such as the one by Coles (2001).

3.5.2.3. Modeling Nonstationary

The extremes of hydrologic variables exhibiting nonstationarity may be independent but not identically distributed. If the form of the distribution remains the same (e.g., GEV) but with varying parameters (related to time or as a function of some covariate), the extreme value distribution can be parameterized using those relationships. For GEV, the general form of such a nonstationary model for the block maxima is denoted as Z_t is,

$$Z_t \sim GEV[\mu(t, c), \sigma(t, c), \xi(t, c)] \quad (6)$$

where t denotes time, and c is a covariate (an external variable) that may influence the parameters of the GEV distribution. Depending on the complexity of the data at hand, various functional forms for the three parameters of the GEV model may be used. Some examples are:

- a. The location parameter is a linear function of time, but other parameters are fixed

$$\mu(t) = \beta_0 + \beta_1 t; \sigma(t) = \sigma; \text{ and } \xi(t) = \xi \quad (7)$$

- b. The location parameter as a quadratic function of time, but other parameters are fixed

$$\mu(t) = \beta_0 + \beta_1 t + \beta_2 t^2; \sigma(t) = \sigma; \text{ and } \xi(t) = \xi \quad (8)$$

- c. Scale parameter as a log-linear function of time and other parameters are fixed. The exponential form is used to ensure that the scale parameter remains positive.

$$\mu(t) = \mu; \sigma(t) = \exp(\beta_0 + \beta_1 t); \text{ and } \xi(t) = \xi \quad (9)$$

- d. Both location and scale parameters are functions of time, but the shape parameter is constant

$$\mu(t) = \beta_0 + \beta_1 t; \sigma(t) = \exp(\beta_2 + \beta_3 t); \text{ and } \xi(t) = \xi \quad (10)$$

- e. The location parameter is a function of the covariate, NINO3 (an index representing the El Niño/La Niña phenomenon) but other parameters are fixed.

$$\mu(t) = \beta_0 + \beta_1 NINO3(t); \sigma(t) = \sigma; \text{ and } \xi(t) = \xi \quad (11)$$

The application of the above is illustrated in Section 3.6.

3.5.2.4. Change Factors of Rainfall Depth-Duration-Frequency (DDF) Estimates

Another approach for modeling nonstationarity, particularly in the case of extreme rainfall expressed in the form of Depth-Duration-Frequency (DDF) curves, is to use the concept of a Change Factor (CF). The values of CF are typically determined from downscaled, climate model data corresponding to the historical period and a future period of interest. They can be used to adjust available DDF curves such as those available from NOAA’s Atlas 14 dataset for planning and design of future stormwater projects associated with Transportation Infrastructure. The theoretical basis of CF is illustrated in Figure 3-18.

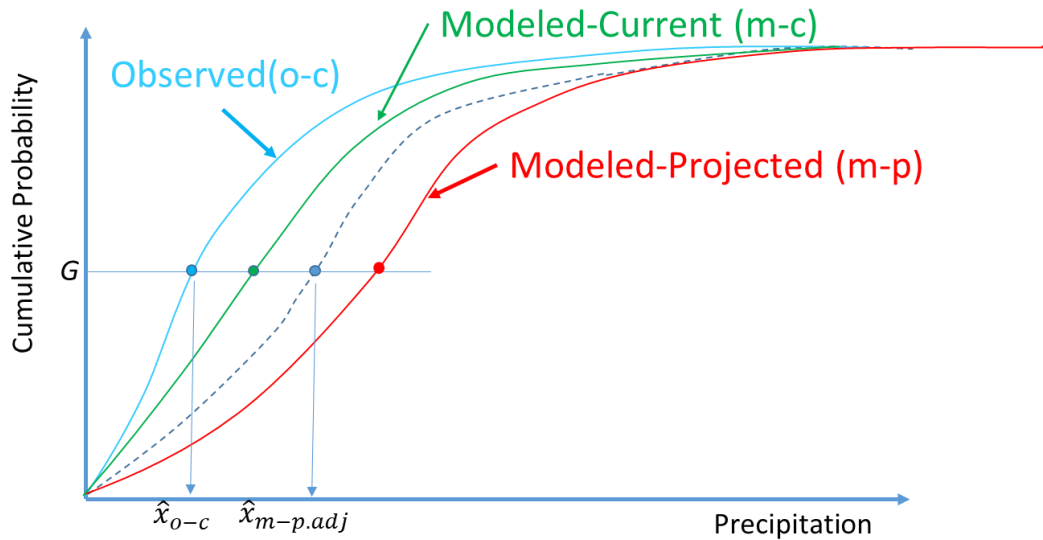


Figure 3-18. Illustration of the concept of the change factor. The dashed curve is the adjusted curve using, observed, modeled-current, and modeled-project probability distributions and the change factor defined in the text below. In most cases, the m-c and o-c curves deviate from each other, even in cases when the current and observed periods are identical.

As shown in Figure 3-18, a CF is associated with three cumulative probability distributions: (1) Observed (F_{o-c}); (2) Modeled-Current (F_{m-c}); and (3) Modeled-Projected (F_{m-p}). Modeled-Current and Observed probability distributions correspond to the same historical period. The Modeled-Projected distribution represents the future precipitation for a specific future period.

It is well known that the extreme rainfall predicted by climate models has a large negative bias. Typically, bias correction techniques are used to correct such biases. For defining CF, it is assumed that the **Multiplicative Quantile Delta Mapping** (MQDM) method is used for adjusting the future. The expression for adjusting future rainfall quantiles is (Irizarry et al. 2016, 2017):

$$\hat{x}_{m-p,adj} = F_{m-p,adj}^{-1}(G) = F_{m-p}^{-1}(G) * \left\{ \frac{F_{o-c}^{-1}(G)}{F_{m-c}^{-1}(G)} \right\} \quad (12)$$

The variables used in MQDM are defined as follows: \hat{x}_{m-padj} is the adjusted quantile for the model (m) projections (p) for the future period, F_{o-c} is the Cumulative Distribution Function, CDF, of the observations (o) in the current baseline period (c), F_{m-c} is the CDF of the model (m) in the current baseline period (c), and F_{m-p} is the CDF for the model (m) projections (p) for the future period. G is the annual non-exceedance probability (CDF value) and is equal to $1-P$, and P is the annual exceedance probability (AEP) which is related to the return period T by $1/P = T$ (i.e., $G=1-1/T$), F^{-1} is the quantile function.

The adjusted rainfall for the future is given by Eq (13) below which allows the adjustment of the rainfall quantile corresponding to a given return period $T = 1/p$ by combining estimates obtained from historical data ($o-c$), the model output for the current period ($m-c$) and the model output for the future period.

$$\hat{x}_{m-padj} = F_{o-c}^{-1}(G) \left[\frac{F_{m-p}^{-1}(G)}{F_{m-c}^{-1}(G)} \right] = F_{o-c}^{-1}(G) * CF \quad (13)$$

The quantity inside the large square brackets is the Change Factor, CF, which may be used to adjust the historical DDF curves (as denoted by F_{o-c}).

3.5.3. Review of Stationary Methods for Return Period and Risk

The stationary approach assumes that extreme values (e.g., floods, sea levels) are independent and identically distributed (i.i.d.) random variables with a specified probability distribution. First, the case of annual maxima (each value represents the maximum value over a block length of one year) will be presented. Denoting the random variable of extremes as Z , assume that it has a Cumulative Distribution Function (CDF) denoted by $F_Z(z, \theta)$ where θ is its parameter set. For a given cumulative probability, q , the corresponding value of the variable, Z , denoted as z_q is called the q -th quantile. In addition, sometimes the notation z_p is utilized, where p denotes the exceedance probability, i.e., $p=1-q$. Traditionally, the concept of Return Period, T , has been used in which $T = 1/p$ (e.g., Gumbel, 1941) and in this case, the corresponding quantiles z_q or z_p as defined above are also written as z_T . In some recent literature, the quantiles are called “return level” (e.g., Coles 2001). The design quantity in this notation, z_T may refer to discharge or an elevation (stage) corresponding to the return period, T .

Figure 3-19(a) shows schematically the hydrologic design problem using the annual maximum flood data which is assumed to be stationary over the historical period. The design life of n years is assumed to start from time t_0 when the project operation begins the following construction. When using the Return Period T as the design criteria, it is useful to represent T as the Expected Waiting Time (EWT) which is also the statistical expectation for the time until the first exceedance of the design value (also known as “waiting time”). This allows a convenient extension of this concept into the nonstationary paradigm. The waiting time, X , is the time it takes from time t_0

for the first flood event exceeding the design quantile, say, z_{q0} , which implies that all other prior annual maxima after t_0 are less than z_{q0} . It can be shown that X is a random variable that follows the geometric distribution (e.g., Mood et al., 1974) in which its expected value is $E[X]=1/p_0$ where p_0 is the exceedance probability of the design level z_{q0} and it can be determined from $p_0 = 1 - F_Z(z_{q0}, \theta)$. It follows that the design return period, T which is equal to $1/p_0$, is the Expected Waiting Time (EWT) for the extreme event to occur. It is also noted that the Return Period (or EWT) is independent of the design life, n . The return period concept may be interpreted as “*the expected waiting time for the T -year event is T years.*” In addition, the variance of X is $\text{Var}(X) = (1 - p_0)/p_0^2$.

Another measure that is important in evaluating and designing projects is the hydrologic risk which incorporates the design life, n . It may be shown that the number of events exceeding z_{q0} in an n -year period is a random variable, Y , which has a Binomial Distribution (BD) (e.g., Bras, 1990)

$$P[Y = y] = \binom{n}{y} (p_0)^y (1 - p_0)^{n-y} \quad y = 0, 1, \dots, n \quad (14)$$

where y is the number of such events over the design life, n . Risk, R , is defined as the occurrence of one or more extremes exceeding the design return level or equivalently $P[Y \geq 1]$. It should be noted that the definition of Risk defined in the context of hydrologic designs here is different from the traditional use of risk as the product of probability and consequence.

Following the above definition, R is given by

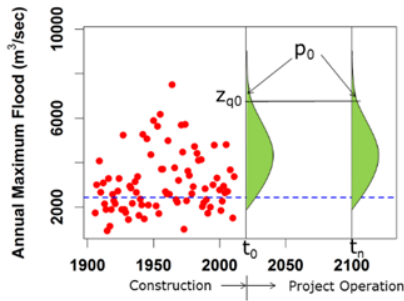
$$R = P[Y \geq 1] = 1 - P[Y = 0] = 1 - (1 - p_0)^n \quad (15)$$

Note that Eq. (25) suggests that risk, R , is only a function of $T = 1/p_0$ and n , and computing it does not require the knowledge of the underlying extreme value distribution. In addition, a more general definition of hydrologic risk may consider the probability of the occurrence of y or more events exceeding the design level, i.e., $P[Y \geq y]$ during the n -year period. This will require integrating Eq. (24) as

$$R = P(Y \geq y) = \sum_{j=y}^n \binom{n}{j} p_0^j (1 - p_0)^{n-j} \quad , \quad y = 1, \dots, n \quad (16)$$

Furthermore, another quantity of interest for project evaluation and design is the expected number of events (ENE) exceeding the design event over the n -year period, i.e. $E[Y] = np_0$.

(a) Stationary Case



(b) Nonstationary Case

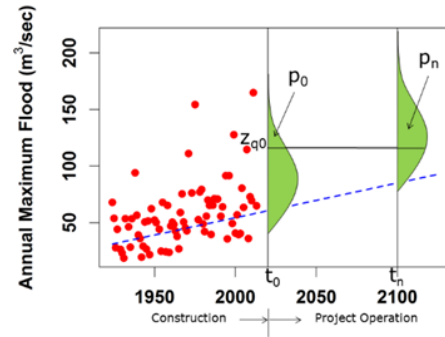


Figure 3-19. Examples of stationary and nonstationary annual maximum floods for (a) stationary, and (b) nonstationary. The dashed line in each figure is the fitted location parameter using a stationary and nonstationary GEV distribution respectively for each case. The variables t_0 and t_n denote the beginning and end of the project design life, n , respectively. In addition, z_{q0} is the design quantile, and p_0 and p_n denote exceedance probabilities (area of PDF above the design quantile) (Adapted from Obeysekera and Salas, 2020).

3.5.4. Extension to a Nonstationary Paradigm

In this section, the evaluation and design methods summarized in the previous section under stationarity will be extended to nonstationarity. Figure 3-19(b) illustrates a situation of nonstationarity where the annual flood maxima show an increasing pattern. At this location, the annual maximum floods have been increasing over the years, likely due to increasing urbanization as indicated by a doubling of population from the 1930s to 1990s. Unlike the stationary case where the probability p_0 is expected to remain constant in the future, the probability exceeding the design quantile z_{q0} will increase over time from p_0 to p_n at the end of the design life, n (Fig. 14b). Since the exceedance probability, p_t increases for $t=1, 2, \dots, n$, the traditional geometric distribution with constant p is not applicable. The time-varying p can be obtained readily from a fitted time-varying model as $p_t = 1 - F_Z(z_{q0}, \theta_t)$ where the subscript t in θ indicates that the underlying Probability Distribution Function (PDF) of annual maxima changes with time, and hence nonstationary (note that we assume that the type of PDF is the same, but the parameters vary with covariates that evolve with time). In this case, the waiting time, X , for the first occurrence of an event exceeding z_{q0} (i.e., waiting time) follows a nonhomogeneous geometric distribution (Mandelbaum et al., 2007; Salas and Obeysekera, 2014). As in the stationary case, the concept of Expected Waiting Time (EWT) will now be extended but for a situation with time-varying probabilities, p_t .

The derivation of EWT under nonstationarity may be found in Cooley (2013) and Salas and Obeysekera (2014). This leads to a convenient formula for EWT, which we denote as T given by

$$T = 1 + \sum_{x=1}^{\infty} \prod_{t=1}^x (1 - p_t) \quad (17)$$

In practice, the increasing values of p_t will converge the product to zero quickly and a finite, but the somewhat large value of x , say x_{max} may be adequate instead of the infinite summation shown in Eq. (27). Since $p_t = 1 - F_Z(z_{q0}, \theta_t)$ and the initial design return period is $T_0 = 1/p_0$, a curve of T versus T_0 can be constructed for a given sequence of p_t values. This is called the “Return Period Curve” (Salas and Obeysekera, 2014) and it is a convenient design tool for nonstationary situations (see Figure 3-20). It can be used to answer questions such as “What should be the design T_0 if the desired EWT, T , is say, 50 years?” Clearly, for increasing extreme events, $T < T_0$. We will illustrate this case with an example in the next section.

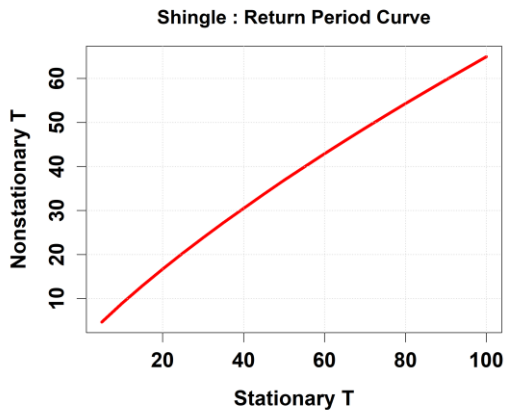


Figure 3-20. Example return period curve.

The risks under nonstationarity can be derived using an approach similar to the stationary case but it is somewhat more complex. Assuming, once again that Y is the number of events exceeding the design quantile z_{q0} over the design life n with possible values $y = 0, 1, 2, \dots, n$, the Probability Mass Function (PMF), which is equivalent to the Binomial Distribution in the stationary case, is given by the Poisson Binomial Distribution (Obeysekera and Salas, 2016),

$$P[Y = y] = \sum_{A \in \mathcal{F}_y} \prod_{j \in A} p_j \prod_{i \in A^c} (1 - p_i) \quad , \quad y = 0, 1, \dots, n \quad (18)$$

where \mathcal{F}_y is the set of all subsets of y integers that can be selected from $\{1, 2, 3, \dots, n\}$, and A^c is the complement of A with respect to $\{1, 2, \dots, n\}$. While Eq. (28) can be used to determine the risk $R = P(Y > y)$, as mentioned in Obeysekera and Salas (2016), the computation of the PMF given by Eq. (28) is cumbersome, particularly for large n . For the particular case where $y=0$, i.e. $R = P(Y > 0) = 1 - P(Y=0)$, one may use the simple nonstationary risk formula (Salas and Obeysekera 2014),

$$R = P[Y \geq 1] = 1 - P[Y = 0] = 1 - \prod_{t=1}^n (1 - p_t) \quad (19)$$

Since the time-varying probabilities, p_t can be determined for a given initial design quantile, z_{q0} , the computation of the risk, R , using Eq. (29) is straightforward. An example demonstrating the effect of nonstationarity on Risk is illustrated in Figure 3-21.

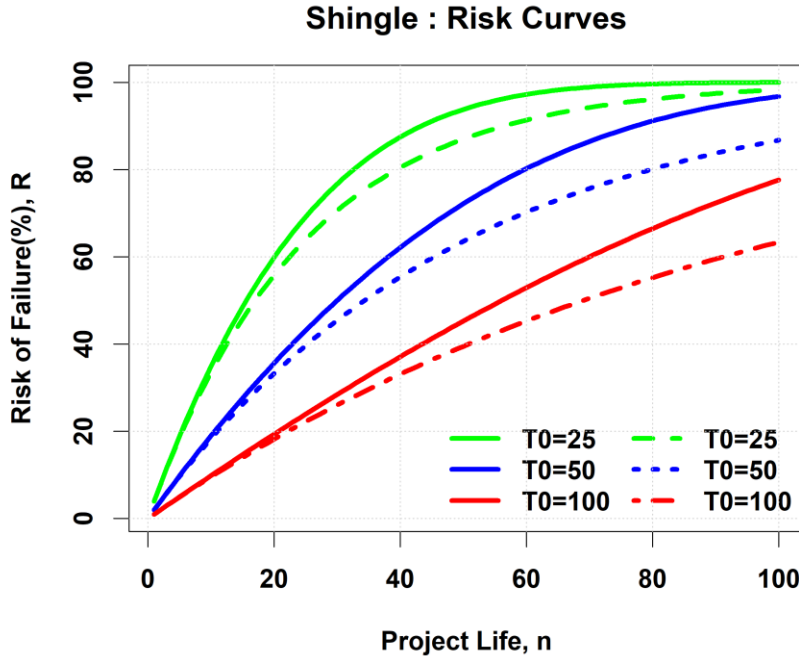


Figure 3-21. An example demonstrating changes in the magnitude of risk due to nonstationarity as a function of the project life, n . The dashed lines in this figure correspond to the stationary case, and as shown, risk naturally increases for projects with longer project life. In each case, the corresponding nonstationary curve is shown as a solid curve. Three cases corresponding to the initial return period, $T_0 = 25, 50,$ and 100 years are shown.

Another quantity of interest is the frequency of extreme events, which varies with time for nonstationary conditions. In case of increasing probabilities of exceedance, the frequency of extreme events exceeding the initial design level z_{q0} will increase with time. The expected number of events, ENE, over the design life n is a measure that may be used for evaluating existing projects or as a design criterion for future projects (Obeysekera and Salas, 2016). Although the computation of the PMF given by Eq. (28) is cumbersome, the expected value and the variance of Y are simpler and can be determined from

$$E[Y] = \sum_{t=1}^n p_t \quad (20)$$

$$Var[Y] = \sum_{t=1}^n p_t (1 - p_t) \quad (21)$$

It is straightforward to show that, under stationarity conditions, i.e., $p_t = p_0$ for all t , then $E[Y] = np_0$ and $Var[Y] = np_0(1 - p_0)$ which correspond to the first two moments of the Binomial Distribution as stated above in the previous section.

Further details of the above concepts can be found in Salas et al. (2018). The application of the methods will be further illustrated in Section 3.6.

3.6. Development of Nonstationary Methods for Key Environmental Drivers

Using the methods described in Section 3.5, it is now possible to demonstrate their application to Florida-specific data described in Section 3.3. In this section, the application focuses on (a) extreme rainfall including the mapping of Change Factors; (b) Peak discharge at USGS gauges, and (c) Sea Level extremes at the four tide gauges identified in the Data Assembly section.

3.6.1. Rainfall

3.6.1.1. Comparison of DDF

DDF curves were generated at the 242 ATLAS 14 stations using the Change Factors from the statistically downscaled LOCA dataset as described in Section 3.3.1. An example of the DDF curves at Jacksonville International Airport is presented in Figure 3-22. The plot shows the ATLAS 14 values, its 5th, and 95th percentile, the ATLAS14 values multiplied by Change Factors (ATLAS 14 x CF), and its 17th and 83rd percentile. The FDOT rainfall is presented in the 1-day plots. In most cases (except some South Florida stations), the 83rd percentile of ATLAS 14 x CF is higher than the upper bound (95th percentile) of the ATLAS14 rainfall depth as shown in Figure 3-22. The complete set of comparison plots will be included in the data transfer as specified in Section 5.2

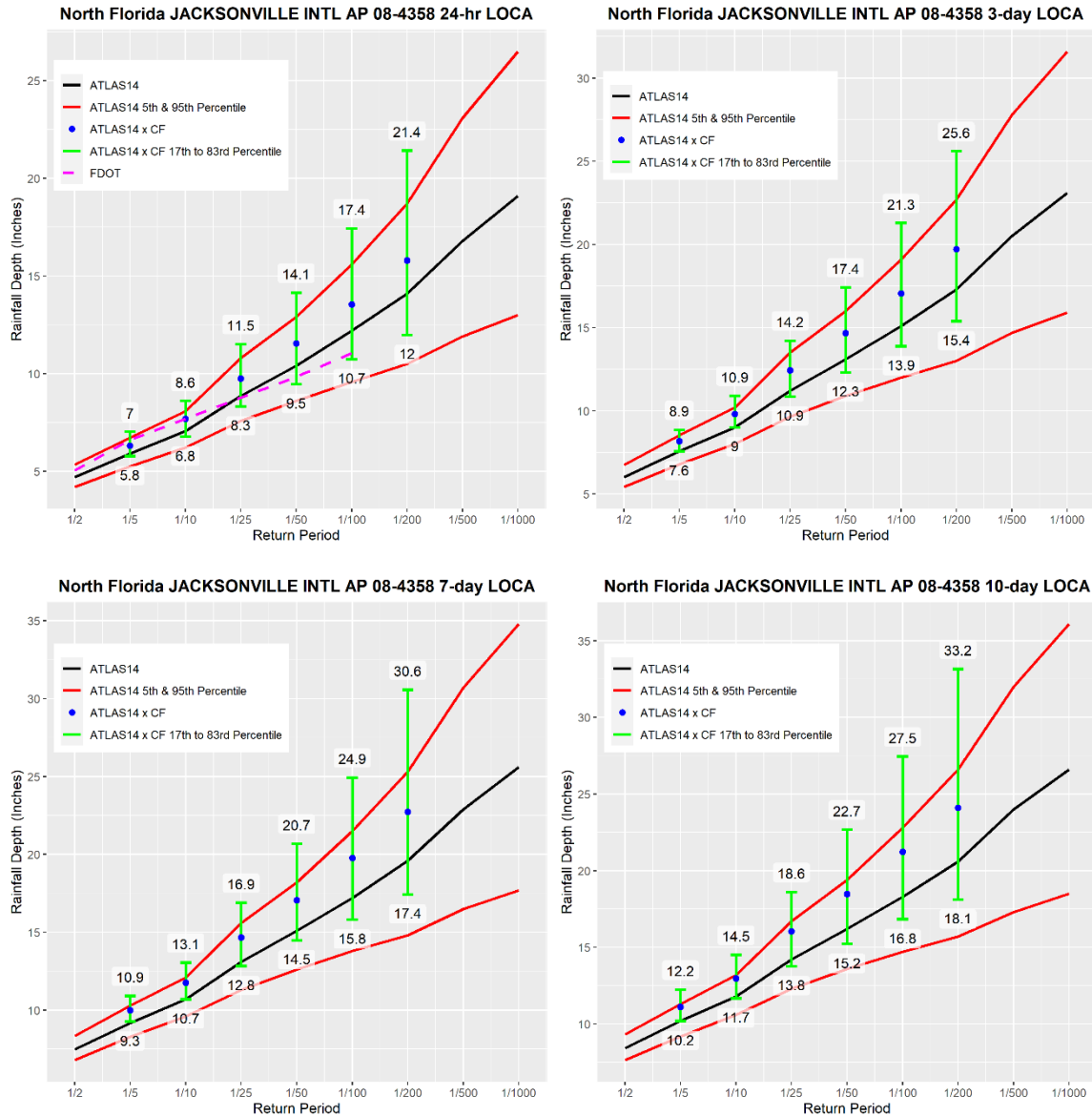


Figure 3-22. DDF curves generated for 1-day, 3-day, 7-day, and 10-day storms using the ATLAS 14 data and change factors from downscaled data at the Jacksonville International Airport station.

3.6.1.2. Spatial Mapping of Change Factor

For computing the spatial distribution of Change Factor, the following downscaled, climate data sets were used.

1. Localized Constructed Analogues (LOCA), statistically downscaled, 1/16thdeg (~ 6 km) resolution
2. Multivariate Adaptive Constructed Analogs (MACA), statistically downscaled, 1/16 deg (4, 6 km) resolution

3. Coordinated Regional Downscaling Experiment (CORDEX), dynamically downscaled, (25 and 50 km) resolution

Typically, each climate model data set is available for the period 1950 through 2099, covering both historical and future periods. The goal was to compute the CF for each grid cell corresponding to the downscaled climate dataset (LOCA, MACA, and CORDEX). A rigorous statistical modeling approach for computing DDF curves from the climate datasets (historical and future periods) was used. For the results shown below, the historical period was 1950:1999 whereas the future period was 2050:2099, both equal 50 years in length. Historical and future DDF curves were produced using the Peaks Over Threshold (POT) approach involving the Generalized Pareto Distribution (GPD). The ratio of the DDF estimates corresponding to future and historical periods computed from climate model datasets yielded the CF for all grid cells. For illustration, the daily rainfall was used, and the CF values were computed for the Return Periods, 5, 10, 25, 50, 100, and 200 years. For determining spatial contours of equal CF, the values were first smoothed by using a two-dimensional LOESS algorithm. An example of resulting spatial maps is shown in Figure 3-23. The complete set of spatial maps is included as part of the data transfer described in Section 4.

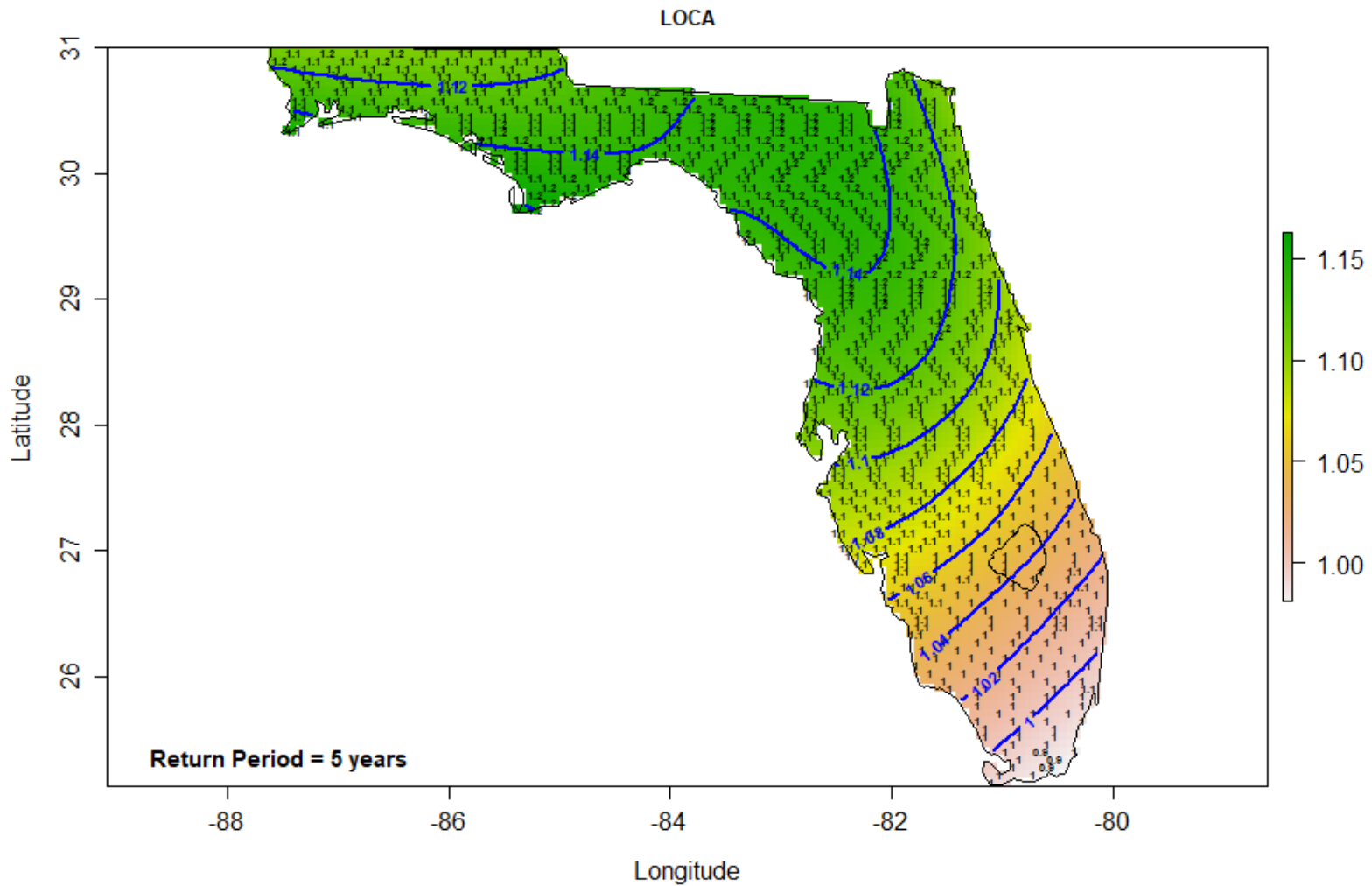


Figure 3-23. Spatial maps of change factors derived from the LOCA dataset corresponding to the return period of five years. Sample values in selected grid points and the contours using a smoothing algorithm are also shown.

3.6.2. Sea Level

This section illustrates the application of nonstationary methods described in Section 3.5 for tide gauge locations (Figure 3-5). Here the same approach used in the NOAA 2022 report (Sweet et al., 2022, Section 3.5) was used with one exception, which is explained below. The SLR scenarios used for this illustration are from the NOAA 2017 report (Sweet et al., 2017) and are required to be used for vulnerability assessments in the State of Florida. The NOAA 2022 report (Sweet et al., 2022) provides a new set of projections based on new science and the extrapolations of observations. It is noted that, if necessary, the applications documented below can be extended easily to the NOAA 2022 report (Sweet et al., 2022) projections.

As stated in NOAA 2022 report (Sweet et al., 2022), one of the primary tasks in coastal infrastructure projects is to determine the design elevation (also known as return level) of a particular structure (e.g., seawall, road crown, or first-floor elevation of a building) for a desired level of risk or probability. They typically require the knowledge of advanced statistical methods associated with extreme values such as those illustrated in the commonly referenced textbook by Coles (2001) (see Section 3.5). Results of the application of such methods (as in Sweet et al., 2022) for all 14 tide gauges in Florida shown in Figure 3-5 are presented below.

The regional frequency analysis (RFA)-based extreme water level (EWL) distribution parameters are provided in **Error! Reference source not found.** These were available from the federal report published by NOAA (Sweet et al., 2022). The EWL probability parameters are necessary to replicate this use case, and they are specifically from a generalized Pareto distribution (GPD) peaks-over-threshold approach (see Section 3.5.2, and Sweet et al., 2022): (a) the local Index, u ; (b) rate of exceedances above the local index, λ ; (c) scale, σ_{RFA} ; and (d) shape, ξ , and the slope of the current sea level curve from 1992 to 2000. In the examples below, NOAA 2017 (Sweet et al., 2017) intermediate-high curve is used. Both the SLR (RSL) scenario and the return level curves are referenced to Year 2000.

As in the NOAA 2022 report (Sweet et al., 2022), it is assumed that only the location parameter (i.e., local index, u in GPD) changes as a function of the SLR scenario (i.e., RSL). This may be expressed as

$$F(z) = GPD(u(RSL), \sigma, \xi) \quad (22)$$

where u is the GPD local index that is a function of RSL, and σ and ξ are scale and shape parameters, respectively, which are assumed to be constant over time. Because of the above assumption, the local index u is adjusted by a magnitude δ (i.e., the regional mean sea level change from the reference year) obtained from the selected scenario.

For planning infrastructure using the scenario's RSL projections and the EWL probabilities, two approaches are illustrated: (1) recurrent flood frequency and (2) time-varying average recurrence interval and risk. While the infrastructure designs are based on a variety of factors, one or both

approaches may be used to support that process (e.g., the height of a sea wall, road crown elevation, or base-flood elevation of a building). In this use case, the term “flood” could pertain to a particular NOAA High Tide Flood (HTF) level or an arbitrary probabilistic EWL level.

Table 3-5. Regional frequency analysis (RFA)-based extreme water level (EWL) distribution parameters.

Tide Gauge Location Details		RFA-based GPD parameters				Slope (m/year)
NOAA ID	Location	Local Index u	λ	σ_{RFA}	ξ	
8720030	Fernandina Beach, FL	0.473	3.01	0.179	0.227	0.0023
8724580	Key West, FL	0.262	2.97	0.195	0.364	0.0025
8729840	Pensacola, FL	0.345	2.85	0.212	0.456	0.0024
8720218	Mayport, FL	0.378	3.01	0.179	0.227	0.0026
8727520	Cedar Key, FL	0.415	2.96	0.270	0.375	0.0022
8726520	St Petersburg, FL	0.337	2.99	0.266	0.354	0.0028
8725520	Fort Myers, FL	0.325	2.98	0.199	0.375	0.0031
8725110	Naples, FL	0.323	2.98	0.199	0.375	0.0029
8728690	Apalachicola, FL	0.390	2.95	0.257	0.402	0.0030
8726724	Clearwater Beach, FL	0.294	2.99	0.266	0.354	0.0071
8729108	Panama City, FL	0.368	2.88	0.238	0.432	0.0025
8723970	Vaca Key, FL	0.249	2.97	0.195	0.364	0.0042
8723214	Virginia Key, FL	0.317	3.00	0.152	0.251	0.0051
8721604	Trident Pier, FL	0.407	3.00	0.178	0.198	0.0051

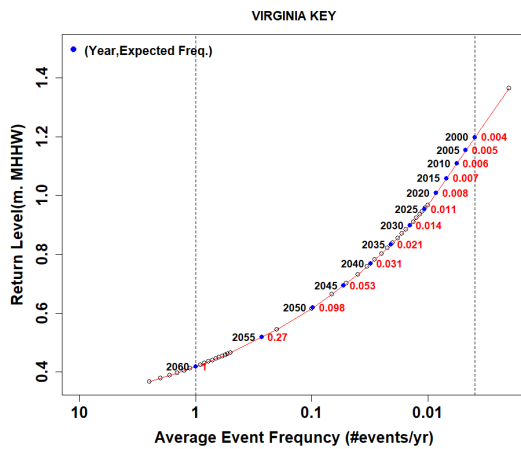
Designs based on Recurrent Flood Frequency. Using the extreme value distributions and the sea level scenarios, it is possible to predict the time-varying change in frequency. In the case of GPD, the recurrent flood frequency (number of exceedances above a return level [z]) may be computed as (Buchanan et al., 2017)

$$N(z, \delta) = \lambda \left(1 + \frac{\xi(z - [u + \delta])}{\tilde{\sigma}} \right)^{-\frac{1}{\xi}} \text{ for } \xi \neq 0 \quad (23)$$

where δ is the change in RSL (relative to the project construction year).

The planning problem may be stated as follows: What should the initial return level (used for the design) be to ensure that the recurrent flood frequency is limited to a specified number of events at the end of the design life? It is now possible to lay this out graphically, as shown in **Error! Reference source not found.** for two tide gauges.

(a)



(b)

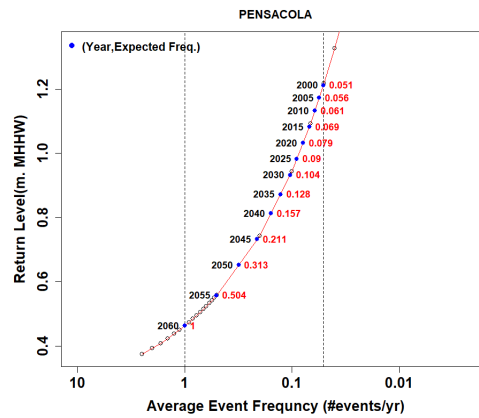


Figure 3-24. Recurrent flood frequency estimates for (a) Virginia Key, Florida, and (b) Pensacola, Florida. Note: to be useful for decision-making, a conversion of the return level to land-based heights (e.g., geodetic datum such as NAVD88) should be made.

In **Error! Reference source not found.**, the number to the right of each point along the curve shows the recurrent flood frequency, N , corresponding to the year indicated on the left. In this case, it was assumed that by 2060, the desired value of $N = 1$, and the design event frequency (#events/yr) necessary for this criterion, are indicated in **Error! Reference source not found.** A summary of results for all 14 tide gauges is shown in **Error! Reference source not found.** The design return period required in 2000 to meet the flood frequency criteria shows significant variability across the sites. The design return level (and the design average recurrence interval) depends on the slope (a function of the scale and shape parameters) of the return level curve.

Design Based on Time-Varying Exceedance Probabilities

The application of time-varying recurrence interval and risk concepts is illustrated by converting the GPD model to an equivalent annual maxima model, which in this case is the GEV distribution (Coles, 2001). The equivalent annual-maxima modeling approach, as used here, will also facilitate the direct application of emerging risk and recurrent interval concepts already developed for situations of time-varying extreme probabilities (Salas and Obeysekera, 2014; Salas et al., 2018; Obeysekera and Salas, 2020).

The cumulative distribution function (CDF) of the GEV model of annual maxima is expressed as

$$F(z) = \exp \left\{ - \left[1 + \xi \left(\frac{z - \mu}{\sigma} \right) \right]^{-1/\xi} \right\} \quad (24)$$

where μ, σ, ξ , are the location, scale, and shape parameters of the GEV (Coles 2001).

Table 3-6. Summary of design parameters (with numbers rounded) to constrain the recurrent flood frequency, N , to one per year by 2060 (end-year of the design life).

NOAA ID	Location	Relative sea level rise (in meters from 2000 to 2060)	Return level (m above 1983-2001 MHHW) corresponding to AEF = 1-year	Return level (m above 1983-2001 MHHW) required in 2005 to ensure $N = 1$ by 2060	Design Average Recurrence Interval (in years) required in 2005 to ensure $N = 1$ by 2060
8720030	FERNANDINA BEACH	0.79	0.597	1.39	73
8720218	KEY WEST	0.78	0.351	1.13	72
8720357	PENSACOLA	0.75	0.462	1.21	20
8720587	MAYPORT	0.79	0.483	1.27	133
8721604	CEDAR KEY II	0.75	0.583	1.33	14
8723214	ST. PETERSBURG	0.8	0.48	1.28	25
8723970	FORT MYERS	0.78	0.436	1.22	41
8724580	NAPLES	0.78	0.433	1.21	41
8725110	APALACHICOLA	0.74	0.55	1.29	14
8725520	CLEARWATER BEACH	0.81	0.456	1.27	34
8726384	PANAMA CITY	0.73	0.505	1.24	16
8726520	VACA KEY	0.79	0.348	1.14	82
8726607	VIRGINIA KEY	0.78	0.419	1.20	255
8726667	TRIDENT PIER	0.78	0.537	1.32	149

For computing μ , the local index is further adjusted to reflect the translation of the return level curve from 2000 to the reference year (i.e., 2005). The GEV scale parameter, $\sigma = \tilde{\sigma}\lambda^\xi$, where the at-site scale parameter $\tilde{\sigma}$, is computed as $\tilde{\sigma} = \sigma_{RFA} * u$. Finally, the time-varying GEV model assumes that only the location parameter, μ , changes with sea level change, δ , and the time-varying annual extreme value distribution is given by

$$F^t(z, \delta) = \exp \left\{ - \left[1 + \xi \left(\frac{z - (\mu + \delta)}{\sigma} \right) \right]^{-1/\xi} \right\} \quad (25)$$

With sea level rise, the exceedance probability, p_t , corresponding to an initial return level (z_{q0} , initial design), changes with time because of the rising RSL, δ . Consequently, the average recurrence interval is not a fixed measure but decreases with increasing sea levels.

The traditional concept of the average recurrence interval or ARI is the average waiting time between two successive exceedances of the return level. Using the same definition but in a time-varying exceedance probability framework an equivalent measure of average recurrence interval, T , may be derived as (Cooley, 2013; Salas and Obeysekera, 2014).

$$T = 1 + \sum_{x=1}^{\infty} \prod_{t=1}^x (1 - p_t) \quad (26)$$

where $p_t = 1 - F^t(z, \delta)$ is the time-varying exceedance probability. If a project is designed for a return period, $T_0[t = t_0]$, then $T < T_0$ implies that the actual recurrence interval due to rising RSL will be less.

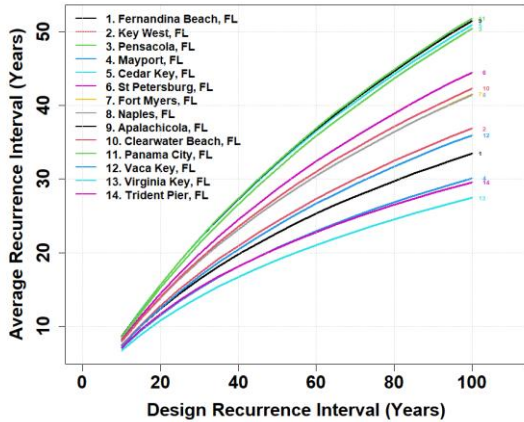
The methods described in the preceding paragraphs are applied to the 14 tide-gauge locations shown in Figure 3-5. For illustration, it was assumed that the projection scenario for each tide gauge would continue beyond 2060. However, the methodology described above can be used with any other scenario. The derived GEV parameters for each gauge are shown in **Error! Reference source not found.**

Table 3-7. The parameters of GEV computed using the peaks-over-threshold GPD model (Coles 2001).

NOAA ID	Location	GEV location parameter	GEV scale parameter	GEV shape parameter
8720030	FERNANDINA BEACH	0.620	0.109	0.227
8720218	KEY WEST	0.371	0.076	0.364
8720357	PENSACOLA	0.484	0.118	0.456
8720587	MAYPORT	0.503	0.087	0.227
8721604	CEDAR KEY II	0.606	0.168	0.375
8723214	ST. PETERSBURG	0.498	0.132	0.354
8723970	FORT MYERS	0.452	0.097	0.375
8724580	NAPLES	0.450	0.097	0.375
8725110	APALACHICOLA	0.567	0.155	0.402
8725520	CLEARWATER BEACH	0.440	0.115	0.354
8726384	PANAMA CITY	0.526	0.138	0.432
8726520	VACA KEY	0.355	0.072	0.364
8726607	VIRGINIA KEY	0.419	0.063	0.251
8726667	TRIDENT PIER	0.537	0.090	0.198

The average recurrence interval curves, T , as a function of T_0 , for all 14 tide gauge locations are shown in **Error! Reference source not found.**(a). This figure demonstrates that, in all cases, the actual average recurrence interval is less than the design recurrence interval. For instance, for a location near Pensacola, Florida, if a project is designed for $T_0 = 100$ years, the actual average recurrence interval, due to accelerating RSL rise, is only about 50 years.

a)



b)

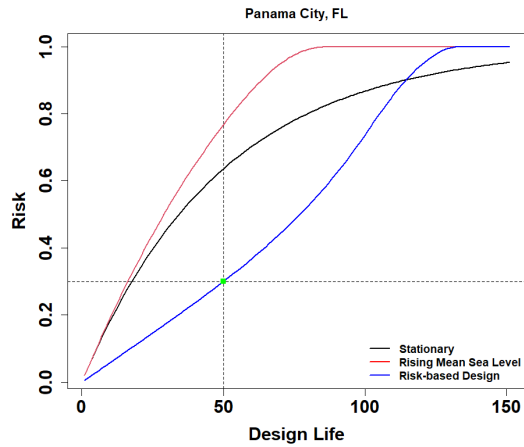


Figure 3-25. (a) Actual average recurrence interval (due to rising mean sea level) curves (T versus T_0) at each tide gauge. (b) Risk curves as a function of design life: Stationary (black curve), the actual risk resulting from rising relative sea level rise (red curve), and risk curve for a specific risk (blue curve).

Risk-Based Design

Under stationary conditions, the risk (defined as the probability of one or more exceedances above the design elevation) is a function of the life of the project, n . The risk formula under stationarity is given by $R = 1 - (1 - \frac{1}{T_0})^n$. As the length of the design life increases, risk also increases. Under conditions of time-varying exceedance probability, p_t , the risk (R) formula is (Salas and Obeysekera, 2014)

$$R = 1 - \prod_{t=1}^n (1 - p_t) \quad (27)$$

With rising relative sea levels, p_t increases and the risk is higher than that under stationarity. This increase in risk is illustrated for the Pensacola, Florida, tide gauge in **Error! Reference source not found.**(b) when the initial design, $T_0 = 50$ years. The black curve in **Error! Reference source not found.**(b) shows the increasing risk as the design life becomes longer even under stationarity. For instance, if the Design Life, $n = 50$ yrs, this risk is about 0.6 (60%). However, when sea level rise is incorporated, the risk over a given life of the project increases more rapidly, exceeding the corresponding risk under stationarity (see the red curve in **Error! Reference source not found.**(b)). In the above example, when $n=50$ yrs, the risk will increase to about 75% due to rising sea levels. Moreover, the rising sea level causes the risk to approach 100% ($R = 1$) when the design life is about 75 years or more. In the risk-based design approach, one can specify the tolerable risk and determine the initial design period (or return level).

One option is to design a project in such a way that the resulting increased risk profile due to the nonlinear RSL trend is at or below that under stationarity. While the risk reduction approach described below is illustrated for a selected RSL scenario for the future, it can be implemented for multiple scenarios leading to a variety of risk-reduction options depending on the future RSL scenarios. In such a broader application, a risk-based framing founded on risk tolerance may be adopted.

Considering uncertainty in the sea level rise projections, one may wish to approach the problem using concepts of dynamically adaptive planning. In the example shown in Figure 3-25(b) (blue curve), two parameters are specified to illustrate this concept. First, it is assumed that the project will be constructed in, for example, two or more phases. Considering such a planning assumption, phase I is 50 years long (i.e., $n = 50$ years), and the maximum tolerable risk during this phase is 0.3 (30%) as opposed to the 75% risk mentioned above. The blue curve shows the risk profile for such a design. This curve was computed by constraining risk, $R=0.3$ when $n=50$, as shown by the green dot in Figure 3-25(b). One implication of this adaptive approach is that the initial return level will need to increase from 1.93-m MHHW to 3.15-m MHHW (Table 3-8), and the corresponding initial average recurrence interval or return period must increase from 50 years to 174 years. Such an increase in the design period is not surprising given the risk tolerance of 30% during the life of the project. If this risk tolerance is less (say 50%), then the required design is smaller. The purpose of this example is to demonstrate how the nonstationary approach may be used for developing a risk-based design.

Finally, in this approach, one must also assume that the project will be expanded after that initial period, and measures must be adopted not to lock in the design and preempt the planners from expanding it into a bigger project after say, the initial 30-year period. For example, the foundation design of the project may need to assume the eventual capacity expansion and allow for it in the initial design. This approach of dynamically adaptive planning is becoming increasingly popular to deal with deep uncertainties associated with sea level rise.

Table 3-8 shows that with a relatively small increase in initial design elevation, the risk can be managed to a desirable level. In this example, however, the ultimate design (at the end of the full design life; e.g., 50 or 100 years) needs to be assessed to ensure that resources (e.g., land) may be needed for the build-out.

Table 3-8. Results of the Risk-Based Design for all tide gauges shown in Figure 3-5. Values in the last column have been rounded to the closest 5-year interval.

NOAA ID	Location	Design return level for $T_0 = 50$ years (m MHHW)	Design return level to constrain risk to 30% over a 25-year period (m MHHW)	Average Recurrence Interval (ARI) of the design to constraint probability (Risk) to 30% over a 25-year period
8720030	FERNANDINA BEACH	1.30	1.93	333
8720218	KEY WEST	1.03	1.72	249
8720357	PENSACOLA	1.76	2.94	174
8720587	MAYPORT	1.05	1.62	419
8721604	CEDAR KEY II	2.10	3.28	176
8723214	ST. PETERSBURG	1.61	2.56	199
8723970	FORT MYERS	1.31	2.12	212
8724580	NAPLES	1.31	2.11	212
8725110	APALACHICOLA	2.03	3.23	173
8725520	CLEARWATER BEACH	1.41	2.27	210
8726384	PANAMA CITY	1.93	3.15	171
8726520	VACA KEY	0.98	1.65	257
8726607	VIRGINIA KEY	0.84	1.37	508
8726667	TRIDENT PIER	1.07	1.62	474

3.6.3. Peak Discharge

Only about 9 gauges in the USGS datasets (out of about 100) showed an increasing trend indicating possible nonstationarity. There was no effort to identify the causes of such nonstationarity at each of the discharge locations. When such an increasing trend is present, planning of infrastructure needs to incorporate nonstationarity concepts described in Sections 2.4 and 3.5. For a demonstration of the nonstationary approach, the data at Shingle Creek at Campbell are used below. As shown in Figure 3-26, the time series plot of annual peak discharge, Q , as a function of time (i.e., Year) shows a statistically significant trend with a p-value of about 0.04.

As a first step, various extreme value models were fitted to determine which type of model (e.g., Gumbel vs. GEV) and nonstationarity would be most appropriate for this discharge location (See Section 3.5.2). In this step, various combinations of nonstationarity in both location and scale parameters were assumed. As a generally accepted guideline, the shape parameter is assumed to be fixed unless there is a valid reason for modeling its nonstationarity. The results of various model combinations are shown in Table 3-9.

Table 3-9. Results summarized for the various combinations of the Gumbel - GEV models.

#	Model	Comparison of Models	Negative Log-Likelihood	Number of Parameters	Deviance Statistic	Tabulated Chi-Squared value	p-Value	Akaike Information Criterion, AIC
1	GUM	NA	327.98	2	NA	NA	NA	660.0
2	GUMMU	2 vs. 1	325.47	3	5.02	3.841	0.025	656.9
3	GUMSC	3 vs. 1	327.92	3	0.11	3.841	0.739	661.8
4	GUMMUSC	4 vs. 2	325.51	4	-0.08	3.841	1.000	659.0
5	GEV	5 vs. 1	327.94	3	0.08	3.841	0.783	661.9
6	GEVMU	6 vs. 5	325.21	4	5.47	3.841	0.019	658.4
7	GEVSC	7 vs. 5	327.52	4	0.84	3.841	0.360	663.0
8	GEVMUSC	8 vs. 6	325.23	5	-0.04	3.841	1.000	660.5

*Model naming follows the following convention: First three letters identify the fitted probability distribution (Gumbel or GEV) followed by the parameters, mu (location), and sc (scale) parameters that were assumed to be nonstationary (function of time)

Details of model selection based on the results of various statistics given in Table 3-9 are well covered in textbooks such as Coles (2001) and they will not be repeated here. Based on the p-value (below .05) and the lowest AIC statistic from the last two columns of the above table, the GUMMU model was chosen as the best model (highlighted in Table 3-9). This model name implies that the best model is Gumbel and the nonstationarity is incorporated as a trend in the location parameter (μ). A plot of the data and the temporal variation of the location parameter is shown in Figure 3-26.

SHINGLE CREEK at CAMPBELL

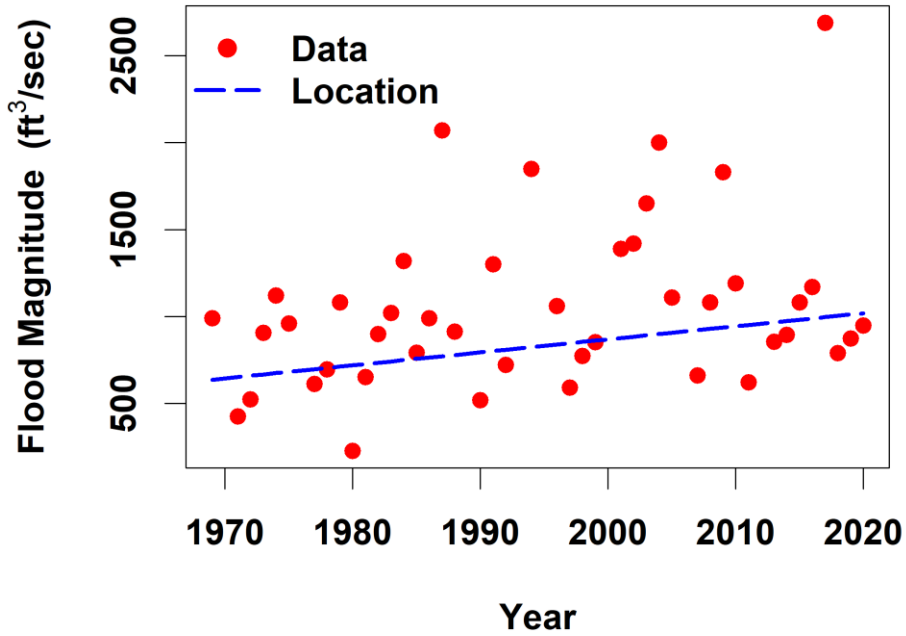
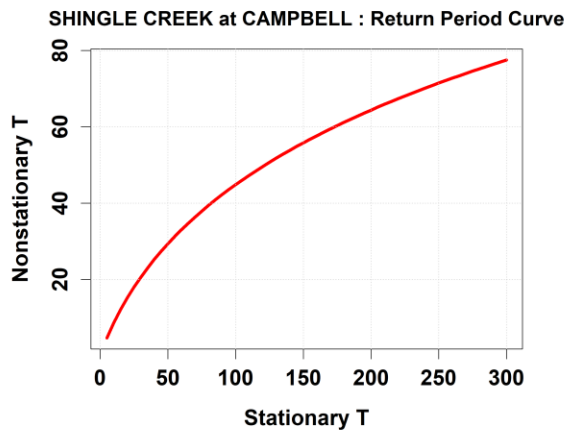


Figure 3-26. Temporal variation of the location parameters with the flood magnitude data.

The nonstationary return period curve and the risk curves are shown in Figure 3-27.

(a) Return Period Curve



(b) Risk Curve

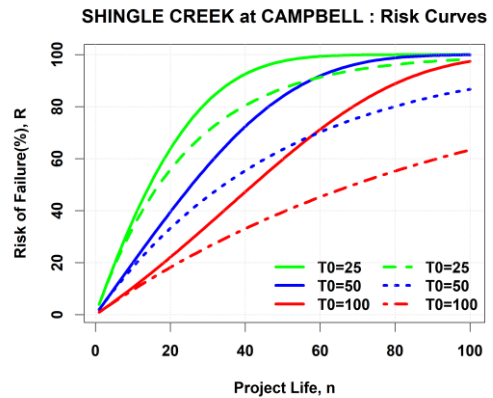


Figure 3-27. The nonstationary return period curve and the risk curves.

3.6.3.1. Example risk-based application of FDOT Projects

Two primary characteristics of projects are important in the context of applying nonstationary methods. First, the type of project (Open Channel, Storm Drains, Cross Drains) and the associated Design Frequency are relevant. Under nonstationarity, the concept of design frequency needs to be revisited. The FDOT Drainage Manual (FDOT, 2021a) provides guidance on this information. The second parameter of importance is the Design Service Life (DSL). For illustrative purposes, a Cross Drain project (e.g. bridge) with a DSL of 50 years and a Design Frequency of 100 years is used in the ensuing sections. The demonstration of how a risk-based nonstationary approach for planning and design may be used is shown in Figure 3-28. The assumption on risk threshold is only for illustration of the approach. Variations of the type of project, Design Frequency, DSL, and the risk threshold will not affect the use of this nonstationary approach based on risk.

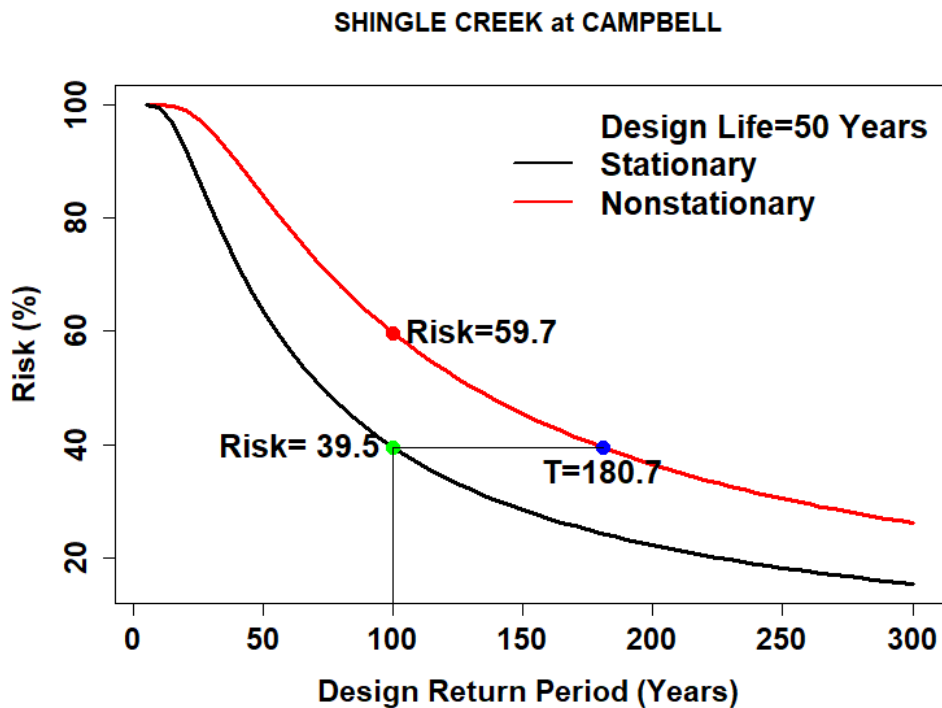


Figure 3-28. Risk-based nonstationary approach for planning and design.

The two curves in this figure show the stationary (lower black curve) and the nonstationary (upper red curve) risk profiles as a function of the design return period for a project with a design life of 50 years. As expected, the risk of failure under nonstationary conditions is higher (the red curve is above the black curve). If a project is designed for $T = 100$ -year return period, the risk of failure is 39.5% and 59.7% under stationary and nonstationary conditions respectively. If there is a desire to reduce the nonstationary risk to say, stationary risk (i.e., 39.5%), then, the figure shows that the project must be designed to $T = 180.7$ years. This will result in a larger design discharge and, the cost will be larger. This is the cost of reducing future risk to address

nonstationarity. It should be noted that increasing the project capacity to address nonstationarity depends on numerous other factors besides cost (e.g., risk tolerance). Ideally, the benefits of maintaining a desired risk profile by avoiding, say, service disruptions under nonstationarity, need to be compared with this additional cost of a design with a higher return period. It was beyond the scope of this research project to carry out such an analysis. It is noted that, in some situations, the current infrastructure practice may already include a sufficiently large safety factor (e.g., larger diameter pipe in a culvert) that will provide the necessary risk drawdown.

3.7. Conclusions

The overall objective of this chapter was the development of datasets and methods for incorporating nonstationarity in transportation project design. The chapter focused on three hydrologic drivers that are typically used for planning and design: (a) extreme rainfall; (b) peak discharge in canals, rivers, and creeks; and (c) sea levels along the coastline.

The first major task was to assemble the historical data for these drivers but only within the State of Florida. As with any nonstationary approach, the first task is to detect statistically significant trends for both current and future periods. Only when such trends are significant, the nonstationary approaches should be considered in future planning. The theoretical basis for trend detection was described in detail. In addition, the recent research for revisiting the traditional concepts of return period and risk was summarized in detail.

In the case of rainfall, the focus was on the best available Depth-Duration-Frequency (DDF) curves published by NOAA and known as Atlas 14. There was no attempt to detect trends in historical rainfall. However, downscaled, climate-downscaled datasets were used to assess the potential changes to such DDF curves. For this analysis, the downscaled LOCA dataset was used. First, Change Factors (CF, percent change in extreme rainfall from current to future) computed for a prior study conducted for the Florida Building Commission (FBC) were compared with the uncertainty bounds of the Atlas 14 estimates. At many locations, the 83rd percentile rainfall of the Change Factor values lay outside the 95th percentile values of the ATLAS 14 upper bounds. DDF curves comparison using Change Factors from MACA and CORDEX datasets will be generated as a next step.

A new, gridded set of CF was created by conducting statistical analysis using the Peaks Over Threshold method for each grid cell. Smoothed contours of the CF were drawn for all three climate datasets and return periods of 5-, 10-, 25-, 50-, 100-, and 200- years. These will be useful for incorporating nonstationarity in rainfall by applying the CF to current DDF curves for any location within the State of Florida.

Peak discharge data were collected and reviewed for over 200 stations across the State. Based on the length of records and the frequency of missing values, 99 stations were selected for further analysis. The application of linear regression for trend detection was not possible due to the non-Gaussian nature of the probability distribution of peak discharge data. Instead, the nonparametric method based on the Mann-Kendall test was chosen for detecting trends. This

analysis demonstrated that, at many stations, there was no positive trend in peak discharge data. However, nine stations showed statistically significant trends. Future infrastructure planning and design at these locations may need to consider the presence of systematic trends and hence use the nonstationary methods illustrated in this report.

For sea level extremes, 14 tide gauge locations around the State were selected. The tests for detecting trends at these locations were not needed as it is well known that sea levels are rising as their trends are significant. The application of nonstationary methods was demonstrated for one tide gauge location. For future mean sea level rise scenarios, the curves recommended in the NOAA 2017 report (Sweet et al., 2017) were used. The curves for extreme sea levels were obtained from the Federal report published by NOAA in 2022 (Sweet et al., 2022). Results for all 14 tide gauge locations are available and included as part of the dataset transfer.

4. DEVELOPMENT OF NEW DATASETS FOR APPLYING THE NONSTATIONARY METHODS

4.1. Objective

The research team will assess and assemble the information available for projections of sea level rise, rainfall, and groundwater levels for applications of the nonstationarity methods. The datasets will include both FDOT and other data that are necessary for applying the nonstationarity methods.

As part of Task 3, the research team has put together a dataset. The datasets will be transferred to the Research Center. The following is a description of the datasets included.

4.2. Description of Datasets Included

4.2.1. Rainfall

- NOAA ATLAS 14 Depth Duration Frequency (DDF) estimates

The dataset consists of statistical rainfall depth developed using Regional Frequency Analysis (RFA). The curves are available at 242 locations in Florida. The dataset provides precipitation frequency estimates for storm durations of 5 minutes through 60 days at average recurrence intervals of 1 year through 1000-years.

This data is stored in the *FDOTdataTransfer_DFF* folder. The folder consists of three Microsoft Excel Worksheet files (.xlsx) – one each for mean, 5th (lower bound), and 95th (upper bound) percentile rainfall depths. Each Excel file contains multiple sheets labeled using the recurrence interval (nine recurrence intervals from 2-years through 1000-years) and each sheet contains a table of estimated rainfall depths (in inches) for 242 stations for 19 storm durations of 5-minutes through 60-days.

The *FDOTdataTransfer_DFF* folder also contains a .csv file named *Atlas14_StationInfo* which provides information about the 242 stations including the longitude, latitude, region (*Region.Name*), and climate division (*Cd.New* used in the processing of Change Factors presented below). The *stationID* values, included in the table, can be used as the unique identifier. The RData file named *FL_Atlas14_PDS_DDF* contains the raw data. R file named *DDF_DataTransfer* contains the script used to process the data tables.

- LOCA, MACA, and CORDEX Change Factors

Change factors (CFs) are calculated from statistically downscaled global climate data products. The CFs can then be used to update the DDF estimates of the ATLAS14 data. Such applications can provide extreme rainfall estimates for future periods under different emission scenarios.

For each dataset, both “NEAR” (2030-2069) and “FAR” (2060-2099) periods are covered. The Change Factor for Return Periods (RPs), 5-, 10-, 25-, 50-, 100-, and 200- years for durations 1, 3, 7, and 10 days are provided. The statistics included are the 17th, 50th (median), and 83rd percentiles of model spread, the 90% confidence intervals (*ci90MedL*, *ci90MedH*) for the median, and the mean. The CFs for all 242 Atlas 14 stations are in the dataset.

- Spatial Maps

Spatial maps of Change Factors across Florida were created from daily MACA, LOCA, and COREX at return periods of 5, 10, 25, 50, 100, and 200 years. For determining spatial contours of equal CF, the values were first smoothed by using a two-dimensional LOESS algorithm. The maps are included in the folder *FDOTdataTransfer_SpatialMaps*. The files are named using the data (*MACA*, *LOCA*, and *CORDEX*) along with the return period (*5yr*, *10yr*, *25yr*, *50yr*, *100yr*, and *200yr*).

- DDF Curves with Change Factors

DDF curves were generated at the 242 ATLAS 14 stations using the Change Factors from the statistically downscaled LOCA dataset. The data is included in the folder *FDOTdataTransfer_DDFwithDF*. There are four folders by duration: 1-day, 3-day, 7-day, and 10-day, each containing the .tif files of the plots at the ATLAS 14 stations. The files are named using the Atlas 14 station names.

4.2.2. Peak Discharge

- Annual Peak Flow Data from USGS stations

Annual peak flow data from the 231 USGS stations across Florida were filtered using an R script to select stations with a minimum 40 years of observations and without data gaps that exceed five years. The data from the resulting 99 stations were transferred as csv files and can be found in the *FDOTdataTransfer_PeakDischarge* folder. The files are named ‘*AnnualPeakFlow_*’ followed by station ID. Each .csv file has a table with *Year* and *Value* (annual peak flow in cfs). The .csv files are formatted so the user may directly upload these files to the United States Army Corps of Engineers (USACE) Time Series Toolbox to perform nonstationarity analysis.

The subfolder also contains a .csv file named *_FileInfo* which provides information like the latitude (*Lat*), longitude (*Lon*), and file names (*NewFileName*), which may be identified using the unique *StationID*.

4.2.3. Sea Level

- Hourly Sea Level Data from NOAA Tide Gauges

Tide gauge data available through NOAA's tides and currents were downloaded for 23 stations in Florida. The downloaded data was in the form of NetCDF (.nc) files. Using a Python script, the observed water levels (in feet referenced to Mean Lower Low Water, MLLW) were extracted from each station and exported as a csv file. The csv files are named '*HourlyTidalValues_*' followed by the station ID. Each .csv file has a table with the following columns: *time* (date-time format dd/mm/yyy hh:ss), *ObservedTide* (in ft MLLW), *Year*, *Month*, *Day*, and *Hour*.

The subfolder also contains a .csv file that provides the latitudes (Lat) and longitudes (Lon) for each gauge station identified using their unique station IDs (*StatID*).

4.2.4. Groundwater

The groundwater data is compiled in the *FDOTdataTransfer_GW* subfolder.

- Broward County 2070 Future Conditions Average Wet Season Groundwater Elevation Map 2017

This map was created using Broward County's hydrologic models with the USACE NRC Curve 3 for anticipated sea level rise and future precipitation patterns from the Center for Ocean-Atmospheric Prediction Studies (COAPS) Community Climate System model (CCSM).

The shapefile for the raster layer is in the *BrowardFutureConditions* subfolder.

- Broward County 2070 Future Conditions Average Wet Season Groundwater Elevation Map 2023 Update

The above map was updated with sea level rise (SLR) projections aligned with Southeast Florida's Climate Compact (3.3 ft SLR by 2070).

- Miami Dade 2040 Future Groundwater Level Maps

For planning purposes, Miami Dade County provides two maps for anticipated groundwater elevations in NAVD 88: 1) dry season – month of May, and 2) wet season – month of October. The maps were created from the NRCII forecast, which uses 1.0 feet of sea level rise increase from 2009 (-0.9 ft mean sea level NAVD88 to 0.1 ft in 2040).

5. KNOWLEDGE TRANSFER

5.1. Objective

Develop a technology transfer and a training program to inform design professionals including engineers, environmental professionals, and right-of-way professionals on how to apply the new methods.

5.2. Description of Task

A one-day, recorded, Technology Transfer webinar was organized on June 21, 2023. The topics covered in the webinar were: (a) concepts of nonstationarity, (b) methods and tools useful for detection nonstationarity in hydrologic drivers, (c) general guidelines when the treatment of nonstationarity may be necessary, and (d) a new paradigm for return period and risk under nonstationarity and the appropriate methods.

6. SUMMARY AND RECOMMENDATIONS

6.1. Summary

With the need to build resilient transportation infrastructure, there has been growing interest in incorporating data and tools that account for climate change in planning and design. The objective of this project was to review the current FDOT manuals of practice and propose potential modifications to incorporate nonstationary datasets and methods. To achieve this objective, the work done through this effort was divided into four tasks:

- 1) Review current FDOT manuals for potential modifications and evaluate the current methods in nonstationarity, along with the frameworks to implement them.
- 2) Recommend and/or develop planning and design tools for incorporating nonstationarity in the design process.
- 3) Develop new nonstationary datasets of environmental variables for the State of Florida.
- 4) Organize a one- or two- day technology transfer webinar for transportation design professionals.

As a result of the review of FDOT manuals, the design team focused on three main environmental variables: 1) rainfall, 2) sea level, and peak discharge. Datasets and the methods included in the manuals are largely based on the stationarity assumption. Rainfall estimates are routinely used in FDOT planning and design processes like storm drain system design, cross drain hydraulics, temporary facility design, and calculating peak flow using the Rational method. The latest versions of FDOTs manuals of practice recommend the use of NOAA's Atlas 14 datasets. Atlas 14 estimates are based on historical data and do not consider the potentially changing extreme rainfall magnitudes. Calculations for sea level rise, which is necessary to estimate tailwater elevations for stormwater systems, ponds, etc., are performed in the FDOT manuals using regression of historical tide gauge data. Similarly, peak discharge, which is used in the design and analysis of open channels, cross drains, bridges, etc., is calculated from gauge data or regional USGS regression equations.

The decision to include nonstationary data and methods should be based on the design life of the project, the cost, criticality, vulnerability, and risk of the project. According to FHWA (2016) designers should consider risk evaluations (asset criticality, vulnerability, and cost) and the service life of the project in their implementation of nonstationary data and methods. In line with this, FHWA (2016) provides a framework with multiple levels of analysis. Typically, a level 1 or a level 2 project, which has a design life of less than 75 years, may only require historical data; whereas higher levels of analysis, with design lives greater than 75 years require the use of projected data as well. Some examples of projected data as well as tools and methods of analysis for rainfall and peak discharge are presented in FHWA (2016). FHWA (2020) provides information on sea level rise projections. Projections may be process-based (such as Kopp et al. 2014) or scenarios-based (such as Sweet et al. 2017). FHWA (2020) recommends using site -specific RSLR estimates for designs, with minimum projections of RLSR throughout the remainder of this

century and higher projections of RSLR when the overall project performance is very sensitive to sea levels and/or the design life and cost are high. Both FHWA circulars emphasize that engineers need to be cognizant of the uncertainty in projected data, as well as the evolutionary nature of climate data and science. The NCHRP reports (Kilgore et al. 2019a and 2019b) also provide guidance on incorporating nonstationarity in the transportation design process. In these reports, a framework is provided based on the factors like criticality of the project, expected service life, vulnerability to climate change, the functional classification (roadway, bridge, or tunnel), regulatory requirements, and resources available for the project. The NCHRP reports (Kilgore et al. 2019a) recommend that for projects with service lives greater than 30 years, at least one lower and one higher climate scenario should be considered for inland hydrological design. For coastal applications, the NCHRP reports (Kilgore et al. 2019b) recommend, at a minimum, the equivalent local projection of Sweet et al. (2017). The engineering demand and structure capacity must be compared and checked for every design. It is noted that there have been some recent efforts to pilot-test the implementation of the methods described in NCHRP 15-61 titled “Applying Climate Change Information to Hydrologic and Coastal Design of Transportation Infrastructure.” In particular, the document NCHRP 20-44(23) demonstrates the computation of design flood elevations and design waves employing NCHRP 15-61 Guidance Level 1 and Level 2 procedures for a bridge that is supposed to be operational from 2021 and 2090.

Before applying nonstationary methods, it is necessary to ensure that any apparent trend in the data is not due to natural variability in a stationary environment. An example of nonstationary trend detection was demonstrated in this report through the analysis of annual peak flow data from 99 USGS gauges. The gauges showed positive trends in 9 stations. In case of an increasing trend, efforts must be undertaken to identify the source of the nonstationarity. Nonstationarity detection may also be performed using the USACE Time Series Analysis Tool as described in Section 3.4.2 and Appendix D.

Section 2.4.2 presents methods for incorporating nonstationarity into the planning process. Some of these methods are demonstrated in Section 3.6. An example of incorporating nonstationarity with peak discharge data from Shingle Creek, FL is presented in Section 3.6.1. Nonstationarity may be incorporated into rainfall estimates using global climate model data. Section 3.6.1 presents an example of how Atlas 14 data may be modified with change factors derived from downscaled climate models, in this case, LOCA data. The modified rainfall estimates vary by location. But for most cases, the 83rd percentile value is higher than the Atlas 14 95th percentile estimate. Projects which require the use of nonstationary rainfall data due to high service life, criticality, risk, cost, etc. should consider the use of the downscaled climate data.

Another concept that is worth considering is the “stationarity” in the return period or fixed return periods. This happens when the level of protection of infrastructure is reduced due to climatic nonstationarity. For example, roadways designed for a 50-year return period may reduce to a 25-year return period at the end of the design life. Section 3.5.3 of this report introduces the concepts of ‘Expected Waiting Time’, ‘Risk’, and ‘Expected Number of Events’ and how they may

be incorporated into the hydrologic design process. Examples of these are presented in Sections 3.6.2 and 3.6.3.

Datasets were compiled with the sources of the climatic data and nonstationary data created from them are presented in Chapter 4. The focus of this work was to use the existing data and tools, instead of creating these from scratch. The datasets compiled will be a part of the technology transfer to FDOT. In addition, a webinar will be scheduled to go over the concepts of nonstationarity, methods, and tools useful for detecting nonstationarity in environmental drivers, results of the reviews of the manuals of practice, areas of practice that are recommended to be revised, the new paradigm of nonstationarity, and the methods that were developed. The next section presents some specific recommendations for the use of these datasets and methods.

6.2. Recommendations

The Task 1 review has highlighted several opportunities to provide new datasets and methods to incorporate nonstationarity due to both climate change and land-use change into current planning and design practices of transportation infrastructure. Many of these new opportunities are included in the latest versions of the FHWA guidance documents including FHWA (2016) and FHWA (2020). Moving forward, it is recommended that this latest information on both datasets and methods be customized for Florida and explore options for updating FDOT planning and design manuals with the latest information. **The focus of future tasks of this project will be to first focus on improving existing tools for incorporating nonstationarity into planning/design practices before new tools are developed.** The project will also explore the transfer of the new datasets and methods to the GeoPlan portal being maintained by the University of Florida.

Before embarking on applying nonstationary techniques for TI planning and design, it is recommended that a formal process be followed to justify their use for a particular project. This report focused on key hydrologic drivers that are relevant to TI projects in both coastal and inland areas of Florida. They include, rising sea levels, potentially changing extreme rainfall magnitudes, and both inland and coastal peak flood discharges. It is recommended that any modeling or applications required for the planning and design of TI use future changes in applicable drivers during the design life or the planning horizon of a project. Because there are many factors (land use change and climate) that may contribute to any apparent nonstationarity in data, careful adherence to this process may be needed. Table 6-1 shows multiple situations relevant to the decision regarding the considerations of nonstationarity.

Table 6-1. Decision matrix for considering nonstationarity.

Historical*	Future	Considerations
Statistically significant trend absent	Projections do not suggest a systematic trend, or there is insufficient information	Current practice based on stationarity is adequate
Statistically significant trends present	Projections do not demonstrate a systematic trend	Most likely due to when the system is built out or climate change is episodic. The decision to use an extrapolation of historical trends may depend on risks and economic aspects. A Dynamic Adaptive Policy Pathway (DAPP) strategy may be warranted
Statistically significant trend absent	Projections do suggest systematic trend	Apply the new nonstationary techniques unless the current safety factors can account for future changes (e.g. freeboard). Consider DAPP
Statistically significant trends present	Projections do suggest a systematic trend	Apply the new nonstationary techniques unless the current safety factors can account for future changes (e.g. freeboard). Consider DAPP

* A careful attribution exercise should be implemented if the trends are statistically significant.

It is prudent to follow up this research project with additional actions that may lead to possible update of the current FDOT guidelines. First, while possible nonstationarity was detected in certain climate drivers (e.g. sea level rise, peak discharge at limited locations), further assessment will be needed to confirm such changes in the vicinity of where they were detected. This is a necessary component of attribution. This is particularly important for peak discharge time series as the projected sea level rise is a clear case of nonstationarity due to acceleration that has been confirmed already. This assessment should include a thorough review of the literature to determine if there are other studies in the area to confirm the presence of systematic trends and possible causes (e.g., urbanization). Second, the updates to some key data sets should be considered. In particular, the USGS peak flow equations may be dated, and they may need to be updated to incorporate recent discharge records. Third, it is prudent to wait for the upcoming statewide products from Florida’s Flood Hub for nonstationary data. These include statewide sea level rise projections and the Change Factors for estimating future rainfall for a range of average recurrence intervals. Flood Hub is not expected to put forth specific recommendations on the use of this data for infrastructure planning, but rather provide the science input necessary for

developing future conditions. Fourth, in situations where nonstationarity is detected and confirmed, the implementation of the Dynamic Adaptive Policy Pathway (DAPP) approach should be considered when the retrofitting of existing TI infrastructure or a new facility is needed in the region. Considering the research nature of this project, additional efforts will be needed to develop specific tools and data that would supplement existing FDOT guidelines.

REFERENCES

- Abatzoglou J.T. & Brown T.J. (2012). *International Journal of Climatology*. "A comparison of statistical downscaling methods suited for wildfire applications, <https://dx.doi.org/10.1002/joc.2312>
- Archfield S.A., Kennen J.G., Carlisle D.M., and Wolock D.M. 2013. An objective and parsimonious approach for classifying natural flow regimes at a continental scale. *River Research and Applications*. DOI: 10.1002/rra.2710.
- Befus, K.M., Barnard, P.L., Hoover, D.J. et al. 2020, Increasing threat of coastal groundwater hazards from sea-level rise in California. *Nat. Clim. Chang.* 10, 946–952 (2020). <https://doi.org/10.1038/s41558-020-0874-1>
- Bras, R.L. (1990). "Hydrology: An Introduction to Hydrologic Science." Addison-Wesley Publishing Co., Reading, Mass., 643 pages.
- Buchanan, M.K., M. Oppenheimer, and R.E. Kopp, 2017: Amplification of flood frequencies with local sea level rise and emerging flood regimes. *Environmental Research Letters*, 12 (6), 064009. <https://doi.org/10.1088/1748-9326/aa6cb3>
- Centre for Ecology and Hydrology, 2013. A review of applied methods in Europe for flood-frequency analysis in a changing environment. H. Madsen, D. Lawrence, M. Lang, M. Martinkova, and T.R. Kjeldsen, eds., Wallingford, U.K.: Centre for Ecology and Hydrology
- Cohn, T. and Lins, H. F., 2005. "Nature's style: Naturally trendy." *Geoph. Res. Letters* 32, 5 p
- Coles, S., 2001. *An Introduction to statistical modeling of extreme values*. Springer-Verlag, London, 208 pages.
- Cooley, D. (2013). "Return periods and return levels under climate change." Chapter 4 in *Extremes in a Changing Climate: Detection, Analysis and Uncertainty*, A. AghaKouchak et al. eds., Springer Science + Business media Dordrecht.
- CSAP. Climate Science Advisory Panel, Tampa Bay. 2019. *Recommended Projections of Sea Level Rise in the Tampa Bay Region*.
- Davison, A.C., and Smith, R.L. (1990). Models for exceedances over high thresholds: *Journal of the Royal Statistical Society. Series B* v. 52, no. 3. p. 393-442.
- Douglas, E. M., Vogel, R. M., and Kroll, C. N., 2000. "Trends in floods in the United States: impact of spatial correlation." *J. Hydrol.* 240, 90-105.
- Draper N.R., and H. Smith., 2014. *Applied Regression Analysis*, 3rd edition, Wiley, New York, 706 pp.

- FDOT. 2012. Local Agency Program Manual. Available at <https://www.fdot.gov/programmanagement/lap/lap-toc.shtm>. (Accessed 3 January 2022)
- FDOT. 2017. Utility Accommodation Manual. Available at <https://www.fdot.gov/docs/default-source/programmanagement/utilities/Docs/UAM/UAM2010.pdf> (Accessed 3 January 2022)
- FDOT. 2018. Manual of Uniform Minimum Standards for Design, Construction and Maintenance for Streets and Highways. Available at <https://www.fdot.gov/roadway/floridagreenbook/fgb.shtm> (Accessed 3 January 2022)
- FDOT. 2019a. Transportation Asset Management Plan. Available at [https://fdotwww.blob.core.windows.net/sitefinity/docs/default-source/planning/performance/fdot-transportation-asset-management-plan_\(june-28-2019\).pdf?sfvrsn=36c94a6b_2](https://fdotwww.blob.core.windows.net/sitefinity/docs/default-source/planning/performance/fdot-transportation-asset-management-plan_(june-28-2019).pdf?sfvrsn=36c94a6b_2) (Accessed 3 January 2022)
- FDOT. 2019b. Pavement Type Selection Manual. Available at https://fdotwww.blob.core.windows.net/sitefinity/docs/default-source/roadway/pm/publications/ptsm201901.pdf?sfvrsn=6f0bb70f_2 (Accessed 3 January 2022)
- FDOT. 2020a. Drainage Design Guide. Florida Department of Transportation Office of Design, Drainage Section, Tallahassee, FL.
- FDOT. 2020b. Drainage Handbook Drainage Connection Permits. Florida Department of Transportation Office of Design, Drainage Section, Tallahassee, FL.
- FDOT. 2020c. Freight Mobility and Trade Plan. Available at https://fdotwww.blob.core.windows.net/sitefinity/docs/default-source/rail/fmtp/april-2020/fmtp-tm-vp-april-2020.pdf?sfvrsn=5ec40f68_8 (Accessed 3 January 2022)
- FDOT. 2020d. Project Development & Environment Manual. Available at https://fdotwww.blob.core.windows.net/sitefinity/docs/default-source/environment/pubs/pdeman/2020/pd-e_part-1-2_pdf_finapi.pdf?sfvrsn=eb032889_2 (Accessed 3 January 2022)
- FDOT. 2021a. Drainage Manual. Topic No. 625-040-002. Florida Department of Transportation Office of Design, Drainage Section, Tallahassee, FL.
- FDOT. 2021b. Soils and Foundations Handbook. Available at <https://fdotwww.blob.core.windows.net/sitefinity/docs/default-source/structures/structuresmanual/archivedstructuresmanuals/sfh2021.pdf?> (Accessed 3 January 2022)

- FDOT. 2021c. Utility Procedures Manual. Available at https://fdotwww.blob.core.windows.net/sitefinity/docs/default-source/programmanagement/utilities/docs/uam/700-030-001-adopted.pdf?sfvrsn=5c101b2c_14 (Accessed 3 January 2022)
- FDOT. 2022a. Structures Manual. Available at <https://www.fdot.gov/structures/structuresmanual/currentrelease/structuresmanual.shtm> (Accessed 3 January 2022)
- FDOT. 2022b. Flexible Pavement Design Manual. Available at <https://fdotwww.blob.core.windows.net/sitefinity/docs/default-source/roadway/pm/publications/2022fpdm.pdf>? (Accessed 3 January 2022)
- FDOT. 2022c. Rigid Pavement Design Manual. Available at <https://fdotwww.blob.core.windows.net/sitefinity/docs/default-source/roadway/pm/publications/2022rpdm.pdf>? (Accessed 3 January 2022)
- FHWA (Federal Highway Administration). 2016. Hydraulic Engineering Circular No. 17 Highways in the River Environment – Floodplains, Extreme Events, Risk, and Resilience. Publication No. FHWA-HIF-16-018.
- FHWA. 2020. Hydraulic Engineering Circular No. 25 Highways in the Coastal Environment. Publication No. FHWA-HIF-19-059.
- Gumbel, E.J., 1941. The return period of flood flows. The Annals of Mathematical Statistics. 12 (2), 163-190
- Hosking, J. R. M. (1990). L-Moments: Analysis and Estimation of Distributions Using Linear Combinations of Order Statistics. Journal of the Royal Statistical Society, Series B, 52, 105-124.
- Hosking, J. R. M. (1996). Fortran Routines for Use with the Method of L-Moments, Version 3. Research Report RC20525, IBM Research Division, Yorktown Heights, NY.
- Irizarry M., Obeysekera J., Dessalegne T. (2016). Determination of Future Intensity-Duration-Frequency Curves for Level of Service Planning Projects. Task 2 - Deliverable 2.1 to SFWMD - Conduct an extreme rainfall analysis in climate model outputs to determine temporal changes in IDF curves.
- Irizarry, M. M., Dessalegne, T., and Obeysekera, J. (2017). Assessment of Methods for Future Depth-Duration-Frequency Curve Development under Climate Change for the State of Florida, World Environmental and Water Resources Congress. 2017. 188–202. <https://doi.org/10.1061/9780784480601.018>
- Irizarry-Ortiz, M.M., and Stamm, J.F., 2021, Change factors to derive future precipitation depth-duration-frequency (DDF) curves at 174 National Oceanic and Atmospheric

Administration (NOAA) Atlas 14 stations in central and south Florida: U.S. Geological Survey data release, <https://doi.org/10.5066/P9KEMHYM>.

Kendall, M.G., 1938. A new measure of rank correlation. *Biometrika*, 30, 81-93

Kendall, M.G., 1976. *Rank Correlation Methods*, 4th edition, Charles Griffin, London, 202 p.

Kilgore, R., Thomas, W.O., Douglas, S., Webb, B., Hayhoe, K., Stoner, A., Jacobs, J.M., Thompson, D.B., Herrmann, G.R., Douglas, E., and Anderson, C. 2019a., *Applying Climate Change Information to Hydrologic and Coastal Design of Transportation Infrastructure Final Report*. NCHRP Project 15-61. Prepared for The National Cooperative Highway Research Program Transportation Research Board.

Kilgore, R., Thomas, W.O., Douglas, S., Webb, B., Hayhoe, K., Stoner, A., Jacobs, J.M., Thompson, D.B., Herrmann, G.R., Douglas, E., and Anderson, C. 2019b., *Applying Climate Change Information to Hydrologic and Coastal Design of Transportation Infrastructure Design Practices*. NCHRP Project 15-61. Prepared for The National Cooperative Highway Research Program Transportation Research Board.

Knutson, T. R., Chung, M. V., Vecchi, G., Sun, J., Hsieh, T-L. and Smith, A. J. P., 2021: ScienceBrief Review: Climate change is probably increasing the intensity of tropical cyclones. In: *Critical Issues in Climate Change Science*, edited by: Corinne Le Quéré, Peter Liss & Piers Forster. <https://doi.org/10.5281/zenodo.4570334>

Kopp, R. E., Horton, R. M., Little, C. M., Mitrovica, J. X., Oppenheimer, M., Rasmussen, D. J., Strauss, B. H. and Tebaldi, C. 2014. Probabilistic 21st and 22nd century sea-level projections at a global network of tide-gauge sites. *Earth's Future*, Vol. 2, No. 8, p. 383–406.

Koutsoyiannis, D., 2002. The Hurst phenomenon and fractional Gaussian noise made easy. *Hydrologic Sciences Journal*, 47 (4), 573-595.

Koutsoyiannis D. and Montanari A, 2014. Negligent killing of scientific concepts: the stationarity case. *Hydrological Sciences Journal*, doi.org/10.1080/02626667.2014.959959.

Lang M., T.B.M.J. Ouarda, B. Bobee., 1999. Towards operational guidelines for over-threshold modeling, *Journal of Hydrology*, 225, 103-117

Lins, Harry F. and Timothy A. Cohn, 2011. Stationarity: Wanted Dead or Alive? *Journal of the American Water Resources Association (JAWRA)* 47(3):475-480. DOI: 10.1111/j.1752-1688.2011.00542.x

Madsen, H., Lawrence, D., Lang, M., Martinkova, M., and Kjeldsen, T.R., 2014. Review of trend analysis and climate change projections of extreme precipitation and floods in Europe. *J. Hydrol.* 519, 3634-3650

- Madsen, H., Pearson, C.P., Rosbjerg, D. (1997). Comparison of annual maxima series and partial duration series methods for modeling extreme hydrologic events. 1. At-site modeling: *Water Resources Research*, v. 33, no. 4, p. 747-757.
- Mandelbaum, M., Hlynka, M., and Brill, P. H. (2007). "Nonhomogeneous geometric distributions with relations to birth and death processes." *Sociedad de Estadística e Investigación Operativa*, Springer, 281-296.
- Mann, H.B., 1945. Nonparametric test against trend, *Econometrica*, 13, 245-259.
- Matalas, N.C., 2012. Comment on the announced death of stationarity. *Journal of Water Resources Planning and Management*, 138, 311–312. doi:10.1061/(ASCE)WR.1943-5452.0000215.
- McCuen, Richard H., Peggy A. Johnson, and Robert M. Ragan (2002). "*Highway Hydrology*," Hydraulic Design Series 2 (HDS 2), Second Edition, FHWA-NHI-02-001.
- Milly, P.C.D., Betancourt, J., Falkenmark, M., Hirsch, R.M., Kundzewicz, Z.W., Lettenmaier, D.P., and Stouffer, R.J., 2008. Stationarity is dead – whither water management?. *Science* 319, 573-574.
- Montanari, A. and Koutsoyiannis, D., 2014. Modeling and mitigating natural hazards: stationarity is immortal!. *Water Resources Research*, 50 (12), pp. 9748–9756.
- Mood, A., Graybill, F., and Boes, D. C. (1974). "Introduction to the theory of statistics." 3rd Edition, McGraw Hill, N. York.
- Nason, G.P. 2006. "Stationary and non-stationary time series", *Statistics in Volcanology*, H. M. Mader, S. G. Coles, C. B. Connor, L. J. Connor
- Obeysekera J. , and Salas, J, 2020. Hydrologic designs for extreme events under nonstationarity. In: *Engineering Methods for Precipitation under a Changing Climate*. Olsen, J.R. and K.T. Adamec, Eds. American Society of Civil Engineers, 63–82.
<http://dx.doi.org/10.1061/9780784415528.ch04>
- Obeysekera, J, and Salas, J., "Frequency of Recurrent Extremes under Nonstationarity," *ASCE J. Hydrol. Eng*, 21(5), 2016
- Panthou, G., Vischel, T., Lebel, T., Quantin, G., and Molinié, G. 2014. Characterising the space–time structure of rainfall in the Sahel with a view to estimating IDAF curves, *Hydrol. Earth Syst. Sci.*, 18, 5093–5107, <https://doi.org/10.5194/hess-18-5093-2014>.
- Perica, S., Martin, D., Pavlovic, S., Roy, I., St. Laurent, M., Trypaluk, C., Unruh, D., Yekta, M., Bonnin, G. 2013. NOAA Atlas 14 Volume 9 Version 2, *Precipitation-Frequency Atlas of the United States, Southeastern States*. NOAA, NationalWeather Service, Silver Spring, MD.

- Pickands, J. (1975). Statistical inference using extreme order statistics: *Annals of Statistics*, v. 3. p. 1190131. <https://dx.doi.org/10.1214/aos/1176343003>
- Pierce D. W., Cayan D. R., Thrasher B. L. (2014). Statistical downscaling using Localized Constructed Analogs (LOCA). *Journal of Hydrometeorology* 15:2558–2585. <https://doi.org/10.1175/JHM-D-14-0082.1>
- Prosdocimi, I., Kjeldsen, T.R., and Svensson, C. 2014. Non-stationarity in annual and seasonal series of peak flow and precipitation in the UK. *Nat. Hazards Earth Syst. Sci.*, 14, 1125-1144.
- Salas, J. and Obeysekera, J. 2014. "Revisiting the Concepts of Return Period and Risk for Nonstationary Hydrologic Extreme Events." *ASCE J. Hydrol. Eng.*, 19(3).
- Salas, J., Obeysekera J. and Vogel R. 2018. Techniques for assessing water infrastructure for nonstationary extreme events: a review, *Hydrological Sciences Journal*, 63:3, 325-352, DOI: 10.1080/02626667.2018.1426858
- Sauer, V., W. Thomas, Jr., V. Stricker, and K. Wilson (1983). "Flood Characteristics of Urban Watersheds in the United States," Water-Supply Paper 2207, U.S. Geological Survey.
- SEFRCC, Southeast Florida Regional Climate Change Compact Technical Ad hoc Work Group (Compact). 2011. A Unified Sea Level Rise Projection for Southeast Florida. A document prepared for the Southeast Florida Regional Climate Change Compact Steering Committee. 27 p.
- Sen PK. 1968. Estimates of the regression coefficient based on Kendall's Tau. *Journal of American Statistical Association* 63(324): 1379-1389.
- SERC (Science Education Research Center) Carleton. 2017. Non-stationary Hydrology. Retrieved November 29, 2022 from https://serc.carleton.edu/integrate/teaching_materials/water_science_society/student_materials/904
- Serinaldi, F. and C.G. Kilsby (2015). "Stationarity is Undead: Uncertainty Dominates the Distribution of Extremes". *Advances in Water Resources*, 77, 17-36, doi:10.1016/j.advwatres. 2014.12.013.
- Shapiro, S. S. and Wilk, M. B. 1965. An analysis of variance test for normality (complete samples). *Biometrika*. 52 (3–4): 591–611. doi:10.1093/biomet/52.3-4.591.
- Simonovic S.P., A. Schardong, D. Sandink, R. Srivastav. 2016. A web-based tool for the development of Intensity Duration Frequency curves under changing climate. *Environmental Modelling & Software* 81.

- SLSC-FIU, Sea Level Solutions Center - Florida International University. 2021. Updating Statewide Extreme Rainfall Projections. Report. A document prepared for the Florida Building Commission.
- South Florida Water Management District (SFWMD). 2016. Environmental Resource Permit Applicant's Handbook Volume II.
- Srivastav R. and Slobodan P. Simonovic. 2015. Computerized Tool for the Development of Intensity-Duration-Frequency Curves under a Changing Climate. Water Resources Research Report no. 089, Facility for Intelligent Decision Support, Department of Civil and Environmental Engineering, London, Ontario, Canada, 52 pages. ISBN: (print) 978-0-7714-3087-9; (online) 978-0-7714-3088-6.
- Stedinger, J.R. and Griffis, V.W., 2011. Getting from here to where? flood frequency analysis and climate". *Journal of the American Water Resources Association*, 47 (3).
- Sweet, W.V., B.D. Hamlington, R.E. Kopp, C.P. Weaver, P.L. Barnard, D. Bekaert, W. Brooks, M. Craghan, G. Dusek, T. Frederikse, G. Garner, A.S. Genz, J.P. Krasting, E. Larour, D. Marcy, J.J. Marra, J. Obeysekera, M. Osler, M. Pendleton, D. Roman, L. Schmied, W. Veatch, K.D. White, and C. Zuzak, 2022: Global and Regional Sea Level Rise Scenarios for the United States: Updated Mean Projections and Extreme Water Level Probabilities Along U.S. Coastlines. NOAA Technical Report NOS 01. National Oceanic and Atmospheric Administration, National Ocean Service, Silver Spring, MD, 111 pp. <https://oceanservice.noaa.gov/hazards/sealevelrise/noaa-nostechrpt01-global-regional-SLR-scenarios-US.pdf>
- Sweet, W.V., Kopp, R.E., Weaver, C.P., Obeysekera, J., Horton, R.M., Thieler, E.R., and Zervas, C. 2017. Global and Regional Sea Level Rise Scenarios for the United States. *NOAA Technical report NOS CO-OPS 083*, Silver Spring, Md., 75 p.
- Theil, H. (1950) A Rank-Invariant Method of Linear and Polynomial Regression Analysis. *Nederlandse Akademie Wetenschappen Series A*, 53, 3860392.
- USACE (United States Department of Transportation). 2018. Guidance for Incorporating Climate change Impacts to Inland Hydrology in Civil Works Studies, Designs, and Projects. *Engineering and Construction Bulletin No. 2018-14*.
- USDOT (United States Department of Transportation). 2015. CMIP Climate Data Processing Tool User's Guide. Prepared by ICF International for the United States Department of Transportation Center for Climate Change and Environmental Forecasting under *The Gulf Coast Study, Phase 2, Impacts of Climate Change and Variability on Transportation Systems and Infrastructure*.

- USDOT. 2014. Assessing Criticality in Transportation Adaptation and Planning. https://www.fhwa.dot.gov/environment/sustainability/resilience/tools/criticality_guidance/criticality_guidance.pdf
- USDOT. 2015. U.S. DOT Vulnerability Assessment Scoring Guide (VAST). Version 1.1.
- Vogel, R.M., Yaindl, C., and Walter, M., 2011. Nonstationarity: flood magnification and recurrence reduction factors in the United States." *Journal of the American Water Resources Association*, 47 (3), 464-474.
- Wang, Y. et al., 2020. Innovative trend analysis of annual and seasonal rainfall in the Yangtze River Delta, eastern China. *Atmospheric Research*, 231: 104673.
- Webb, B.M. 2017. *A Primer on Modeling in the Coastal Environment*. FHWA–HIF–18–002, Washington, D.C.: Federal Highway Administration. 71 pp.
- Yue S., Z. W. Kundzewicz, and L. Wang. 2012. Detection of Changes, Chapter 22, in Kundzewicz, Z. (Ed.). (2012). *Changes in Flood Risk in Europe*. London: CRC Press, <https://doi.org/10.1201/b12348>.

APPENDIX A. SUMMARY OF FDOT DOCUMENT REVIEW

APPLICATIONS/CRITERIA/RECOMMENDATIONS IN FDOT, FHWA & NCHRP DOCUMENTS

Guidance/Report	Applications/Criteria/Recommendation	Comments																								
Design Parameter: Rainfall																										
FDOT Drainage Manual (2021)	<ul style="list-style-type: none"> ➤ Use statistical rainfall depth data for Florida in the National Oceanic and Atmospheric Administration (NOAA) Atlas 14 Rainfall Data available at: https://hdsc.nws.noaa.gov/hdsc/pfds/pfds_map_cont.html?bkmrk=fl ➤ Open Channel - Design Storm Frequencies <table border="1" data-bbox="531 505 1421 748"> <thead> <tr> <th>Type Channel</th> <th>Frequency</th> </tr> </thead> <tbody> <tr> <td>Roadside, median, and interceptor ditches or swales</td> <td>10-year</td> </tr> <tr> <td>Outfalls</td> <td>25-year</td> </tr> <tr> <td>Canals</td> <td>25-year</td> </tr> <tr> <td>Temporary roadside and median ditches or swales</td> <td>2-year</td> </tr> <tr> <td>Temporary outfalls and canals</td> <td>5-year</td> </tr> </tbody> </table> ➤ Storm Drain Systems – Design Storm Frequencies <table border="1" data-bbox="531 865 1421 1300"> <thead> <tr> <th>Type Storm Drain</th> <th>Frequency</th> </tr> </thead> <tbody> <tr> <td>General design</td> <td>3-year</td> </tr> <tr> <td>General design work that involves the replacement of a roadside ditch with a pipe system by extending side drainpipes</td> <td rowspan="2">10-year</td> </tr> <tr> <td>General design on work to interstate facilities</td> </tr> <tr> <td>Outfalls</td> <td>25-year</td> </tr> <tr> <td>Interstate facilities for which roadway runoff would have no outlet other than a storm drain system such as in a sag inlet or cut section</td> <td rowspan="2">50-year</td> </tr> <tr> <td>Outlets of systems requiring pumping stations</td> </tr> </tbody> </table> 	Type Channel	Frequency	Roadside, median, and interceptor ditches or swales	10-year	Outfalls	25-year	Canals	25-year	Temporary roadside and median ditches or swales	2-year	Temporary outfalls and canals	5-year	Type Storm Drain	Frequency	General design	3-year	General design work that involves the replacement of a roadside ditch with a pipe system by extending side drainpipes	10-year	General design on work to interstate facilities	Outfalls	25-year	Interstate facilities for which roadway runoff would have no outlet other than a storm drain system such as in a sag inlet or cut section	50-year	Outlets of systems requiring pumping stations	<ul style="list-style-type: none"> ➤ Design storm frequencies are used for the design of open channels, storm drain systems, and cross-drain hydraulics ➤ Use of Return Period (RP) is already the current practice. ➤ The FIU project will propose the use of RP and AEP under nonstationary conditions ➤ Most FDOT projects have a design life of 75-years or less. This may influence the level of analysis that is required for considering nonstationarity ➤ NOAA Atlas 14 rainfall depth data for Florida is recommended for use in the Drainage Manual
Type Channel	Frequency																									
Roadside, median, and interceptor ditches or swales	10-year																									
Outfalls	25-year																									
Canals	25-year																									
Temporary roadside and median ditches or swales	2-year																									
Temporary outfalls and canals	5-year																									
Type Storm Drain	Frequency																									
General design	3-year																									
General design work that involves the replacement of a roadside ditch with a pipe system by extending side drainpipes	10-year																									
General design on work to interstate facilities																										
Outfalls	25-year																									
Interstate facilities for which roadway runoff would have no outlet other than a storm drain system such as in a sag inlet or cut section	50-year																									
Outlets of systems requiring pumping stations																										

APPLICATIONS/CRITERIA/RECOMMENDATIONS IN FDOT, FHWA & NCHRP DOCUMENTS

Guidance/Report	Applications/Criteria/Recommendation	Comments										
	<p>➤ Cross Drain Hydraulics - Permanent Facilities – Design Storm Frequencies</p> <table border="1" data-bbox="531 350 1419 553"> <thead> <tr> <th>Facility</th> <th>Frequency</th> </tr> </thead> <tbody> <tr> <td>Mainline Interstate</td> <td>50 years</td> </tr> <tr> <td>High Use or Essential: Projected 20-year AADT¹>1500</td> <td>50 years</td> </tr> <tr> <td>Other: Projected 20-year AADT¹<1500</td> <td>25 years</td> </tr> <tr> <td>Road ditch culverts, pedestrian and trail bridges</td> <td>10 years</td> </tr> </tbody> </table> <p>¹AADT (Annual Average Daily Traffic) is preferred. If it is not available, use ADT</p> <p>➤ For temporary facilities, if there are no flooding or scour concerns, a 10-year design storm event is the minimum design frequency for temporary culverts, bridge culverts, and bridges</p> <p>➤ Use the highest tailwater elevation coincident with the design storm event for the sizing of cross drains and determining headwater and backwater elevations</p> <p><u>Cross Drain Hydraulics: Tidal Flow – Creeks/rivers flowing into tidal water bodies</u></p> <p>➤ Hurricane rainfall is dependent on the peak surge stage; hence, the USACE tropical storm rainfall-runoff procedure from the 1986 Engineering and Design Storm Surge Analysis Manual should be used to estimate runoff from any design surge regardless of the surge return frequency</p> <p>➤ May also use a steady discharge equal to the peak flow from a 10-year storm instead of the above USACE procedure</p>	Facility	Frequency	Mainline Interstate	50 years	High Use or Essential: Projected 20-year AADT ¹ >1500	50 years	Other: Projected 20-year AADT ¹ <1500	25 years	Road ditch culverts, pedestrian and trail bridges	10 years	
Facility	Frequency											
Mainline Interstate	50 years											
High Use or Essential: Projected 20-year AADT ¹ >1500	50 years											
Other: Projected 20-year AADT ¹ <1500	25 years											
Road ditch culverts, pedestrian and trail bridges	10 years											
<p>FDOT Drainage Design Guide (2020)</p>	<p>The Intensity-Duration-Frequency (IDF) Curves for 11 zones in Florida were developed using HYDRO-35 and TP-40 developed by the Department. According to the Drainage Design Guide, the curves provide a reasonable basis for design.</p>	<p>➤ The Drainage Design Guide expands on some applications in the Drainage Manual with</p>										

APPLICATIONS/CRITERIA/RECOMMENDATIONS IN FDOT, FHWA & NCHRP DOCUMENTS

Guidance/Report	Applications/Criteria/Recommendation	Comments
	<p><u>Open channel design</u></p> <ul style="list-style-type: none"> • Roadside or median ditches or swales designed to convey a 10-year frequency storm without damage • Outfall ditches or canals should convey a 25-year frequency storm without damage • Unless flood rights are obtained or flow is contained in the ditch, pre-development stages for all frequencies up to and including the 100-year event must not be exceeded <p><u>Side drains</u></p> <ul style="list-style-type: none"> ➤ 10-year frequency like for open channel design <p>USACE reference ‘Engineering and Design Storm Surge Analysis’</p> <ul style="list-style-type: none"> ➤ Methodology for estimating the rainfall associated with the landfalling hurricanes ➤ Graphs of point rainfall depth for a given frequency and a given distance from the left or right of the storm track ➤ Point rainfall graphs for selected frequency levels at either 6-hour or 12-hour intervals before landfall and after landfall <p><u>Storm Drain – Shoulder Gutter</u></p> <ul style="list-style-type: none"> ➤ Intercept all flow from a 10-year storm <p><u>Precipitation Data (Appendix A.2.3)</u></p> <p>Intensity-duration-frequency curves or photographs for historic or design storm conditions from:</p> <ul style="list-style-type: none"> ➤ HYDRO-35 <ul style="list-style-type: none"> ○ Depth-duration-frequency data useful for small drainage areas 	<p>the Drainage Manual taking precedence</p> <ul style="list-style-type: none"> ➤ FDOT is moving into ATLAS 14 as the standard dataset for IDF (refer to the new latest version of the Drainage Manual) ➤ FIU will explore more recent work on ATLAS 14 changes due to nonstationarity ➤ FIU will propose consideration of state-wide Change Factors computed as a part of the Florida Building Commission (FBC) study. This may be included in the UF Sketch Tool

APPLICATIONS/CRITERIA/RECOMMENDATIONS IN FDOT, FHWA & NCHRP DOCUMENTS		
Guidance/Report	Applications/Criteria/Recommendation	Comments
	<ul style="list-style-type: none"> ○ Rainfall depths for durations from 5 to 60 mins and return periods from 2 to 100 years ➤ Technical Paper 40 (TP-40) <ul style="list-style-type: none"> ○ Rainfall depths for durations from 0.5 to 24 hours and return periods from one to 100 years ➤ TP-49 <ul style="list-style-type: none"> ○ Extends to 2, 4, 7, and 10 days and return periods of 2, 5, 10, 25, and 100 years ➤ FDOT distributions derived from HYDRO-35, TP-40, and TP-49 ➤ NOAA Atlas 14 data 	
Design Parameter: Sea Level		
FDOT Drainage Manual (2021)	<p><u>Design of Storm Drains</u></p> <ul style="list-style-type: none"> ➤ For tailwater elevation of storm drains discharging into tidal bays, use mean high tide ➤ Sea Level Rise (SLR) Analysis <ul style="list-style-type: none"> ○ To assess the vulnerability of flooding over the design life of the facility ○ Recommends using the relative sea level trend data from historical records gathered by the National Water Level Observation Network (NWLON) and managed by NOAA ○ Straight-line extrapolation based on the design service life of the project with the nearest station ○ NOAA SLR trend supporting documentation must be included for the determination of design tailwater <p><u>Design of Cross Drains</u></p> <ul style="list-style-type: none"> ➤ Tidally influenced culverts must adjust the Mean High Water (MHW) elevation for SLR using the straight-line extrapolation <p><u>Stormwater Management: Coastal Ponds</u></p>	<ul style="list-style-type: none"> ➤ Sea level data is required for the selection of tailwater elevations of storm drains, tidally influenced culverts, coastal ponds, etc. ➤ To account for SLR a straight-line extrapolation method is recommended in the Drainage Manual ➤ Source of SLR data recommended NOAA NWLON

APPLICATIONS/CRITERIA/RECOMMENDATIONS IN FDOT, FHWA & NCHRP DOCUMENTS		
Guidance/Report	Applications/Criteria/Recommendation	Comments
	<ul style="list-style-type: none"> ➤ Adjust tailwater elevation to account for SLR using the straight-line extrapolation 	
FDOT Design (2020) Drainage Guide	<p><u>Cross Drain Sizing</u></p> <ul style="list-style-type: none"> ➤ Use the highest tailwater elevation that can reasonably be expected to occur coincident with the designed storm event ➤ For tidal conditions, use the SLR analysis described in Section 3.4.1 of the Drainage Manual <p><u>Sources of Tidal Bench Marks (Bridge hydraulics)</u></p> <ul style="list-style-type: none"> ➤ NOAA Center for the Operational Oceanographic Products and Services (CO-OPS) ➤ Florida Department of Environmental Protection (FDEP) Land Boundary Information Systems (LABINS) 	<ul style="list-style-type: none"> ➤ Recommends the straight-line extrapolation method in the Drainage Manual ➤ Sources of tidal data recommended include NOAA CO-OPS and FDEP LABINS
Design Parameter: Stream/Canal Discharge		
FDOT Manual (2021) Drainage	<p><u>Open Channel: Hydrologic Analysis</u></p> <ul style="list-style-type: none"> ➤ Frequency analysis of observed gauge data ➤ If no gauge data is available: <ul style="list-style-type: none"> ○ use USGS regional or local regression equations ○ the rational equation for drainage areas up to 600 acres ○ for outfalls from stormwater management facilities, use the method for the design of the stormwater management facility ➤ If a regulated/controlled canal, request data from the controlling agency and verify the data <p><u>Cross Drain Hydraulics: Freshwater Flow</u></p> <ul style="list-style-type: none"> ➤ Frequency analysis of observed gauge data ➤ If no gauge data is available: <ul style="list-style-type: none"> ○ use USGS regional or local regression equations 	<ul style="list-style-type: none"> ➤ The current FDOT practice is to use peakFQ ➤

APPLICATIONS/CRITERIA/RECOMMENDATIONS IN FDOT, FHWA & NCHRP DOCUMENTS

Guidance/Report	Applications/Criteria/Recommendation	Comments
	<ul style="list-style-type: none"> ○ the rational equation for drainage areas up to 600 acres ➤ If a regulated/controlled canal, request data from the controlling agency and verify the data 	
<p>FDOT Design (2020)</p> <p>Drainage Guide</p>	<p>Same as FDOT Drainage Manual (2021) for open channel design</p> <p>Bridge Hydraulics Analysis</p> <p>Gauge data is used to:</p> <ul style="list-style-type: none"> ➤ Determine the peak flow rates (statistical analysis of streamflow data done by USGS) ➤ Provide starting water surface elevations or boundary conditions for the bridge model ➤ Calibrate the bridge model 	<ul style="list-style-type: none"> ➤ The use of regression equations under future conditions needs to be explored

APPENDIX B. THEORETICAL CONCEPTS

Linear Model for Single Trends

The general form of the linear model is,

$$y_t = \beta_0 + \beta_1 X_{t1} + \beta_2 X_{t2} \dots + \beta_p X_{tp} + \varepsilon_t \quad (\text{B1})$$

where y is the dependent variable with its subscript t denoting time (1 to n), X values denote the predictors, and ε is the error term.

In matrix form, the linear model may be written as,

$$Y = X\beta + \varepsilon \quad (\text{B2})$$

where Y is a vector of size ($n \times 1$) and X is a matrix of size ($n, p+1$) consisting of unity as the first column and the remaining columns correspond to each time series of the predictors, X . The size of the parameter vector β is equal to $p+1$. The error term is a vector of size ($n \times 1$).

Using the least squares methodology, the estimator of the parameter vector β is given by

$$\hat{\beta} = (X^T X)^{-1} X^T Y \quad (\text{B3})$$

A property of the least squares estimation approach is that the estimators given by Eq. (3) are unbiased. Assuming the error term ε_t has a Gaussian distribution, the estimators of β have a multivariate normal distribution:

$$\hat{\beta} \sim N_{p+1}[\beta, \sigma^2 (X^T X)^{-1}] \quad (\text{B4})$$

where N_{p+1} denotes a multivariate normal distribution of dimension $p+1$ and σ^2 is the variance-covariance matrix of the error term. This in turn, can provide confidence intervals for each parameter.

For diagnostic testing purposes, it is often convenient to decompose the variability of the dependent variable, Y , in the form of an Analysis of Variance (ANOVA) table (**Error! Reference source not found.**).

Table B1. ANOVA table for multiple linear regression.

Source	Sum of Squares	Degrees of Freedom	Mean Square	F Ratio
Regression	$SSR = \hat{\beta} X^T Y - n\bar{Y}^2$	p	$MSR = \frac{SSR}{p}$	$F = \frac{MSR}{MSE}$
Error	$SSE = \varepsilon^T \varepsilon$	$n-p-1$	$MSE = \frac{SSE}{n-p-1}$	

Total	$SSTO = \mathbf{Y}^T \mathbf{Y} - n\bar{Y}^2$			

Given the sample data, the estimate of σ^2 can be obtained as $S^2 = SSE/(n-p-1)$ and the standard error of each parameter is estimated as $S_{\hat{\beta}_i} = S\sqrt{C_{ii}}$ where C_{ii} is the corresponding diagonal element of $(\mathbf{X}^T \mathbf{X})^{-1}$. Assuming the standardized values of estimated parameters to follow a Student-t distribution with $n-p-1$ of degrees of freedom, the $100(1-\alpha)$ Percent confidence interval for $\hat{\beta}_i$ is given by

$$[\hat{\beta}_i - t_{1-\frac{\alpha}{2}}(n-p-1)S_{\hat{\beta}_i}, \hat{\beta}_i + t_{1-\frac{\alpha}{2}}(n-p-1)S_{\hat{\beta}_i}] \quad (B5)$$

Diagnostic tests for individual parameters estimated from data can be conducted using the Student-t variate, $t = (\hat{\beta} - \beta_{i0})/S\sqrt{C_{ii}}$. If the absolute value of t is greater than $t_{1-\frac{\alpha}{2}}(n-p-1)$, then the null hypothesis $\beta_i = \beta_{i0}$ is rejected. For detecting the presence or absence of a trend, often $\beta_{i0} = 0$ is used (i.e., zero slope).

A simultaneous test for all coefficients, whether they are all equal to zero, may be conducted using the results of the ANOVA table. Since the F ratio (last column in **Error! Reference source not found.**) has an F-distribution with p and $(n-p-1)$ degrees of freedom, the null hypothesis that all coefficients $\beta_i=0, i=1, \dots, p$ is rejected if the computed $F > F_{\alpha}(p, n-p-1)$. Another common approach for rejecting the null hypothesis is to demonstrate that $\alpha_c = Prob[F_{\alpha}(p, n-p-1) > F]$ is greater than α .

Shapiro Wilk Statistic

The Shapiro-Wilk test statistic is given by

$$W = \frac{(\sum_{i=1}^n a_i x_{(i)})^2}{\sum_{i=1}^n (x_i - \bar{x})^2} \quad (\text{B6})$$

where $x_{(i)}$ is the i^{th} order statistic (i^{th} -smallest), and \bar{x} is the sample mean. Further details of this method can be found in Shapiro and Wilk (1965). The “shapiro.test” script available in the stats library of R was used to compute W and its p-value associated with the hypothesis testing to determine if data follows a Normal Distribution.

Trend Detection Using the Mann-Kendall

The test consists of summing the signs of the difference between all pairs of sequential time series values

$$S = \sum_{k=1}^{n-1} \sum_{j=k+1}^n \text{sgn}(X_j - X_k) \quad (\text{B7})$$

where n is the length of the time series, X_j and X_k are sequential time series values for times t_j and t_k ($j > k$) and sgn is the sign function defined as

$$\text{sgn}(X_j - X_k) = \begin{cases} 1 & \text{if } X_j - X_k > 0 \\ 0 & \text{if } X_j - X_k = 0 \\ -1 & \text{if } X_j - X_k < 0 \end{cases} \quad (\text{B8})$$

The null hypothesis, H_0 , for the test is that the data, X , are a sample of n independent and identically distributed random variables (i.e., there is no trend and $S=0$). The alternative hypothesis, H_a , states that the distribution of X_j and X_k are not identical for all $k, j \leq n$, and $k \neq j$ (i.e., there is a trend, and $S \neq 0$). The null hypothesis is rejected when S is significantly different from zero, and there is a monotonic trend over time. The test requires the calculation of the standardized test statistic, Z_s , which is assumed to come from a standard normal distribution, $N(0,1)$. The test statistic is given by

$$Z_s = \begin{cases} \frac{s-1}{\sigma_s} & \text{if } S > 0 \\ 0 & \text{if } S = 0 \\ \frac{s+1}{\sigma_s} & \text{if } S < 0 \end{cases} \quad (\text{B9})$$

The standard deviation of S is given by Kendall (1976) as

$$\sigma_s = \sqrt{\frac{1}{18} \left[n(n-1)(2n+5) - \sum_{p=1}^q t_p(t_p-1)(2t_p+5) \right]} \quad (\text{B10})$$

where q is the number of tied groups, and t_p is the size of the p^{th} tied group.

Sen-Theil Regression Tests

The method consists of computing the simple pairwise slope estimate: $S_{kj} = (X_j - X_k)/(t_j - t_k)$ for all possible distinct pairs of measurements, (X_k, X_j) where $t_j > t_k$. For a sample of size n , there will be $N = n(n-1)/2$ pairs of slopes. The Sen-Theil trend slope can then be computed as the median of all pairwise slopes, $b = \text{median}(S_{kj})$, and the intercept of the trend line is given by $a = \text{median}(X - bt)$. By taking the median pairwise slope instead of the mean, extreme pairwise slopes usually caused by outliers have little impact on the final slope estimate.

APPENDIX C. EXAMPLES OF INDICATORS AND THEIR POTENTIAL DATA SOURCES

Table C-1. Temperature indicators provided as examples in Vulnerability Assessment Tool (VAST).

Temperature Indicator	Description and Rationale	Potential Data Source(s)
Change in Total Number of Days per Year above/below a Threshold Temperature	Above a certain temperature, workforce or operational restrictions may come into effect. Materials such as pavement binders may have design temperature ranges, and temperatures above or below that range may cause structural damage. For example, the Gulf Coast study vulnerability assessment for Mobile used the projected number of days above 95°F per year as the exposure indicator, based on stakeholder input that 95°F represented a key operational threshold.	Climate model outputs (e.g., DOT CMIP Climate Data Processing Tool)
Change in Longest Number of Consecutive Days per Year above/below a Threshold Temperature	For some assets, the duration of heat waves or cold snaps may be more influential than the number of times a certain temperature is reached.	<ul style="list-style-type: none"> • Climate model outputs (e.g., DOT CMIP Climate Data Processing Tool)
Change in Number of Freeze-Thaw Cycles per Year	In some areas, freeze-thaw cycles may be the biggest cause of temperature-related damage. More frequent temperature variations around freezing point may be the best way to capture potential temperature-induced damage to infrastructure.	<ul style="list-style-type: none"> • Climate model outputs (e.g., DOT CMIP Climate Data Processing Tool) • Local university
Change in Annual Maximum or Minimum Temperature	The projected change in average annual temperatures (either daily highs or lows) is normally readily available and can provide a sense of the magnitude of projected warming in your area.	<ul style="list-style-type: none"> • Climate model outputs (e.g., DOT CMIP Climate Data Processing Tool) • Regional climate projections -- National Climate Assessment or FHWA Climate Change Effects Typology • Local university
Change in Annual Mean Temperature	The projected change in average annual temperatures is normally readily available and can provide a sense of the magnitude of projected warming in your area.	<ul style="list-style-type: none"> • Climate model outputs (e.g., DOT CMIP Climate Data Processing Tool) • Regional climate projections -- National Climate Assessment or FHWA Climate Change Effects Typology • Local university

Table C-2. Precipitation indicators provided as examples in Vulnerability Assessment Tool (VAST).

Precipitation Indicator	Rationale	Potential Data Source(s)
Change in Amount of Rain associated with 100-year 24-hour Storm	Some types of infrastructure are more sensitive to short-term, extreme precipitation events. Changes in the volume of rainfall from a 24-hour storm may influence the effectiveness of stormwater detention systems.	<ul style="list-style-type: none"> • Climate model outputs (e.g., DOT CMIP Climate Data Processing Tool) • Local university
Location in FEMA 100-Year Flood Zone	Assets located in floodplains are more likely to be exposed to flooding from changes in precipitation. The flood zone return period to focus on depends on the assessment.	<ul style="list-style-type: none"> • FEMA Digital Flood Insurance Maps (DFIRMs)
Location in FEMA 500-Year Flood Zone	Assets located in floodplains are more likely to be exposed to flooding from changes in precipitation. The flood zone return period to focus on depends on the assessment.	<ul style="list-style-type: none"> • FEMA Digital Flood Insurance Maps (DFIRMs)
Location in 10-Year Floodplain	Assets located in floodplains are more likely to be exposed to flooding from changes in precipitation. The flood zone return period to focus on depends on the assessment.	<ul style="list-style-type: none"> • Flood Insurance Studies • Maintenance and emergency management staff
Location in 25-Year Floodplain	Assets located in floodplains are more likely to be exposed to flooding from changes in precipitation. The flood zone return period to focus on depends on the assessment.	<ul style="list-style-type: none"> • Flood Insurance Studies • Maintenance and emergency management staff
Change in Number of Consecutive Days with Precipitation	Soil moisture influences performance of drainage systems as well as slope stability for roads and bridges.	<ul style="list-style-type: none"> • Climate model outputs (e.g., DOT CMIP Climate Data Processing Tool) • Local university
Change in Total Seasonal Precipitation	Total seasonal precipitation impacts landscapes and vegetation and is therefore an important consideration in wetland mitigation projects.	<ul style="list-style-type: none"> • Climate model outputs (e.g., DOT CMIP Climate Data Processing Tool) • Local university

Table C-2. Continued.

Precipitation Indicator	Rationale	Potential Data Source(s)
Change in Total Annual Precipitation	If total seasonal precipitation is unknown, annual precipitation can serve as an indicator for impacts landscapes and vegetation.	<ul style="list-style-type: none"> • Climate model outputs (e.g., DOT CMIP Climate Data Processing Tool) • Local university
Change in Peak Discharge	Culvert design can be based on peak discharge associated with a flooding event of a given return period (e.g., 1 in 100-year flood).	<ul style="list-style-type: none"> • Climate model outputs (e.g., DOT CMIP Climate Data Processing Tool) • Local university
Change in Flow Velocity	Flow velocity is often one factor considered in the design of stormwater management systems for transportation infrastructure.	<ul style="list-style-type: none"> • Climate model outputs (e.g., DOT CMIP Climate Data Processing Tool) • Local university
Change in Discharge Volume	Discharge volume is often one factor considered in the design of stormwater management systems for transportation infrastructure.	<ul style="list-style-type: none"> • Climate model outputs (e.g., DOT CMIP Climate Data Processing Tool) • Local university

Table C-3. Sea Level Rise indicators provided as examples in Vulnerability Assessment Tool (VAST).

Sea Level Rise Indicator	Rationale	Potential Data Source(s)
Modeled SLR Inundation Depth	Assets projected to be inundated by sea level rise are, definitionally, the most exposed to sea level rise.	GIS Sea Level Rise model
Elevation	Elevation can serve as natural protection from sea level rise. The higher an asset, the less exposed it may be to sea level rise.	<ul style="list-style-type: none"> • National Elevation Dataset (NED) • LiDAR • Asset management system
Proximity to Coastline	Assets closer to the coast may be more likely to be exposed to sea level rise.	<ul style="list-style-type: none"> • GIS analysis • Google Earth
USGS Coastal Vulnerability Index	The Coastal Vulnerability Index (CVI) calculates the relative risks to a coastal area due to future sea level rise, and includes factors such as tidal range, wave height, coastal slope, shoreline change, geomorphology, and historical rate of sea level rise. The Index is scored on a scale of 1 to 4.	http://pubs.usgs.gov/of/2004/1020/html/cvi.htm

Table C-4. Storm surge indicators provided as examples in Vulnerability Assessment Tool (VAST).

Storm Surge Indicator	Rationale	Potential Data Source(s)
Modeled Surge Inundation Depth	The assets inundated under the most water based on the ADCIRC storm scenarios are the most exposed to storm surge.	<ul style="list-style-type: none"> • ADCIRC model • STWAVE - Steady State spectral WAVE model • USGS Coastal Change Hazards: Hurricanes and Extreme Storms web viewer • NOAA Sea, Lake and Overland Surge from Hurricanes (SLOSH) model (http://www.nhc.noaa.gov/surge/slosh.php)
Proximity to Coastline	Assets closer to the coast may be more likely to be exposed to storm surge.	<ul style="list-style-type: none"> • GIS analysis • Google Earth
Elevation	Elevation serves as natural protection from storm surge. The higher an asset, the less exposed it may be to storm surge.	<ul style="list-style-type: none"> • National Elevation Dataset (NED) • LiDAR • Asset management system
USGS Coastal Vulnerability Index	The Coastal Vulnerability Index (CVI) calculates the relative risks to a coastal area due to future sea level rise, and includes factors such as tidal range, wave height, coastal slope, shoreline change, geomorphology, and historical rate of sea level rise. The Index is scored on a scale of 1 to 4.	http://pubs.usgs.gov/of/2004/1020/html/cvi.htm
Presence in FEMA Coastal Flood Zone	Assets located in floodplains are more likely to be exposed to flooding from storm surge. The flood zone return period to focus on depends on the assessment.	https://msc.fema.gov/webapp/wcs/stores/servlet/FemaWelcomeView?storeId=10001&catalogId=10001&langId=-1
Presence of Protective Structures	Protective structures may divert storm surge from an asset, reducing its exposure.	<ul style="list-style-type: none"> • Asset management system • Google Earth

Table C-5. Wind exposure indicators provided as examples in Vulnerability Assessment Tool (VAST).

Wind Exposure Indicator	Rationale	Potential Data Source(s)
Modeled Wind Speed	The assets that experience the highest wind speeds in the ADCIRC storm scenarios are the most exposed to hurricane winds.	<ul style="list-style-type: none"> • ADCIRC model • USGS Coastal Change Hazards: Hurricanes and Extreme Storms web viewer
Observed Wind Speed Records	Historical wind speeds at a location can provide a proxy for how likely a location is to be exposed to winds in future storms.	<ul style="list-style-type: none"> • NOAA Weather Stations • State climatologist

APPENDIX D. REPORT ON NONSTATIONARY DETECTION USING USACE'S
TIME SERIES TOOLBOX

1. Introduction

This report includes demonstration results from using USACE’s Time Series Analysis toolbox to detect different types of nonstationarity in environmental time series. The webtool can be found here: https://climate.sec.usace.army.mil/tst_app/ along with a detailed user guide. Here the tool is used and applied to three different types of environmental variables and the associated time series (aggregated or pre-processed in different ways): sea level, streamflow, and precipitation. Sea level data is available at hourly resolution and as monthly and annual means. We first analyze the monthly and annual mean time series and then derive a time series of annual maxima water levels after removing the annual mean sea level from the raw data. Finally, we perform a tidal analysis and derive time series of annual maxima surge values and analyze those. Precipitation and discharge data is available at daily resolution, and we use that to derive annual maxima time series and also derive and analyze annual mean time series (see Table 1 for a summary of the different time series that were analyzed).

Table 1 - Data types and their temporal resolution used in the analysis

Data Type	Monthly mean	Annual Mean	Annual Max
Sea-level	x	x	x (from hourly data)
Precipitation		x	x (from daily data)
Discharge		x	x (from daily data)
Surge			x (from hourly data)

In general, the analysis procedure consists of 7 different steps, as outlined in the following (for more details see User Guide):

1. Uploading data in the correct format
2. The tool provides summary information of the data, basic statistics, and visualization (including the seasonal cycle)
3. Trend analysis: the toolbox uses regression techniques to fit linear trend lines to the data (traditional and Sen’s slope) and performs hypothesis tests to determine significance of trends
4. Identifying seasonality: the toolbox uses a series of statistical methods to identify and define seasonal patterns in the data. [WE DO NOT SHOW RESULTS FOR THIS STEP]
5. Nonstationarity detection: the toolbox uses statistical testing to detect changes in the time series mean, variance, or distribution
6. Breakpoint analysis: the toolbox identifies sudden changes in the time series
7. Time series modeling: the toolbox provides three models (time series linear model, autoregressive integrated moving average (ARIMA), and exponential smoothing (ETS)) to

determine the appropriate time series model that accounts for seasonality, trend and nonstationarities. [WE DO NOT SHOW RESULTS FOR THIS STEP]

The following limitations exist and have to be taken into account when selecting data to analyze with the tool:

- Time series toolbox has limits to upload size (failed to take 16 MB and above)
- The toolbox requires that there are at least 30 points of continuous data in the dataset, otherwise it is unable to perform the analysis.

The following sections include the results from steps 3, 5, and 6, as those are most relevant to the detection of nonstationarity and its consideration in extreme value analysis. Results are first shown for sea level data (Section 2), then for precipitation (Section 3), and streamflow (Section 4).

2. Sea Level Data

Monthly mean sea level time series

The annual and monthly mean sea-level time series for the St Petersburg tide gauge was obtained from the Permanent Service for Mean Sea Level (PSMSL) database and covers the period from 1947 to 2021 (with 100% completeness) (see Figure 1 for the monthly time series).

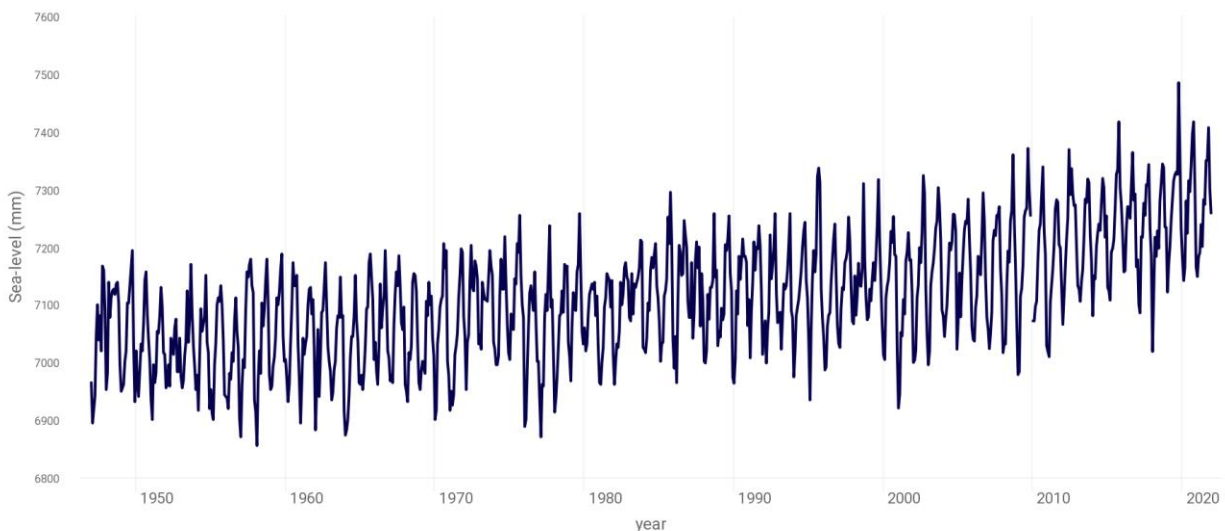


Figure 1 – Monthly mean sea-level time series

Both the traditional and Sen's slopes indicate a positive trend (Figure 2); 2.9996 (traditional slope) and 3.0112 (Sen's slope). Results from the trend hypothesis tests shown in Fig. 3 indicate that the trend is significant at the 5% level.

Data with Slope Fits (Traditional and Sen's Slope)

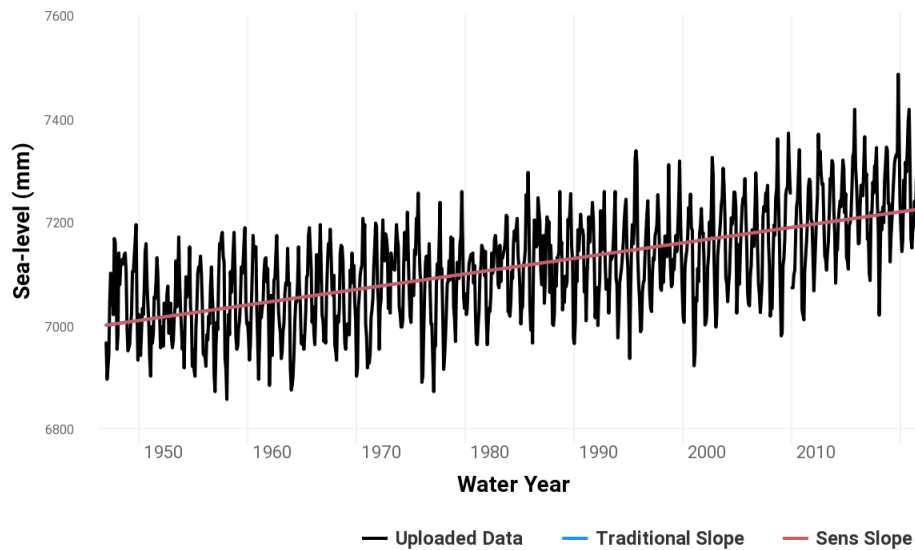


Figure 2 - Fitting trends: traditional and Sen's slope

Test	PValue
t-Test	3.593e-95
Mann-Kendall	< 2.2e-16
Spearman Rank-Order	1.7709e-90

Figure 3 - Trend hypothesis tests

The results from the nonstationarity analysis are displayed in Figures 4 to 7. Figure 4 shows the areas of potential (abrupt) nonstationarity, while Figure 5 shows the results for the individual statistical tests highlighting only the ones which indicate that nonstationarity is significant at a pre-defined level. In the case of St Petersburg that leads to the conclusion that there is a significant change in the distribution in the mid-1970s, where two different tests agree. Figure 6 shows key metrics (mean, variance, and standard deviation) for different segments of the time series, when segmentation is based on the results shown in Figure 4. Statistical test results for a breakpoint analysis are shown in Figure 7, which indicate here that three breakpoints exist where sharp changes in the time series behavior occur; this could warrant segmented analysis of the data based on these breakpoints. The User Guide included helpful information on consensus (i.e. multiple tests indicate same type of nonstationarity), robustness (i.e. changes in multiple

statistical properties), and magnitude (i.e. strengths of changes in statistical properties) to help interpreting results from using multiple tests for different statistical properties.

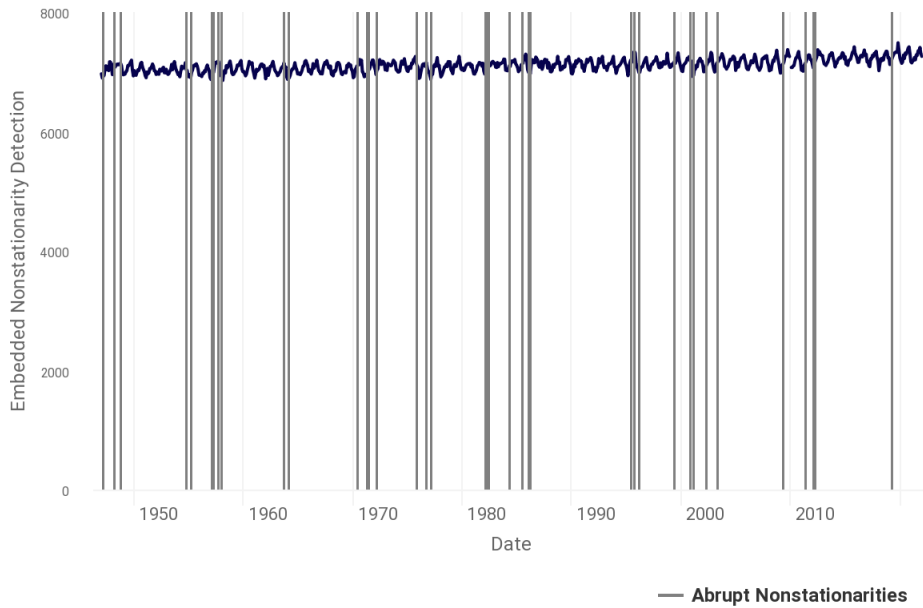


Figure 4 – Nonstationarity detection, vertical lines indicate possible areas of nonstationarity

Statistical Tests

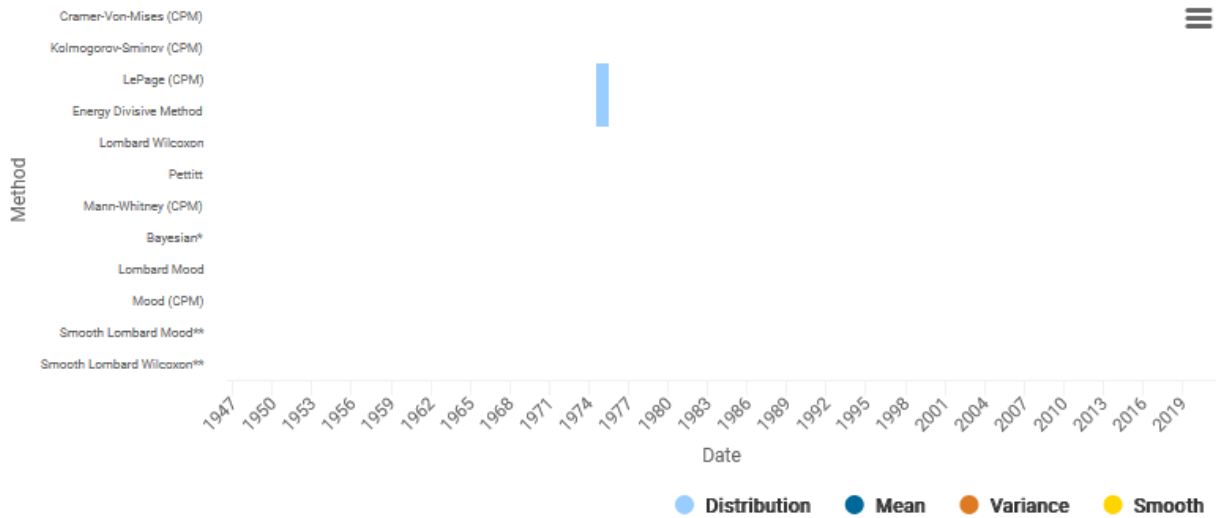


Figure 5 - Statistical tests applied to detect nonstationarity

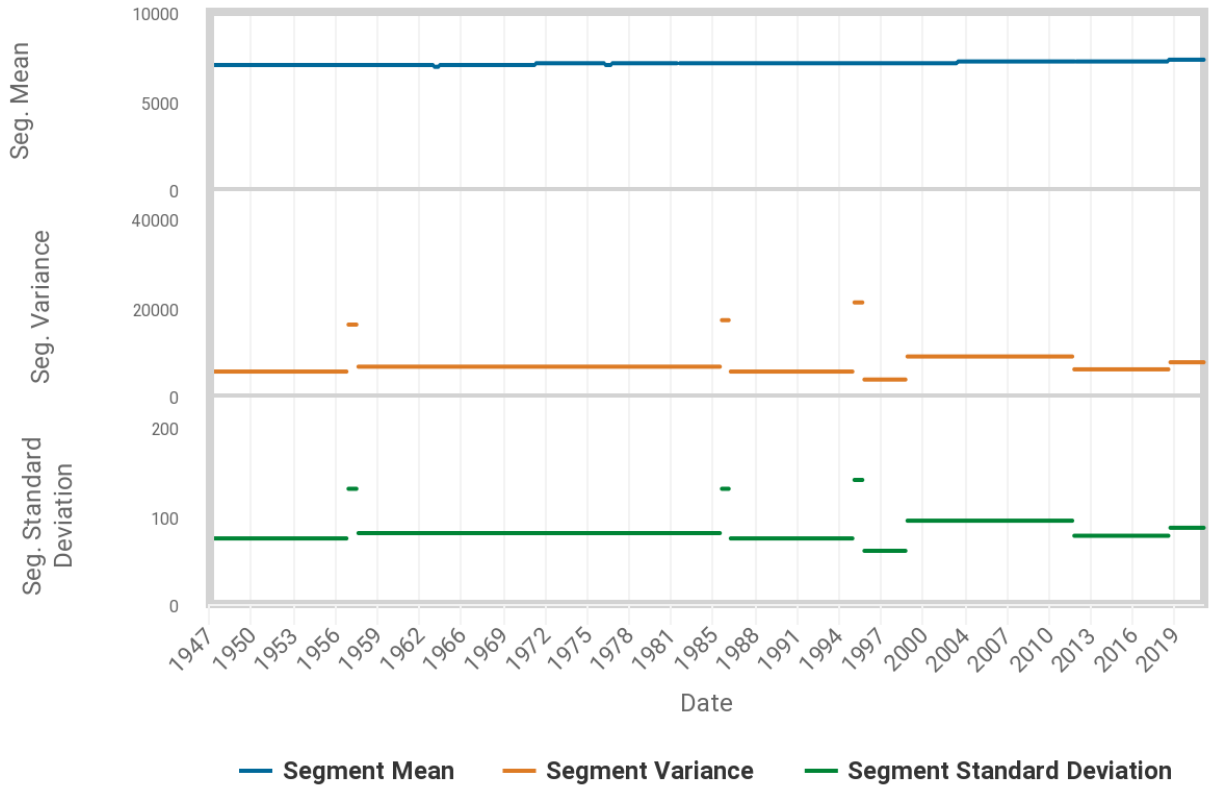


Figure 6 - Segment statistics, detecting changes in the mean, variance, and standard deviation of the time series

Plotted Data with Identified Breakpoints

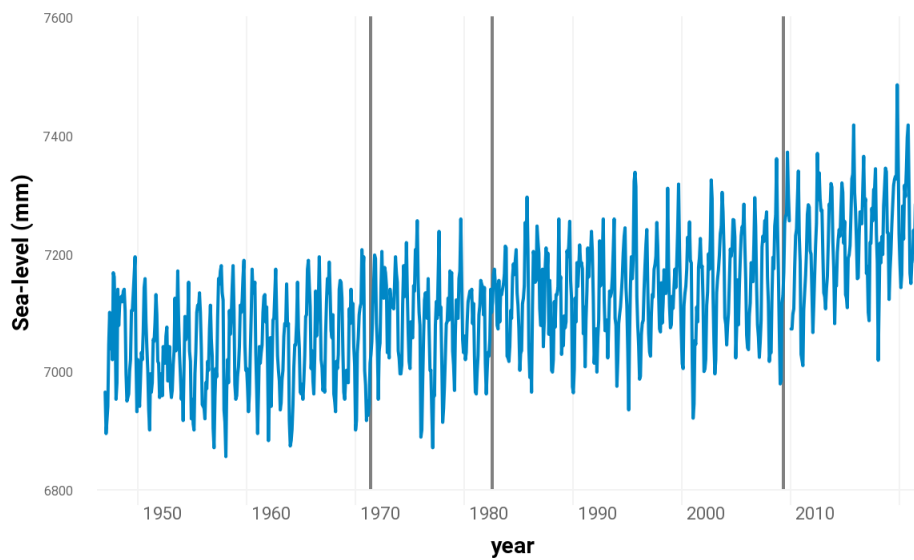


Figure 7 - Breakpoint detection, 1971 and 1982, and 2009 identified as breakpoints

Annual mean sea-level time series

Figures 8 to 14 show the same results as above but for the annual mean sea level time series in St Petersburg. Again, the trend analysis indicates the presence of significant trends and all tests agree on this result (this is to be expected given the clear sea level rise signal). In contrast to the monthly mean sea level analysis, where only abrupt nonstationarity was detected (vertical grey lines in Figure 4), Figure 11 indicates that smooth nonstationarity is detected for the entire period. This is a result of the same trend being present in the monthly and annual mean sea level time series, but much lower variance in the annual time series, which leads to statistically significant results in many cases. At the same time fewer points of potentially abrupt nonstationarity are identified due to the reduced variability. Four breakpoints are identified for the annual mean sea level time series.

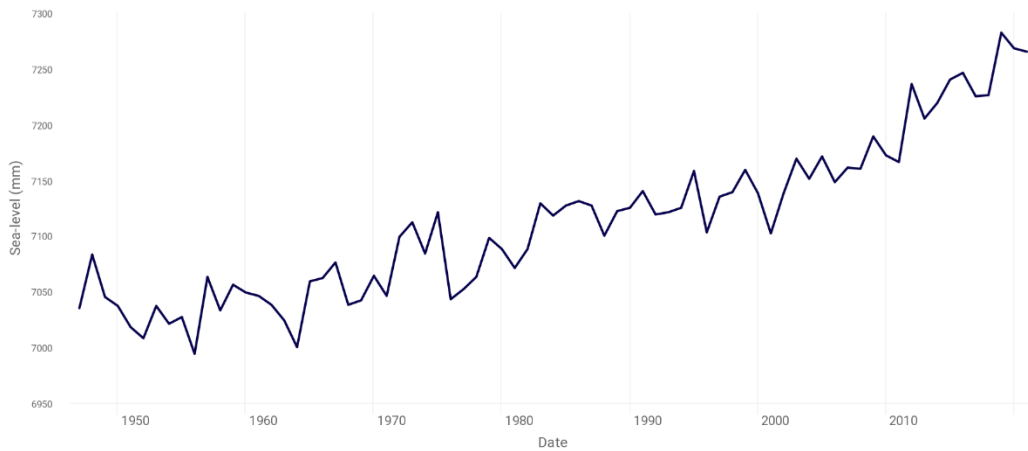


Figure 8 - Annual mean sea-level time series

Data with Slope Fits (Traditional and Sen's Slope)

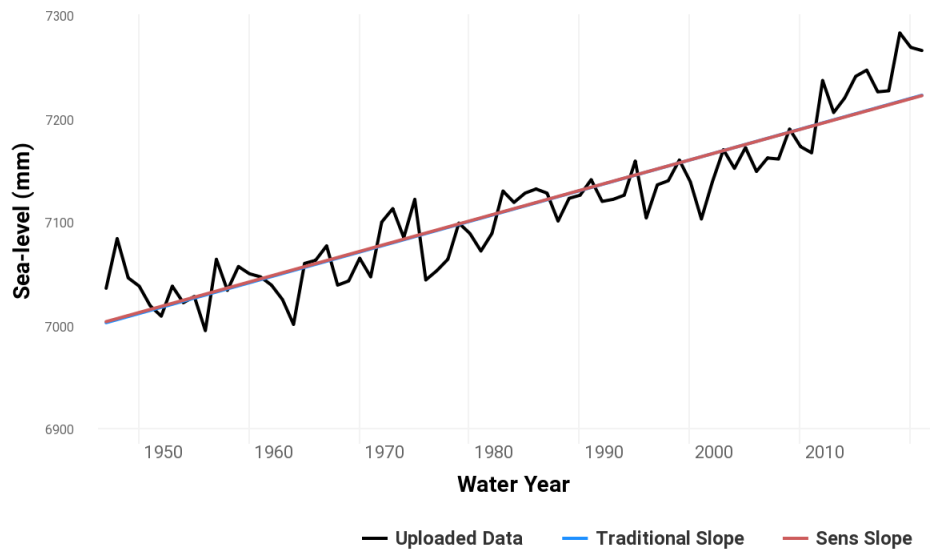


Figure 9 - Fitting trends: traditional and Sen's slope

Test	PValue
t-Test	4.9007e-32
Mann-Kendall	< 2.2e-16
Spearman Rank-Order	9.422e-36

Figure 10 - Trend hypothesis tests

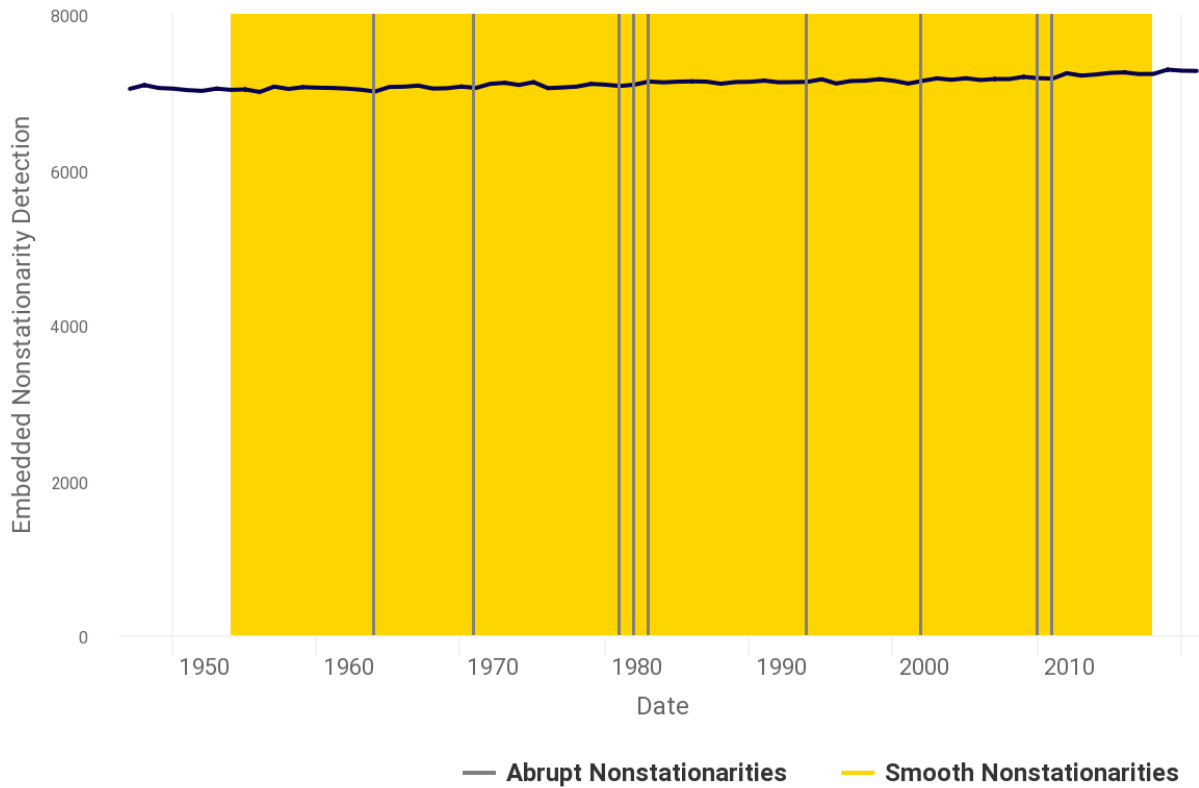


Figure 11 – Nonstationarity detection

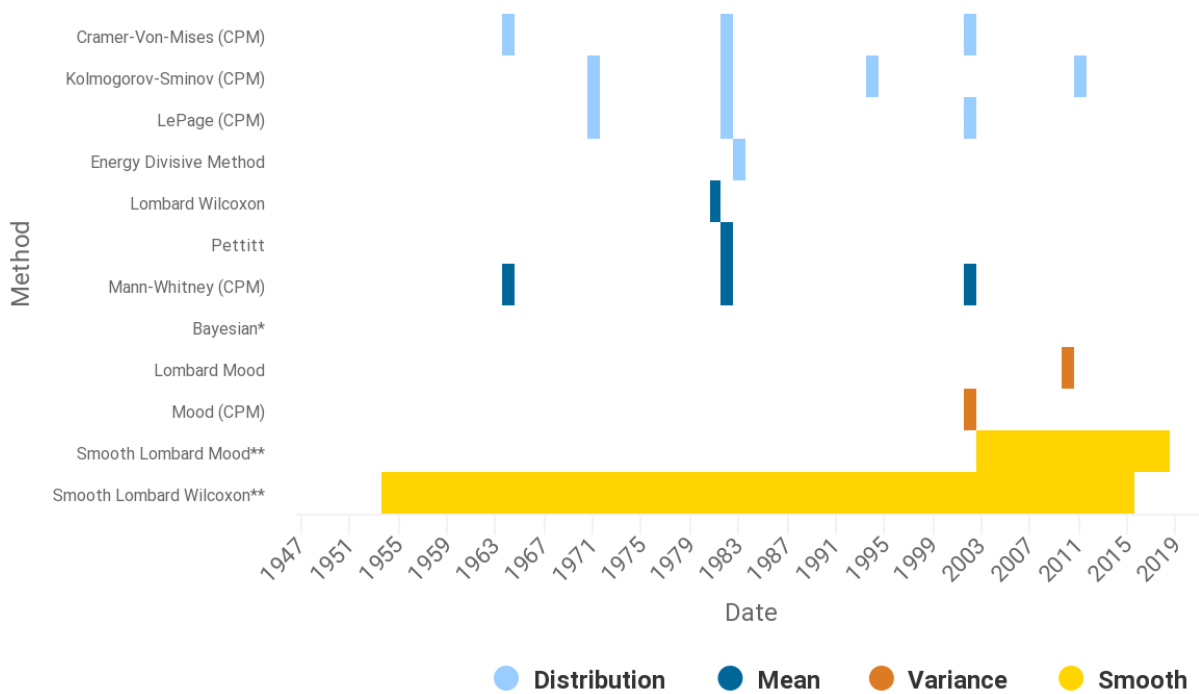


Figure 12 - Statistical tests applied to detect nonstationarity

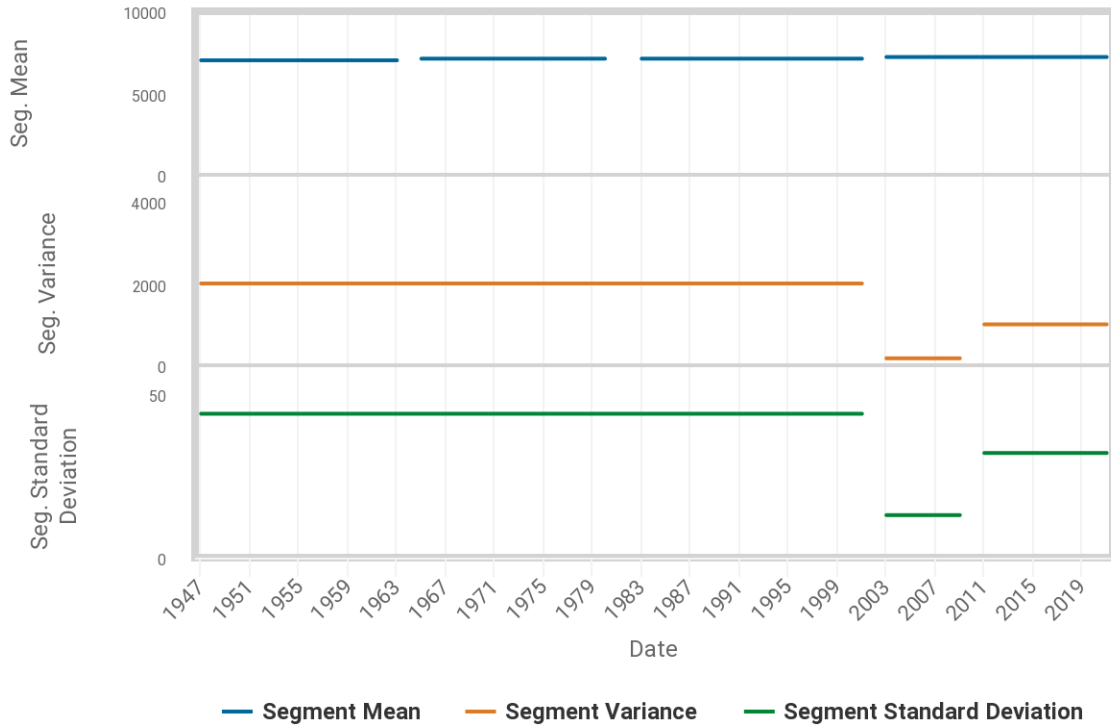


Figure 13 - Segment statistics, detecting changes in the mean, variance, and standard deviation of the time series

Plotted Data with Identified Breakpoints

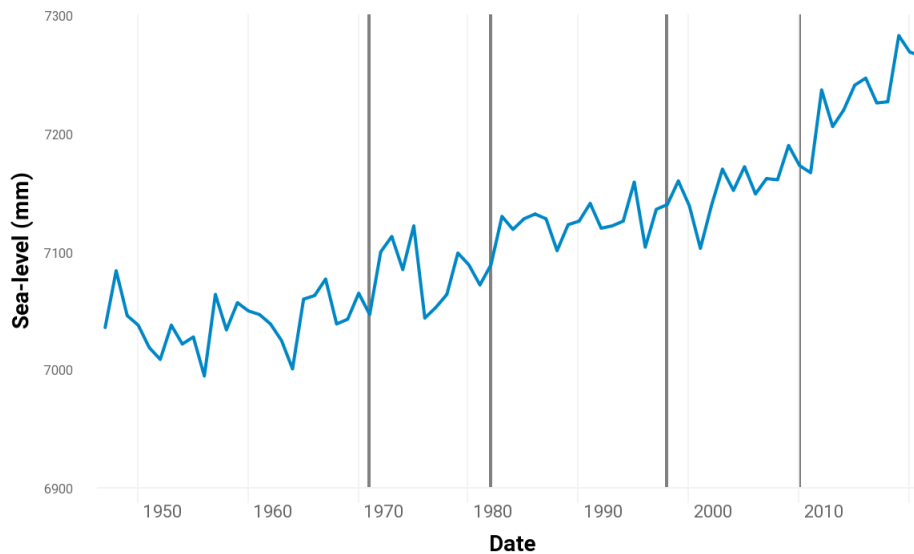


Figure 14 - Breakpoint detection, 1971, 1982, 1998, and 2010 detected as breakpoints

Annual maximum water level time series

Extreme value analysis is often conducted based on annual maxima time series. This requires at least hourly resolution of the underlying data. Here we use hourly data from the GESLA-2 database for the St Petersburg tide gauge from 1947 to 2012 to derive annual maxima values (Figure 15). Since we already established the important role of mean sea level rise from analyzing monthly and annual mean sea level time series, we removed the annual mean values from the hourly data before deriving annual maxima values. The trend tests still indicate the existence of significant positive trends, despite the much larger variability as compared, for example, to the annual mean sea level time series (Figures 16 and 17). Isolated instances of significant nonstationarity in the distribution and mean are found (Figures 18 and 19) but only from one test in each case and for different time periods (see comments on “consensus” and “robustness” above and in the User Guide). No breakpoints are identified (Figure 21).

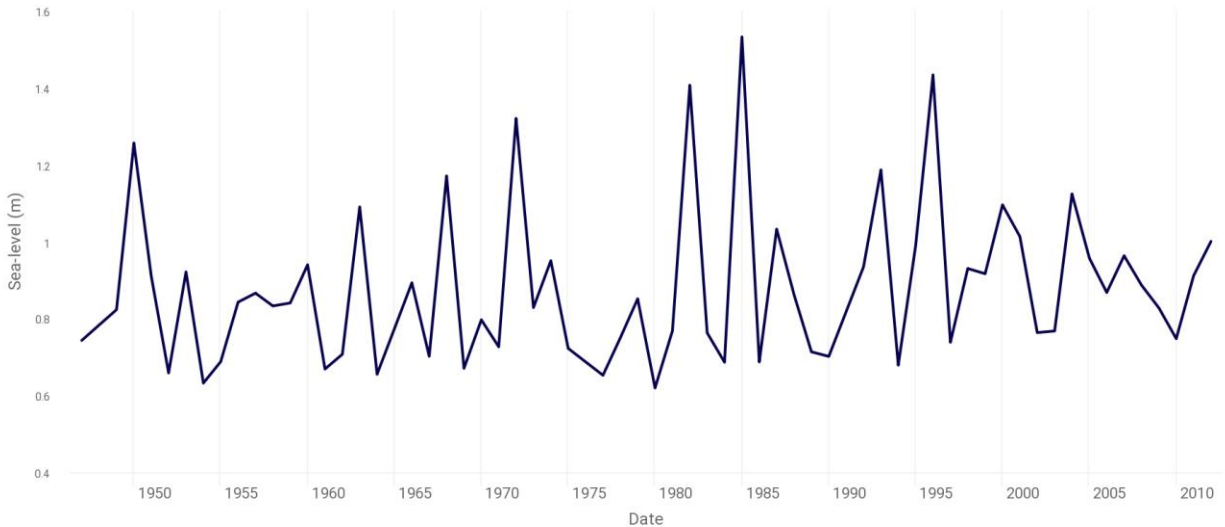


Figure 15 - Annual maximum sea-level time series

Data with Slope Fits (Traditional and Sen's Slope)

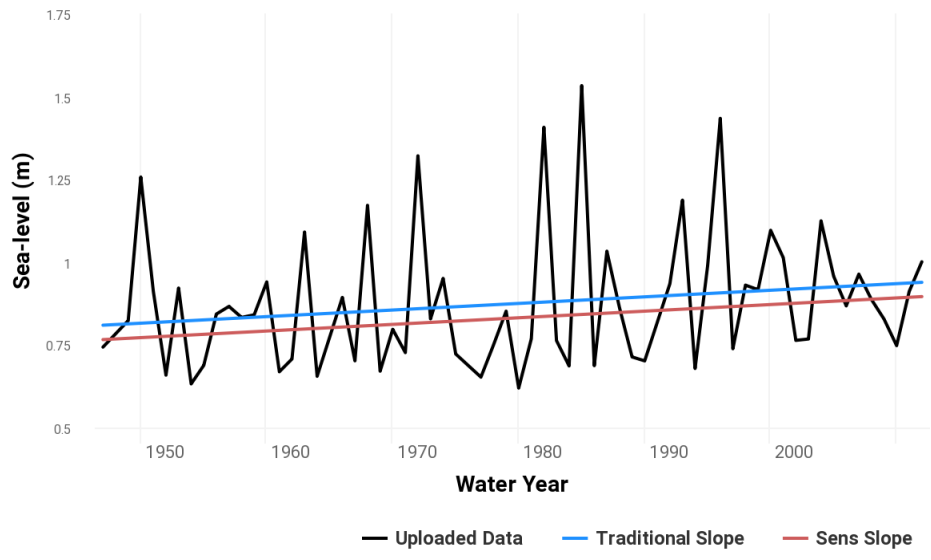


Figure 16 - Fitting trends: traditional and Sen's slope

Test	PValue
t-Test	0.12978
Mann-Kendall	0.052753
Spearman Rank-Order	0.040115

Figure 17 - Trend hypothesis tests

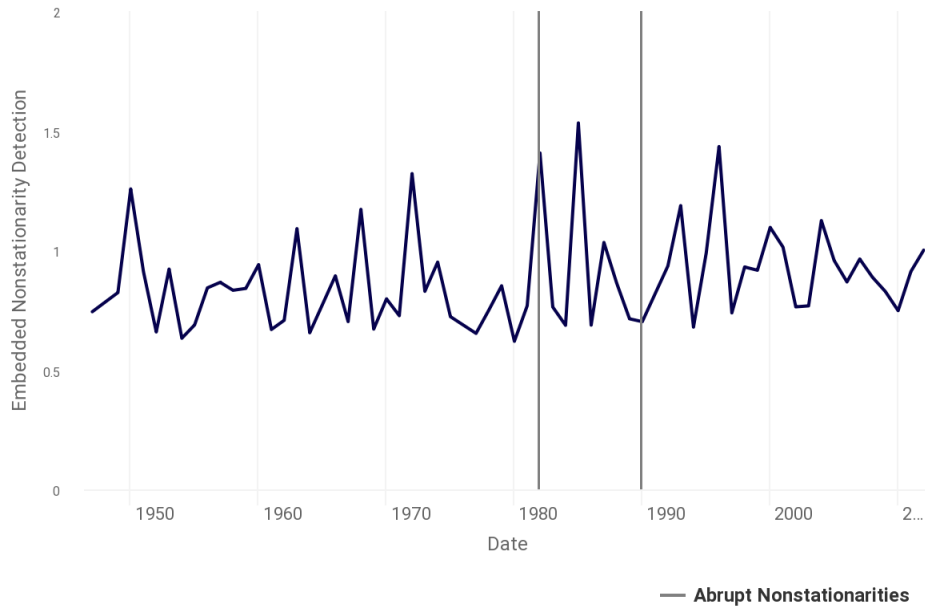


Figure 18 – Nonstationarity detection, vertical lines indicate abrupt nonstationarities

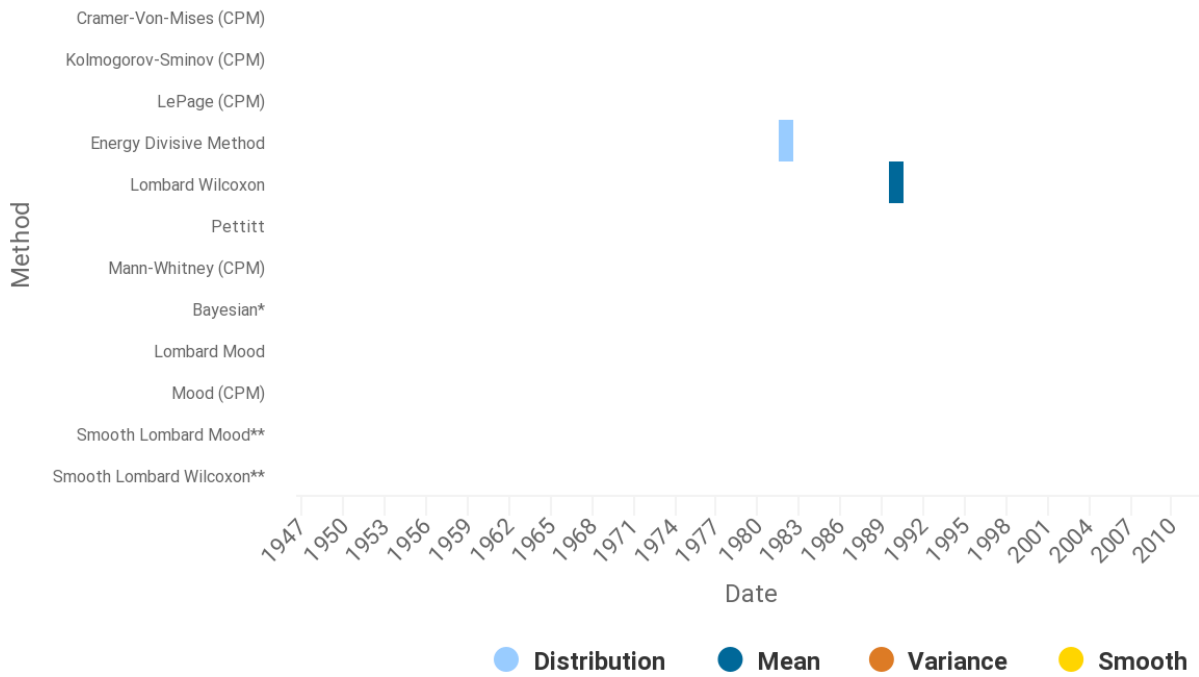


Figure 19 - Statistical tests applied to detect nonstationarity

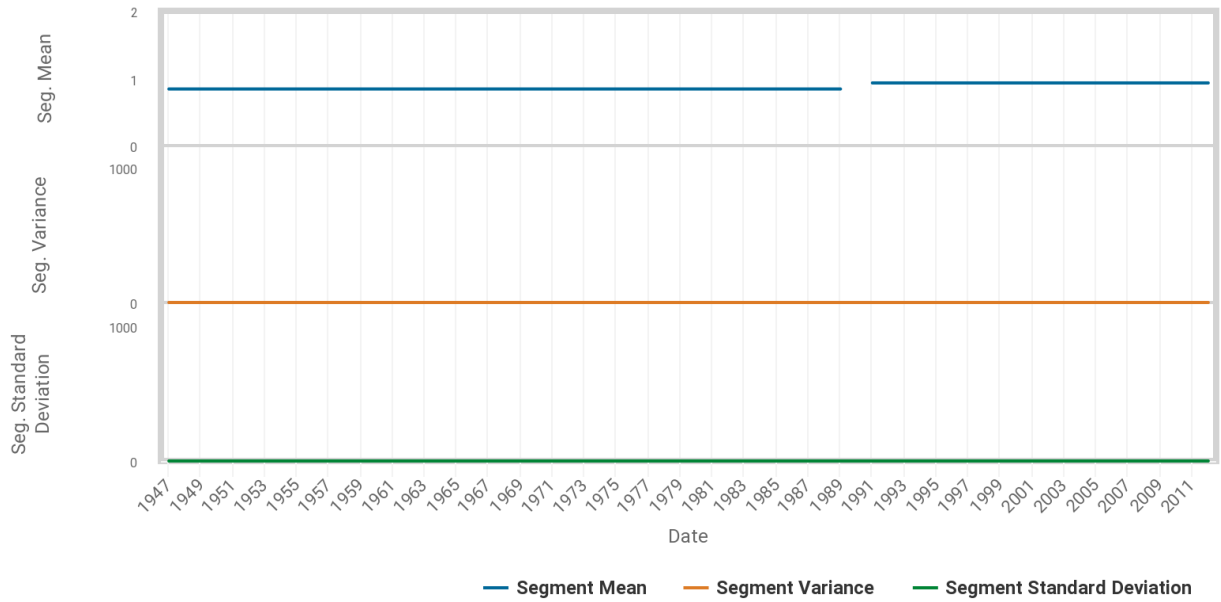


Figure 20 - Segment statistics, detecting changes in the mean, variance, and standard deviation of the time series

Plotted Data with Identified Breakpoints

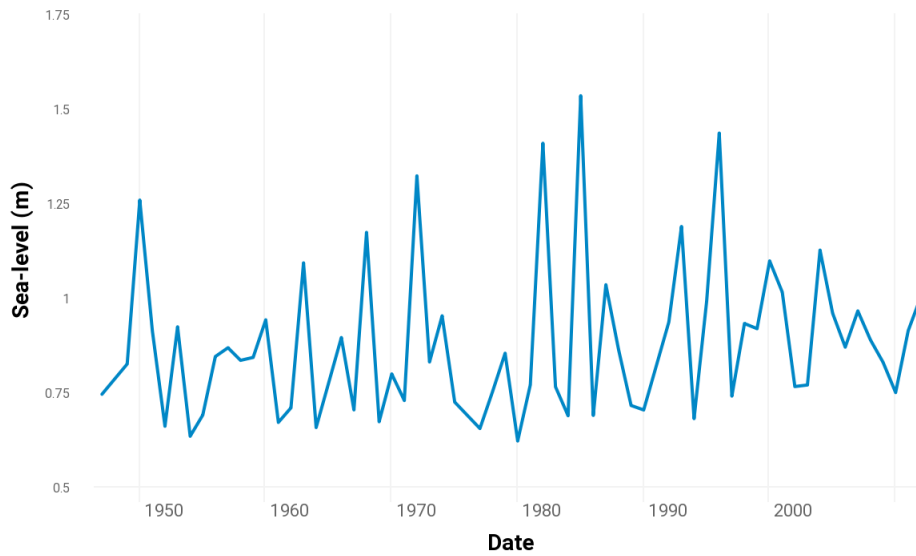


Figure 21 - Breakpoint detection, no breakpoints detected

3. Precipitation Data

In this section the same results as above are shown but for precipitation data. We use annual mean precipitation time series and annual maxima values (derived from daily cumulative rainfall). We use data for Fernandina Beach from 1898 to 2018.

Annual mean precipitation time series

The annual mean precipitation time series for Fernandina Beach is shown in Figure 22. Both the traditional and Sen's slopes indicate a positive trend; 0.0033 (traditional slope) and 0.0034 (Sen's slope) (Figure 23) and trend hypothesis tests indicate significance at the 5% level (Figure 24). Only abrupt nonstationarity is identified (Figure 25) and especially in the 2000s and 2010s multiple tests for various statistical time series attributes agree on the existence of nonstationarity in the mean, variance, and distribution (Figure 26). No break points are detected (Figure 28).

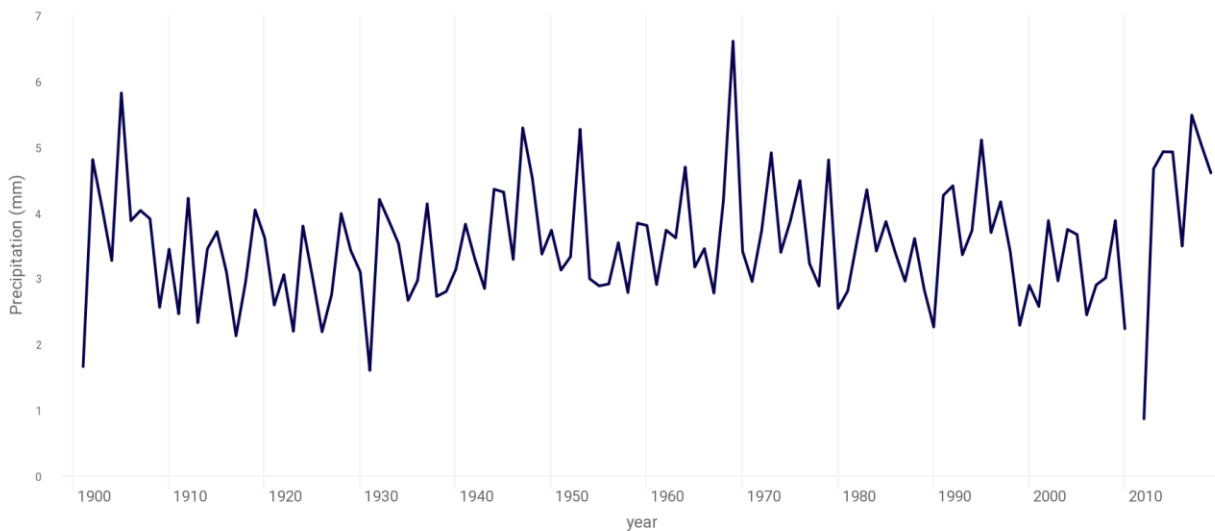


Figure 22 - Annual mean precipitation time series

Data with Slope Fits (Traditional and Sen's Slope)

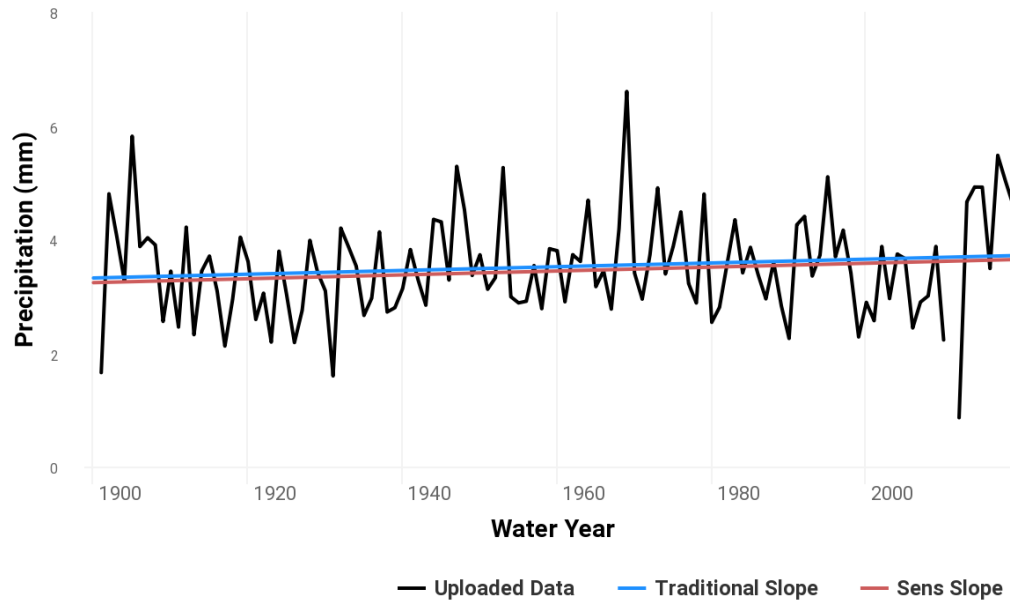


Figure 23 - Fitting trends: traditional and Sen's slope

Test	PValue
t-Test	0.17559
Mann-Kendall	0.17584
Spearman Rank-Order	0.19333

Figure 24 - Trend hypothesis tests

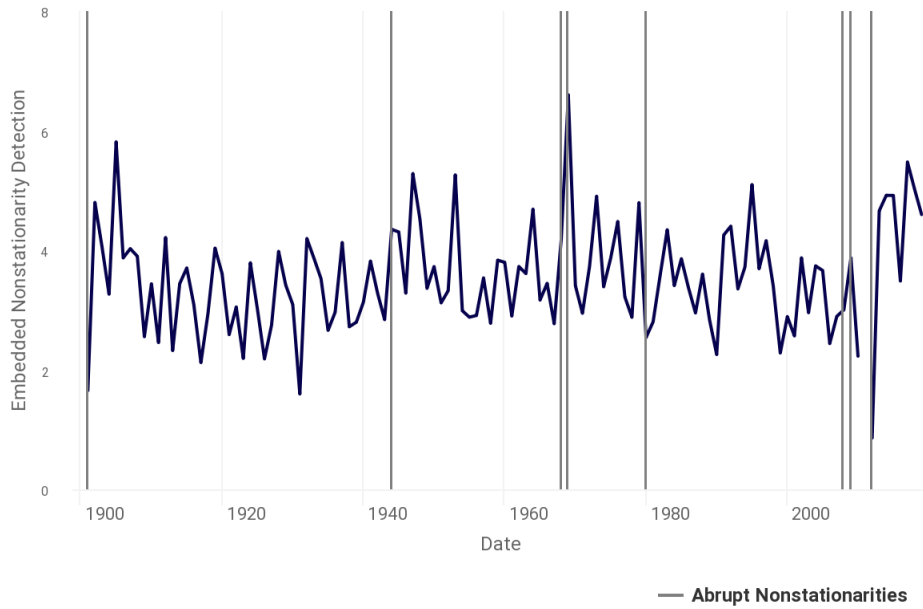


Figure 25 – Non-stationary detection, vertical lines indicate abrupt non-stationarities

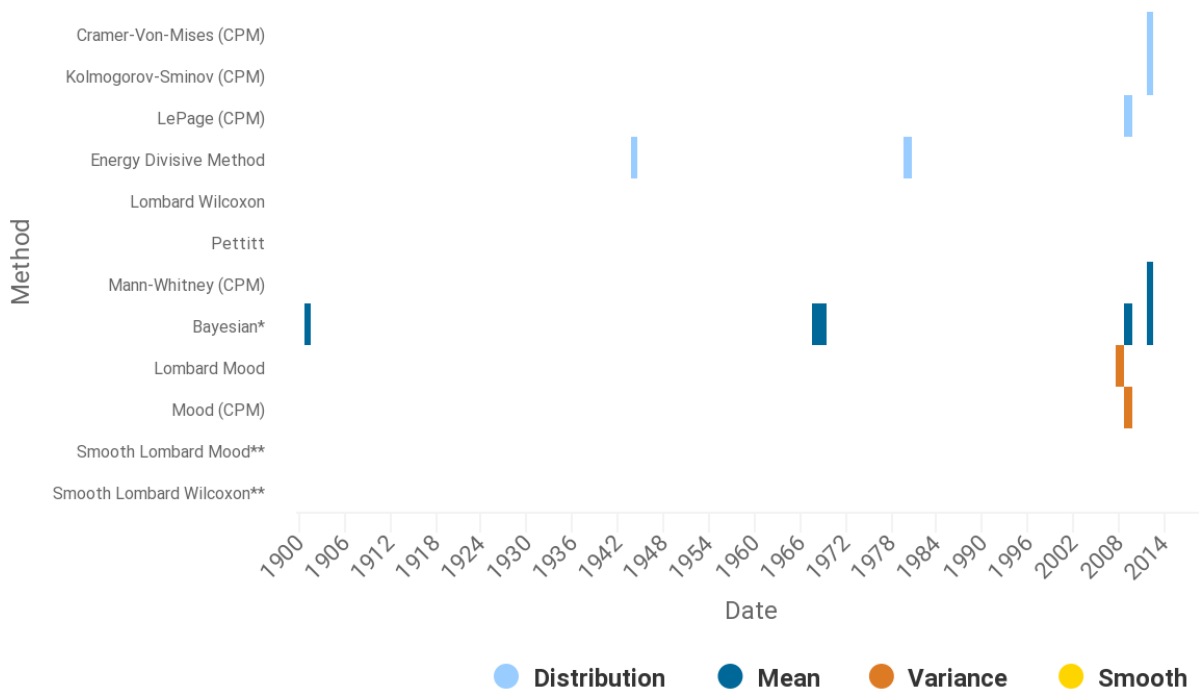


Figure 26 - Statistical tests applied to detect nonstationarity

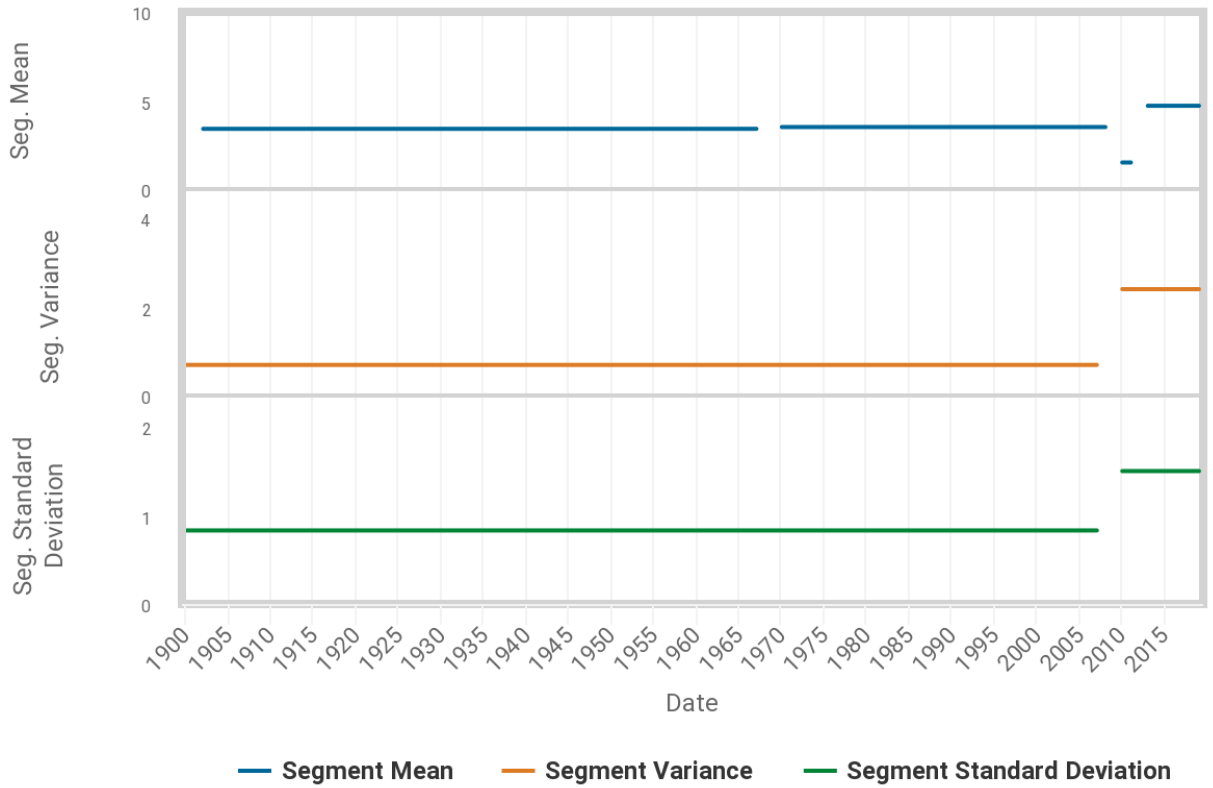


Figure 27 - Segment statistics, detecting changes in the mean, variance, and standard deviation of the time series

Plotted Data with Identified Breakpoints

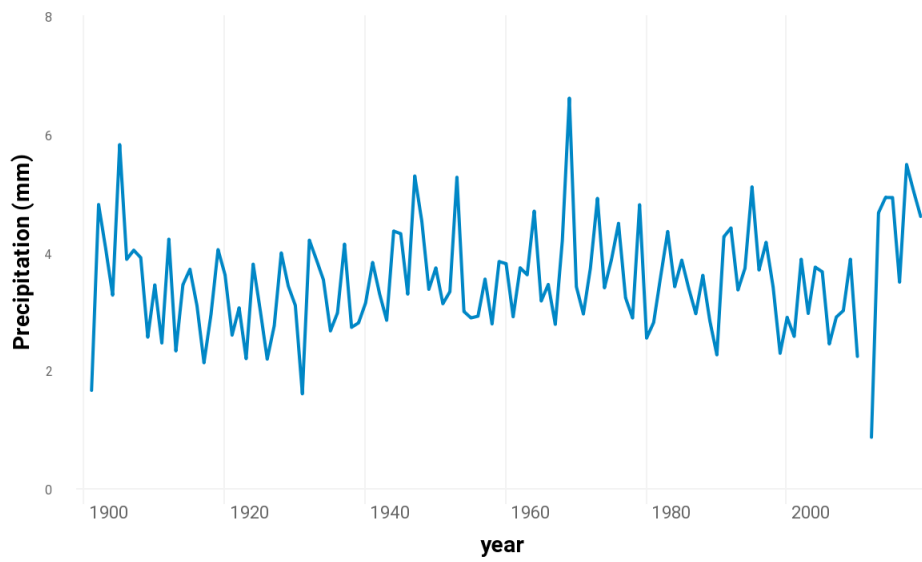


Figure 28 - Breakpoint detection, no breakpoints detected

Annual Maximum Precipitation Time Series

As outlined above, extreme value analysis often is performed using block maxima, where 1-year blocks are commonly used, leading to the use of annual maximum values. The annual maximum precipitation time series for Fernandina Beach is shown in Figure 29. In this case, both the traditional and Sen's slopes indicate a negative trend; -0.103 (traditional slope) and -0.163 (Sen's slope) (Figure 30) and trend hypothesis tests indicate significance at the 5% level (Figure 31). Only abrupt nonstationarity is found and only by individual tests for different years (Figures 32 and 33). No breakpoints are detected (Figure 35).

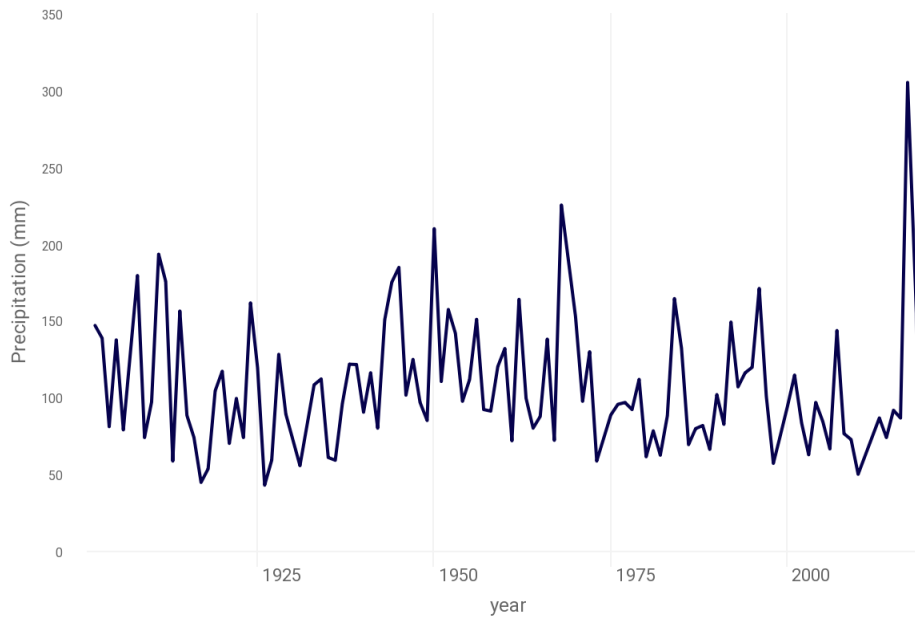


Figure 29 - Annual maximum precipitation time series

Data with Slope Fits (Traditional and Sen's Slope)

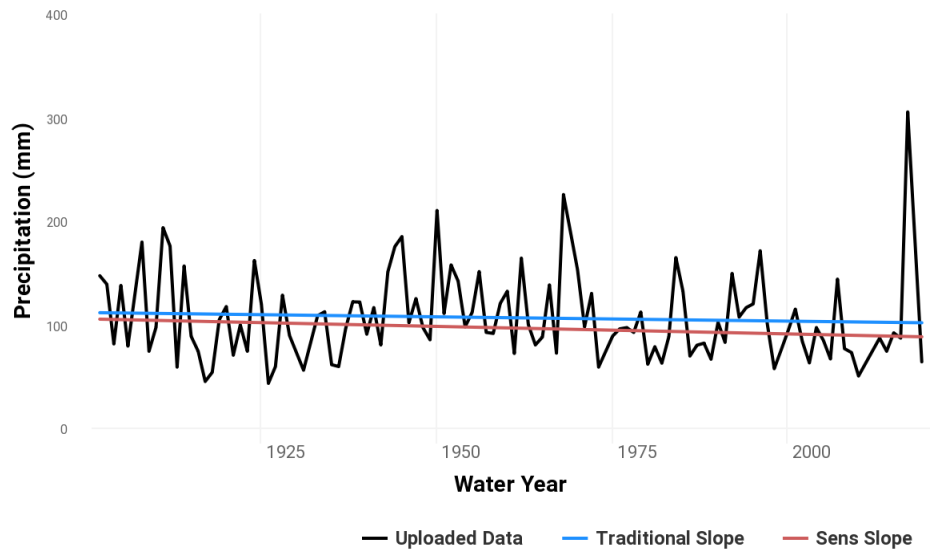


Figure 30 - Fitting trends: traditional and Sen's slope

Test	PValue
t-Test	0.39331
Mann-Kendall	0.1262
Spearman Rank-Order	0.14919

Figure 31 - Trend hypothesis tests

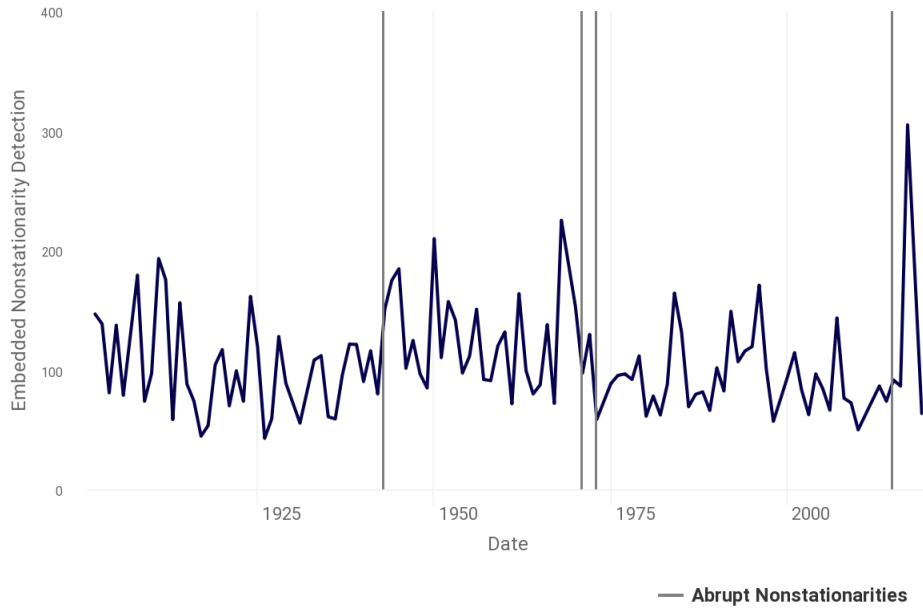


Figure 32 – Nonstationarity detection, vertical lines indicate abrupt nonstationarities

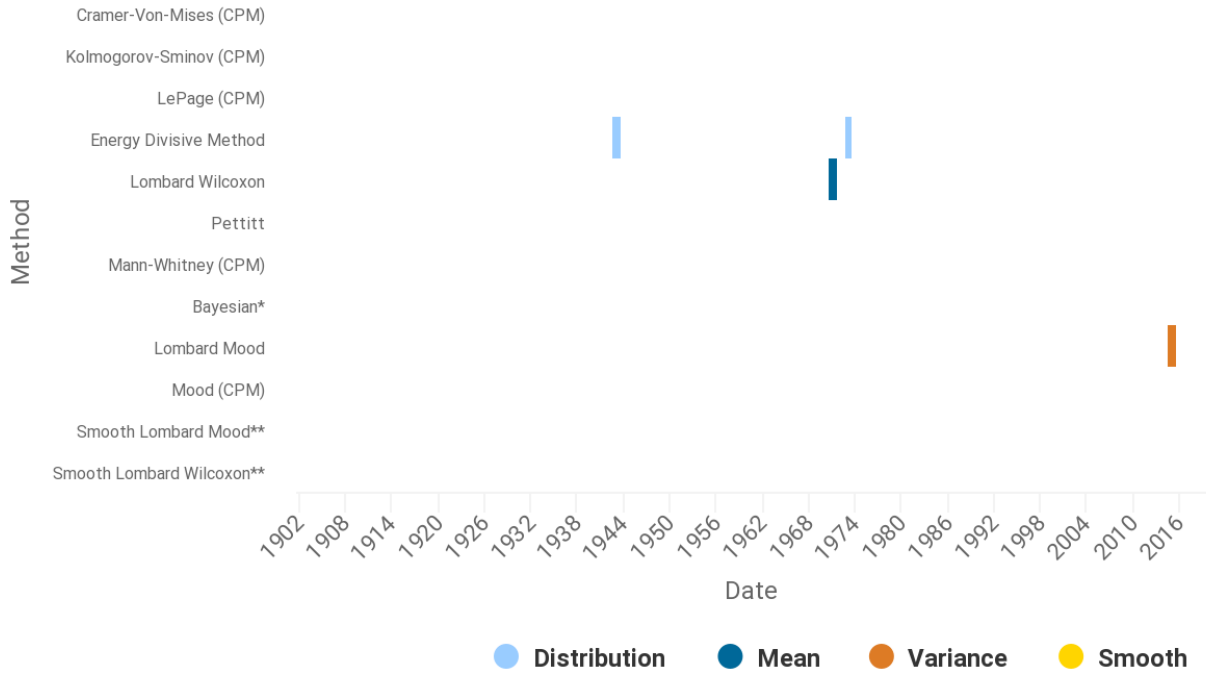


Figure 33 - Statistical tests applied to detect nonstationarity

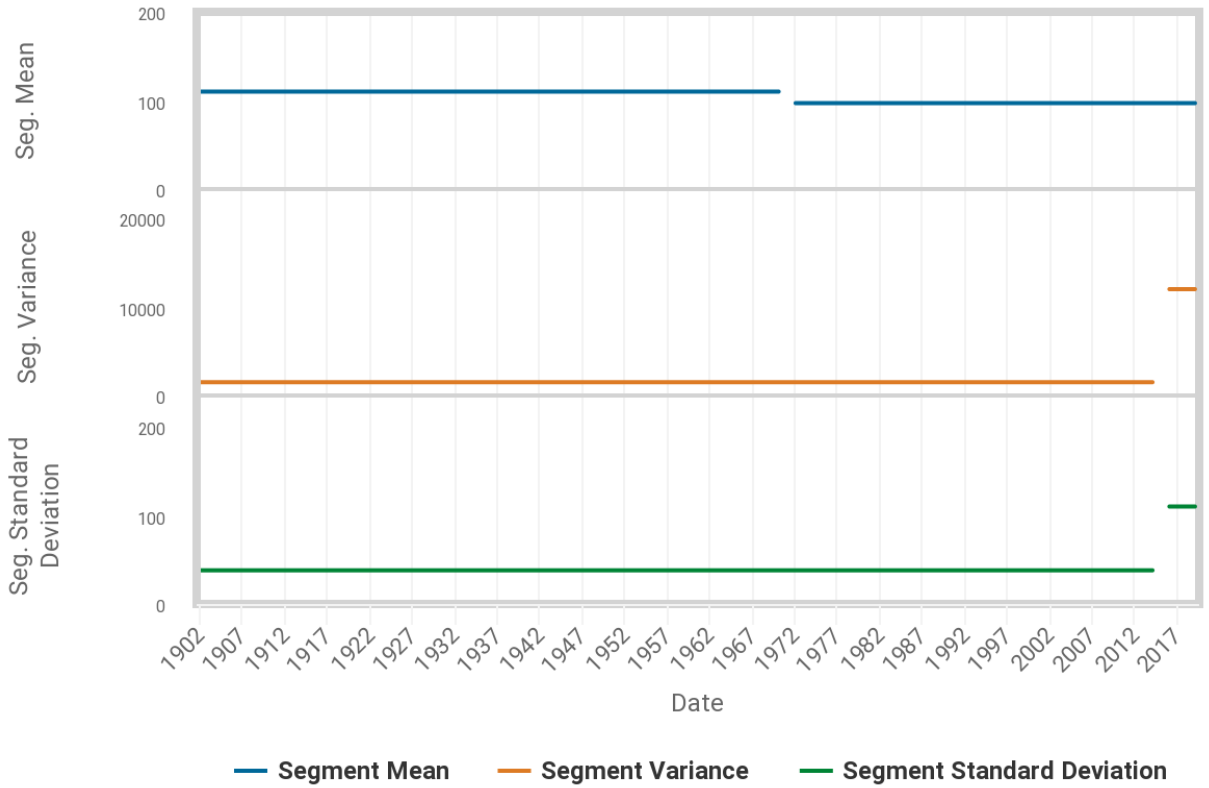


Figure 34 - Segment statistics, detecting changes in the mean, variance, and standard deviation of the time series

Plotted Data with Identified Breakpoints

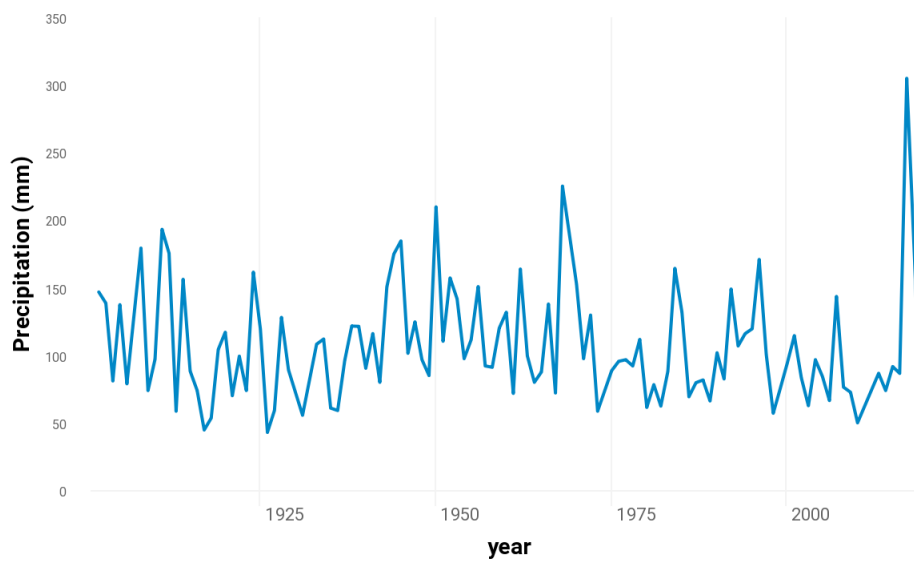


Figure 35 - Breakpoint detection, no breakpoints detected

4. Streamflow Data

The following shows the same results as displayed above for streamflow data from the Lithia gauge, which covers the period from 1932 to 2019. The data was derived from the Global Runoff Data Center (GRCD). Similar to the precipitation analysis, we apply the nonstationarity tool to annual mean and annual maxima (derived from daily mean values) streamflow data.

Annual mean streamflow time series

The annual mean stream time series for the Lithia gauge is shown in Figure 36. Both the traditional and Sen's slopes indicate a negative trend; -0.0315 (traditional slope) and -0.0293 (Sen's slope) (Figure 37) and trend hypothesis tests indicate significance at the 5% level (Figure 38). Abrupt nonstationarity is identified for three instances, clustered in the late 1960s to early 1970s (Figure 39), where two tests indicate a change in the mean and one test indicates a change in distribution (but all in different years) (Figure 40) No breakpoints are found (Figure 42).

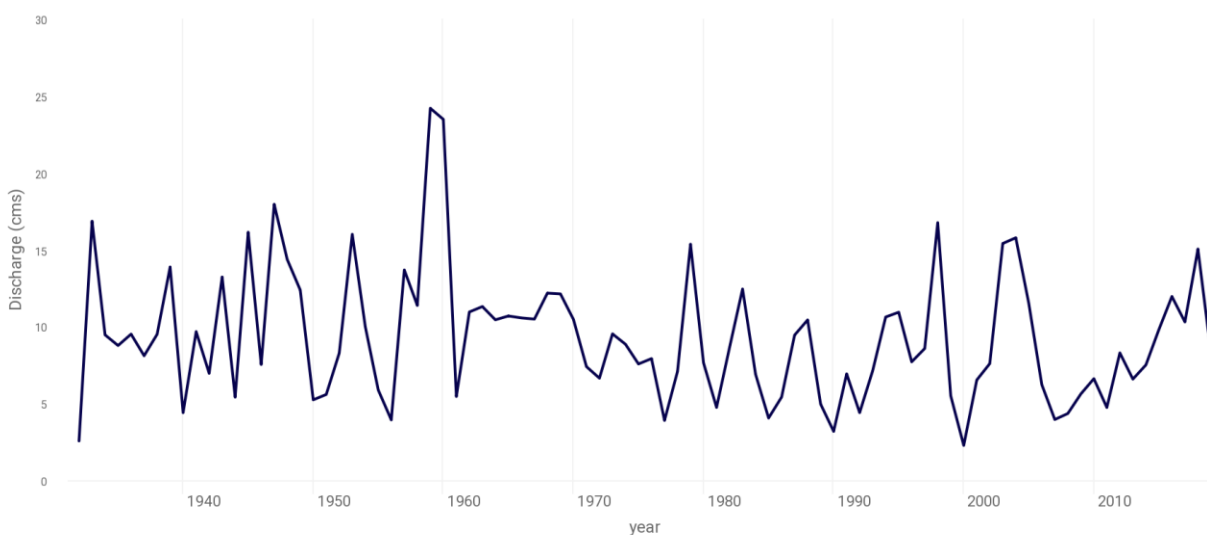


Figure 36 - Annual mean discharge time series

Data with Slope Fits (Traditional and Sen's Slope)

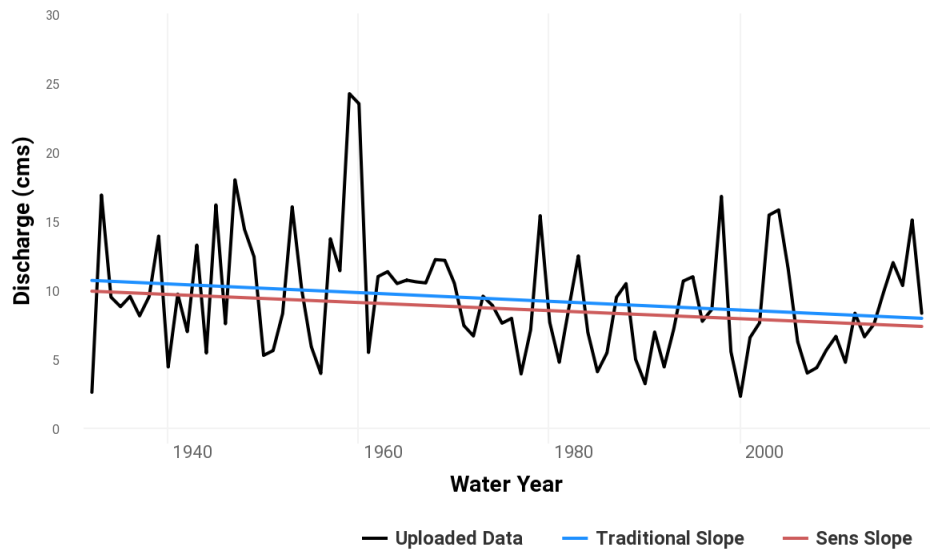


Figure 37 - Fitting trends: traditional and Sen's slope

Test	PValue
t-Test	0.078991
Mann-Kendall	0.074419
Spearman Rank-Order	0.087405

Figure 38 - Trend hypothesis tests

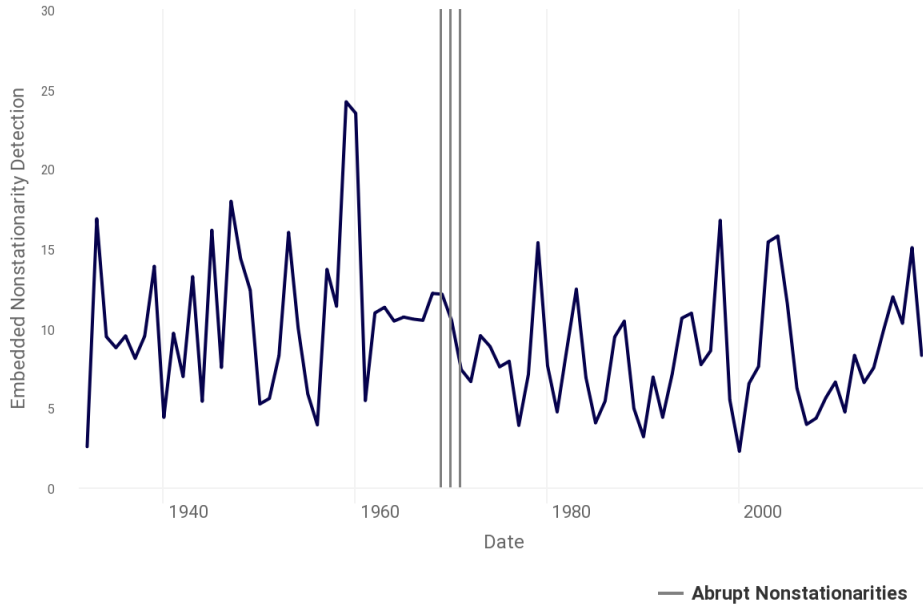


Figure 39 - Nonstationarity detection, vertical lines indicate abrupt nonstationarities

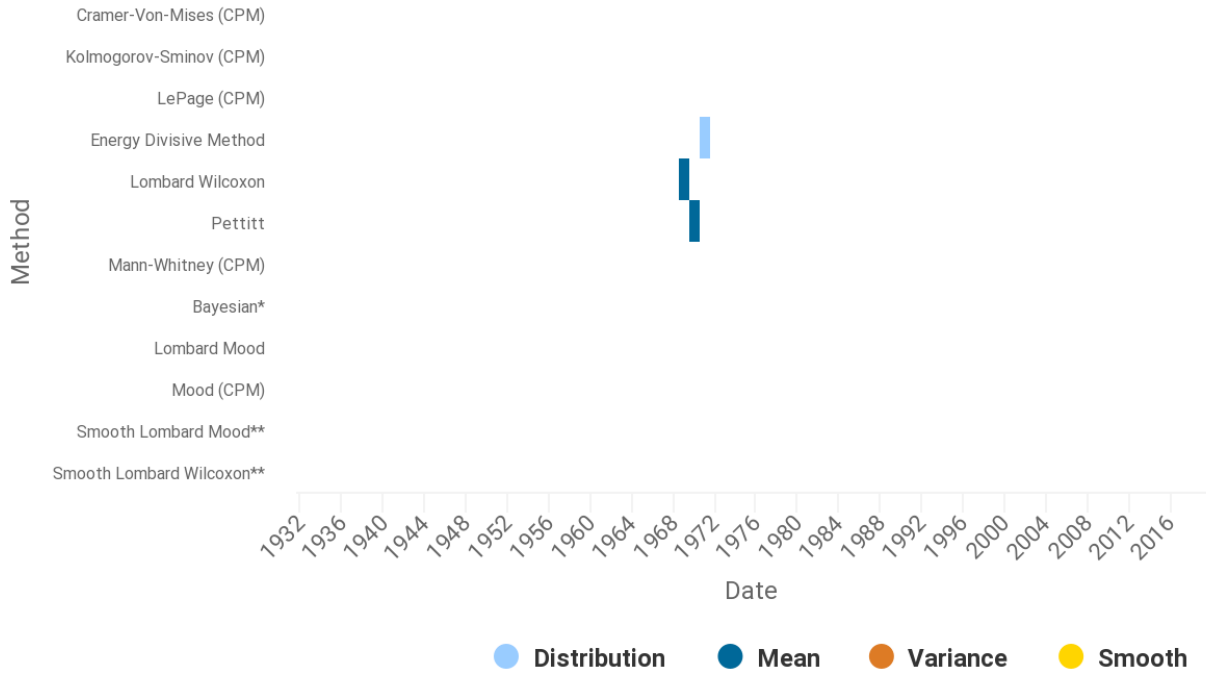


Figure 40 - Statistical tests applied to detect nonstationarity

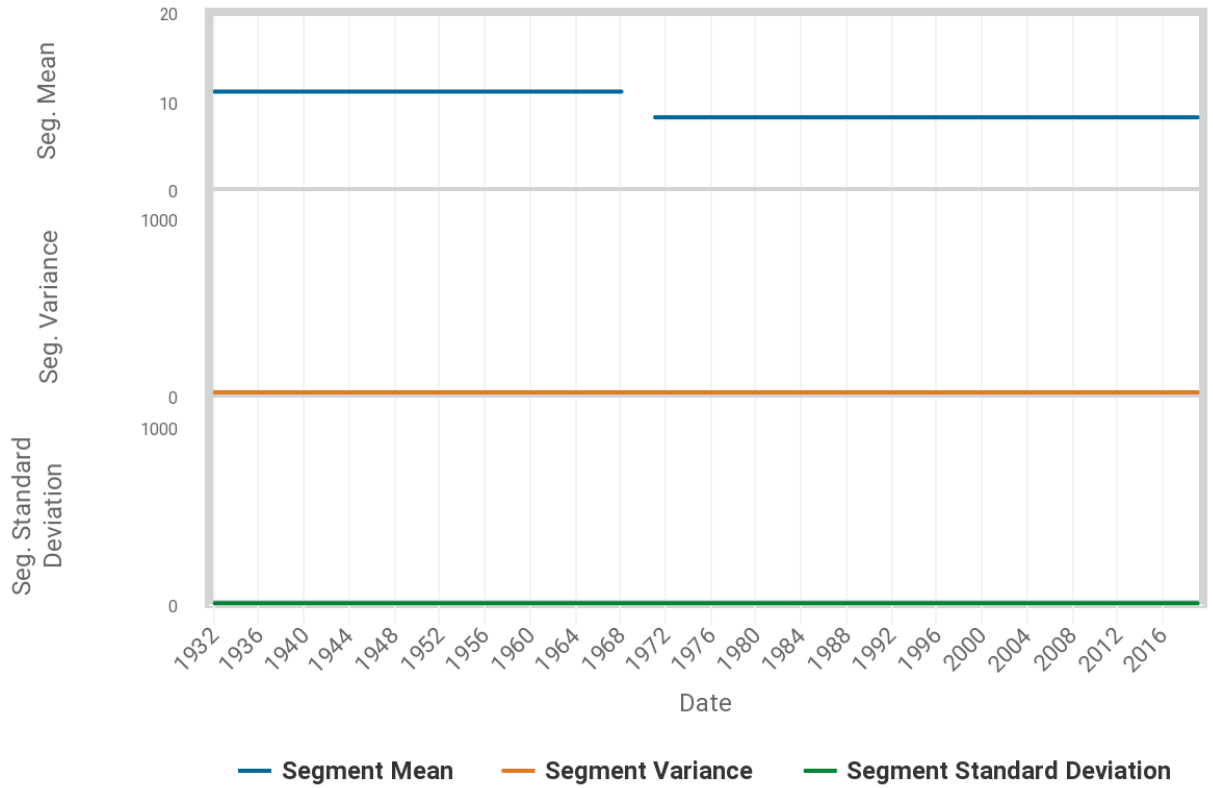


Figure 41 - Segment statistics, detecting changes in the mean, variance, and standard deviation of the time series

Plotted Data with Identified Breakpoints

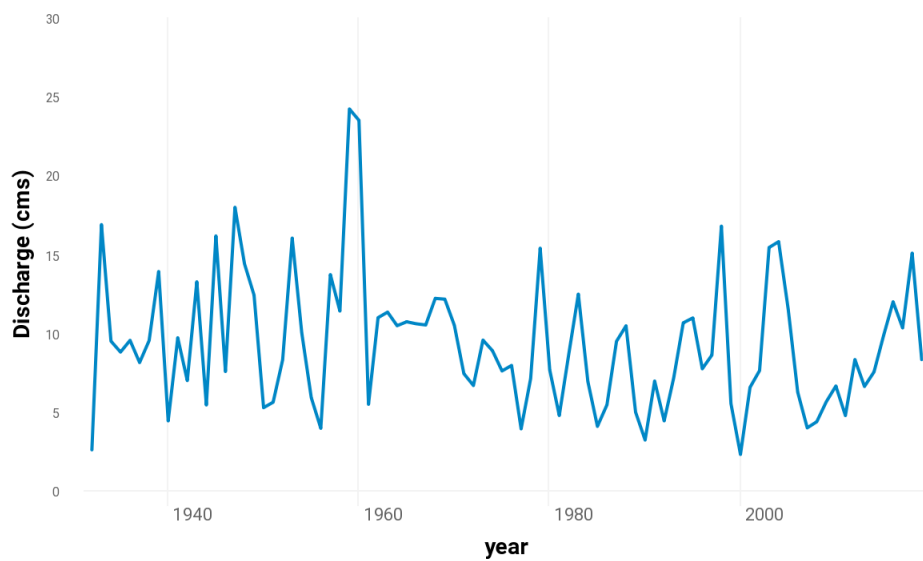


Figure 42 - Breakpoint detection, no breakpoints detected

Annual maximum streamflow time series

The annual maximum streamflow time series for the Lithia gauge is shown in Figure 43, with an obvious outlier in the first year of the record in 1932 (which is possibly an artifact). The existence of this outlier leads to negative trends from both the traditional and Sen's slopes; -1.721 (traditional slope) and -0.531 (Sen's slope) (Figure 44). Trend hypothesis tests indicate significance at the 5% level (Figure 45). Abrupt nonstationarity is found, particularly around 1960 (Figure), by different tests and for different statistical properties of the time series (mean and distribution) (Figure 47). This also leads to a breakpoint in 1960 (Figure 49).

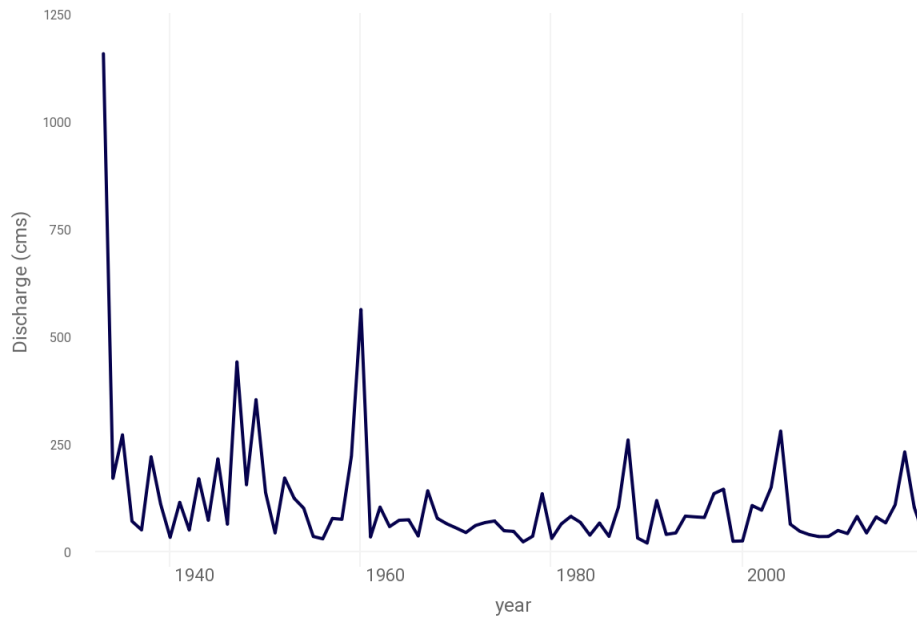


Figure 43 - Annual maximum discharge time series

Data with Slope Fits (Traditional and Sen's Slope)

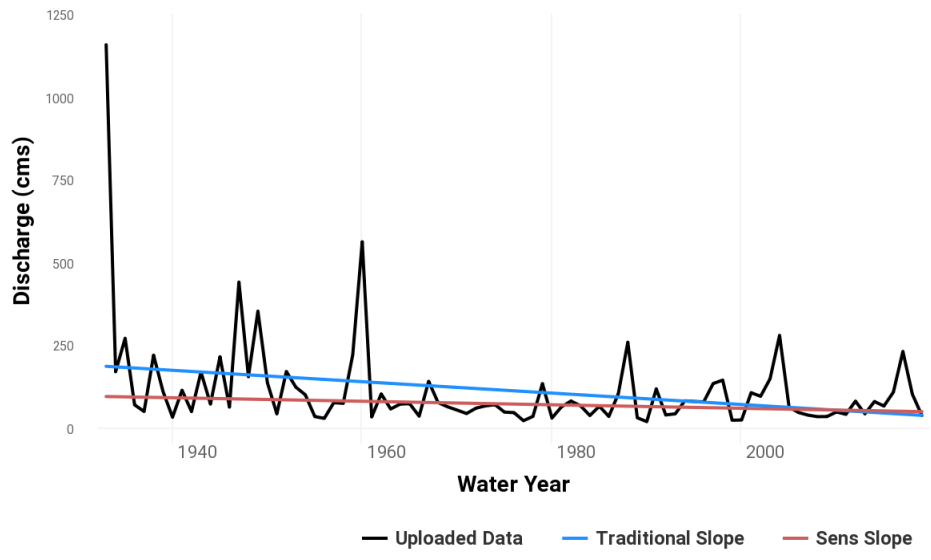


Figure 44 - Fitting trends: traditional and Sen's slope

Test	PValue
t-Test	0.0048875
Mann-Kendall	0.018223
Spearman Rank-Order	0.016756

Figure 45 - Trend hypothesis tests

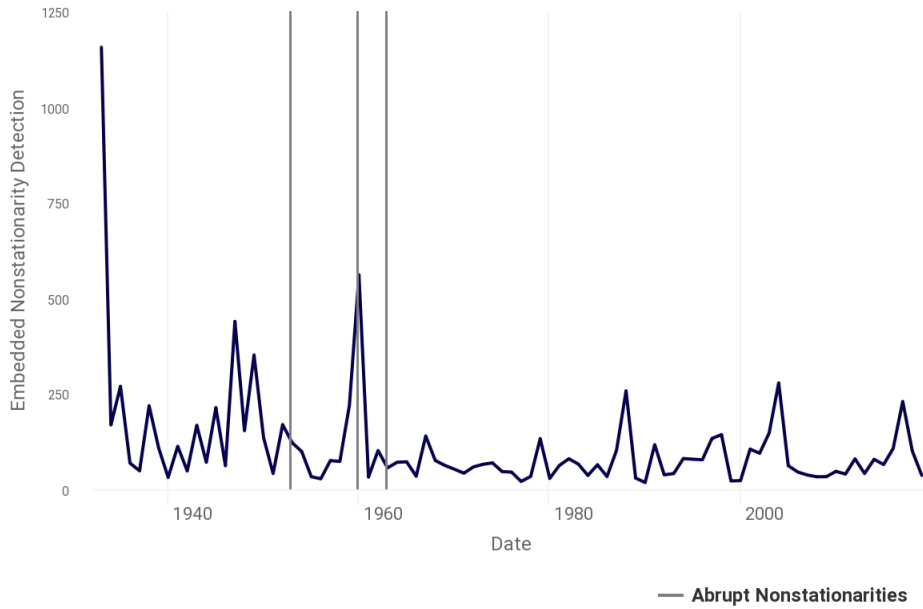


Figure 46 - Nonstationary detection, vertical lines indicate abrupt nonstationarities

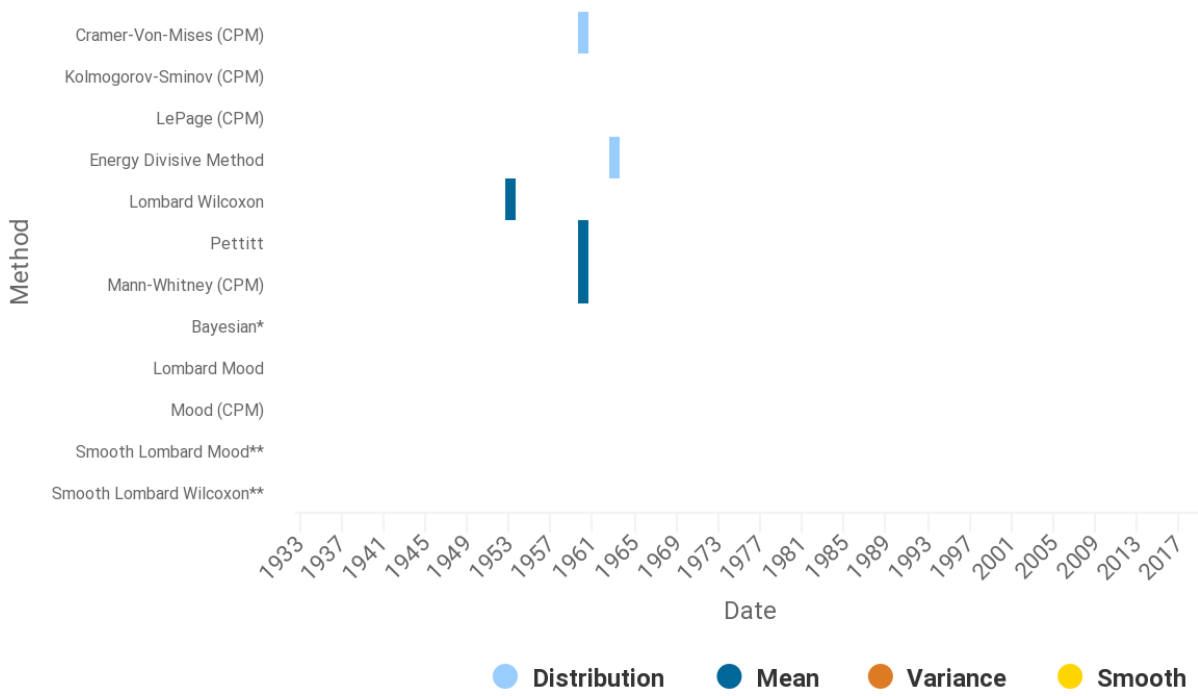


Figure 47 - Statistical tests applied to detect nonstationarity

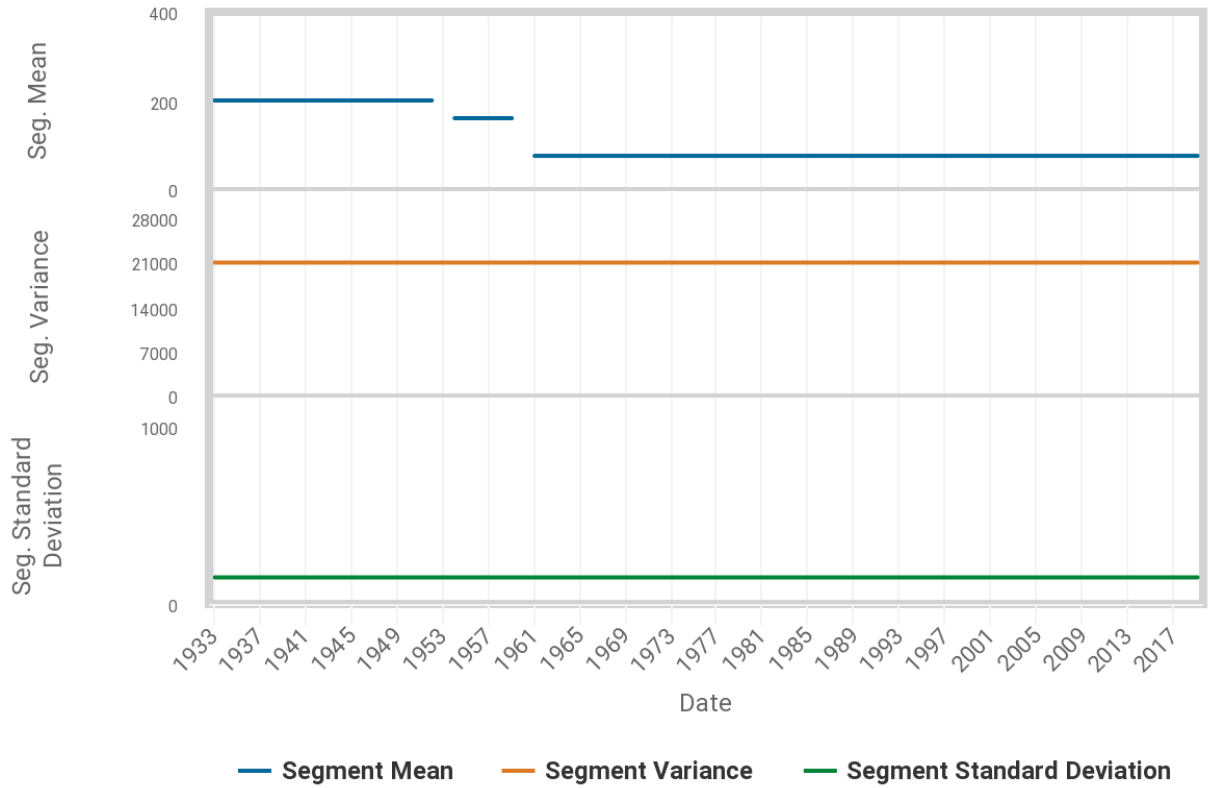


Figure 48 - Segment statistics, detecting changes in the mean, variance, and standard deviation of the time series

Plotted Data with Identified Breakpoints

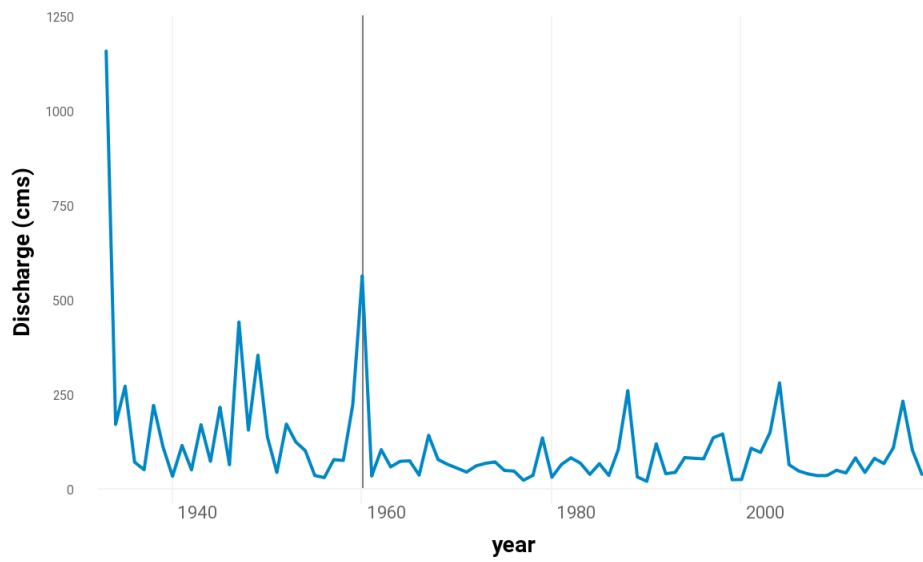


Figure 49 - Breakpoint detection, 1960 identified as breakpoint

5. Downloading and preprocessing data

Sea Level Data

Sea levels recorded at gauges situated around the U.S. coast can be obtained from The National Oceanic and Atmospheric Administration (NOAA) Center for Operational Oceanographic Products and Services (CO-OPS). The CO-OPS homepage directs users to select a state as shown in Figure 50.



Figure 50 - CO-OPS homepage.

Clicking on Florida returns the following map showing the spatial distribution of the tide gauges around the Gulf and south-eastern U.S. coasts (Figure 51).

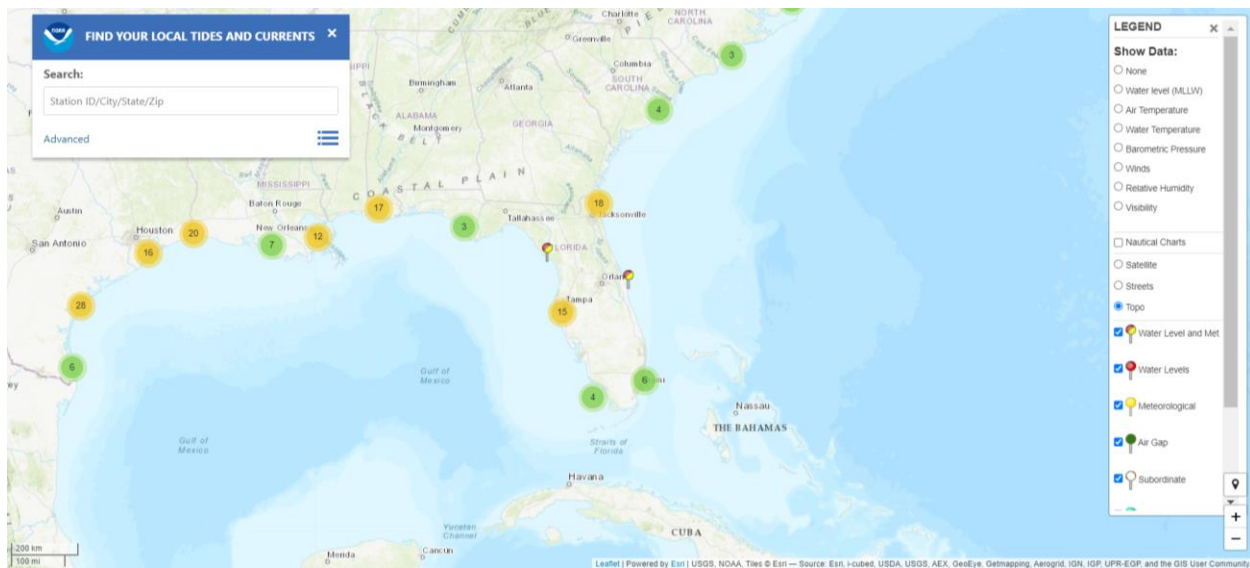


Figure 51 - Spatial distribution of tide gauges.

The tide gauges are visible by zooming in closer to south Florida as shown in Figure 52.

Tide gauges in south Florida

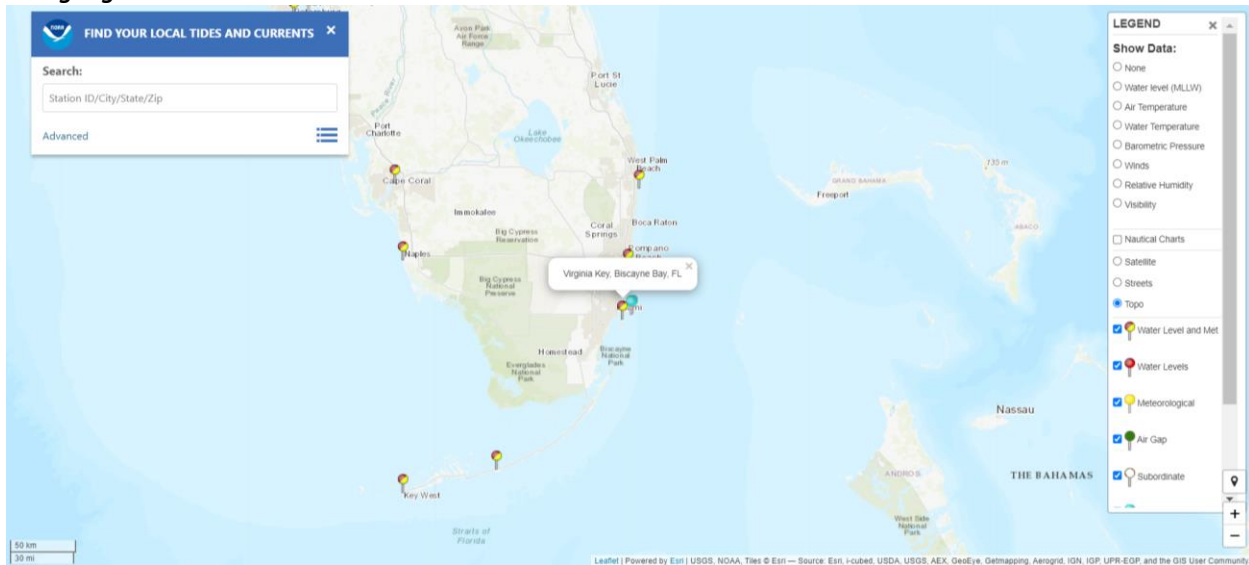


Figure 52 - Tide gauges in south Florida

To view the sea level data at a tide gauge simply click on the pin denoting its location. Figure 53 shows the homepage for the Virginia Key tide gauge.

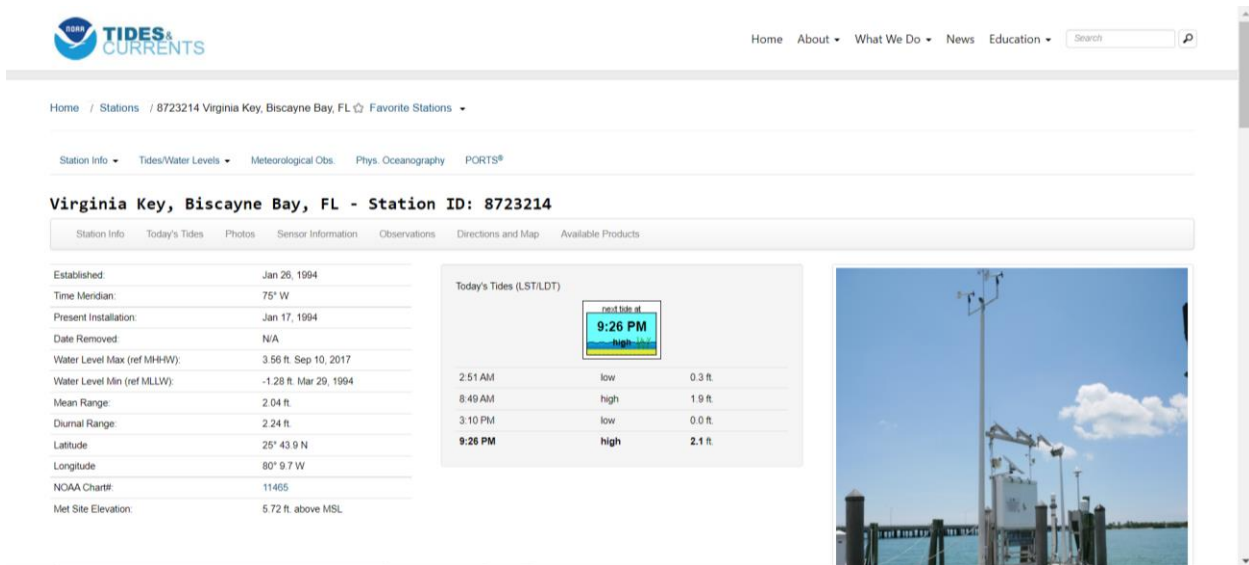


Figure 53 - Homepage of the Virginia Key gauge.

To find the sea level data, select 'Water Levels' from the 'Tide/Water Levels' dropdown menu. Water levels are typically provided at 6min and hourly time scales relative to a range of datums. Water level over short time periods (<31 days) can be plotted and exported to a '.csv' file (see bottom right corner of Figure 54). A MATLAB script to download water level data for longer time periods can be found at https://figshare.com/articles/code/Automatically_Download_sea_level_data_from_NOAA_tide_gauge/10304807/3.



Figure 54 - Plotting water levels over the previous 30 days at Virginia Key. Notice the 'Export to CSV' icon in the bottom right corner.

Streamflow Data

The United States Geological Society (USGS) National Water Information System provides access to water data from over 13,500 stations in the U.S. at <https://waterdata.usgs.gov/nwis/rt> (Figure 55).

USGS Home Contact USGS Search USGS

National Water Information System: Web Interface

USGS Water Resources

Data Category: Current Conditions Geographic Area: United States GO

Click to hide News Bulletins

- Explore the [NEW USGS National Water Dashboard](#) interactive map to access real-time water data from over 13,500 stations nationwide.
- [Full News](#)

USGS Current Water Data for the Nation

Predefined displays: Introduction go

Daily Streamflow Conditions

Thursday, July 20, 2022 09:30ET

Select a state from the map to access real-time data

Current data typically are recorded at 15- to 60-minute intervals, stored onsite, and then transmitted to USGS offices every 1 to 4 hours, depending on the data relay technique used. Recording and transmission times may be more frequent during critical events. Data from current sites are relayed to USGS offices via satellite, telephone, and/or radio telemetry and are available for viewing within minutes of arrival.

All real-time data are **provisional and subject to revision**.

Build Current Conditions Table	Show a custom current conditions summary table for one or more stations.
Build Time Series	Show custom graphs or tables for a series of recent data for one or more stations.

Explanation

- High
- > 90th percentile
- 76th - 90th percentile
- 25th - 75th percentile
- 10th - 24th percentile
- < 10th percentile
- Low

The colored dots on this map depict streamflow conditions as a **percentile**, which is computed from the period of record for the current day of the year. Only stations with at least 30 years of record are used. The **gray circles** indicate other stations that were not ranked in percentiles either because they have fewer than 30 years of record or because they report parameters other than streamflow. Some stations, for example, measure stage only.

Figure 55 - National Water Information System homepage.

To view the streamflow gauges located along a river more clearly users are urged to select a state as shown in Figure 56

The screenshot displays the USGS National Water Information System (NWIS) web interface for Florida. At the top, the USGS logo and navigation links are visible. The main content area features a map of Florida with numerous streamflow gauges indicated by colored dots (green, yellow, red, blue). To the right of the map, there are links for 'Statewide Streamflow Table', 'Statewide Groundwater Table', 'Statewide Precipitation Table', and 'Statewide Water-Quality Table'. Below these links, a text block explains that current data is recorded at 15-60 minute intervals and is provisional. At the bottom right, a table provides details for 'Build Current Conditions Table' and 'Build Time Series' options.

Build Current Conditions Table	Show a custom current conditions summary table for one or more stations.
Build Time Series	Show custom graphs or tables for a series of recent data for one or more stations.

Figure 56 - Location of streamflow gauges in the state of Florida.


Clicking on a station takes users to the gauge’s homepage which contains information on the types of measurements taken and period of record. Figure 57 presents the homepage of the gauge near the town of Bell on the Suwannee River.

USGS 02323000 SUWANNEE RIVER NEAR BELL, FLORIDA
PROVISIONAL DATA SUBJECT TO REVISION

Available data for this site Time-series Current/Historical Observations GO

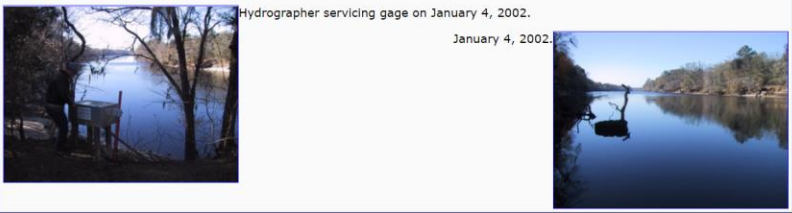
Click to hide station-specific text

This gage is monitored as part of the [National Groundwater and Streamflow Information Program](#).



Hydrographer servicing gage on January 4, 2002.

January 4, 2002.



Available Parameters	Available Period	Output format	Days (7)
<input type="checkbox"/> All 4 Available Parameters for this site		<input checked="" type="radio"/> Graph	<input type="text" value="7"/>
<input checked="" type="checkbox"/> 00010 Temperature, water	2021-02-25 2022-07-28	<input type="radio"/> Graph w/ stats	-- or --
<input checked="" type="checkbox"/> 00060 Discharge	2000-08-03 2022-07-28	<input type="radio"/> Graph w/o stats	<input type="text" value="Begin date"/>
<input checked="" type="checkbox"/> 00065 Gage height	2007-10-01 2022-07-28	<input type="radio"/> Graph w/ (up to 3) parms	<input type="text" value="2022-07-21"/>
<input checked="" type="checkbox"/> 00095 Specific cond at 25C	2021-02-25 2022-07-28	<input type="radio"/> Table	<input type="text" value="End date"/>
		<input type="radio"/> Tab-separated	<input type="text" value="2022-07-28"/>

[Summary of all available data for this site](#)
[Instantaneous-data availability statement](#)

Figure 57 - Homepage for the Suwannee River Near Bell (<https://waterdata.usgs.gov/nwis/uv?02323000>).

The *dataRetrieval* R package provides an efficient way of downloading and processing USGS hydrological data. The instantaneous value data retrieval from USGS (NWIS) function 'readNWISuv' downloads data from <https://waterservices.usgs.gov/>. The function requires the gauge's site identification number (*siteNumbers*), measurement type (*parameterCd*) as well as start (*StartDate*) and end (*endDate*) dates. The following code downloads the daily mean discharge recorded at the Suwannee River Bell gauge between 04-08-2000 and 20-07-2022 and reformats it to form the input for the USACE's Time Series Analysis toolbox:

```
#Loading the dataRetrieval package

library(dataRetrieval)

#Defining 'readNWISuv' inputs

siteNo <- "02323000"

pCode <- "00060"

start.date <- "2000-08-04"

end.date <- "2022-07-20"

#Downloading the data

data <- readNWISuv(siteNumbers = siteNo,
                    parameterCd = pCode,
                    startDate = start.date,
                    endDate = end.date)
```

```
colnames(data) <- c("agency_cd", "site_no", "dateTime", "Discharge", "X_00060_00000_cd", "tz_cd")
#Writing the data to a '.csv' file
write.csv(data, "C://Users//Documents//USGS_02323000_SUWANNEE_RIVER_NEAR_BELL_FLORIDA.csv")
#Formatting for the USACE's Time Series Analysis toolbox
#Reading in the data
Data <- read.csv("C://Users//Documents//USGS_02323000_SUWANNEE_RIVER_NEAR_BELL_FLORIDA.csv")
#Retaining only the date and discharge value columns
data <- data[ ,c(4,5)]
#Reformatting the date to that required by the Time Series Analysis toolbox
data$dateTime <- format(as.Date(substr(data$dateTime,1,10)), '%m/%d/%Y')
```

APPENDIX E. USGS TREND ASSESSMENT TABULAR DATA

Table E-1. Tabular results from the normality test for the USGS annual peak flow data.

STATION ID	STATION NAME	p-VALUE
2270500	ARBUCKLE CREEK DE SOTO CITY, FL	0
2231000	ST. MARYS RIVER MACCLENNY, FL	0
2326900	ST. MARKS RIVER NEWPORT, FLA.	0
2307000	ROCKY CREEK SULPHUR SPRINGS FL	0
2313000	WITHLACOOCHEE RIVER SR 200 NEAR HOLDER, FL	0
2358700	APALACHICOLA RIVER BLOUNTSTOWN,FLORIDA	0.001
2264100	BONNET CREEK VINELAND, FL	0.001
2324000	STEINHATCHEE RIVER CROSS CITY, FLA.	0
2310947	WITHLACOOCHEE RIVER CUMPRESSCO, FL	0.003
2312500	WITHLACOOCHEE RIVER CROOM, FL	0
2232000	ST. JOHNS RIVER MELBOURNE, FL	0
2365500	CHOCTAWHATCHEE RIVER CARYVILLE, FLA.	0
2266200	WHITTENHORSE CREEK VINELAND, FL	0
2243960	OCKLAWAHA R RODMAN DAM NEAR ORANGE SPRINGS, FL	0.005
2312640	JUMPER CREEK CANAL BUSHNELL, FL	0.001
2301500	ALAFIA RIVER LITHIA PINECREST RD AT LITHIA, FL	0
2303330	HILLSBOROUGH R MORRIS BR NEAR THONOTOSASSA FL	0.001
2301000	NORTH PRONG ALAFIA RIVER KEYSVILLE FL	0
2252500	NORTH CANAL VERO BEACH, FL	0.015
2236000	ST. JOHNS RIVER DE LAND, FL	0.049
2298830	MYAKKA RIVER SR 72 NEAR SARASOTA, FL	0
2320500	SUWANNEE RIVER BRANFORD, FLA.	0
2309848	SOUTH BRANCH ANCLOTE RIVER ODESSA FL	0.004
2301300	SOUTH PRONG ALAFIA RIVER LITHIA FL	0
2307359	BROOKER CREEK TARPON SPRINGS FL	0
2243000	ORANGE CREEK ORANGE SPRINGS, FL	0
2235000	WEKIVA RIVER SANFORD, FL	0
2299950	MANATEE RIVER SR 64 NEAR MYAKKA HEAD, FL	0
2300200	SOUTH FORK LITTLE MANATEE RIVER DUETTE FL	0
2370000	BLACKWATER RIVER BAKER, FLA.	0
2310000	ANCLOTE RIVER LITTLE RD NEAR ELFERS, FL	0
2300700	BULLFROG CREEK WIMAUMA FL	0
2239501	SILVER RIVER OCALA, FL	0.253
2266300	REEDY CREEK VINELAND, FL	0
2266480	DAVENPORT CREEK LOUGHMAN, FL	0
2303400	CYPRESS CREEK SAN ANTONIO FL	0
2232200	WOLF CREEK DEER PARK, FL	0
2271500	JOSEPHINE CREEK DE SOTO CITY FL	0
2306500	SWEETWATER CREEK SULPHUR SPRINGS FL	0

Table E-1. Continued.

STATION ID	STATION NAME	p-VALUE
2232400	ST. JOHNS RIVER COCOA, FL	0.418
2319500	SUWANNEE RIVER ELLAVILLE, FLA	0
2234990	LITTLE WEKIVA RIVER ALTAMONTE SPRINGS, FL	0
2244420	LITTLE HAW CREEK SEVILLE, FL	0
2327100	SOPCHOPPY RIVER SOPCHOPPY, FLA.	0
2369000	SHOAL RIVER CRESTVIEW, FLA.	0
2300500	LITTLE MANATEE RIVER US 301 NEAR WIMAUMA, FL	0
2322500	SANTA FE RIVER FORT WHITE, FLA.	0
2233200	LITTLE ECONLOCKHATCHEE RIVER UNION PARK, FL	0
2301900	FOX BRANCH SOCRUM, FL	0
2295637	PEACE RIVER US 17 AT ZOLFO SPRINGS, FL	0
2319000	WITHLACOOCHEE RIVER PINETTA, FLA.	0
2237293	PALATLAKAHA R STRUCTURE M-1, NR OKAHUMPKA, FL	0
2303800	CYPRESS CREEK SULPHUR SPRINGS FL	0.002
2297310	HORSE CREEK SR 72 NEAR ARCADIA, FL	0
2233500	ECONLOCKHATCHEE RIVER CHULUOTA, FL	0
2359170	APALACHICOLA RIVER SUMATRA,FLA.	0
2300100	LITTLE MANATEE RIVER FT. LONESOME FL	0
2294650	PEACE RIVER SR 60 AT BARTOW, FL	0
2324500	FENHOLLOWAY RIVER FOLEY, FLA.	0
2310300	PITHLACHASCOTEE RIVER NEW PORT RICHEY FL	0
2325000	FENHOLLOWAY RIVER PERRY, FLA	0.011
2264000	CYPRESS CREEK VINELAND, FL	0
2253500	SOUTH CANAL VERO BEACH, FL	0.18
2247510	TOMOKA RIVER HOLLY HILL, FL	0
2359500	ECONFINA CREEK BENNETT, FLA.	0
2256500	FISHEATING CREEK PALMDALE, FL	0
2303000	HILLSBOROUGH RV STATE PARK NR ZEPHYRHILLS, FL	0
2235200	BLACKWATER CREEK CASSIA, FL	0
2232500	ST. JOHNS RIVER CHRISTMAS, FL	0.029
2264495	SHINGLE CREEK CAMPBELL, FL	0.019
2303350	TROUT CREEK SULPHUR SPRINGS FL	0
2329600	LITTLE RIVER MIDWAY, FLA.	0
2248000	SPRUCE CREEK SAMSULA, FL	0.018
2312200	LITTLE WITHLACOOCHEE RIVER RERDELL, FL	0
2358000	APALACHICOLA RIVER CHATTAHOOCHEE FLA	0
2366500	CHOCTAWHATCHEE RIVER BRUCE, FLA.	0
2231600	JANE GREEN CREEK DEER PARK, FL	0
2326000	ECONFINA RIVER PERRY, FLA.	0.001

Table E-1. Continued.

STATION ID	STATION NAME	p-VALUE
2263800	SHINGLE CREEK AIRPORT NEAR KISSIMMEE, FL	0
2312700	OUTLET RIVER PANACOOCHEE RETREATS, FL	0.12
2312000	WITHLACOOCHEE RIVER US 301 AT TRILBY, FL	0
2312180	LITTLE WITHLACOOCHEE RIVER TARRYTOWN, FL	0
2329000	OCHLOCKONEE RIVER HAVANA, FLA.	0
2253000	MAIN CANAL VERO BEACH, FL	0.081
2245500	SOUTH FORK BLACK CREEK PENNEY FARMS, FL	0
2303420	CYPRESS CREEK SR 54 AT WORTHINGTON GARDENS, FL	0
2297100	JOSHUA CREEK NOCATEE FL	0
2236500	BIG CREEK CLERMONT, FL	0
2302500	BLACKWATER CREEK KNIGHTS FL	0
2296500	CHARLIE CREEK GARDNER FL	0
2330000	OCHLOCKONEE RIVER BLOXHAM, FLA.	0
2312720	WITHLACOOCHEE RIVER WYSONG DAM, AT CARLSON, FL	0.043
2234324	HOWELL CREEK SLAVIA, FL	0.001
2237700	APOPKA-BEAUCLAIR CANAL ASTATULA, FL	0
2262900	BOGGY CREEK TAFT, FL	0
2267000	CATFISH CREEK LAKE WALES, FL	0
2321500	SANTA FE RIVER WORTHINGTON SPRINGS, FLA.	0

Table E-2. Tabular results from the Kendall Test for the USGS Annual Peak Flow Data

STATION ID	STATION NAME	p-VALUE	SEN-SLOPE
2270500	ARBUCKLE CREEK DE SOTO CITY, FL	0.1231	-8.067
2231000	ST. MARYS RIVER MACCLENNY, FL	0.7822	4.643
2326900	ST. MARKS RIVER NEWPORT, FLA.	0.7728	-1.835
2307000	ROCKY CREEK SULPHUR SPRINGS FL	0.6523	1.128
2313000	WITHLACOOCHEE RIVER SR 200 NEAR HOLDER, FL	0.0065	-15.614
2358700	APALACHICOLA RIVER BLOUNTSTOWN,FLORIDA	0.0634	-535.714
2264100	BONNET CREEK VINELAND, FL	0.0015	8.586
2324000	STEINHATCHEE RIVER CROSS CITY, FLA.	0.9422	1.16
2310947	WITHLACOOCHEE RIVER CUMPRESSCO, FL	0.3262	-4.384
2312500	WITHLACOOCHEE RIVER CROOM, FL	0.0558	-9.68
2232000	ST. JOHNS RIVER MELBOURNE, FL	0.9675	-0.723
2365500	CHOCTAWHATCHEE RIVER CARYVILLE, FLA.	0.7538	18.519
2266200	WHITTENHORSE CREEK VINELAND, FL	0.0169	0.4
2243960	OCKLAWAHA R RODMAN DAM NEAR ORANGE SPRINGS, FL	0.5115	-10.769
2312640	JUMPER CREEK CANAL BUSHNELL, FL	4.00E-04	-1.188
2301500	ALAFIA RIVER LITHIA PINECREST RD AT LITHIA, FL	0.0382	-18.359
2303330	HILLSBOROUGH R MORRIS BR NEAR THONOTOSASSA FL	0.8026	2.251
2301000	NORTH PRONG ALAFIA RIVER KEYSVILLE FL	0.457	5.783
2252500	NORTH CANAL VERO BEACH, FL	0.0885	-3.167
2236000	ST. JOHNS RIVER DE LAND, FL	0.9241	1.429
2298830	MYAKKA RIVER SR 72 NEAR SARASOTA, FL	0.3103	-5.775
2320500	SUWANNEE RIVER BRANFORD, FLA.	0.9557	2.174
2309848	SOUTH BRANCH ANCLOTE RIVER ODESSA FL	0.2727	1.044
2301300	SOUTH PRONG ALAFIA RIVER LITHIA FL	0.2742	-4.739
2307359	BROOKER CREEK TARPON SPRINGS FL	0.741	0.501
2243000	ORANGE CREEK ORANGE SPRINGS, FL	0.0014	-6.343
2235000	WEKIVA RIVER SANFORD, FL	0.4467	0.731
2299950	MANATEE RIVER SR 64 NEAR MYAKKA HEAD, FL	0.7439	4.455
2300200	SOUTH FORK LITTLE MANATEE RIVER DUETTE FL	0.5275	0.95
2370000	BLACKWATER RIVER BAKER, FLA.	0.4586	-15.954
2310000	ANCLOTE RIVER LITTLE RD NEAR ELFERS, FL	0.7315	-1.486
2300700	BULLFROG CREEK WIMAUMA FL	0.5571	-3.2
2239501	SILVER RIVER OCALA, FL	0	-4.792
2266300	REEDY CREEK VINELAND, FL	0.0266	5.462
2266480	DAVENPORT CREEK LOUGHMAN, FL	0.0058	1.435
2303400	CYPRESS CREEK SAN ANTONIO FL	0.7338	0.294
2232200	WOLF CREEK DEER PARK, FL	0.3496	6.136
2271500	JOSEPHINE CREEK DE SOTO CITY FL	0.0729	3.156
2306500	SWEETWATER CREEK SULPHUR SPRINGS FL	0.0247	0.636

Table E-2. Continued.

STATION ID	STATION NAME	p-VALUE	SEN-SLOPE
2232400	ST. JOHNS RIVER COCOA, FL	0.6604	6.688
2319500	SUWANNEE RIVER ELLAVILLE, FLA	0.8065	11.765
2234990	LITTLE WEKIVA RIVER ALTAMONTE SPRINGS, FL	0.3035	1
2244420	LITTLE HAW CREEK SEVILLE, FL	0.7463	0.826
2327100	SOPCHOPPY RIVER SOPCHOPPY, FLA.	0.8813	-2.093
2369000	SHOAL RIVER CRESTVIEW, FLA.	0.1212	40.526
2300500	LITTLE MANATEE RIVER US 301 NEAR WIMAUMA, FL	0.0159	-18.8
2322500	SANTA FE RIVER FORT WHITE, FLA.	0.0314	-19.762
2233200	LITTLE ECONLOCKHATCHEE RIVER UNION PARK, FL	0.1913	3.607
2301900	FOX BRANCH SOCRUM, FL	0.4885	1.183
2295637	PEACE RIVER US 17 AT ZOLFO SPRINGS, FL	3.00E-04	-33.629
2319000	WITHLACOOCHEE RIVER PINETTA, FLA.	0.1461	49.6
2237293	PALATLAKAHA R STRUCTURE M-1, NR OKAHUMPKA, FL	0.2487	0.825
2303800	CYPRESS CREEK SULPHUR SPRINGS FL	0.0156	-9.571
2297310	HORSE CREEK SR 72 NEAR ARCADIA, FL	0.0238	-19.385
2233500	ECONLOCKHATCHEE RIVER CHULUOTA, FL	0.6926	3.2
2359170	APALACHICOLA RIVER SUMATRA,FLA.	0.578	-334.502
2300100	LITTLE MANATEE RIVER FT. LONESOME FL	0.0179	-6.391
2294650	PEACE RIVER SR 60 AT BARTOW, FL	0.4456	-2.134
2324500	FENHOLLOWAY RIVER FOLEY, FLA.	3.00E-04	-7.541
2310300	PITHLACHASCOTEE RIVER NEW PORT RICHEY FL	1	0
2325000	FENHOLLOWAY RIVER PERRY, FLA	0.0058	-7
2264000	CYPRESS CREEK VINELAND, FL	0.8476	0.034
2253500	SOUTH CANAL VERO BEACH, FL	0.4099	-2.186
2247510	TOMOKA RIVER HOLLY HILL, FL	0.2419	4.906
2359500	ECONFINA CREEK BENNETT, FLA.	0.0116	7.667
2256500	FISHEATING CREEK PALMDALE, FL	0.0233	-24.821
2303000	HILLSBOROUGH RV STATE PARK NR ZEPHYRHILLS, FL	0.1323	-9.108
2235200	BLACKWATER CREEK CASSIA, FL	0.3298	-1.043
2232500	ST. JOHNS RIVER CHRISTMAS, FL	0.8055	3.182
2264495	SHINGLE CREEK CAMPBELL, FL	0.0226	7.353
2303350	TROUT CREEK SULPHUR SPRINGS FL	0.3326	2.653
2329600	LITTLE RIVER MIDWAY, FLA.	0.9068	-7.825
2248000	SPRUCE CREEK SAMSULA, FL	0.375	1.291
2312200	LITTLE WITHLACOOCHEE RIVER RERDELL, FL	0.6309	-1.297
2358000	APALACHICOLA RIVER CHATTAHOOCHEE FLA	0.8487	-26
2366500	CHOCTAWHATCHEE RIVER BRUCE, FLA.	0.897	-11.01
2231600	JANE GREEN CREEK DEER PARK, FL	0.003	-37.607
2326000	ECONFINA RIVER PERRY, FLA.	0.9921	0

Table E-2. Continued.

STATION ID	STATION NAME	p-VALUE	SEN-SLOPE
2263800	SHINGLE CREEK AIRPORT NEAR KISSIMMEE, FL	0.0154	7.5
2312700	OUTLET RIVER PANACOOCHEE RETREATS, FL	0.0784	-2.585
2312000	WITHLACOOCHEE RIVER US 301 AT TRILBY, FL	0.044	-7.619
2312180	LITTLE WITHLACOOCHEE RIVER TARRYTOWN, FL	0.7825	0.7
2329000	OCHLOCKONEE RIVER HAVANA, FLA.	0.0543	41.877
2253000	MAIN CANAL VERO BEACH, FL	0.2614	-2.5
2245500	SOUTH FORK BLACK CREEK PENNEY FARMS, FL	0.0973	-17.826
2303420	CYPRESS CREEK SR 54 AT WORTHINGTON GARDENS, FL	0.2598	-2.933
2297100	JOSHUA CREEK NOCATEE FL	0.1034	-11.404
2236500	BIG CREEK CLERMONT, FL	0.6751	-0.245
2302500	BLACKWATER CREEK KNIGHTS FL	0.5919	-1.66
2296500	CHARLIE CREEK GARDNER FL	0.8078	-1.778
2330000	OCHLOCKONEE RIVER BLOXHAM, FLA.	0.0896	49.167
2312720	WITHLACOOCHEE RIVER WYSONG DAM, AT CARLSON, FL	0.319	-9.529
2234324	HOWELL CREEK SLAVIA, FL	0.0816	2.012
2237700	APOPKA-BEAUCLAIR CANAL ASTATULA, FL	0.0463	-3.25
2262900	BOGGY CREEK TAFT, FL	0.0026	8.414
2267000	CATFISH CREEK LAKE WALES, FL	0.0962	-0.429
2321500	SANTA FE RIVER WORTHINGTON SPRINGS, FLA.	0.093	-25.88